1-1-2013

Investigation into the Effect of Strong Oxidizers on the Electrokinetic Removal of Chromium, Copper, and Arsenic from CCA Impregnated Wood Waste

John Amos Broussard

Investigation into the effect of strong oxidizers on the electrokinetic removal of chromium, copper, and arsenic from CCA impregnated wood waste

By

John Amos Broussard, III

A Thesis
Submitted to the Faculty of
Mississippi State University
in Partial Fulfillment of the Requirements
for the Degree of Master of Science
in Chemical Engineering
in the Dave C. Swalm School of Chemical Engineering

Mississippi State, Mississippi

May 2013

Investigation into the effect of strong oxidizers on the electrokinetic removal of chromium, copper, and arsenic from CCA impregnated wood waste

By

John Amos Broussard, III

Approved:

R. Mark Bricka Associate Professor of Chemical Engineering (Major Professor)	Hossein Toghiani Associate Professor of Chemical Engineering (Committee Member)
Billy B. Elmore Associate Professor of Chemical Engineering (Committee Member)	Keisha B. Walters Associate Professor of Chemical Engineering (Graduate Coordinator)
Sarah A. Rajala Dean of the Bagley College of Engineering	

Name: John Amos Broussard, III

Date of Degree: May 10, 2013

Institution: Mississippi State University

Major Field: Chemical Engineering

Major Professor: R. Mark Bricka

Title of Study: Investigation into the effect of strong oxidizers on the electrokinetic removal of chromium, copper, and arsenic from CCA impregnated wood waste

Pages in Study: 289

Candidate for Degree of Master of Science

The focus of this research is to determine the effects of particle size reduction and chemical pretreatment with strong base oxidizers on the effectiveness of the electrokinetic remediation of wood waste contaminated with chromated copper arsenate. Selection of an oxidative chemical pretreatment solution involved an initial screening between three pre-selected chemicals followed by optimization of oxidative chemical solution strengths and solid to liquid ratios. Samples of each of the three particle sizes were chemically treated with the final oxidative pretreatment and loaded into electrokinetic units where a direct current was applied for approximately fifty days. Similar experiments were performed without subjecting the contaminated wood to oxidative pretreatment to serve as an experimental control. It was identified that oxidative pretreatment of the lowest particle size prior to electrokinetic treatment was able to remove the highest percentages of chromium (75 %), copper (95 %), and arsenic (92 %) from the contaminated wood.

ACKNOWLEDGEMENTS

The author would like to thank the faculty and the staff of the Mississippi State University Chemical Engineering Department for all of their support over the past several years and for their extreme patience and understanding in dealing with a student attempting to complete all of the requirements for graduation remotely. Of particular note in this category are my thesis committee members Dr. Toghiani, Dr. Elmore, and Dr. Walters. And above all, thank you Dr. Bricka for helping me along all this time.

In addition the author would like to thank graduate students: Annu Marwaha, Monty Singeltary, Prashanth Buchnireddy, and Otho Barnes for much appreciated help in the laboratory. And also thanks to research assistant Rosemary Weathersby.

TABLE OF CONTENTS

LIST OF TABLES

LIST OF FIGURES

CHAPTER I

INTRODUCTION

Wood products are attacked and degraded by many different agents. Insects, microorganisms, weather, mechanical stresses, and fire are all examples of agents that can contribute to the degradation of wood products. Preservatives are applied to wood products to combat the different wood degradation agents. Chromated Copper Arsenate (CCA) is one such preservative. CCA treatments are designed primarily to protect against biological decay and insect infestation. The application of CCA preservative to a wood product can increase the average service life of the wood product from between one and five years to an average service life of twenty to fifty years (Cooper, 2003). This is one of the reasons why CCA has been the most commonly used wood preservative in the US for the past twenty years (Gezer, 2005).

Most wood products enter the waste stream as construction and demolition (C&D) debris. C&D debris is typically disposed of by landfilling or incineration. Until recently, neither of the traditional disposal methods has posed a serious environmental threat. However, the volume of CCA products entering the C&D waste stream is expected to increase in coming years and the long term impact of this change in C&D composition is unknown (Solo-Gabriele, 1999).

Studies show that CCA waste cannot be incinerated in an environmentally friendly manner (Decker et al, 2002). Incineration of CCA products causes the volatile

release of a toxic form of arsenic. There is also a dramatic increase in the concentration of arsenic and chromium in the post incineration ash product (Table 1.1). As such, the disposal of CCA waste by incineration results in the generation of two wastes, each with a higher toxicity than the original product (Solo-Gabriele, 1999).

Landfilling is currently the most common disposal method for waste wood products. Modern landfills utilize different types of liners to contain waste. The three types of landfill liners are listed in Table 1.2. Waste products are assigned to different landfill types according to the potential threat they pose to the environment (Hughes, 2005).

In most US states, the toxicity characteristic leaching procedure (TCLP) is performed to determine whether or not a solid waste will be classified as a toxicity characteristic (TC) hazardous waste. A material that tests positive as a TC hazardous waste must be discarded in a Subtitle C landfill (40CFR264). When a solid waste product comprised mainly of CCA is subjected to a TCLP test, it will usually test positive for arsenic (Townsend, 2004). This should result in the classification of the material as a TC hazardous waste, which would call for disposal in a Subtitle C landfill. But since it is not common practice to separate materials containing CCA from the bulk waste and since CCA waste makes up such a small percentage of the overall waste stream, solid waste containing CCA will normally test negative as a TC hazard and be discarded into single and Subtitle D landfills

The possibility of the disposal issues mentioned above developing into legitimate problems in the future has lead government organizations to begin to phase out production of CCA products in the US. In 2002 a voluntary decision was made by the

pressure-treated wood industry to phase treated wood products containing CCA out of consumer markets. In 2004 the Environmental Protection Agency (EPA) banned the use of wood products containing CCA in residential areas in the US (Gezer, 2005). The EPA has allowed the production of CCA products to continue for use exclusively in industrial and commercial applications in the US.

It has been estimated that the wood preservation industry annually produces 30 million cubic meters of treated wood worldwide. It has also been estimated that approximately two thirds of all the treated wood products produced since 1970 contain CCA. It is estimated that the volume of CCA treated wood being removed from service in the US will have increased to over 16 million cubic meters per year by 2020 (Humphrey, 2002 or Cooper, 2003). Some measures have been taken to reduce the volume of CCA materials entering service in the US. But the use of CCA products will continue on an industrial scale, and CCA products will continue to accumulate in the US waste stream.

1.1 Wood Products

1.1.1 Wood as an Engineering Material

As an engineering material wood products have high strength to weight ratios, are easy to shape and fasten, and are effective insulators. The economic advantages of using wood as an engineering material include the relatively low cost of wood compared to other engineering materials and the high availability of wood in virtually all of Earths global regions. Over the course of history, many developments have been made in the materials field. Some of these developments have resulted in the displacement of wood products as engineering materials (ie. concrete, steel, composites). However, there are still areas where wood products continue to out perform all other engineering materials.

The continued use of wood products is due not only to the favorable physical properties of wood, but in a large part to technological advances made by the wood production industry. The measurement of wood properties has become much more precise in recent years due to advances in analytical technology. The development and application of analytical methods and standards specific to wood products has also made it possible for the wood producing industry to classify wood products by their inherent strengths and weaknesses. Progress has also been made in the timber manufacturing process as well as in wood preservation techniques. All of these developments have been effective in increasing the serviceability, economy, and overall efficiency of wood products.

1.1.2 Wood Deterioration

Perhaps the least desirable characteristic of wood products is their susceptibility to deterioration. Wood deterioration agents can be grouped into the following categories: fungi and bacteria, insects, weathering, fire, and mechanical wear.

Fungi and bacteria are two categories of organisms that can cause extensive damage to wood products. They are known to infect natural wood as well as treated wood, and they have the potential to cause the complete failure of a product. As a general rule, a wood product containing a minimum of 20 percent moisture will be at higher risk of becoming infested with fungi and bacteria. Consequently, damage to wood products by fungi and bacteria will be more extensive in high humidity environments and below the waterline of submerged wood products. Wood species that naturally retain high levels of moisture are also at risk (Hunt and Garratt, 1967). There are many different mechanisms by which fungi and bacteria degrade wood products. To elaborate on the different types

of microrganisms and the mechanisms by which they degrade wood would be beyond the scope of this report. A broad overview of wood degrading species can be found in Hunt and Garrat (1967) and Richardson (1993).

Insects are known to attack natural wood as well as treated wood products, and they too have the potential to cause the complete failure of a wood product. Replacing and/or repairing wood products damaged by insect attack costs the end users of the wood product millions of dollars annually. The threat of insect attack on wood products exists in virtually all climates and global regions where wood products are utilized. There are many different mechanisms by which insects degrade wood products. To elaborate on all of the different types of species of insects and the methods by which they attack wood is beyond the scope of this report. An overview of can be found in Hunt and Garratt (1967) and Richardson (1993).

Mechanical wear is a wood degrading mechanism that affects load-bearing wood products. Cyclic loads and constant loads can affect the physical properties of the wood product negatively. This is especially true in situations where the abrasion of wood with metals is unavoidable. If a wood product is subjected to loading stresses for extended periods of time without inspection or replacement, then mechanical wear can cause a product failure. It should be noted that damage due to mechanical wear is often accelerated when in the presence of other wood degrading agents.

Weathering is a wood degrading mechanism that affects natural wood and treated wood. It occurs in areas where wood products are exposed to harsh climates or periodic changes in weather. Weathering is closely related to the ability of wood products to absorb and desorb water. The repeated absorption and desorption of water causes the

wood to expand and contract. After many cycles of expansion and contraction, the structural value of the wood can be affected negatively. The degree to which wood absorbs water depends on the type of wood, humidity of the surrounding environment, and changes in ambient temperature. Weathering is normally restricted to the surface of the wood product. However, if a product is exposed to weathering conditions for extended periods of time without inspection or replacement then it is likely that the material will experience some degree of weathering degradation internally.

Fire can cause extensive damage to wood products in relatively short periods of time. Wood products provide a flame ignition source and a large flame propagation surface area. Fire spreads more easily over wood products with small particle size and low moisture content. Also, decayed wood is known to ignite more readily than healthy wood. Fire can result in the failure of wood product, especially when the product is bearing a load.

1.1.3 Wood Preservation

The primary objective of a preservative treatment is to increase the service life of the material (Hunt and Garratt, 1967). Industrial scale wood preservation began in 1832 when an Englishman named John Kyan obtained the first patent for the chemical treatment of wood products. In Kyan's process, a timber was submerged into a tank containing 0.67% mercuric chloride solution for several days.

In the years since Kyan, an untold number of preservative treatment formulations and application methods have been developed. Each formulation and method has its own strengths and weaknesses. Characteristics of effective wood preservatives are listed in Table 1.3.

1.1.4 Main Groups of Wood Preservatives

There are three main classifications of chemical preservative formulations for wood treatment: tar oils, organic solvents, and waterborne preservatives. Examples of the most commonly used solutions in each category are published annually in the American Wood Protection Association (AWPA) Standards Manual.

1.1.4.1 Tar Oils

Tar oil wood preservatives are products of the distillation of coal tars, wood oils, low cost solvents, petroleum oils, and light fuel oils. Tar oils are commonly referred to as creosote. They contain several hundred organic compounds. Nearly all of the organic compounds present in tar oils can be grouped into one of the three following categories: tar acids, tar bases, and hydrocarbons (Hunt and Garratt, 1967).

Hydrocarbons make up the largest portion of organic compounds in tar oil preservatives. Toxicity due to hydrocarbon content in tar oil preservatives is low. For this reason, the hydrocarbon fraction is typically referred to as “dead oil”. The hydrophobic nature of the hydrocarbon fraction protects the wood product from water damage. The hydrocarbon fraction also prevents water-soluble portions of the preservative from leaching out of the wood by forming a heavy, black, tar-like layer on the exterior of the wood product. The tar layer acts as a waterproof barrier between the soluble species within the wood and any water-based leaching agents external to the wood. For the most part, hydrocarbons have little or no effect on the toxicity of the preservative formulation. However a small fraction of the hydrocarbon portion known as polycyclic-aromatic hydrocarbons (PAH), are known to be relatively mobile as well as carcinogenic to humans. Some examples of toxic PAH’s are listed in Table 1.4.

In terms of mass, tar acids and tar bases will typically make up less than ten percent of the total preservative formulation. The tar acid and tar base fraction is toxic to many wood deterioration agents. The tar acid and tar base fraction is also highly mobile within the wood matrix which allows tar oil preservative treatments to achieve high degrees of penetration and therefore preserve a larger portion of the wood product.

Tar oil preservatives dominated the wood preservation market from the time of their discovery by John Bethel in 1838 until the 1930's. Advantages associated with the use of tar oils include excellent resistance to biological deterioration, insect attack, and good resistance to damage due to fluctuations in moisture content. Disadvantages include the odors they emit, their tendency to leach mobile portions of preservative solution over time, and the surfaces of products treated with tar oils cannot be painted. In addition, the recent decrease in availability of tar oil preservatives due to rising petroleum costs has had a negative effect on the tar oil preservative industry.

1.1.4.2 Organic Solvents

Some chemicals have the ability to protect against wood deterioration agents, but are ineffective as preservative treatments. They are ineffective because of preservative volatilization upon treatment and low degree of fixation within products. In some cases, this can be remedied by mixing the chemicals into low cost petroleum oils (Hunt et al, 1967). Preservatives made this way are known as organic solvents.

The earliest known occurrences of organic solvent preservatives were in the 1880's. Since then, many combinations of toxic chemicals and organic solvents have been developed (Richardson, 1993). The most widely used preservative of this type is pentachlorophenol (PCP). Advantages of using organic solvents include ease of

manufacture, high moisture resistance, and the ability to control chemical concentrations within the preservative solutions. It is also possible to achieve high penetration depths with organic solvent preservative treatments. Disadvantages associated with the use of organic solvents include their low resistance to insect attack, high volatility upon application to wood, and the low degree of chemical fixation within the wood. Despite their shortcomings, organic solvent preservatives experienced a period of rapid growth in the 1930's. During this decade, they found extensive use as a temporary replacement for tar oil preservatives, which had become scarce due to fuel conservation tactics implemented in 1930's US. The increased use of organic solvent preservatives continued until the 1960's, at which point water-borne preservatives began to dominate the wood preservative market.

1.1.4.3 Waterborne Preservatives

Waterborne preservatives are made by dissolving a mixture of inorganic ions into water. There are many advantages of using water as a solvent for wood preservative treatments. Water is cheap and widely available. It is able to penetrate into wood matrices deeper and more uniformly than most organic solvents. And relative to tar oils and organic solvents, there is a lower risk of combustion or explosion during the preservative treatment process.

Waterborne preservatives are usually made up of two or more of the following components: mercury, zinc, copper, arsenic, chromium, and ammonium. The most commonly used type of this preservative in the past fifty years has been CCA. CCA is inexpensive, highly effective, and poses negligible environmental risk when in service (Freeman, 2003). The main disadvantage of waterborne preservatives is the public

perception of CCA. Concern over arsenic exposure has caused the US government to withdraw CCA treated wood products from the residential market. As a result of this, several arsenic-free waterborne preservatives have been made available to the public to be used as alternatives. Three examples of these treatments are alkaline copper quat (ACQ), amine copper azole (CA), and copper bis-N-cyclohexyldiazeniumdioxy (Cu-HDO). While these alternatives are believed to be more environmentally friendly than CCA, they are less effective preservatives and approximately three times more expensive (Bricka, 2008).

A graph illustrating the amounts of creosote, PCP, and CCA products consumed annually in the US can be seen in Figure 1.1. A graph representing the increased production of CCA products in the US relative to the total production of preserved wood in the US can be seen in Figure 1.2.

1.1.5 Preservative Application Methods

Wood preservative formulations are applied to wood products by various methods. Some of the more common techniques are the brush and spray method, steeping (dipping), the hot and cold bath, vapor phase pressure treatment, and the liquid phase pressure treatment. In the case of CCA, liquid phase pressure treatment is the most commonly used application method.

All treatment methods make use of different levels of the following four factors that define the maximum attainable retention level of a preservative treatment in a particular wood species:

- Fluid Penetration
- Treatment Time

- Treatment Temperature
- Treatment Pressure

These factors will be elaborated upon in the following four sections.

1.1.5.1 Fluid Penetration

Liquid is absorbed into porous solids as a function of the surface tension of the liquid, the diameter of the solid pore, and the angle of contact along the solid-liquid interface of the pore. A rough sketch of a hydrophilic pore can be seen in Figure 1.3. The driving force that causes a liquid-based preservative to flow into pores is known as capillary force "*F*", and it is given by the following equation.

$$F = f\,\pi\, d\,\cos(\alpha) \tag{1.1}$$

where: "f" = surface tension associated with the two phase interface

"d" = pore diameter

"α" = contact angle

The pressure "*P*" developed by the capillary force is given by the following equation.

$$P = \frac{F}{\pi\, r^2} = \frac{4\, f\, \cos(\alpha)}{d} \tag{1.2}$$

where: "r" = pore radius

The pore penetration rate "*R*" is then given by substitution of equation (1.2) into Poiseuille's equation.

$$R = \frac{P \pi r^4}{8 \nu} = \frac{\pi d^3 f \cos(\alpha)}{32 \nu} \tag{1.3}$$

where: "ν" = the coefficient of viscosity of the preservative fluid

Equation 1.3 shows that the rate of penetration is largely influenced by pore diameter. The rate of penetration is also proportional to the surface tension at the solid-liquid interface and the cosine of the contact angle, both of which are associated with the wettability of the wood species. The rate of penetration is inversely proportional to the viscosity of the preservative fluid.

1.1.5.2 Treatment Time

The treatment time varies greatly between different application techniques. Selection of an efficient treatment time is an arduous process. First, the expected end use of the final product must be defined. Then the agents of deterioration that are of primary concern can be identified. Then a preservative formulation and a specific retention level are selected based upon the expected agents of deterioration that were identified. Finally, an application technique is chosen based on the ability of that technique to achieve the target retention level. The target retention level is the weight of preservative per unit volume of preserved wood product and it is typically reported in pounds per cubic foot.

Products that require high retention levels (ie 0.8-2.5 lb/ft^3), such as saltwater marine pilings and marine bulkheads, will typically need to be treated with a pressure treatment method to achieve the target retention level. Total treatment times in pressure processes can range from between 1 and 5 hours to several days depending on the physical properties of the wood species and the size and dimensions of the product.

Products that require smaller retention levels (ie less than 0.25 lb/ft^3), such as stint lumber or indoor furnishings, can be treated with an immersing process or a brush and spray method. Dipping and steeping are two examples of immersing processes. Dipping is a process where immersion time is about 10 to 15 minutes. Steeping is a process where immersion time is more than one hour. A general rule for brush and spray methods is that a conscientiously applied flood spray is equivalent to 10 to 15 minutes of immersion (Richardson, 1993).

1.1.5.3 Treatment Temperature

The effect of temperature on preservative treatment involves the distribution of heat over the liquid and solid phases present within the reaction zone. Sometimes it is better to have a heated preservative solution and sometimes it is better to have a heated wood surface. For example, when using oil-based preservatives, solutions that are heated prior to treatment will achieve higher retentions. This is due to the fact that shear interaction within the preservative fluid phase decreases as temperature increases (Hunt et al, 1967). Equation 1.3 shows that lower preservative solution viscosities are able to achieve higher pore penetration rates. The velocity profile depicted in Figure 1.4 helps to illustrate this point.

Increases in solution temperature have less of an effect on the overall treatment of wood products when water based solvents are used. This is because the temperature effect on the viscosity of water based solvents is less pronounced than it is for oil based solvents (Hunt et al, 1967). An important factor to consider when applying heat to water based solvents is that water based solvents do not retain heat as well as oil based solvents. Also, heat is not easily transferred between the wood phase and the preservative fluid

phase due to the low thermal conductivity of wood. This results in a high temperature gradient at the interface between the wood product and the preservative solution. Since water based solvents do not retain heat as effectively as oil based solvents, contacting the wood with heated water based preservative solution causes the solution to cool more quickly than it causes the wood to heat. A better utilization of heat in such a case would be to heat the wood prior to chemical treatment. By pre-heating the wood the contact angle within the wood phase is reduced and the pore diameter is expanded; which according to equation 1.3 would result in an increase in pore penetration rate.

1.1.5.4 Treatment Pressure

The use of pressure in treatment methods will typically result in a deeper and more uniform overall preservative treatment. Generally, softwoods respond to pressure treatment better than hardwoods because they have lower wood mass densities and higher porosities. This fact is supported by equation 1.3. Equation 1.3 shows that the pore penetration rate is proportional to the size of the average pore radius in the wood and the pressure developed by capillary force within that pore radius.

1.1.5.5 The Pressure Treatment Method

Most of the CCA products that are currently in service have been impregnated with CCA metals using a full cell pressure treatment method. In this method:

- a wood specimen is placed in a pressure vessel
- approximately ninety percent of atmospheric pressure is drawn from the vessel
- vacuum conditions are held for a period of time
- preservative solution is flooded into the vessel

- vacuum is released
- positive pressure is applied
- preservative is radially impregnated into the wood specimen

On average, a pressure of 7 to 14 atmospheres is maintained for a period of 1 to 5 hours during the positive pressurization stage. When dealing with a non-porous wood specimen, the positive pressure may have to be maintained on the vessel for several days for the desired retention level to be achieved (Hunt et al, 1967).

Once the target retention level is reached, the pressure on the vessel is released and the remaining preservative solution is allowed to drain. A final vacuum is pulled on the wood specimen to remove any remaining preservative solution and to relieve any residual compression stresses remaining in the wood after completion of the positive pressurization stage. Once the final vacuum stage is complete, vacuum is released and the treated specimens are removed from the vessel. A qualitative schematic example of a full cell pressure treatment pressure profile is shown in Figure 1.5.

When pressure-treating wood with water based preservatives, it is necessary to allow the final treated specimens to dry for an extended period of time. Setting the wood out to dry allows for any excess preservative solution remaining either on the exterior of the product to evaporate. After the product is dry, chemical fixation of preservative chemicals is considered to be complete and the product is ready for handling and shipping. A diagram illustrating the full cell pressure treatment process can be seen in Figure 1.6.

1.2 CCA Waste Regulations

1.2.1 CCA Disposal in the Past

The first large wave of CCA products was put into service in the 1970's. The separation of CCA materials from the bulk waste stream is not practiced because the waste containing CCA is not legally classified as hazardous, therefore CCA products are typically incinerated or landfilled along with other wood waste in the bulk waste stream.

In 1983, a report was published that traced symptoms of arsenic exposure to the incineration of CCA wood waste**.** Symptoms including loss of hair, severe recurring nosebleeds, extreme fatigue, debilitating headaches, blackouts followed by long periods of extreme disorientation, and violent seizures were observed in a Wisconsin family of eight that heated their home by burning scrap pieces of CCA wood in a stove (McMahon, 1985).

When CCA wood products are incinerated, toxic forms of CCA metals are released into the atmosphere and the concentration of CCA metals in the ash product increase dramatically (Table 1.1). The primary threat to humans is exposure to arsenic through inhalation. In CCA treated products arsenic is present primarily as arsenate (As^{+5}) and arsenite (As^{+3}). Both forms of arsenic are known carcinogens, however arsenate is perceived as less of a toxicity threat to humans because it is less mobile in the environment at atmospheric conditions. The suspected reaction scheme for the bulk volatization of arsenic during incineration is shown in equations 1.4 through 1.6 (Helsen, 2000).

$$4\,CrAsO_4 \cdot 6\,H_2O\,(s) \rightarrow 24\,H_2O\,(g) + 2\,Cr_2O_3\,(s) + 2\,As_2O_5\,(s) \qquad (1.4)$$

$$2\,As_2O_5\,(s) \rightarrow 2\,As_2O_3\,(l) + 2\,O_2\,(g) \quad (1.5)$$

$$2\,As_2O_3\,(l) \rightarrow As_4O_6\,(g) \quad (1.6)$$

It is important to note that this reaction scheme does not account for all of the arsenic contained in CCA wood waste. It is based on the assumption that the bulk of the arsenic in CCA wood waste is present at $CrAsO_4$ (Pizzi, 1982).

The mechanism for arsenic volatilization is the reduction of arsenate to arsenite. The degree to which arsenate is reduced depends on the combustion temperature and the burn time. In a study conducted by McMahon it was found that at 800 ^oC, the amount of arsenic volatized increased from 22 % to 44 % when combustion time was extended from 10 minutes to 60 minutes. Over 70 % of the arsenic contained in the CCA product was volatized when the temperature of the furnace was raised to 1000 ^oC for a period of 60 minutes (McMahon, 1985).

It is known that small amounts of preservative chemicals leach out of CCA products over the course of their service lives. Although research in this area has been extensive, the lack of standardization has made it difficult to compare the results from one study to another (Townsend, 2004). Nonetheless, a few trends in the in-service leaching of CCA products have been recognized. In general, arsenic and copper leach at higher rates than chromium (Kennedy et al, 2001), leaching rates of all CCA metals increases as the pH of the surrounding environment decreases (Cooper, 2001), and leaching rates of CCA metals are much higher in situations where the wood product is below ground or in contact with water (Hingston, 2001). Research conducted on the characteristics of metals leached from CCA products has shown the short-term environmental impact to be minimal (Lebow, 2002). In Lebow's study, slight increases in

the concentration of CCA contaminants were observed in the environment adjacent to CCA products that were in-service. However, the mobility of the contaminants through the adjacent soils was observed to be low. As a result, Lebow concluded that the overall environmental impact of the contaminants was negligible due to the poor environmental mobility of the contaminants.

1.2.2 Classifying CCA Waste

Solid wastes are labeled as hazardous if they exhibit one or more of the following characteristics: ignitability, corrosivity, reactivity, toxicity. Descriptions of the types of materials that apply to each of these categories and the waste characteristic qualification limits are published annually in the United States Code of Federal Regulations (40CFR261.20). Toxicity is the only waste characteristic that applies to CCA. The toxicity characteristic limit for chromium and arsenic is 5 ppm. Copper is not included in the list of toxicity characteristic metals; therefore a waste cannot be labeled as a TC hazardous waste due to the presence of copper in high concentrations.

When an individual CCA product is tested for toxicity, it will pass the TCLP test for toxicity due to chromium content but it will normally fail for toxicity due to arsenic content (Townsend, 2004). This only means that if CCA materials were separated from the bulk waste product before disposal, the concentrated CCA waste product would qualify as a TC hazardous waste. Since it is not common practice to screen waste for CCA products, CCA waste is disposed as a fraction of the overall waste stream. Most wastes containing only a fraction of CCA will not test positive for metal contamination and they will be placed into subtitle D landfills (Solo-Gabriele, 1999). In instances where the wastes fail the TCLP test due to arsenic contamination, the waste is excluded from

being labeled as hazardous because of an exemption in the US Code of Federal Regulations. Title 40, part 264.4b of the US Code of Federal Regulations excludes the following from the definition of a hazardous waste:

> Solid waste which consists of discarded aresenical-treated wood or wood products which fails the test for the Toxicity Characteristic for Hazardous Wastes Codes D004 through D017 and which is not a hazardous waste for any other reason if the waste is generated by persons who utilize the aresenical-treated wood or wood product for these materials' intended end use.

1.2.3 Restrictions Involving CCA

Recent research has demonstrated that the environmental risk associated with the volume of CCA wood waste being dumped into subtitle D landfills is minimal (Saxe, 2007). However, the environmental impact of continuing current disposal practices is unknown. For this reason, many nations and US state governments have placed restrictions on the production of CCA and use of products containing CCA. In 1994 the state of New Jersey restricted the use of CCA products in marine settings where shellfish are present. In 2002 the state of New York banned the use of CCA wood products in the construction of any new public or school playground. In 2003 a ban on the sale of CCA products to the general public was enforced in all nations belonging to the European Union (EU). The state of Maine followed suit in June 2003, banning the sale of CCA products to the general public. In 2004, the phase-out of CCA products that was jointly initiated in 2002 by the US EPA and the wood preservation industry concluded with a nationwide ban on the use of arsenical treated wood products in residential settings (Gezer, 2005). In 2005, the Australian Pesticide and Veterinarian Medical Authority

(PVMA) ruled that CCA products would begin to be phased out for use in playground equipment.

1.2.4 Expected Waste Stream

It has been estimated that the wood preservation industry annually produces 30 million cubic meters of treated wood worldwide. It has also been estimated that two thirds of treated wood contains CCA (Humphrey, 2002). The bans and restrictions involving CCA have reduced the volume of CCA products entering into service. However, CCA has been the most extensively used wood preservative in the world for the past 40 years. Because of this it is reasonable to expect the rate of CCA waste generation to remain relatively constant for another 20 to 30 years.

In the United States alone, it has been estimated that the amount of CCA treated wood being removed from service will increase to over 16 million cubic meters per year by 2020 (Humpherey, 2003). After 2020 it is expected that the rate of generation of CCA waste will be reduced because of the recent restrictions placed on the use of CCA products.

Since there will be such a large volume of CCA contaminated waste entering the waste stream over the next 20-30 years, and since the long term impact of this large volume of waste is unknown at this time the remediation of metals from CCA-treated products has become an important area of research. Several waste remediation methods for CCA contaminated waste are presented in the following sections of this report.

1.3 CCA Waste Treatment Alternatives

Researchers have examined many different CCA waste remediation methods. All of these alternatives exhibit advantages, disadvantages, and various degrees of waste minimization efficiency.

1.3.1 Reuse

Reuse of CCA contaminated wood waste is being implemented in an effort to decrease the volume of waste that is expected to be available for disposal within the next twenty years. Reuse is defined as using spent CCA products in different applications instead of disposing of the product. An example of reusing would be collecting pieces of CCA wood from a storm damaged patio or boat house and using them as a garden border or as fence material.

Since separating CCA wood from other wood waste is not practiced, it would be hard to implement reuse on an industrial scale. It is also known that CCA wood waste continuously leaches out small amounts of copper and arsenic, which must be considered before finding reuse applications for a particular product. Care must be taken to protect the environment from further exposure to the reused product. This can be done by re-finishing the surface of the product with paint or varnish or by placing of the product in covered areas where it will not be exposed to rainfall.

1.3.2 Composite Materials

A composite material is defined as a system composed of a mixture of two or more constituents that differ in chemical properties and composition. An example of a composite material including CCA would be a particleboard product laced with CCA

wood. Another example would be using CCA waste as a filling material in cement slabs. In both of these examples the final product is improved by taking on some of the preservative properties associated with CCA material, and the level of CCA exposure to the environment is reduced.

A drawback of using CCA waste in composite materials is that the end product becomes contaminated to a certain degree with CCA. Incorporation of CCA in composite materials is an effective way of temporarily reducing the volume of CCA wood waste. However, incorporation of CCA in composite materials does nothing to eliminate the toxicity hazard.

1.4 Extraction of CCA Metals

1.4.1 Chemical Extraction

Chemical extraction is a process by which a soluble fraction of a material is separated and removed from the material by an extractive media. To be effective the extractive media must be able to remove, isolate, and contain the soluble fraction.

Many chemical extraction methods are effective in removing high percentages of CCA metals from waste wood. Kazi obtained removal efficiencies of 85 % chromium, 98% copper, and 78% arsenic with aqueous extraction solutions of 2.5 % hydrogen peroxide at 90^{o} C for periods of 2 hours (Kazi, 2006). Comparable results have been achieved through the use of extraction solutions containing organic acids and/or ligands (Velizarova, 2004; Clausen, 2000; Cooper, 1991; Kanjo, 1994; Hingston et al, 2001; Gezer, 2006; Kartal et al, 2003). Supercritical fluids extractions modified with ligands have also achieved comparable removal efficiencies (El-Fatah, 2004; Takeshita, 2000). Kakitani developed a single step extraction technique using a pH-adjusted bioxalate

solution with a sodium hydroxide additive. This method was effective in extracting approximately 90 % of CCA metals from waste wood in under 6 hours at a solid waste to extraction fluid ratio of 1g : 20ml (Kakitani, 2006).

One drawback of chemical extraction methods is the capital investment. Chemicals, handling, and equipment for multistage processes all raise costs for chemical extraction techniques. Also, most chemical extraction methods are harsh on the wood components and have low metal selectivity. After the extraction process is complete, the structural and the thermodynamic value of the cleaned wood product has been reduced to the point that the remaining wood fraction is no longer of use. If a suitable chemical extraction method is going to be used for CCA waste treatment it will likely have to make use of the purified wood product as well as the extracted metals to be economically feasible.

1.4.2 Biological Extraction

Some biological agents are able to achieve fair metal removal efficiencies. Successful extractions have been achieved by fermenting CCA sawdust in a bacterial media identified as Bacillus licheniformis. Copper, chromium, and arsenic removal efficiencies of 93%, 6%, and 45% were observed in the experiments (Clausen, 1997).

An advantage of biological extraction is that it can be carried out in relatively mild conditions. In addition, it also has a higher metal selectivity than chemical extractions. Disadvantages include the added cost of supporting the microorganisms and the slow rates at which the extractions proceed relative to chemical extractions.

For biological extraction to remain competitive as a CCA remediation method, it is likely that it will have to be paired with another remediation technique. Some research

has been done in this area already. For example, through the combination of acid extraction with oxalic acid and subsequent bacterial fermentation of CCA wood waste with Bacillus licheniformis, Clausen was able to achieve copper, chromium, and arsenic removal efficiencies of 99%, 79%, and 100% (Clausen, 1998). Another combination method that might be worth investigating is the combination of electrokinetic remediation with biological extraction. The passage of current through a bed of combined CCA waste and biological agents might be able to support the biological media by supplying heat and oxygen through electrokinetic transport while at the same time facilitating the remediation of CCA metals from the base waste product.

1.4.3 Thermal Methods

1.4.3.1 Low Temperature Pyrolysis

Pyrolysis is defined as the partial combustion of a feedstock under oxygen free conditions. In a pyrolytic reaction a feed material is converted into three products: gas, oil, and char. Advantages of pyrolysing CCA wood waste include the reduction of waste volume and decreased production of oxidized species. Researchers consider decreased production of oxidized species a huge advantage since oxidation is known to cause arsenic volatilization at temperatures below 200^{o} C (Helsen, 2000). A disadvantage of using pyrolysis as a CCA remediation technique is the fact that the char product is even more heavily contaminated with CCA metals than the original waste product. This is a particular concern with arsenic, which is present in pyrolysis residues as mobile arsenites (Ottosen, 2005). For pyrolysis to become a viable CCA remediation technique, researchers must demonstrate that they can control arsenic emissions during the pyrolysis

process and either recover or effectively contain the metals remaining in the post pyrolysis char product.

1.4.3.2 High Temperature Gasification

Gasification is similar to pyrolysis except in gasification processes: a small amount of oxygen is used, temperatures are higher, and the feedstocks are converted completely into syngas and char. Also, much of the char generated during gasification reactions is further broken down into hydrogen gas, carbon monoxide, and various other volatile compounds at temperatures greater than 1100 ^{o}C. A disadvantage of using gasification as a CCA remediation technique is the emission of arsenic vapors. Also, a higher energy investment is required in order to maintain the high temperatures necessary for gasification.

1.5 Electrokinetic Remediation

In electrokinetic (EK) remediation, an electric field is created by surrounding a wetted material with electrodes and then applying a low voltage direct current across the electrodes surrounding the material. The electric field causes ions in the wetted material to be mobilized and migrate towards the electrodes.

Advantages of EK relative to the alternative extraction methods presented in Section1.4 include: the limited use of solvents, the limited use of temperature manipulations, and the limited use of pressure manipulations. EK parameters such as current density and potential difference are also relatively easy to measure and manipulate. Different driving forces are responsible for the movement of ions in EK remediation. These phenomena are electroosmosis, electrophoresis, streaming potential,

electromigration, diffusion, and sedimentation potential. These phenomena are discussed in the following paragraphs.

1.5.1 Electroosmosis

Electroosmosis is defined as the transport of pore fluid from a material as a result of the application of an electric field. The mechanism of electroosmotic flow is not fully understood at this time. Many theories have been developed over the years (Mitchell, 1976). The most widely accepted of these theories is known as the Hemholtz-Smoluchowski (HS) Theory, which is described in the following paragraphs.

A particle surface has a net charge. When the particle is submerged in a conductive media then the surface attracts a layer of oppositely charged ions. Once the surface has been neutralized, a randomly arranged diffuse layer of ions will cover the ion layer. Then an even larger dissociated layer of ions will form outside of the diffuse layer. Figure 1.7 illustrates this arrangement of ions relative to a negatively charged particle surface. This arrangement of ions is known as the ionic double layer theory.

In the presence of an electric field, the ion layer will remain fixed on the surface. The diffuse layer, although it is comprised of a random arrangement of ions, has a net charge opposite of the charge on the adjacent ion layer. The net charge of the diffuse layer causes a net flux of the diffuse layer of ions towards the electrode of opposite charge. The net flux of the diffuse layer of ions displaces pore fluid in the same direction. Electroosmosis is the flow of pore fluid towards an electrode induced by the application of an electrical field across a solid particle.

According to the HS Theory, the bulk electroosmotic velocity can be approximated by the following equation.

$$U_{EO} = \frac{\varepsilon \xi E}{\mu} \tag{1.7}$$

where:

U_{EO} = Electroosmotic Velocity $\left(\frac{cm^2}{volt \cdot \sec} \right)$

ε = Permittivity of the Solution $\left(\frac{amp \cdot \sec}{volt \cdot cm} \right)$

ξ = Zeta Potential $(volt)$

E = negative Gradient of Electric Potential $\left(\frac{volt}{cm} \right)$

μ = Solution Viscosity $\left(\frac{gram}{cm \cdot \sec} \right)$

1.5.2 Electrophoresis

The same forces that cause the electroosmotic phenomenon also cause the electrophoretic phenomenon. The ionic double layer existing around solid particles causes a net flow of ions and pore fluid towards the electrode of opposite charge, but in electrophoresis the solid particle itself is induced to migrate towards an electrode of opposite charge along with the diffuse ion layer pore fluid solution. Electrophoresis is typically observed in situations where loosely packed, highly permeable solid particles are suspended in a fluid medium.

1.5.3 Streaming Potential

Streaming potential is an electrokinetic phenomenon caused by the flow of fluid through a porous medium induced by a pressure gradient. The fluid flow induced by the

pressure gradient displaces ions from their stable positions in the ionic double layer arrangement. The displacement of ions causes a charge imbalance to exist across the porous medium. The result is an overall electrical potential difference (or streaming potential) across the porous medium.

1.5.4 Electromigration

Electromigration is the transport of ions under the influence of an electric field. Inducing an electric potential difference across a solution containing ions causes the ions to migrate through the medium. In general, anions migrate towards the anode and are oxidized and cations migrate toward the cathode and are reduced. The effective ionic mobility is an estimation of how fast an ionic species will migrate towards its respective electrode. It can be approximated using the following equation.

$$U^* = \frac{D^* Z F}{R T} \tag{1.8}$$

where:

U^* = Effective Ionic Mobility $\left(\frac{cm^2}{volt \cdot \sec}\right)$

D^* = Effective Diffusion Coefficient $\left(\frac{cm^2}{\sec}\right)$

Z = Ionic Valence $\left(\pm e^-\right)$

F = Faradays Constant $\left(coulombs\right)$

R = Universal Gas Constant $\left(\frac{joule}{kelvin \cdot mole}\right)$

T = Absolute Temperature $(kelvin)$

The effective diffusion coefficient is given by the following equation.

$$D^* = D\,\tau\,\eta \tag{1.9}$$

where:

D = Ionic Diffusion Coefficient at infinite dilution $\left(\frac{cm^2}{\sec}\right)$

τ = Tortuosity of the medium

η = Porosity of the medium

1.5.5 Ionic Diffusion

Ionic diffusion is the migration of ions from regions of higher concentrations to regions of lower concentrations. The diffusive molar flux of a chemical species is expressed by Fick's Law.

$$J = -D^* \frac{d(c)}{dx} \tag{1.10}$$

where:

J = Molar Flux $\left(\frac{mole}{cm^2 \cdot \sec}\right)$

D^* = Effective Diffusion Coefficient $\left(\frac{cm^2}{\sec}\right)$

c = concentration at some point x $\left(\frac{mole}{cm^3}\right)$

x = distance (cm)

1.5.6 Sedimentation Potential

In sedimentation potential, the movement of charged solid particles through a conductive medium results in an electric potential difference across the conductive medium. The movement of the particle causes ions in the diffuse layer of the ionic double layer surrounding the particle to be displaced from their equilibrium positions. The charged solid particle gains a dipole moment as a result of the departure from equilibrium. The net effect of collective dipole moments across the conductive medium is known as the sedimentation potential.

1.5.7 Water Electrolysis

Applying direct current across a wetted medium results in the transport of water toward electrodes. Reactions of water at electrode interfaces result in the breaking of the water molecules. Water reacting with the anode is oxidized and produces oxygen gas and hydrogen ions (equation 1.11). Water reacting with the cathode is reduced and produces hydrogen gas and hydroxyl ions (equation 1.12).

$$2H_2O \rightarrow O_2(g) + 4H^+ + 4e^- \tag{1.11}$$

$$2\ H_2O + 2e^- \rightarrow H_2(g) + 2OH^- \tag{1.12}$$

The type of reaction that occurs at an electrode surface depends upon the availability of chemical species and the electrochemical potential of the reactions at the interfaces. Water electrolysis accounts for only a fraction of the reactions occurring at electrode interfaces in electrochemical cells. The overall rate at which ions are produced at electrodes can be approximated using Faradays Law of Equivalence of mass and charge (1.13).

$$J = \left(\frac{I}{Z F} \right) \tag{1.13}$$

where:

J = molar flux of ions $\left(\frac{moles}{cm^2 \cdot \sec} \right)$

I = current density $\left(\frac{amps}{cm^2} \right)$

Z = Ionic Valence $\left(\pm e^- \right)$

F = Faradays Constant $\left(coulombs \right)$

1.5.8 Adsorption and Desorption Reactions

Adsorption is generally defined as the formation of a layer of gas, liquid, or solid on a surface. Adsorption can be classified as either chemisorption or physisorption. In chemisorption molecules form chemical bonds to surfaces. In physisorption molecules form ionic bonds to surfaces.

Desorption is the opposite of adsorption. It is defined as the process of removing sorbed materials from a surface. Generally, chemisorbed molecules are more difficult to desorb than physisorbed molecules. Desorption usually takes place in extreme pH environments.

The ability of a particular surface to adsorb or desorb materials is dependant upon the conditions surrounding the surface. If a surface has a net positive charge, then absorption is defined as the attraction of anions to the surface. The point of zero charge (PZC) of a surface is the point at which the positive charge of the surface is completely neutralized by the sorption of anions onto the surface. The pH of the solution at the point

of zero charge controls the charge of the particle being adsorbed. If the pH of the solution is less than the PZC-pH, then adsorption of anions is favored. If the pH of the solution is more than the PZC-pH, then adsorption of cations is favored.

1.6 Research Objectives

1.6.1 Overview

A scientist named Reuss first observed electoosmotic flow in the early 1800's. Since then electrokinetic theory and technology has been developed to the degree that the possibility of using electric current to remove charged contaminants from porous media is beginning to be considered as a commercially viable remediation technique. Many experiments have been performed that have been successful in applying electrochemical technology to contaminated samples. Recent research has demonstrated effective removal of charged contaminants from large volumes of saturated soils through in-situ electrokinetic remediation. Successful remediation of soils has lead to further research of electrokinetics as a possible remediation technique for other contaminated media.

1.6.2 Goals of the Study

Public concerns over the safe disposal of CCA contaminated wastes have provided another research opportunity in the area of electrokinetic remediation. Presently in the US, large amounts of CCA waste are being disposed of in subtitle D landfills. Although risks associated with this practice are considered to be minimal at this juncture, the long term ramifications of continuing this disposal practice at the current rate are unknown. This research is an attempt to evaluate the possibility of using EK and base

oxidizers to remove chromium, copper, and arsenic from waste wood containing CCA prior to disposal of the materials by conventional means (incineration or landfilling).

1.6.3 Levels of Parameters Examined in this Study

These experiments were designed to compare metal remediation efficiencies different with respect to the parameters of particle size and oxidative pre-treatment. Three levels of particle size were examined at two levels of oxidative treatment in duplicates for a total of 12 experiments. This research will hopefully provide some insights into EK remediation as well as answers to the following questions:

1. What mass percentage removals are attainable using EK to remove arsenic, chromium, and copper from CCA contaminated wood samples?
2. What effect, if any, does particle size/alignment have on the EK removal efficiency of CCA metals from contaminated wood waste?
3. Does oxidative pre-treatment with base oxidizing chemicals increase the removal efficiency or rate of removal of CCA metals from contaminated wood waste?
4. Is the fraction of arsenic, chromium, and copper that is remaining in the post-treated wood more or less environmentally mobile than the arsenic, chromium, and copper contained in the initial sample?
5. Are arsenic, chromium, and copper ions more likely to behave as anions or cations in EK condtions?
6. At what rates are arsenic, chromium, and copper removed from the CCA contaminated wood samples?
7. How much power is consumed during the experimental runs?

8. Were any of the treatment levels examined in this study more effective at removing CoC selectively as a function of EK power used? (EK power specifically, not total power)
9. Are there any anomalies in the chemical environment during EK experimental runs (ie pH spikes, Eh spikes, etc) that correspond to increased removal CCA removal rates?

Table 1.1 Comparison of the concentrations of CoC contained in unburned CCA wood and CCA wood ash (Solo-Gabriele, 1999)

	Concentration	
	unburned	**CCA**
Metal	CCA wood	ash
Arsenic	1,200 ppm	33,000 ppm
Chromium	2,100 ppm	16,000 ppm
Copper	1,100 ppm	22,000 ppm

Table 1.2 Different classes of lined landfills

Liner	**Regulation**	**Wastes**
type	level	Accepted
single	State	construction and demolition debris (C&DD), including concrete, asphalt, shingles, wood, bricks, and glass
composite (subtitle D)	Federal	non-hazardous municipal solid wastes from residential, commercial, and industrial sources
double (subtitle C)	Federal	hazardous wastes that are, or once were, classified as either ignitable, toxic, reactive, or corrosive

Table 1.3 Six main characteristics of an effective wood preservative

1	The preservative must be toxic to wood deterioration agents.
2	The preservative must be effective in penetrating deep into the wood product.
3	The preservative must remain fixed within the wood structure for an extended period of time.
4	The preservative must be relatively harmless to wood.
5	The different components used to preserve the wood product must be readily available.
6	There must be a cheap and environmentally safe method of producing the preservative.

Table 1.4 Categories of organic compounds found in tar oil preservatives

Category	Percentage	Some Examples
tar acids	< 5%	phenol, cresol, xylenol, napthol
tar bases	< 5%	pyridine, quinoline, acridine
hydrocarbons	> 90%	napthalene, fluorene, anthracene, phenanthrene

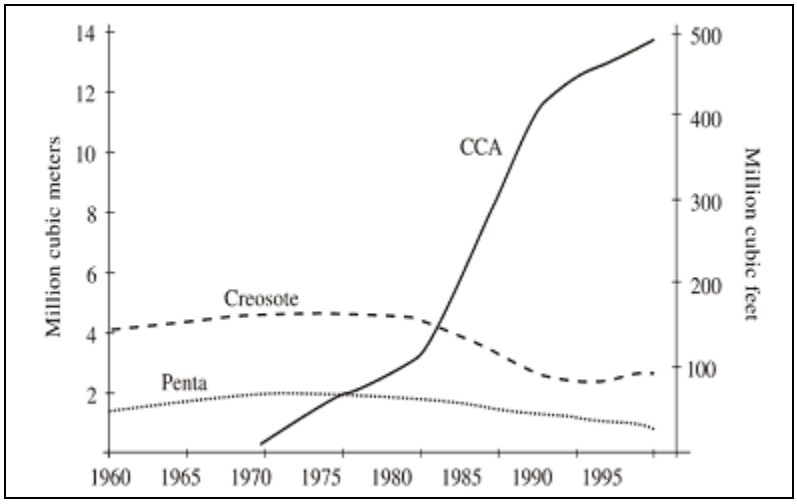

Figure 1.1 Annual consumption of CCA, creosote, and pentachlorophenol in the US from 1960-1996 (Felton, de Groot 1996)

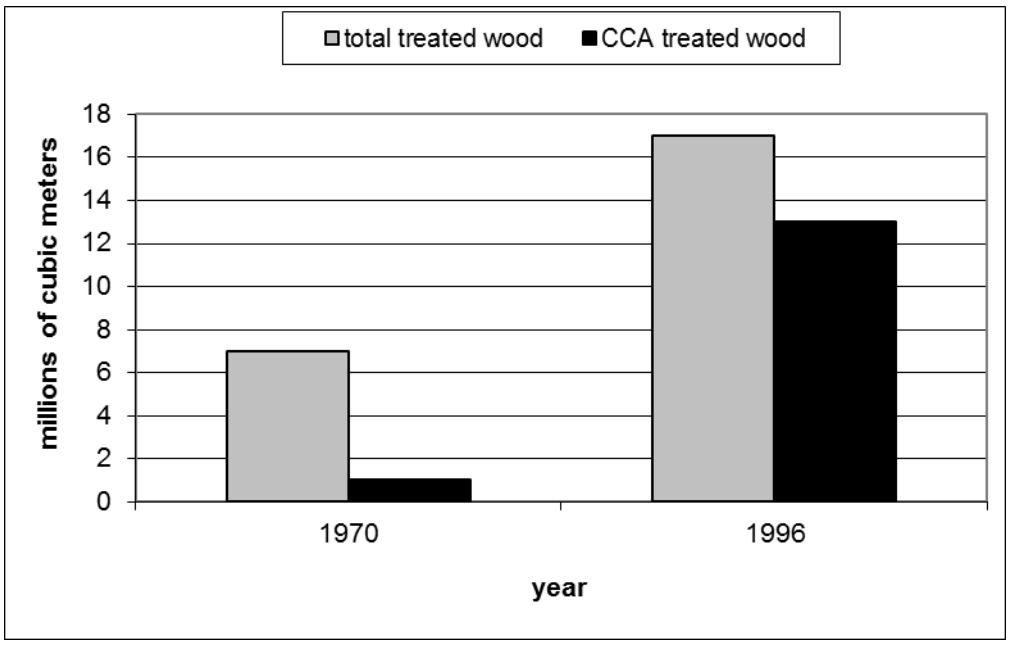

Figure 1.2 The increased production of CCA treated wood relative to the total production of preserved wood in the US (Solo-Gabriele, Townsend 1999)

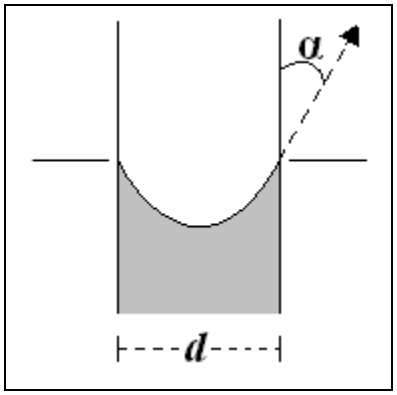

Figure 1.3 Sketch of a hydrophilic pore where the shaded area represents air, and the unshaded area represents treatment solution

"α" represents the water contact angle of the hydrophilic pore
"d" represents the diameter of the hydrophilic pore

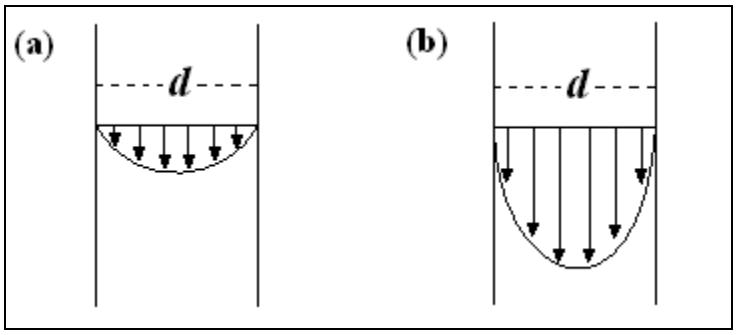

Figure 1.4 Pore velocity flow profile of a high viscosity fluid (a) and a low viscosity fluid (b)

"d" represents pore diameter

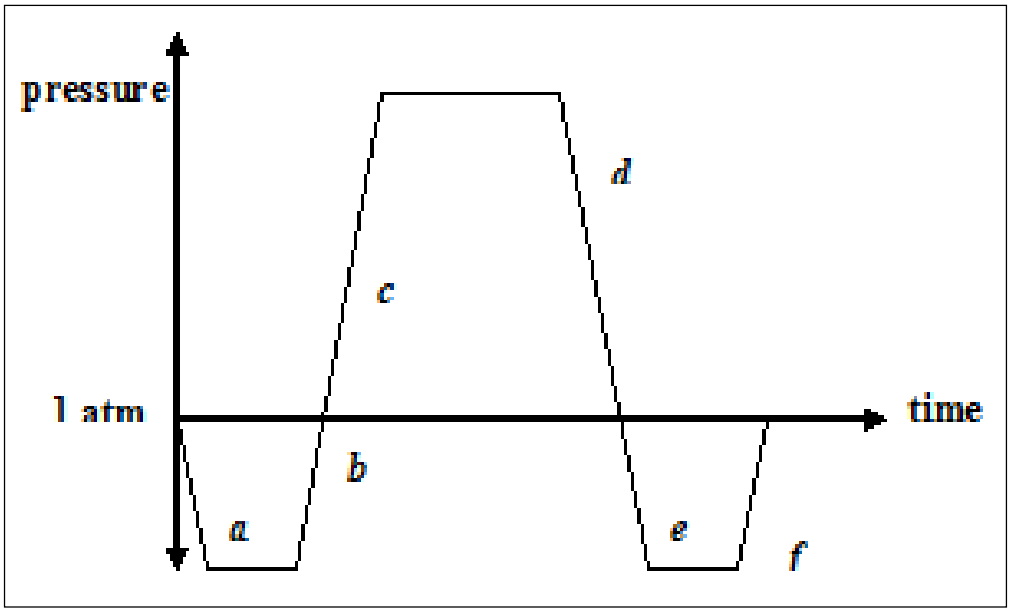

Figure 1.5 Pressure profile for a full cell pressure treatment process

"a" represents the preliminary vacuum period
"b" represents the flooding of the pressure vessel
"c" represents pressurization period
"d" represents the draining of the pressure vessel
"e" represents the vacuum period
"f" represents the release of vacuum

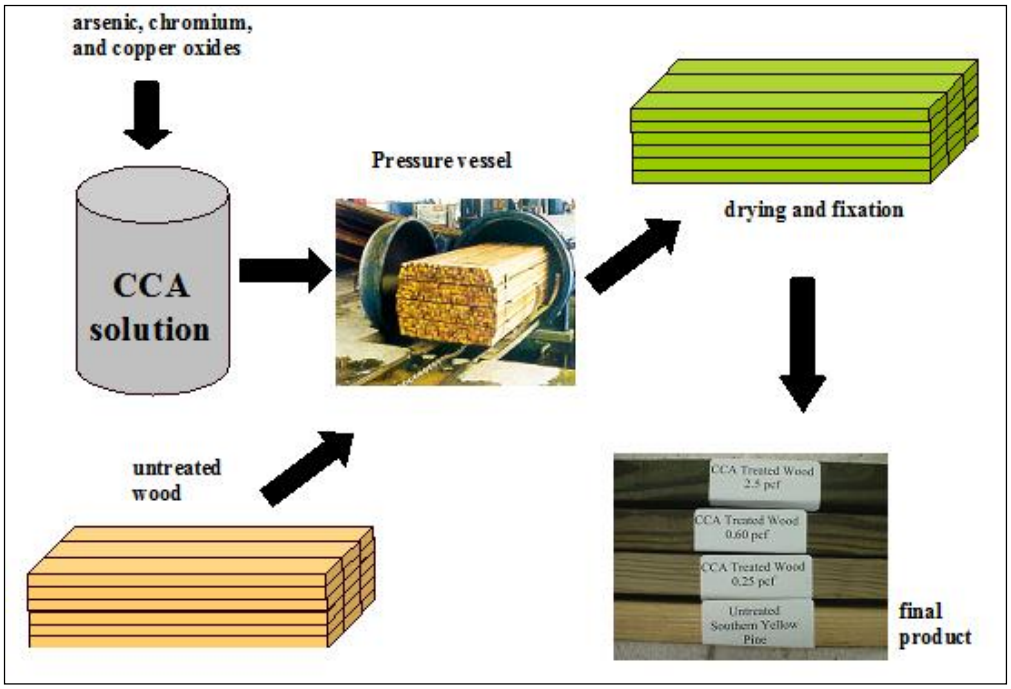

Figure 1.6 Diagram of the full cell pressure treatment method

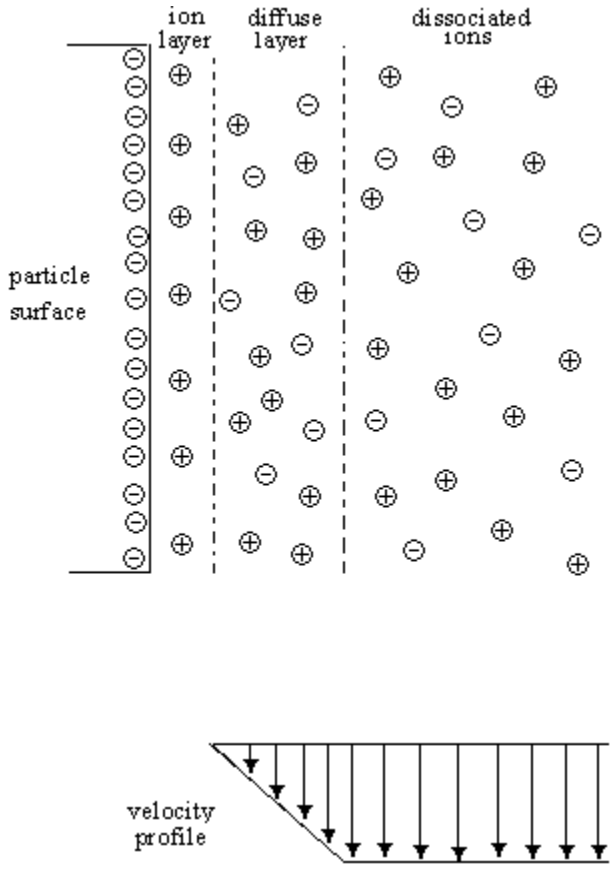

Figure 1.7 Schematic representation of ionic layers relative to a negatively charged surface including an offset velocity profile

CHAPTER II

LITERATURE REVIEW

2.1 Brief Overview of the Discovery of Electrokinetics

The first known observation of EK phenomena was recorded in 1809 by a German scientist named Ferdinand F. Reuss. Reuss was studying the effects of electrolysis on the speed of gas emissions from the electrodes of a simple battery when he observed what would come to be called electroosmosis. For Reuss' experiment he buried several simple batteries in the ground at different locations along a river in Moscow. Reuss chose the location of each battery based on the condition of the soil at the site because he theorized that the speed of the emission of the electrolytically produced gases would be affected by the differences in the electrical resistance produced by soils with different characteristics. During the experiments, Reuss observed that there was a net migration of water towards the cathodic electrodes of his batteries. This observation became the basis that a number of 19th century scientists would build upon to form the basic theories of electrochemistry; which would lead to the development of the ion double layer theory by a scientist named Herman von Hemholtz in 1879. His basic ion double layer theory would be refined through work done by Louis Georges Gouy, David Chapman, Otto Stern (and others) to eventually become the mathematical basis by which contemporary EK theory is based.

The capacity of EK to move ionic contaminants through saturated porous media will be the area of focus for this research. This capacity has already been proven on large scales with soils that have been contaminated with heavy metals; and this success with soil remediation has improved the possibility of using similar techniques to remediate other contaminated media (waste wood in the case of this research). The following sections provide a summary of the research conducted in the area of the EK remediation of CCA wood waste.

2.2 Laboratory Scale Investigations

Several studies have been conducted in the area of EK remediation of CCA wood waste. Different types of experimental setups and techniques have been used; and most of them have produced different levels of success. Contaminants of concern (CoC) are defined as chromium, copper, and/or arsenic containing ions. An overview of the parameters utilized in each of the studies summarized in section 2.2 is provided in Table 2.1.

2.2.1 Ribeiro, 2000

These experiments were performed using an EK experimental unit that was developed at the Technical University of Denmark (TUD) in 1992. A rough sketch of the unit is provided in Figure 2.1. The unit is described in detail in theses of Riberio (1998) and Ottosen (1995) which are both cited in the References section of this report; and an overview of the parameters utilized in this particular study is provided in Table 2.1.

Prior to placing sawdust (CCA dust particles sized < 20 mm mesh in diameter) in the central compartment of the EK cell the sawdust was saturated in solutions of

deionized water, 2.5 % oxalic acid, 5.0 % oxalic acid, and 7.5 % oxalic acid (all solution strengths are reported on a weight basis). The saturated sawdust was then placed in the central compartment of a TUD EK cell and a constant current of 0.2 mA/cm^2 was applied to the sawdust for a period of 30 days. Data reported in this study includes the voltage drop between working electrodes over the course of the experiment, the mass of CoC collected in the catholyte and anolyte solutions, the overall CoC removal efficiency, and the distribution of CoC across the TUD EK cell at the conclusion of the experiment.

The level of voltage drop between working electrodes for each experimental condition was inversely proportional to the solution strength of the oxalic acid applied prior to loading the sawdust into the TUD EK cell (ie: sawdust treated with the stronger solutions of oxalic acid experienced lower voltage drops). Ribeiro's explanation for this was that additional ions were added to the sawdust during the oxalic acid treatments:

- Due to the dissociation of the oxalic acid into ions
- Due to a number of non-CoC ions being mobilized into solution on account of the acidity of the oxalic acid solution

The availability of additional ions in the center compartment of the TUD EK cell caused a decrease in the overall resistance of the cell and contributed to a lower overall voltage drop across the TUD EK cell. It was also noted that the possibility of an increased number non-CoC ions being mobilized into solution may have resulted in a lower overall current yield; but that the increase in overall removal of CoC more than compensated for the perceived loss in overall current yield.

Regarding the overall CoC removal efficiencies, it was found that for the experiment where the sawdust was saturated with deionized water, over 90 % of the

copper contained in the sawdust was removed using EK alone. The results of the CoC mass accumulation analysis of the catholyte and anolyte suggest that copper electromigrated almost exclusively as a cation in the deionized water experiment. Copper, however, was the only CoC that responded favorably to the deionized water treatment. Only 26.7 % of the arsenic was removed during this experiment (primarily as an anion according to the mass balance information) and no chromium was removed.

It was found that by saturating sawdust in oxalic acid prior to treatment in the DUT EK cell, the overall removal efficiency of arsenic and chromium could be improved drastically. The removal efficiency of arsenic increased from 26.7% in the deionized water treatment to 98.7 % in the 2.5 % oxalic acid treatment; and the removal efficiency of chromium increased from 0% in the deionized water treatment to 94.8 % in the 2.5 % oxalic acid treatment. Both arsenic and chromium were removed primarily as anions during the 2.5 % oxalic acid experiment and secondarily as cations. According to the results of the mass accumulation analysis of CoC's in the catholyte and anolyte both arsenic and chromium accumulated in the anolyte very rapidly over the first 10-15 days of the EK experiment. After this initial period there was no observable increase in the amount of arsenic or chromium in the anolyte. According to the same analysis both arsenic and chromium accumulated in the catholyte at a very slow rate for the entire 30 day EK test period duration.

To explain the increase in arsenic removal as an anion in the 2.5% oxalic acid experiment Ribeiro referenced previous research (Ribeiro 1998) and concluded that arsenic was removed primarily as an anion in this situation because arsenic containing species that are stable as anionic complexes at pH levels of 4-8. To explain the increase

in chromium removal as an anion in the 2.5% oxalic acid experiment Ribeiro referenced previous research done by herself and others (Ribeiro 1998; Charlet 1992; and Bartlett 1988) and concluded that chromium was removed primarily as an anion in this situation because:

- Chromium III is known specifically to form the stable anionic complex $CrOx^{3-}$ in the presence of oxalate and that this complex would migrate toward the anode when exposed to EK conditions
- Chromate can be reduced in the presence of oxalate under acidic conditions to form various reduced oxalate complexes that migrate toward the anode when exposed to EK conditions

The removal efficiency of copper increased only slightly from 91.4 % to 93.1 % during the 2.5 % oxalic acid experiment. It is interesting to note that there was a noticeable change in the mechanism of copper removal for the 2.5% oxalic acid experiment. In the deionized water experiment copper was removed exclusively as a cation. In the 2.5% oxalic acid experiment copper still behaved primarily as a cation, but approximately 30% of the copper removed was removed in an anionic form. According to the results of the mass accumulation analysis of CoC's in the catholyte and anolyte copper accumulated primarily in the anolyte over the first 10-15 days of the experiment; but after approximately 7 days the copper began to accumulate overwhelmingly in the catholyte. To explain this observation Ribeiro referenced previous research done by others (Martell 1964; Stephan 1996) and concluded that the initial removal of copper as an anion was driven by a combination of:

- the reaction of copper with oxalates to form anionic complexes that would migrate toward the anode under the influence of EK conditions
- simultaneous reaction of copper with oxalate to form copper oxalate, which will not electromigrate to either electrode because it has a limited level of solubility in water

Riberio then theorizes that once all of the free oxalic acid in the central compartment becomes spent then the copper remaining in the central compartment will be in the form of immobile copper oxalate that is in equilibrium with an excess of copper cations and some oxalate anions. When this condition is encountered in the central compartment of the DUT EK cell there will be a net removal of copper with the copper migrating primarily as a cation towards the cathode. In the final summary of this paper Ribeiro reported the max removal efficiency of CoC for the 2.5 % oxalic acid treatment to be successful in removing 93 % of copper, 95 % of chromium, and 99 % of arsenic when subjected to the electrodialytic process examined in this study.

2.2.2 Velizarova, 2004

Velizarova builds upon previous research (Ribeiro, 2000) by further examining the effects of different extracting solutions on the EK remediation of CCA wood waste. In previous research it was observed that the CoC removal efficiency, the overall ionic flux across the DUT EK cell, and the removal of CoC towards the anode were all improved by soaking the waste wood in an extracting solution containing oxalic acid prior to EK treatment. Velizarova theorizes that the increase in CoC removal efficiency towards the anodes of the DUT EK cell and the overall increase in ionic flux across the DUT EK cell are not related. It is difficult to directly associate the increase in CoC

removal efficiency towards the anode with higher degrees of ionic flux across the DUT EK cell because it is possible that some of the organic acid present in the extracting solutions is dissociating into organic ions and electromigrating towards the anode without forming complexes with metal cations. Velizarova tests this theory by treating CCA contaminated wood chips with several different extracting solutions (including some extracting solutions that do not form metal complexes) prior to treating the wood chips electrokinetically. The effects of those solutions on the voltage drop experienced across the DUT EK cell, the removal rates of copper and chromium, and the net direction of flux of the copper and chromium ions are reported in this paper. The effects of the different solutions on arsenic were not reported in this paper. The experiments were performed using an EK experimental unit that was developed at the Technical University of Denmark (TUD) in 1992 (Figure 2.1).

Prior to placing wood chips in the central compartment of the EK cell the wood chips were saturated in solutions of deionized water, 2.5 % oxalic acid, 5.0 % formic acid, a mixture containing 2.5 % oxalic acid and 5.0 % formic acid, 2.5 % EDTA disodium salt, and 1.5 % sodium chloride (all solution strengths are reported on a weight basis) for a period of 24 hours. The saturated wood chips were then placed in the central compartment of a TUD EK cell and a direct current was applied to the wood chips for a period of 14 days. In addition to the applied current experiments; three experiments were run dialytically (no current applied across the electrodes of the TUD EK cell) to serve as a basis for comparison to the EK experiments. The saturation solutions for the three experiments that were run dialytically were the deionized water, 2.5% oxalic acid, and the mixture containing 2.5 % oxalic acid and 5.0 % formic acid.

In the experiment where the wood chips were saturated in deionized water prior to being treated electrokinetically the initial voltage drop across the DUT EK cell was approximately 82 volts. Over the course of the experiment the voltage drop stayed relatively consistent, reaching a peak of approximately 87 volts at the end of the first day and then gradually dropping back down to a voltage drop of 84 volts by the end of the experiment. This trend is an indication of high electrical resistance across the DUT EK cell throughout the experiment which is consistent with previous research where wood chips were saturated with deionized water prior to being treated electrokinetically (Ribeiro, 2000). The following observations were also consistent with previous research:

- no evidence of copper or chromium migration towards the anode
- evidence of copper migration towards the cathode
- compared to the other pre-EK saturation solution treatments the removal efficiencies for copper and chromium were the lowest observed

Velizarova suggests that this is due to the low conductivity of deionized water as well as the poor potential for deionzied water to effectively solubilize ions within the CCA contaminated wood medium being treated electrokinetically.

For all of the other pre-EK saturation solutions however, a voltage drop of approximately 20 volts was observed between the working electrodes of the DUT EK cell initially, followed by a rapid asymptotic increase in voltage drop to an upper limit. The rate of increase in voltage drop and the level at which each of the voltage drop plateaus is different for each pre-EK saturation solution. A high rate of increase in voltage drop is an indication that the level of availability of charged particles in the center compartment of the DUT EK cell is decreasing (ie: EK cell is losing ability to electromigrate ions); and a

high upper limit of voltage drop is an indication that there is a high level of resistance between the working electrodes in DUT EK cell once the EK process reaches equilibrium (ie: the higher the upper limit, the lesser the chance of electromigrating ions within the EK cell). The ranking of the rate of the increase in voltage drop between working electrodes from the initial condition at the start of the EK experiment until upper limit of voltage drop experienced during the EK experiment from fastest to slowest is as follows:

NaCl > EDTA > formic acid > oxalic acid > oxalic/formic acid mixture

The ranking of the upper limit level of voltage drop experienced for each pre-EK saturation solution from highest to lowest is as follows:

NaCl > oxalic/formic acid mixture > oxalic acid > EDTA > formic acid

In the case of the NaCl pre-EK saturation solution the rate at which the EK experiment reaches equilibrium is the most rapid and the level of resistance across the EK cell once the equilibrium condition is reached is the highest. Velizrova theorizes that the reason for this is that the NaCl dissociates into ions in the DUT EK cell center compartment and migrates towards the electrodes as individual ions without forming complexes with other available free ions. The EK process is then forced to oxidize water at the anode and reduce water at the cathode with no contribution from electromigration or electroosmosis. The result is an EK experiment that rapidly reaches an equilibrium with a high resistance across the DUT EK cell center compartment due to electrodes producing an excess of ions locally instead of electromigrating ions from the center compartment towards the working electrodes.

A strong dependence was observed between the pre-EK saturation solution used and the anolytic/catholytic concentration profiles for copper and chromium. The ranking

of the accumulation of chromium in the anolytic half of the TUD EK cell from highest concentration to lowest concentration was as follows:

oxalic/formic acid mixture > oxalic acid > formic acid > EDTA > NaCl

The ranking of the accumulation of chromium in the catholytic half of the TUD EK cell from highest concentration to lowest concentration was as follows:

formic acid > oxalic acid > oxalic/formic acid mixture > EDTA > NaCl

The ranking of the accumulation of copper in the anolytic half of the TUD EK cell from highest concentration to lowest concentration was as follows:

EDTA > oxalic acid > oxalic/formic acid mixture > formic acid > NaCl

The ranking of the accumulation of copper in the catholytic half of the TUD EK cell from highest concentration to lowest concentration was as follows:

NaCl > oxalic acid > oxalic/formic acid mixture > formic acid > EDTA

Velizarova made the following observations regarding the effects of different pre-EK saturation solutions on the direction of chromium and copper removal:

- copper has a strong tendency to migrate towards the cathode while chromium is relatively unaffected when either deionized water or NaCl is used as the pre-EK saturation solution
- no one organic acid pre-EK saturation solution outperformed another because each of the organic acids react with the wood chips to form different complexes with unique shapes as well as different overall charges
- the EDTA pre-EK saturation solution was extremely effective at mobilizing copper towards the anode during EK treatment, however EDTA was less

effective at mobilizing chromium to the anode during EK treatment than oxalic and/or formic acids

Regarding the overall removal efficiency of copper and chromium, Velizarova observed that oxalic acid was most effective at solubilizing copper and chromium and extracting the target metals in some ionic form via the combination of chemical extraction followed by electrokinetic treatment. Velizarova also observed that similar overall removal efficiencies were attainable with the mixture of oxalic acid and formic acid.

2.2.3 Velizarova, 2002

The initial applied current is another parameter that has been investigated as to its effect on the EK remediation of CCA waste (Velizarova, 2002). In this study CCA wood chips were incubated in a solution containing 2.5 % oxalic acid for 24 hours prior to being treated electrokinetically. The wood chips that were incubated in oxalic acid were loaded into a DUT EK cell and the initial current was varied at levels of zero milliamperes (mA), 40 mA, 60 mA, and 120 mA in four separate experiments. To serve as an experimental control, wood chips were also incubated in a solution of deionized water prior to being treated electrokinetically in a fifth experiment. The control experiment was subjected to an initial applied current of only 11.6 mA because that was the maximum current that could be applied to the EK cell with the power supplies used in the study. These experiments were performed using an EK experimental unit that was developed at the Technical University of Denmark (TUD) in 1992 (Figure 2.1).

The experimental results were analyzed according to three different methods in this study. First the current applied to the wood chips in the EK experiments was

monitored on a daily basis to confirm trends in the drop in applied current as the experiments progressed. Second, the initial accumulation rate (IAR) of each CoC was calculated by taking the change in concentration of CoC in either the anolyte or the catholyte over the first 24 hours of the EK experiment and simply dividing the change in concentration by 24 hours. And finally the overall removal efficiency for each CoC was evaluated at the end of the experiment to confirm whether or not the initial applied current had an effect.

Regarding the effects of initial applied current on the EK system; for the experiments where the wood chips were treated with oxalic acid prior to EK treatment and an external power supply was used the results showed that the higher the initial applied current across the DUT EK cell, the faster the current drops to a level of equilibrium. Velizarova attributes this to the rapid depletion of available charged particles in the center compartment of the DUT EK cell. This is consistent with EK theory states that ion velocities are proportional to the electric field strength under EK condtions (ie: decrease in availability of charged particles causes an increase in the resistance across the DUT EK cell which results in a decrease in the ability of the DUT EK cell to support a large electrical current across the electrodes of the DUT EK cell).

For the experiment where the wood chips were treated with de-ionized water prior to EK treatment, the TUD EK cell could not achieve an initial applied current of more than 11.6 mA. Velizarova attributes this to the lower availability of charged particles in the center compartment of the EK cell at the start of the experiment. Velizarova interprets this as evidence of the role of the oxalic acid solution as assisting agents for the initial mobilization of contaminates.

In general it was observed that for all of the CoC's in experiments where the wood chips were treated with oxalic acid prior to EK treatment, the IAR in the anolyte was greater than the IAR in the catholyte. Velizarova attributes this to the initial availability of charged particles as negatively charged oxalate complexes formed during the oxalic acid treatment period prior to EK treatment.

The IAR of copper in the anolyte are greater than the IAR of copper in the catholyte for all of the experiments except for the experiment where deionized water was used as the EK pre-treatment solution. This trend requires some explanation since copper is typically stable as a cation under acidic, water wetted conditions and would therefore be expected to migrate toward the cathode. Velizarova theorizes that the migration of copper as an anion is primarily due to the formation of negatively charged copper oxalates during the EK pre-treatment period. A secondary cause of the anionic migration of copper might be the occurrence of unknown dissolution and precipitation processes that occur while copper is migrating through the TUD EK center compartment. The affinity of copper to react with larger negatively charged organic compounds and to form negatively charged ionic complexes with arsenic and chromium could also cause copper to migrate towards the anolyte as a part of a larger negatively charged complex. Regardless of the explanation, the trend of copper migrating towards the anode instead of the cathode as when oxalic acid is used as the EK pre-treatment solution is consistent with research done by others (Ribeiro, 2000). The highest copper IAR's were observed in the experiment where wood chips were treated with oxalic acid prior to EK treatment with the initial current set a 40 mA. The copper IAR's for all other experiments were significantly lower. Since the relationship between IAR and starting current level is non-

linear, the results suggest that the mechanism for copper migration under EK conditions is complex and cannot be controlled by simply varying the level of initial applied current.

The anionic and cationic IAR's for chromium in the experiment where deionized water was used as the EK pre-treatment solution were non-existent in this study. This demonstrates that the fixation mechanism for chromium in CCA treated wood is much stronger than the fixation mechanisms for copper or arsenic. The fixation mechanism for chromium is so strong that some form chemical pretreatment is necessary to begin the solubilization of chromium ions from CCA treated wood. The highest chromium IAR's in the anolyte were observed in the experiment where wood chips were treated with oxalic acid prior to EK treatment with the initial current set a 40 mA. No clear relationship between chromium IAR's in the anolyte and the amount of initial current applied could be observed because the chromium IAR's in the anolyte were significantly lowere for all experiments other than the experiment where wood chips were treated with oxalic acid prior to EK treatment. The chromium IAR's in the catholyte however showed a clear relationship to the amount of initial current applied. Chromium IAR's in the catholyte increased as the amount of initial current applied to the DUT EK cell increased. Velizarova proposed a three part explanation for these observations:

- treatment with oxalic acid prior to EK treatment was necessary to solubilize chromium to a degree where EK treatment could effectively mobilize it towards the electrodes
- the concentration of chromium in the anolyte when higher initial applied currents were used decreased/slowed due to the fact that negatively charged chromium oxalate complexes became trapped in the the anion exchange

membrane; and those trapped complexes were not allowed to concentrate in the anolyte

- the concentration of chromium in the catholyte actually increases as a function of increasing applied currents; the authors theorize that this is due to the fact that positively charged chromium oxalate complexes become the dominant chromium containing species as the initial applied current is increased and that they are mobilized towards the catholyte by EK more quickly and easily than the negatively charged chromium oxalate complexes

The IAR's of arsenic in the anolyte are consistently an order of magnitude higher than the IAR's of all other CoC's in all of the experimental conditions examined in this study including the experiment run under dialytic (no external power supply) conditions. Velizarova attributes this to the faster solubilization of arsenic when oxalic acid is used as the EK pre-treatment solution and the ability of applied current to mobilize arsenic in the form of acidized arsenic ($H_2AsO_4^-$) at the pH's experienced in the center compartment of the TUD EK cell.

It was observed that with respect to overall removal efficiency, copper was the CoC most strongly influenced by the application of electric current. Net removal of copper improved from approximately 48 % when no initial current was applied to approximately 82 % when an initial current of 40 mA was applied. Chromium and arsenic were more strongly affected by the application of pre-EK oxalic acid treatments than by the level of initial applied current. This trend is most evident in the case of chromium, where the net removal jumped from approximately 1 % when deionized water was used as the pre-EK treatment solution to approximately 72 % in the experiment

where a 2.5% solution of oxalic acid was used as the EK pre-treatment solution and no external power source was used. Increasing the initial applied current from 40 mA to levels of 60 and 120 mA proved to have little effect on the net removal of any CoC over the 14 day EK experimental period used in this study.

2.2.4 Virkutyte, 2004

The position of contaminated CCA material relative to working electrodes in an EK cell is another parameter that has been investigated as to its effect on the EK remediation of CCA waste (Virkutyte, 2004). In this study CCA wood chips were incubated in a solution containing 2.5 % oxalic acid for 36 hours prior to being treated electrokinetically. The wood chips were loaded into a DUT EK cell in three different contamination zone arrangements:

- pre-treated wood chips were loaded in the EK center compartment, adjacent to the anodic half cell
- pre-treated wood chips were loaded in the EK center compartment, in the relative center of the center compartment
- pre-treated wood chips were loaded in the EK center compartment, adjacent to the cathodic half cell

In each of the experimental units the remaining volume of the center compartment was filled with non-CCA treated sawdust that had not been incubated in an oxalic acid solution. These experiments were performed using an EK experimental unit that was developed at the Technical University of Denmark (TUD) in 1992 (Figure 2.1). A DC current of 40mA was then applied to the wood chips for a period of 14 days. At the conclusion of each experiment, the center compartment of the EK cell was sliced into

five sections and analyzed for copper and chromium separately (the effect of the experimental program on arsenic was not reported in this study). Results of the analyses confirmed that the placement of contaminated zones relative to the working electrodes did affect the mechanism by which copper and chromium were removed.

It was observed that when the contaminated zone was located adjacent to the anode, solubilized copper behaved primarily an anion and migrated towards the anode. Some migration toward the cathode was also observed; however the small amount of copper that did migrate toward the cathode was found to be equally present in the catholyte and precipitated into the filler sawdust. Virkutyte attributes the anionic migration of copper primarily to the formation of negatively charged copper oxalate species that were generated during the incubation period with oxalic acid. Virkutyte also allows that the placement of contaminated media on the more acidic side of the TUD EK cell may have encouraged the increased desorbtion of copper from the wood matrix into a mobile cationic form. Virkutyte suggests that although the cationic copper was migrating toward the cathode, the decreasing acidity of the environment in the EK center compartment caused most of the cationic copper to precipitate out of solution as copper hydroxides. It should be noted that a large amount of the copper was found to remain in the contaminated zone adjacent to the anode after the conclusion of the experiment.

When the contaminated zone was located in the center of the TUD EK cell center compartment a large concentration of copper remained accumulated in the middle of the TUD EK cell center compartment, indicating that insoluble and immobile copper species prevail in the middle of the center compartment. The copper that was solubilized behaved equally as a cation and as an anion. Virkutyte theorizes that the anionic migration of

copper towards the anion is solely due to the presence of copper oxalates and the availability of free oxalic acid at the start of the experiment. Once the free oxalic acid species are spent the predominant solubilized copper species are free copper cations that migrate toward the cathode.

It was observed that when the contaminated zone was located adjacent to the cathode, solubilized copper behaved almost exclusively a cation and migrated towards the cathode. According to Virkutyte the conditions of the EK cell adjacent to the cathode are favorable for the formation of copper hydroxides and free copper cations. The mechanism for copper mobilization towards the cathode is a combination of the electromigration of free copper cations and the movement of desorbed yet non-precipiated copper complexes toward the cathode induced by electroosmotic flow.

It was observed that when the contaminated zone was located either adjacent to the anode or in the center of the TUD EK cell center compartment, solubilized chromium behaved almost exclusively as anion and migrated towards the anode. Virkutyte cites previous research to indicate that the dominant form of chromium under the conditions of these experiments is hexavalent chromium (Cr^{6+}) which is known to form soluble and mobile anionic chromium complexes. A relatively small amount of chromium was mobilized towards the cathode in both of these experiments as well. Virkutyte attributes this to the formation of positively charged chromium (Cr^{3+}) complexes and free chromium ions.

It was observed that when the contaminated zone was located adjacent to the cathode, solubilized chromium still behaved almost exclusively as anion and migrated towards the anode. However, a significant amount of chromium remained fixated to the

wood chips in the contaminated zone in this case. Virkutyte theorizes that the mechanism of chromium mobilization is similar to the other cases examined in this study; but that more chromium remains fixated to the wood chips in the contaminated zone because the precipitation of chromium (III) containing complexes is encouraged in the pH and Eh environment experienced in that section of the TUD EK cell.

In summary, for this study the behavior of chromium remained consistent regardless of the placement of the contaminated zone relative to the TUD EK cell electrodes, with chromium ions being removed from CCA wood primarily as anions with a very small concentration of chromium beign removed as cations. Copper removal, however, was highly affected by its placement relative to electrodes. The cation to anion ratio of extracted copper was observed to increase exponentially as the proximity of the contaminated zone to the cathode increased.

2.2.5 Isosaari, 2010

In this research the effect of performing chemical extractions and EK treatments in alternating sequences was investigated for its effect on the overall removal of CoC. Two basic experiments are performed in this research. For chemical extractions 350 grams of dry CCA contaminated wood chips were put into a container with a 0.8 % solution of oxalic acid at a solid:liquid ratio of 1:8. The contents of the containers were mixed for 6 hours by tumbling them end over end at a rate of 70 rpm. For the EK treatments approximately 350 grams of dry wood chips were packed into a dense mesh bag and placed in an EK cell center compartment with dimensions of 150 mm long, 150 mm wide, and 95 mm tall. An initial potential difference of 30 volts was applied to the wood chips for a period of 7 days. These two experiments were performed as stand-alone

tests to serve as experimental controls and then they were performed in alternating succession (ie: a chemical extraction treatment followed by an EK treatment; an EK treatment followed by a chemical extraction treatment; a chemical extraction treatment followed by an EK treatment then followed by an additional chemical extraction; etc).

Regarding the overall removal efficiency of copper it was found that EK treatment alone was a more effective treatment than chemical extractions or any combination of EK treatment and chemical extraction. The highest removal efficiency for copper was 91 % in this study and was encountered when the CCA contaminated sample was subjected to a series of 2 EK treatments in succession. Isosaari attributes this to the formation of Cu^{2+} ions in conditions of low pH and with an oxidizing environment Oxalic acid hampers copper removal during the EK treatment because it induces a reducing environment in the center compartment of the EK cell. Isosaari also suggests that as long as the pH stays below 10 and the center compartment of the EK cell remains as an oxidizing environment, divalent copper cations will be the dominant copper species and will migrate towards the cathode.

Regarding the overall removal efficiency of chromium it was found that EK treatment alone was an ineffective treatment, and that chemical extraction is required to solubilize chromium to a point where EK treatment can be even marginally effective in removing chromium. The highest removal efficiency for chromium was 68 % in this study and was encountered when the CCA contaminated sample was subjected to a chemical extraction and an EK treatment in series. Isosaari attributes this to the formation of cationic complexes containing chromium in conditions of low pH and with reducing environment induced by the presence of oxalic acid in the EK cell center compartment.

Isosaari goes on to suggest that as the pH rises to above 3, chromium precipitates begin to form and neutrally charged complexes containing chromium begin to prevail. Isosaari concluded that to improve chromium removal a stronger oxalic acid extracting solution would have to be used prior to any EK treatment and that the duration of the EK treatment would have to be controlled to ensure that a low pH and a reducing environment is maintained in the center compartment of the EK cell.

Regarding the overall removal efficiency of arsenic it was found that arsenic behaves similarly to chromium. While EK treatment alone was effective in removing a small amount of arsenic (~ 15 %), chemical extraction helped to solubilize arsenic to a point where the effect of a subsequent EK treatment was greatly enhanced (~ 78 %). The highest removal efficiency for arsenic was 81 % in this study and was encountered when the CCA contaminated sample was subjected to a chemical extraction, an EK treatment, then another chemical extraction in series. It should be noted that the final extraction did not add much value to the overall process, only removing an additional 3 % of the arsenic. Isosaari attributes the mobility of arsenic towards the anodic half cell solely to the formation of anionic complexes containing arsenic in a relatively neutral pH environment. Isosaari goes on to suggest that increasing the solution strength of the chemical extraction step might impede the electromigration of arsenic to the anode if it effectively lowers the pH of the EK cell center compartment to less than 2.

The best overall sequence for removing CoC was found to be the three step chemical extraction/EK treatment/chemical extraction sequence; which yielded removal efficiencies of 67 % for copper, 64 % for chromium, and 81 % for arsenic.

2.3 Pilot Scale Investigations

Successful CoC removal efficiencies at the laboratory scale have influenced researchers to examine the effectiveness of CCA EK remediation on a larger scale. In the laboratory scale investigations EK extractions were performed over a small sample volume. The volume of the center compartment in the laboratory scale investigations were approximately 252 cm^3 (16 in^3) in all of the studies summarized in Section 2.2. Also, neither the electrode spacing nor the mass of sample treated per experiment was reported. In the studies listed below, the effects of sample size, average particle size of sample, pre-EK extraction solutions, and electrode spacing on EK remediation of CCA waste are examined. An overview of the parameters used in these studies is provided in Table 2.2.

2.3.1 Pedersen, 2005

In this study the effects of electode spacing and different pre-EK soaking solutions on the EK remediation of CCA wood waste were examined on a pilot scale. The center compartment of the EK pilot plant used in this study was approximately 3.5 meters long, 1 meter wide, 1 meter high, and capable of treating up to 250 kilograms of CCA contaminated wood in a single experiment. Six different experimental conditions were examined in this study. The conditions of each of the six overall experiments are listed in Table 2.2 as the first 6 items in the table. Due to the size of the EK pilot plant collection units (CU) were placed at intermediate locations along the length of the center compartment of the EK pilot plant. A collection unit is a 'flow-through' apparatus used to collect ions at intermediate points along the length of the reactor. It is a small tank designed with an anion exchange membrane facing the cathode and a cation exchange

membrane facing the anode. Each collection unit allows ions of opposite charge into the collection unit and prevents the flow of similarly charged ions out of the unit. The function of the collecting units was to shorten the distance that the ions have to travel before they are removed from the wood-containing compartments.

Electrode spacing in this study ranged from 60 cm to 150 cm. The average mass of contaminated chips placed into 60 cm EK cell was 100 kilograms. The mass of contaminated chips placed into the 150 cm EK cell was 248 kilograms. Comparison of experiments #3 and #6 shows that increasing the electrode spacing from 60 cm to 150 cm causes a 28 % decrease in the removal efficiency of copper and a 25 % decrease in the removal efficiency of chromium. The removal efficiency of arsenic was unaffected by the increase in electrode spacing. Over 95 % of arsenic was removed from the contaminated media in both experiments. The authors attributed the decrease in chromium and copper removal to the pre-EK soaking of wood chips. In previous laboratory scale studies, soaking solutions had been reused up to four times without any negative effects on CoC removal. That trend was not observed in this pilot-scale study. In this study, the pre-EK soaking solution was reused three times in experiment #6. The average CoC removal during pre-EK soaking dropped from 58 % in experiment #3 to 25 % in experiment #6. The authors theorized that the decrease in pre-EK CoC removal was encountered due to the large amount of wood being treated in experiment #6. Essentially, they believe that the liquid phase became saturated with ions during the pre-EK soaking phase and this caused a reduction of the effectiveness of the pre-EK soak and resulted in a lower overall removal of chromium and copper.

The effect of soaking solutions prior to EK treatment can be observed by comparing the results of experiments #1 and #3. In experiment #1, wood chips were soaked in a 5.0 % solution of oxalic acid prior to EK treatment. In experiment #3, wood chips were soaked in a dual 5.0 % oxalic acid, 0.5 molar phosphoric acid solution prior to EK treatment. The addition of phosphoric acid to the soaking solution caused pre-EK copper removal to increase from 20 % to 66 %. It also resulted in an increase in the pre-EK chromium removal from 41 % to 58 %. The effect on pre-EK arsenic removal was not reported.

The most effective treatment examined in this study was experiment # 3. In experiment # 3 approximately 100 kilograms of CCA contaminated waste was subjected to a pre-soak with 0.5 molar H_3PO_4; and then followed by another pre-soak in 5.0 % (by weight) oxalic acid. The pre-soaked material was then placed in the EK pilot plant where the electrode spacing was approximately 60 cm; and a direct current of 2-5 amps was applied to the material for a period of 3 weeks. The overall removal efficiency for copper was 88%. The overall removal efficiency for chromium was 82 %. The overall removal efficiency for arsenic was > 96 %.

2.3.2 Sarahney, 2005

In this research the following three tasks were addressed in series:

1. evaluate oxalic acid, citric acid, ascorbic acid, EDTA, or any combination of these chemicals for their effectiveness in leaching CoC in a batch chemical extraction experimental setup
2. conduct EK experiments using distilled water as the process solution as an experimental control

3. conduct an EK experiment using the most effective extraction solution from task 1 as the process solution

The chemical extraction experiments were performed by adding contaminated wood samples to bottles containing approximately 150 mL of extracting solution and tumbling the bottles for a total of 96 hours. The EK experiments were performed using an experimental unit that was constructed out of acrylic material. It is comprised of a center compartment, anodic half cell, and cathodic half cell that are sized as follows:

- center compartment – 40 cm long, 5 cm wide, 14 cm high acrylic box
- anodic half cell and cathodic half cell – 35 cm long, 10 cm wide, 14 cm high

The center compartment was separated from the anodic and cathodic half cells by a synthetic, non-reactive permeable plate. The electrodes used were 14 cm by 14 cm graphite plates and were powered by an external source. No recirculation was used in these experiments. A rough sketch of the unit is provided in Figure 2.2.

First the ability of acidic solutions to extract CoC from CCA wood chips was evaluated. The chemicals used in these experiments were oxalic acid, citric acid, Ethylenedinitrilotetraacetic acid (EDTA), and ascorbic acid. This task was divided into two phases.

In the first phase of task one, the extraction efficiencies of single acid solutions were examined. In these experiments CoC were chemically extracted from contaminated wood samples in a two stage, 96 hour process. Wood chips were placed in a bottle with 150 milliliters of an extraction agent at a 2.5 % (by volume) solution strength and tumbled end over end for a period of 48 hours. After the first 48 hours the extraction fluid was separated from the solid phase to be analyzed for CoC. Then the bottle was refilled

with 150 milliliters of the same extraction agent at a 5.0 % (by volume) solution strength and tumbled end over end for another 48 hours. After the first 48 hours the extraction fluid was separated from the solid phase to be analyzed for CoC.

Sarahney found that the solutions made with oxalic acid were the most effective for extracting chromium and arsenic with a 68 % and a 76 % extraction efficiency over a period of 96 hours. The extraction of copper with solutions of oxalic acid after 96 hours, however, was less than 50 %. Solutions containing EDTA were found to be the most effective for copper extraction, removing 86 % of the copper but failing to remove more than 5 % of chromium.

In the second phase of task one, extraction of CoC with different combinations of the extractive chemicals examined in the first phase of task one was evaluated. The extractions were carried out over a period of 96 hours without changing the extraction fluid. Of the extraction solutions examined in phase two, the most efficient removal efficiency for all three CoC was observed with the '5 % oxalic acid + 2.5% EDTA' solution. This solution was able to remove arsenic, copper, and chromium at levels of 99 %, 95%, and 35%. It should be noted that although the '5 % oxalic acid + 2.5% EDTA' solution was identified as being the most effective combination of extractive chemicals in this study, the extraction efficiency achieved by combining extractive solutions was only marginally improved. The combination of different individual extractive solutions into a mixed solution does not result in an additive effect on the overall extraction efficiency of CoC for the solutions examined in this study.

The second task involved EK extraction of CoC from CCA wood using distilled water as the process solution. The contaminated CCA sample was subjected to EK

conditions for a period of 14 days (additional EK experimental parameters included in Table 2.1). Sarahney observed that after 14 days of EK treatment, 32 % of arsenic, 8% of chromium, and 29 % of copper were recovered. Copper was observed to accumulate overwhelmingly in the cathodic half cell. Arsenic was observed to accumulate overwhelmingly in the anodic half cell. And chromium was observed to accumulate in both the anodic and cathodic half cells with slightly more chromium accumulating in the anodic half cell.

The third task involved EK extraction of CoC from CCA wood using a solution of '5 % oxalic acid + 2.5% EDTA' as the process solution. The contaminated CCA sample was subjected to EK conditions for a period of 21 days (additional EK experimental parameters included in Table 2.1). Sarahney observed that after 21days of EK treatment, 88 % of arsenic, 74% of chromium, and 97 % of copper were recovered. Unlike the control experiment all CoC's including copper were observed to accumulate overwhelmingly in the anodic half cell. Sarahney attributes this to the reaction of CoC with oxalic acid and EDTA under the acidic conditions that were observed to be within the center compartment of the EK cell ($2.5 < pH < 3.8$). Sarahney proposed that mechanisms by which the CoC were mobilized towards the anode were similar to the mechanisms indicated in previous research. The only major difference was that Sarahney attributed the solubilization and mobilization of copper as anions to copper-containing species reacting with oxalic acid and to copper-containing species reacting with EDTA. It was also observed that the recovery rate for arsenic in the anodic half cell was much slower than the recovery rate of copper and chromium in the anodic half cell for the first 14 days of the experiment. After 14 days however, the recovery rate of arsenic in the

anodic half cell increased rapidly. Sarahney attributes this to the fact that arsenic complexes are single valent and therefore they electromigrate at a fraction of the speed of copper and chromium species, which are divalent and trivalent.

2.3.3 Christensen, 2006

Christensen studied the effect of wood particle size on the EK remediation of CCA wood in pilot scale. Christensen conducted one experiment using the same experimental setup as Pederson (Pederson, 2005). Conditions of the experiment are included in Table 2.2. Christensen used the data from Pederson's experiments as a basis for comparison.

To examine the effect of particle size, the contaminated sample was chipped and then sieved into three separate fractions. The fraction of wood that was less than 2 cm was designated as the fine fraction, the fraction of wood greater than 2 cm and less than 4 cm was designated as the medium fraction, and the fraction of wood greater than 4 cm was designated as the large fraction. All three fractions were homogenized into a single sample and electrokinetically treated in a single EK experiment.

At the conclusion of the experiment, the three wood fractions were re-separated, and analyzed for chromium and copper content. It was found that the final concentration of both chromium and copper in the fine fraction was significantly lower than that of the medium and large fractions. Christensen concluded that the pre-soak and EK treatment was more effective for the fine fraction; and that the effect of particle size on removal of copper and chromium at the medium and large fractions was negligible. The effect of particle size on the pre-soak and EK remediation of arsenic was not reported. Christensen attributes the decrease in copper and chromium removal efficiencies at higher particle

sizes to insufficient wetting of the cores of the larger wood chips during the pre-soak and EK remediation processes.

Table 2.1 Summary of laboratory scale EK experimental conditions

author, date	central compart. Dim.	Electrode material & dim.	Electrode spacing	pre-EK extraction solution/ duration	process solution	pH ; pH control fluid	sample weight, sample size	current, current density	EK duration	maximum removal efficiency
Ribeiro, 2000	L = 3 cm ID = 8 cm	platinized titanium bars; L = 5 cm D = 3 mm	NR	DI water; 2.5 % OA; 5.0 % OA; 7.5 % OA/ NR	0.1 M $NaNO_3$	2.0; conc. HNO_3	NR; sawdust < 0.085 mm	0.2 mA/cm^2	30 days	Cu: 93% Cr: 95% As: 99%
Velizarova, 2002	L = 3 cm ID = 8 cm	platinized titanium bars; L = 5 cm D = 3 mm	NR	DI water; 2.5% OA/ NR	0.1 M $NaNO_3$	3.0; conc. HNO_3	NR; chips L=10-15mm W=2-10mm D=1mm thick	0 mA 40 mA 60 mA 120 mA	14 days	Cu: 84% Cr: 87% As: 95%
Velizarova, 2004	L = 3 cm ID = 8 cm	platinized titanium bars; L = 5 cm D = 3 mm	NR	DI water; 1.25 % NaCl; 2.5 % OA; 5.0 % FA; 2.5%OA+5.0%FA; 2.5 % EDTA/ 24 hours	0.1 M $NaNO_3$	3.0; conc. HNO_3	NR; chips L=10-15mm W=2-10mm 1mm thick	40 mA	14 days	Cu: 80.5% Cr: 87.4% As: NR
Virkutyke, 2004	L = 5 cm ID = 8 cm	platinized titanium bars; L = 5 cm D = 3 mm	NR	2.5 % OA/ 36 hours	0.1 M $NaNO_3$	2.0; 1 M HNO_3	NR; chips (size NR)	40 mA	14 days	Cu: 93% Cr: 95% As: 99%

Table 2.1 continued.

author, date	central compart. Dim.	Electrode material & dim.	Electrode spacing	pre-EK extraction solution/ duration	process solution	pH ; pH control fluid	sample weight, sample size	current, current density	EK duration	maximum removal efficiency
Isosaari, 2010	L = 150 mm W= 150 mm H= 95 mm	Plat coated titanium dioxide mesh; 40 cm^2	NR	0.8% OA	Ion exchange water	2.1-2.8; NA	3-7 mm; chips	30 V	7 days	Cu: 67% Cr: 64% As: 78%
Isosaari, 2010	L = 150 mm W= 150 mm H= 95 mm	Plat coated titanium dioxide mesh; 40 cm^2	NR	NA	Ion exchange water	2.5-11; NA	3-7 mm; chips	30 V	7 days	Cu: 57% Cr: 0% As: 17 %

Table 2.2 Pilot scale EK experimental conditions

author, date	central compart. dim.	electrode material; dim.	electrode spacing / CU	pre-EK extraction solution/duration	process solution	pH; pH control fluid	sample weight, sample size	current, voltage	EK duration	removal efficiency
Pedersen, 2005	L = 3.5 m W = 1m H = 1m	platinized titanium bars; L = 1m D = 3 mm	60 cm / 1	5 % OA / 48 hours	water	2.0; conc. HNO_3	94 kg medium fraction	1.4-2A, 24-25V	11 days	Cu: 57% Cr: 66% As: >85%
Pedersen, 2005	L = 3.5 m W = 1m H = 1m	platinized titanium bars; L = 1m D = 3 mm	60 cm / 0	5 % OA / 48 hours	water	2.0; conc. HNO_3	106 kg medium fraction	2A, 14-18V	11 days	Cu: 34% Cr: 66% As: >85%
Pedersen, 2005	L = 3.5 m W = 1m H = 1m	platinized titanium bars; L = 1m D = 3 mm	60 cm / 1	0.5 M H_3PO_4 / 18 hours 5 % OA / 24 hours	water	2.0; conc. HNO_3	97 kg medium fraction	2-5A, 30-58V	21 days	Cu: 88% Cr: 82% As: >96%
Pedersen, 2005	L = 3.5 m W = 1m H = 1m	platinized titanium bars; L = 1m D = 3 mm	60 cm / 1	no pre-EK extraction	5 % OA	2.0; conc. HNO_3	99 kg medium fraction	0.2-3A, 14-60V	15 days	Cu: 13% Cr: 65% As: NR

Table 2.2 continued

author, date	central compart. dim.	electrode material; dim.	electrode spacing / CU	pre-EK extraction solution/duration	process solution	pH; pH control fluid	sample weight, sample size	current, voltage	EK duration	removal efficiency
Pedersen, 2005	L = 3.5 m W = 1m H = 1m	platinized titanium bars; L = 1m D = 3 mm	90 cm / 2	0.5 M H_3PO_4 / 18 hours 5 % OA / 24 hours	water	2.0; conc. HNO_3	178 kg combo. fine, medium, and large fractions	2-3A, 23-29V	15 days	Cu: 77% Cr: 56% As: NR
Pedersen, 2005	L = 3.5 m W = 1m H = 1m	platinized titanium bars; L = 1m D = 3 mm	150 cm / 4	0.5 M H_3PO_4 / 18 hours 5 % OA / 24 hours	water	2.0; conc. HNO_3	248 kg, medium fraction	2-3A, 40-63V	21 days	Cu: 60% Cr: 57% As: >96%
Sarahney, 2004	L = 40 cm W = 5 cm H = 15 cm	Graphite plates; L = 14 cm W = NR H = 14 cm	NR	no pre-EK extraction	5% OA + 2.5% EDTA solution	2.5-3.8; conc. HNO_3	Weight NR, chips L = 5 cm W = 0.3 cm H = 10cm	9-20 mA, 40-120 V	21 days	Cu: 97% Cr: 74% As: 88%
Sarahney, 2004	L = 40 cm W = 5 cm H = 15 cm	Graphite plates; L = 14 cm W = NR H = 14 cm	NR	no pre-EK extraction	Distilled water	2.8-9.9; NA	Weight NR, chips L = 5 cm W = 0.3 cm H = 10cm	0.2-0.26 mA/cm^2	14 days	Cu: 29 % Cr: 8% As: 32%
Christensen, 2006	L = 3.5 m W = 1m H = 1m	platinized titanium bars; L = 1m D = 3 mm	270 cm / 8	0.5 M H_3PO_4 / 24 hours 5 % OA / 24 hours	water and sodium benzoate	2.0; conc. HNO_3	469 kg, From < 2 cm to > 4 cm	1-1.5 A, 23-39 V	21 days	Cu: NR Cr: NR As: NR

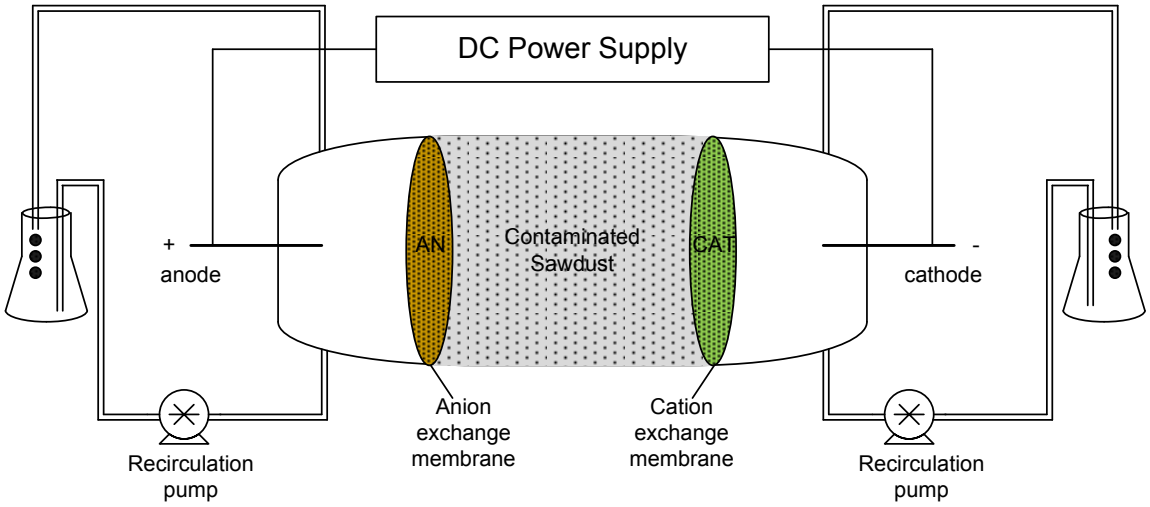

Figure 2.1 Schematic representation of the batch laboratory electrodialytic cell developed at Technical University of Denmark

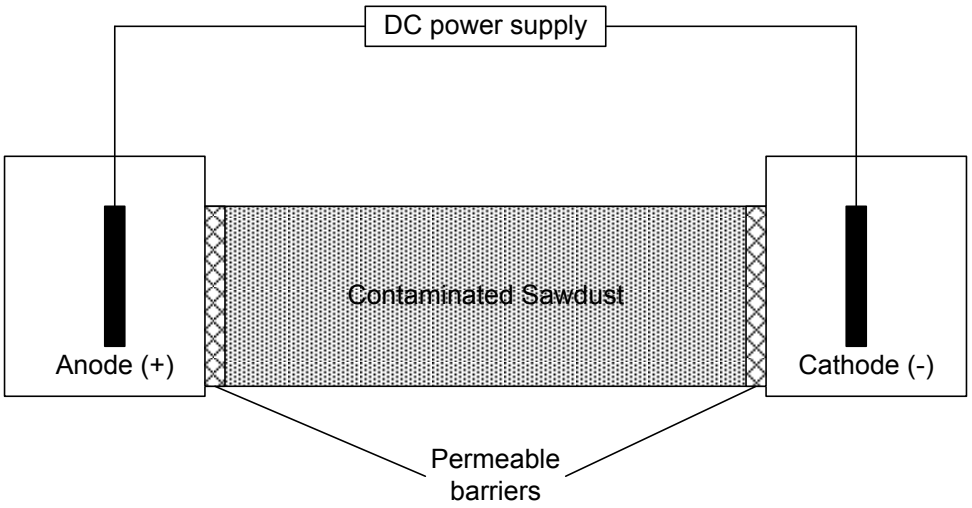

Figure 2.2 Schematic Representation of the Batch Laboratory Electrodialytic Cell Used in Sarahney 2005

CHAPTER III

MATERIALS AND METHODS

The mobility of an ion under the influence of an electric field is affected by many parameters and properties. This study is an investigation into the effects of particle size reduction and oxidative pre-treatment onto the overall effectiveness of the EK remediation of CCA wood waste. The three contaminants of concern (CoC) are chromium, copper, and arsenic. All analytical methods presented in this chapter will be directed towards determining the concentrations of these metals in CCA wood waste and in the post remediation products generated for utilization in this study.

An overview of the experimental phases in this study is shown in Figure 3.1. The study can be divided into phase I experiments, phase II experiments, and the EK phase experiments. The phase I experiments deal mainly with the characterization of the source CCA sample from which all samples of CCA contaminated material were taken over the course of the experimental program (Figure 3.2). The phase II experiments deal mainly with the selection of the oxidative pre-treatment chemical and the optimization of the solution strength and solid to liquid ratio of the oxidative pre-treatment (Figure 3.3). The EK phase experiments involved the assembly of the EK experimental units, the EK experimental sampling, the post-EK experimental unit disassembly, and collection of the post-EK experimental samples (Figure 3.4).

3.1 Phase I Experiments

3.1.1 Sample Collection

The source of all of the CCA samples used in the following experiments was donated for research to Mississippi State University by Starkville Electric Company. The sample was a cylindrical utility pole with approximate dimensions of 16 feet in length and 14 inches in diameter. The utility pole remained in-service for a period of 15.5 years, with a service life beginning in December 1990 and ending in May 2005.

3.1.2 Evaluation of Raw Sample CoC Content

Preparation of samples for the evaluation of CoC content began with particle size reduction. First the utility pole was divided into two sections. The exposed portion of the utility pole was labeled 'surface' and the buried portion of the utility pole was labeled 'subsurface'. Both sections were then split into longitudinal pieces using a one-pound hammer and a spike wedge. The split pieces were no greater than 3 inches in cross section and no longer than 4 feet in length. The split sections were chipped using a Yard Machines Brand 6.5 horsepower chipper shredder. The chipped wood was then separated into two fractions by sieving them through a 9.5 millimeter sieve. The larger fraction of shredded wood was labeled as wood chips and stored for use in the EK experiments. The smaller fraction of wood chips was ground into dust using a Thomas Scientific Brand Model 5 Wiley Mill Grinder. Photos of all of the particle size levels examined in this study are included in Figure 3.5.

The sawdust was subjected to microwave digestion according to a slightly altered version of US EPA Method 3051. In this altered method, 0.4000 ± 0.0010 grams of dry wood fines was weighed using a Mettler-Toledo Model AG204 analytical balance then

transferred to a 60 milliliter CEM XP-1500 digestion vessel. After the transfer of the CCA wood to the digestion vessel, 8 milliliters of 15.8 molar nitric acid and 3 milliliters of 30% by volume hydrogen peroxide was added. The addition of the hydrogen peroxide is accompanied by a violent reaction between the contents of the vessel, so the vessel was allowed to vent for a period of 15 minutes under a fume hood until the intensity of the reaction subsided. The vessels were then capped and placed in a CEM MARS5 microwave to be digested.

Once digestion of the wood samples was complete, the digested material was vacuum filtered. The filtered samples were analyzed for CoC content using a Perkin Elmer Instruments Optima 4300 DV Inductively Coupled Plasma Optical Emissions System (ICP-OES) according to US EPA Method 6010B.

3.1.3 Evaluation of Raw Sample TCLP

The toxicity of the CCA material used in this study was measured using a slightly altered version of EPA Method 1311. First, the particle size of the sample wood was reduced to a size of less than 9.5 millimeters by chipping the wood and passing the wood through a 9.5 millimeter sieve. Then an extraction fluid selection pre-screening was performed exactly according to US EPA Method 1311. The pre-screening step consistently resulted in the selection of extraction fluid #1. After the wood sample was pre-screened, 2.0000 ± 0.0010 grams of dry wood chips was weighed out on an analytical balance and placed in a 60 milliliter Nalgene high density polyethylene (HDPE) bottle. After addition of the wood chips, 40 milliliters of TCLP extraction fluid #1 was added to the bottle. The bottles were then capped and tumbled end over end for a period of 18 ± 2 hours. Once the tumbling period was complete, the contents of the bottles were vacuum

filtered. The pH of the filtrate was then measured using an Oakton Model 310 pH meter with an Orion Model 9206B gel-epoxy probe according to EPA Method 9040C. The filtrate was analyzed for CoC content using ICP-OES equipment according to US EPA Method 6010B.

3.1.4 Evaluation of Raw Sample Moisture Content

Evaluation of the moisture content of CCA wood was performed on CCA sawdust. The method involves six steps, which are listed sequentially in Table 3.1. The moisture content was then calculated using equation 3.1.

$$percent\ moisture = \frac{(b-a)-(c-a)}{(c-a)} \times 100 \tag{3.1}$$

where "*a*" = weight of sample tin

"*b*" = combined weight of sample tin and wet wood sample

"*c*" = combined weight of sample tin and dry wood sample

3.2 Phase II Experiments

In phase II experiments, pre- EK chemical treament agents were evaluated in two separate experimental stages. In stage one, monobasic potassium phosphate (KH_2PO_4), sodium hypochlorite (NaOCl), hydrogen peroxide (H_2O_2), and deionized water were tested for their ability to leach CCA metals from CCA wood fines. In stage two, the highest performing leaching agents from phase one were tested for their ability to leach CCA metals from CCA wood fines at varying solid to liquid ratios and solution strengths. Selection of the final leaching agent was based upon the ability of the pre-treatment solution to selectively leach CCA metals without causing excessive degradation of the wood mass during the process.

3.2.1 Chemical Treatment Agent Selection: Stage One

In stage one experiments the ratio of CCA wood weight to volume of leaching agent was fixed at 4.0000 ± 0.0010 grams of CCA wood to 100 ± 1 milliliters of leaching agent. The amounts of leaching agent added in each experiment were selected so that a similar weight percent of active leaching chemicals would be present in each treatment. The actual amounts of leaching chemicals added in each treatment are listed in Table 3.2.

Each of the four solutions described in Table 3.2 were prepared in 125 milliliter Nalgene HDPE sample bottles. The experimental sample bottles were then tumbled for a period of 15 hours, vacuum filtered, and analyzed for CoC according to US EPA Method 6010B. During experimentation, it was found that these leaching solutions were damaging the wood mass significantly. An attempt was made to analyze the weight loss percentages however, it was impossible to account for 100% of the solids remaining in the bottles after the tests. Therefore, as much of the remaining woody mass was collected as possible, placed in a tin and dried at 75^{o} C overnight in a forced air oven. The samples were removed the next day, desiccated for 30 minutes, and then the degradation of woody mass was estimated by visual inspection.

3.2.2 Chemical Treatment Agent Selection: Stage Two

Based on the results from the phase one experiments, NaOCl and H_2O_2 treatments were selected for possible use as a pre-EK treatment agent. In stage two experiments the leaching solution strength and the solid to liquid ratio of wood mass to leaching solution volume were varied. The levels in variation of these two parameters are shown in Table 3.3.

Each level of solid to liquid ratio was combined with each level of solution strength for both chemical treatments and run in duplicates. A total of 48 experiments were run in the second stage of leaching agent selection. In each of the experiments a dry wood sample was prepared in a 125 milliliter Nalgene HDPE bottle, mixed with a chemical treatment solution as described in Table 3.3, and then tumbled for a period of 15 hours. Once tumbling was complete the samples were vacuum filtered. The filtrate was then analyzed for CoC according to US EPA Method 6010B. After filtration the solid portion of the woody mass was collected, dried overnight at a temperature of 75 ^{o}C, placed in a dessicator for a period of 30 minutes, and re-weighed. This was done so that the loss of wood mass during experiments could be calculated.

3.3 Electrokinetic Phase

3.3.1 Electrokinetic Cell Fabrication

The EK cell design consists of three separate parts: an anode half cell, a cathode half cell, and a center compartment. The half cells were constructed using 3" ID schedule 40 clear rigid PVC pipe, 3" ID clear rigid PVC Tees, 3" schedule 80 gray PVC union flanges, 3" schedule 80 gray PVC blind flanges, 3" ID by 1/8" thickness full face Neoprene gaskets, and approximately 1/3 pie cut piece of a 2" ID schedule 40 clear rigid PVC pipe with a notch burned into the center to serve as a mount for the carbon electrodes. All taps into the half cells were made using a Delta Rockwell Ball Bearing ½ horsepower AC motor drill press and a ¼" drill bit. Taps were threaded with a ¼"-18 NPT threading tool. A schematic diagram of a half cell is included in Figure 3.6. The center compartment of the EK cell was constructed using a 12" joint of 3" ID schedule 40 clear rigid PVC pipe, and two 3" schedule 80 adjustable Vanstone flanges. All taps into

the center compartments were made using the previously mentioned drill press and a 1/8" drill bit. Taps were threaded with an 1/8"-27 NPT threading tool. All pieces were fused together using Oakley brand PVC pipe cleaner and IPS Weld-On PVC plastic pipe cement. A schematic diagram of a center compartment is also shown in Figure 3.6. Figures 3.6 through 3.8 are diagrams of the EK experimental unit.

Pore sampling ports were drilled into the center compartment so that fluid samples could be collected during the experiment. This type of sampling was conducted to determine the ionic mobility of different metals accurately. Pore sampling ports on the center compartment were placed at 3" intervals and consisted of low pressure Teflon® tubing (Dionex model 14157), two ¼"-28 PEEK® thermoflare bolt fittings (Dionex model 37627), two ¼"-28 PEEK® unions (Dionex model 39056), a ¼"-28 PEEK® bolt (Dionex model 37627), a 1/8" Kynar® male straight adapter compression tube fitting (McMaster-Carr model 5533K433), and a threaded high pressure end line filter (Dionex model 45987). A picture of a pore sampling device is shown in Figure 3.9.

The secondary electrodes were designed to measure the voltage drop across the center compartment. Secondary electrode ports on the center compartment were also placed at 3" intervals and consisted of a 0.035" tungsten clean and straight wire (ED Fagan) sealed into a 1/8" Kynar® male straight adapter compression tube fitting (McMaster-Carr model 5533K433) using General Electric clear rubber silicon sealant. Secondary electrodes were connected to a 5 circuit VAC 20 amp circuit block (McMaster-Carr model 7527K65) using 16 gauge copper wiring. A picture of a secondary electrode is shown in Figure 3.9.

3.3.2 Recirculation Tanks

Two recirculation tanks were used for each EK cell, one tank for each half cell. The bases of both types of recirculation tanks were made of 8" by 8", ¼" thick plexiglass sheets. A 6" ID by 12" tall plexiglass pipe having a ¼" wall thickness was glued to each base with a dichloromethane solution. Taps were drilled into the recirculation tanks using the previously mentioned drill press and a ¼" drill bit. All taps on the recirculation tanks were threaded with an ¼"-27 NPT threading tool. On anode recirculation tanks, three taps were made on the front side of the tank at heights of ½", 4 ½", and 6 ½" for fluid transport back into the half cell, half cell overflow, and fluid entry into the recirculation tank. On cathode recirculation tanks, two taps were made on the front side of the tank at heights of ½", 4 ½" for fluid transport back into the half cell and half cell overflow and one tap was drilled in the backside at a height of 7 ½" for fluid entry into the recirculation tank. Schematic diagrams of both anode and cathode recirculation tanks are shown in Figure 3.10. A smaller, pH control reservoir was added on the backside of the cathode recirculation tank. The function of the pH control reservoir was to provide an easily accessible source of cathodic fluid for continuous pH sampling and control. The pH control reservoir was made from a 3 ½"section of 2" ID clear PVC pipe, two 1/8" Kynar® male straight screw nipples, and a 2" ID clear PVC pipe cap. A 1/8" fluid entry tap was drilled through the bottom of the base and another 1/8" fluid exit tap was drilled through the top of the reservoir. Both taps were threaded with an 1/8"-27 NPT threading tool. A schematic diagram of a pH control reservoir can be seen in Figure 3.11.

3.3.3 Carbon Electrode Fabrication

Electrodes were fabricated by drilling a 0.040" hole into a 2 ¾" diameter, 3/8" thick resin impregnated carbon electrode disc (Bay Carbon Inc). Once drilled, a mixture of silver epoxy and silver nitrate was fed into the drilled hole and a 12" joint of 0.035" diameter tungsten wire coated with heat shrinkable tubing was inserted into the drill hole along with the epoxy mixture. Once assembled the electrodes were baked in an oven at 85^{o} C for 24 hours so that the epoxy mixture would cure and fix the tungsten wire in place. Once cured the junction between the tungsten wire and carbon electrode was sealed with General Electric clear rubber silicon sealant. A picture of a complete carbon electrode is shown in Figure 3.12.

3.3.4 Power Supply

Direct current was passed through the center compartment of the EK cell by applying a potential difference across two electrodes with an Agilent model E3612A,120 VAC, DC power supply. The electrodes were connected to the previously mentioned 5 circuit VAC 20 amp circuit block and the circuit block was then connected to the power supply. All connections were made with 16 gauge copper wiring.

3.3.5 Pumps

Fluid was pumped from half cells to their respective recirculation tanks using a Masterflex L/S variable speed pump model 7553-80, 1-100 RPM, 115 VAC motor. Attached to each pump were two Masterflex L/S Easy-Load pump heads, one for each half cell. Two types of tubing were used to circulate fluid. Masterflex L/S 17 ¼" ID black

tubing was used in places where tubing came into contact with pump heads and Nalgene 180 ¼" ID clear PVC tubing was used in all other areas.

3.3.6 pH Controller

The pH of the cathode half cell was regulated throughout the experiment. The pH control apparatus consisted of the pH control reservoir, a 1 molar solution of nitric acid, a pH electrode, and a pH control system. The nitric acid was prepared by diluting approximately 63.2 milliliters of concentrated, 15.8 normal nitric acid to 1 liter, and it was held in a Nalgene 1000 mL polypropylene graduated cylinder. The type of pH probe used was a Sensorex model 450C probe with a BNC connection. The type of pH meter-controller used was a Barnart standing DLXB-pH/M Series metering pump with proportionating output.

3.4 Electrokinetic Cell Loading and Operation

3.4.1 Preparing Samples for EK Cell Loading: Control Experiments

3.4.1.1 Preparing Fines and Chips for EK Cell Loading

Samples of wood chips and wood fines were generated by the same particle size reduction methods described in Section 3.1.2. Before loading into the center compartment, the wood chips and wood fines were moistened with tap water. This involved weighing out 100 grams of wood sample at a time, placing the sample into a large mixing bowl, and spraying the sample with tap water from a spray bottle while gently mixing the sample for 2 minutes. The samples were then transferred to plastic ziplock bags so that the moisture level could be maintained until the samples were ready to be loaded into the EK cells. The wood chips were wetted at an approximate ratio of 1.9

grams of wood chips to 1.0 grams of water. The sawdust was wetted at an approximate ratio of 1.0 grams of sawdust to 1.0 grams of water. The purpose of wetting the wood was to prevent contamination of the lab with CCA-contaminated dust. Also, wetting the sample causes the wood to expand prior to cell loading, which improves the packing of the wood.

3.4.1.2 Preparing Wood Plugs for EK Cell Loading

First, CCA wood slats that were less than one inch in cross section and longer than 12 inches were packed as tightly as possible into the center compartment of an EK cell. Then the slats were slowly pushed out of one end of the center compartment in plug form by lightly tapping the other end of the compartment the with a rubber hammer. When three inches of the bundle became visible outside of the center compartment, the slats were fastened together using two tie wraps and sawn into cylindrical wood plug sections that were approximately 3" in diameter and 3" in length. The tapping, fastening, and sawing steps were repeated until four plugs of CCA wood waste were produced. A picture of a plug is shown in Figure 3.5. It was not necessary to add moisture to the plug samples to aid in cell loading. However, the plug samples were wetted in an attempt to remain consistent with the preparation methods described in Section 3.4.1.1.

The wood plugs were wetted by adding two plugs to a 2 liter Nalgene HDPE sample bottle, filling the bottle with tap water, and soaking the samples for 4 hours. Once the samples were removed from the HDPE bottles, they placed under a fume hood in tin trays and allowed to dry under atmospheric conditions for a period of 24 hours. The samples were then transferred to plastic ziplock bags so that a level of moisture could be maintained until the samples were ready to be loaded into the EK cells.

3.4.2 Preparing Samples for EK Cell Loading: Chemical Pre-treat Experiments.

Wood samples for the chemical pre-treatment EK experiments were prepared according to the control samples preparation methods described in Section 3.4.1. The only exception is that instead of wetting the samples with tap water, the samples were subjected to chemical pre-treatment as described below. Based on the results of Phase II experiments, it was decided to treat CCA wood with a 16.7 % solution of NaOCl at an approximate ratio of 3 grams of wood to 60 milliliters of extracting solution.

3.4.2.1 Preparing Wood Chips and Wood Fines for EK Cell Loading

This was accomplished by weighing approximately 100 grams of sample and placing the sample in a 4 liter Nalgene HDPE bottle. Then 320 milliliters of 4-6 % NaOCl solution and 2 liters of deionized water were added to the bottle. Bottles were then tumbled end over end for 15 hours. After tumbling, solid and liquid phases were separated by passing them through a ¼" sieve. A 400 milliliter sample of post-extraction liquid was taken from each bottle during the filtering process. The liquid samples were then digested according to EPA Method 3015, vacuum filtered, and analyzed for CoC according to EPA Method 6010B. The remaining solids were placed under a fume hood in separate tin trays and allowed to dry under atmospheric conditions for a period of 24 hours. The samples were then transferred to plastic ziplock bags so that a level of moisture could be maintained until the samples were ready to be loaded into the EK cells.

3.4.2.2 Preparing Wood Plugs for EK Cell Loading

The weight of each wood plug ranged from 110 grams to 130 grams. Because of this, each wood plug was treated with pre-EK chemical treatment solutions individually.

The following equations were used to calculate the total volume of liquid (y_1) in milliliters that had be added to 2 liters of solution to achieve the 3g:60ml solid to liquid ratio; the fraction of that total volume of liquid that had to be NaOCl (y_2) in milliliters to achieve the proper solution strength; and the volume of deioninzed water that would need to be added to the concentrated NaOCl to achieve the target level of dilution/S:L ratio/total volume.

$$y_1 = \frac{60}{3}(x - 100) \tag{3.2}$$

$$y_2 = 0.167 * (2{,}000 + y_1) \tag{3.3}$$

$$y_3 = 2{,}000 + y_1 - y_2 \tag{3.4}$$

where: x = weight of the wood plug in grams

Then the plug was placed in a 4 liter Nalgene HDPE sample bottle, combined with volume y_2 of active chemical, topped off with volume y_3 of deionized water, and tumbled end over end for 18 hours. After tumbling, solid and liquid phases were separated by passing them through a ¼" sieve. A 400 milliliter sample of post-extraction liquid was taken from each Nalgene HDPE bottle during the filtering process. The liquid samples were then digested according to EPA Method 3015, vacuum filtered, and analyzed for CoC according to EPA Method 6010B. The remaining solids were placed under a fume hood in separate tin trays and allowed to dry under atmospheric conditions for a period of 24 hours. The samples were then transferred to plastic ziplock bags so that a level of moisture could be maintained until the samples were ready to be loaded into the EK cells.

3.4.3 Loading the Center Compartment

3.4.3.1 Wood Chips and Wood Fines EK Cell Loading: Control Experiments

Cell loading procedures described in this section apply to the wood materials prepared according to the method described in Section 3.4.1.1. First the center compartment was sealed on one end by bolting on a full-face gasket and a blind flange. Then the initial weight of the center compartment was taken using a Denver Instruments Company Model TL-8102D top loading scale. Once the initial weight was recorded, CCA wood was scooped with a hand shovel and carefully funneled into the center compartment. When the level of wood rose to be even with the pore sampling and secondary electrode ports, the wood was packed down lightly with a 5 pound compaction hammer to remove any air pockets, and then the sampling device and secondary electrode was put into place. This was repeated until all of the sampling devices were in place. Then the center compartment was topped off with sample wood, packed down lightly, and weighed a second time on the above mentioned top loading scale.

3.4.3.2 Wood Plugs EK Cell Loading: Control Experiments

This method of packing was used for the samples prepared according to the method described in Section 3.4.1.2. A photo of a "wood plug" is included in Figure 3.5 along with the photos of the other wood particle size levels examined in this study. Once the plugs were prepared, a center compartment of the EK cell was sealed on one end by bolting on a full-face gasket and a blind flange. Then the initial weight of the center compartment was taken using a Denver Instruments Company Model TL-8102D top loading scale. Once the initial weight was recorded, a single plug was placed in the center compartment and packed down to the bottom using a 5 pound compaction hammer. The

tie wraps were removed from the plug as the plug was being packed down into the bottom of the EK cell center compartment. Since the plugs were cut to lengths of 3" each plug was at the appropriate height to add a center compartment sampling device and a secondary electrode. This was repeated until all of the sampling devices were in place. Then the center compartment was topped off with one last plug, packed down lightly, and weighed a second time on the above mentioned top loading scale.

3.4.3.3 EK Cell Loading: Chemical Pre-Treat Experiments

This method of packing was used for wood samples that were chemically pre-treated with the oxidative solution prior to being loaded into the EK cell (ie: the materials prepared according to the method described in Section 3.4.2). Before adding any wood to the center compartment, moisture balances were performed on each of the samples so that the dry weight of CCA material loaded into the EK cell could be calculated. Once the moisture balances were complete the wood chips and wood fines samples were packed into a center compartment according to the method described in Section 3.4.2.1 and the wood plug samples were packed into a center compartment according to the method described in Section 3.4.3.

3.4.4 Cell Operation

Once the center compartments were prepared and weighed they were flanged to the EK half cells. Then all of the tubing connecting the half cells to the recirculation tanks, the overflow tanks, the pump heads, and the nitric acid injection pump was assembled onto the EK cell as well as all of the electrical components required to run the EK equipment. Then the half cells and recirculation tanks were filled with approximately

5 liters of tap water and the power was turned on. The voltage drop across the power supply units was set at the maximum possible electrical potential difference attainable by the power supply units. The power supply units were then adjusted to a constant current setting of 140 milliamperes.

As the EK experiments were running a one molar solution of nitric acid was used to maintain the pH of the catholyte below 3.0. Also the hydraulic head across the assembled EK cell was maintained at zero by manually monitoring the liquid levels of the half cells and recirculation tanks and adding tap water when the level of solution in the cells became uneven. A photograph of an EK cell during operation is shown in Figure 3.7 and a schematic diagram of an EK cell during operation is shown in Figure 3.8.

3.4.5 Analysis and Measurements During Experiments

The following measurements were taken on a daily basis: potential difference across the cell, electrical current flow through the cell, potential difference between the anode and each secondary electrode, volume of anode and cathode overflows, volume of tap water added to the anode and cathode half cells to maintain zero hydraulic head pressure, and the volume of one molar nitric acid consumed for the purpose of pH control. All electric measurements were taken using an Allied Electronics Inc. Model 23XT digital multimeter.

The following samples were collected on a weekly basis. To evaluate the movement of ions through the EK cell, 7 milliliters of pore fluid was collected from each pore fluid sampling port. To evaluate the concentrations of ions in each of the half cells, a 12-inch spatula was used to stir up the contents of the half cell and then approximately 10 milliliters of fluid was collected at each of the half cells from the half cell sampling ports.

All of the fluid samples were analyzed for CoC content according to US EPA Method 6010B using ICP-OES equipment. In addition to concentration analyses, the pH and oxidation-reduction potential (Eh) of the fluid samples were also measured. The pH was measured with the same apparatus described in Section 3.1.3 according to EPA Method 9040C. The Eh was measured with an Accumet portable pH/mV Model AP62 meter attached to a Ag/AgCl combination electrode probe according to ASTM D-1498-93.

3.4.6 Cell Breakdown and Post-Run Analysis

After the EK cells were run for 50-60 days the power to the system was turned off and all wiring was disconnected. The tubing between the recirculation tanks and the half cells were clamped. Anode and cathode half cell solutions were thoroughly mixed and pumped into separate 5 gallon buckets. The recirculation tank solutions were then collected in 3 liter containers. The total volume of each solution was recorded and approximately 400 milliliter samples were taken from each of the EK cell sections containing experimental fluids and stored in two 250 milliliter HDPE sample bottles. All liquid samples were digested according to EPA method 3015, the Microwave Assisted Acid Digestion of Aqueous Samples and Extracts. Following digestion the samples were analyzed for CoC using ICP-OES equipment.

After fluid sampling was complete, the anode and cathode half cells were removed from the center compartment and the pressure plates were stored in Ziplock bags. The pressure plates are 1/8” thick coarse grade polyethylene materials that fit in between the half cells and the center compartment. The purpose of the pressure plates is to contain the wood within the center compartment but to allow ions to migrate from the center compartment into the half cells. Pressure plates were cut into pieces less than one

inch in cross section and placed in a 500 milliliter beaker. After adding 200 milliliters of 20 volume % nitric acid, the beakers were placed on a stir plate and set to stir for approximately two hours. Once the stir cycle was complete, the samples were vacuum filtered and the filtrate collected was analyzed for CoC according to EPA Method 6010B using ICP-OES equipment.

The electrokinetically treated CCA wood was removed by section from the center compartment by section and placed into Ziplock bags. The sections into which the contents of the center compartment were divided can be seen in Figure 3.13. The solid samples were placed under a fume hood and allowed to dry at room temperature for a period of 24 hours. Once the samples were dried significantly, wood chip and wood plug samples were ground to sawdust using the Wiley Mill grinder mentioned in Section 3.1.2.

To ensure that no soluble forms CCA metals remained loosely bound to the wood surface, a multistage rinse with deionized water was performed. First, 4.000 ± 0.0010 grams of post-EK CCA sawdust was weighed out on the Mettler-Toledo balance mentioned above and placed in 50 milliliter polypropylene, round bottom centrifuge tubes. Then 30 milliliters of deionized water was added to the centrifuge tubes and the tubes were tumbled end over end for a period of 30 minutes. After tumbling, the samples were centrifuged in a Thermo Electorn Corporation IEC Centra Model GP6 centrifuge at a speed of 2050 rpm for a period of 10 minutes. Then a 6 milliliter sample of supernatant fluid was collected using a mechanical pipette. The remaining liquid was decanted, then another 30 milliliters of deionized water was added to the centrifuge tube and the centrifuge step was repeated. The samples of supernatant fluid were analyzed for CoC according to EPA Method 6010B using ICP-OES equipment. Once the rinsing procedure

was completed, the wood samples were dried overnight in a forced air oven set at 85° C and then dessicated for 30 minutes. Once all of the post EK solid wood samples were rinsed and dried, the analyses of the CoC content of the wood samples was performed according to the methods described in Section 3.1.2. The analyses for the toxicity characteristic/ionic mobilities were performed according to the methods described in Section 3.1.3.

Table 3.1 Six step method for calculating moisture content

1	sample tin is weighed (*a*)
2	sample tin + wet wood sample is weighed (*b*)
3	sample tin + wood sample is placed in a forced air oven at a temperature of 85 C until sample weight became constant
4	sample tin + dry wood sample is dessicated for a period of 30 minutes
5	sample tin + dry wood sample is weighed ©
6	moisture content is calculated according to equation 3.1

Table 3.2 Chemical solutions used in phase I experiments

chemical	**physical description**	**chemical added**	**final volume**
KH_2PO_4	solid crystalline	7.0000 ± 0.0010 grams	100 ± 1 milliliters
NaOCl	liquid 6% weight	100 ± 1 milliliters	100 ± 1 milliliters
H_2O_2	liquid 30% weight	30 ± 1 milliliters	100 ± 1 milliliters
H_2O	18 mΩ deionized	100 ± 1 milliliters	100 ± 1 milliliters

Table 3.3 Levels of variation used in stage II experiments

solid:liquid ratio	**solution strength by volume %**
1 g: 60 ml	0.08%
3 g: 60 ml	1.70%
5 g: 60 ml	6.70%
	16.7%

Table 3.4 Summary of Test Methods for Characterization and Analysis

Analytical Objective / Test Identification	Method and/or citation
pH	EPA Method 9040C (USEPA, 2004)
Oxidation-Reduction Potential (Eh)	ASTM D-1498-93
Vacuum Filtration	Filter method in EPA Method1311 (USEPA, 1992)
DI Water Rinse	Mod. Stegemann and Cote, 1991
TCLP	Mod. EPA Method 1311 (USEPA, 1992)
Sample Digestions	Mod. EPA Method 3051 (USEPA, 1994)
Solid Phase	EPA Method 3015 (USEPA, 1994)
Liquid Phase	EPA Method 6010B (USEPA, 1996)
Metal Content of Digested Samples	

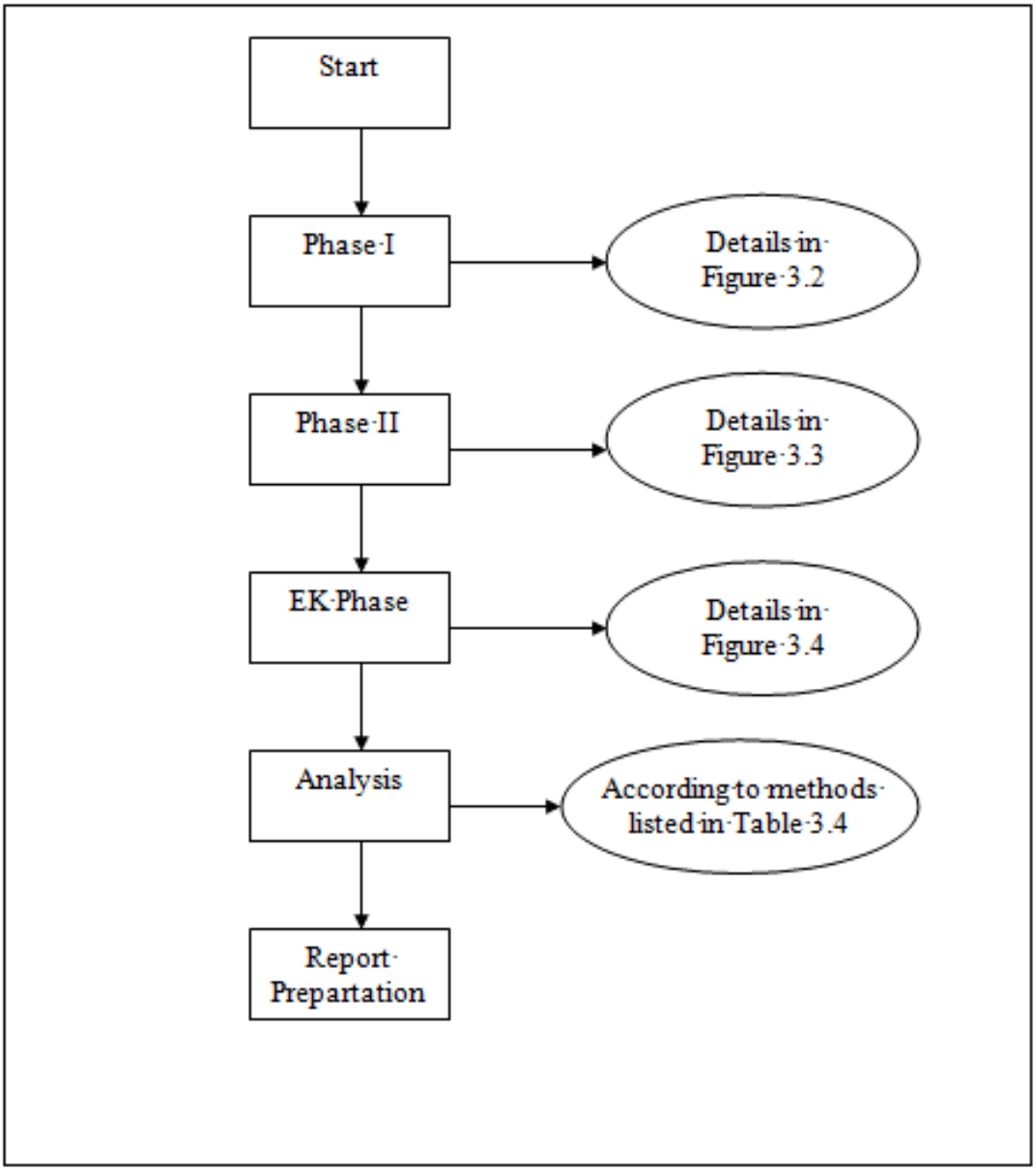

Figure 3.1 Overall experimental setup

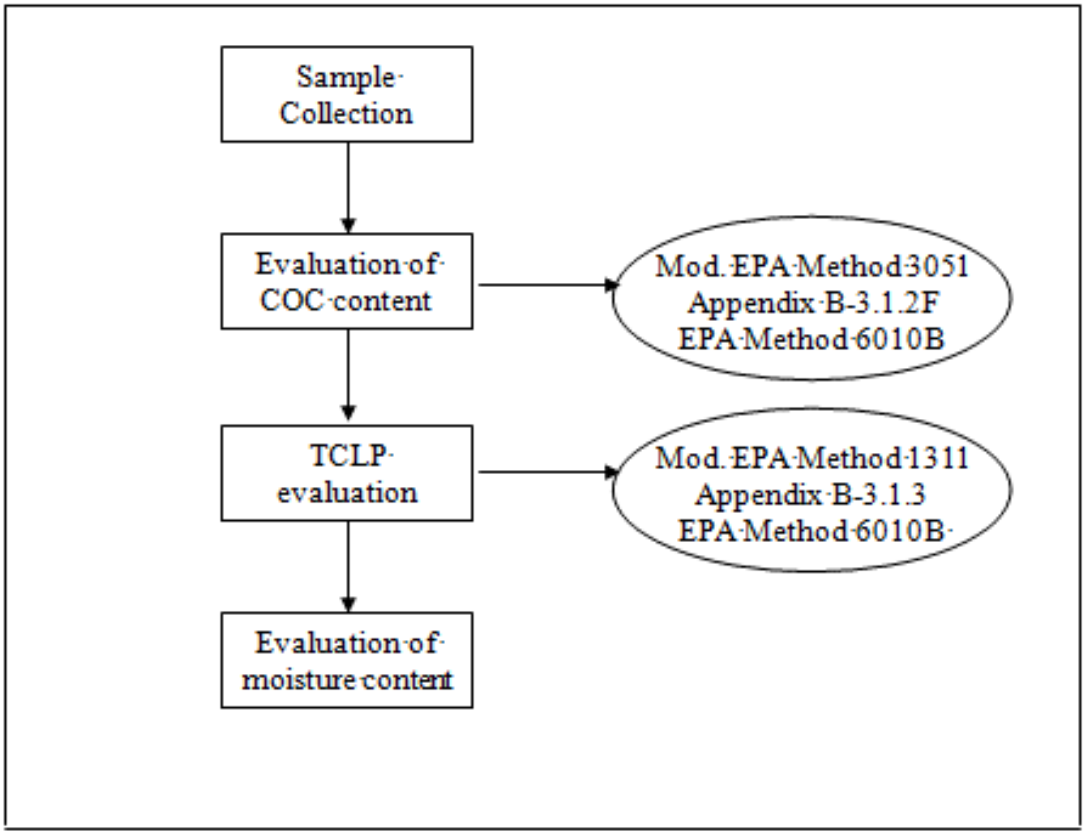

Figure 3.2 Phase I experimental setup

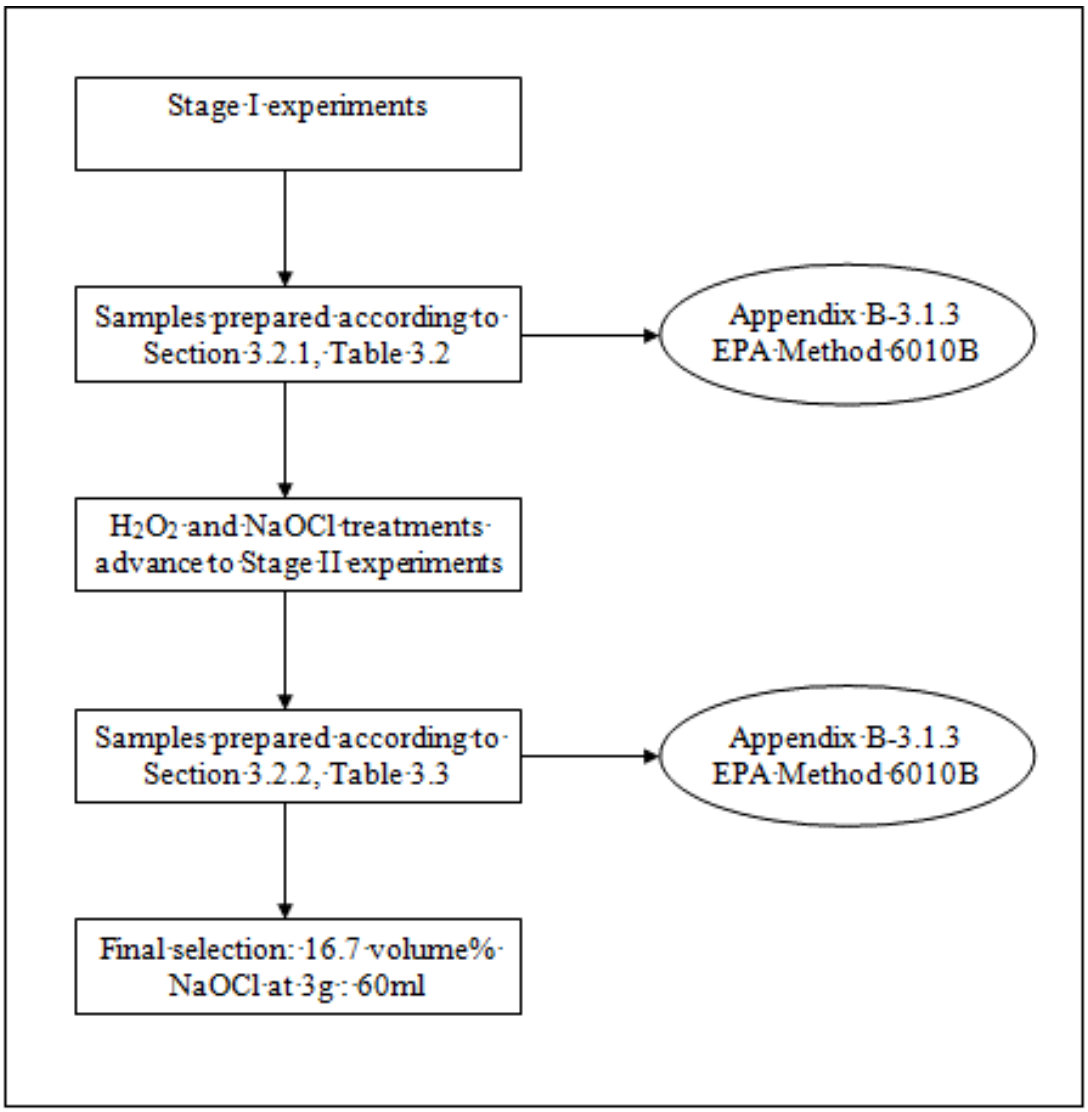

Figure 3.3 Phase II experimental setup

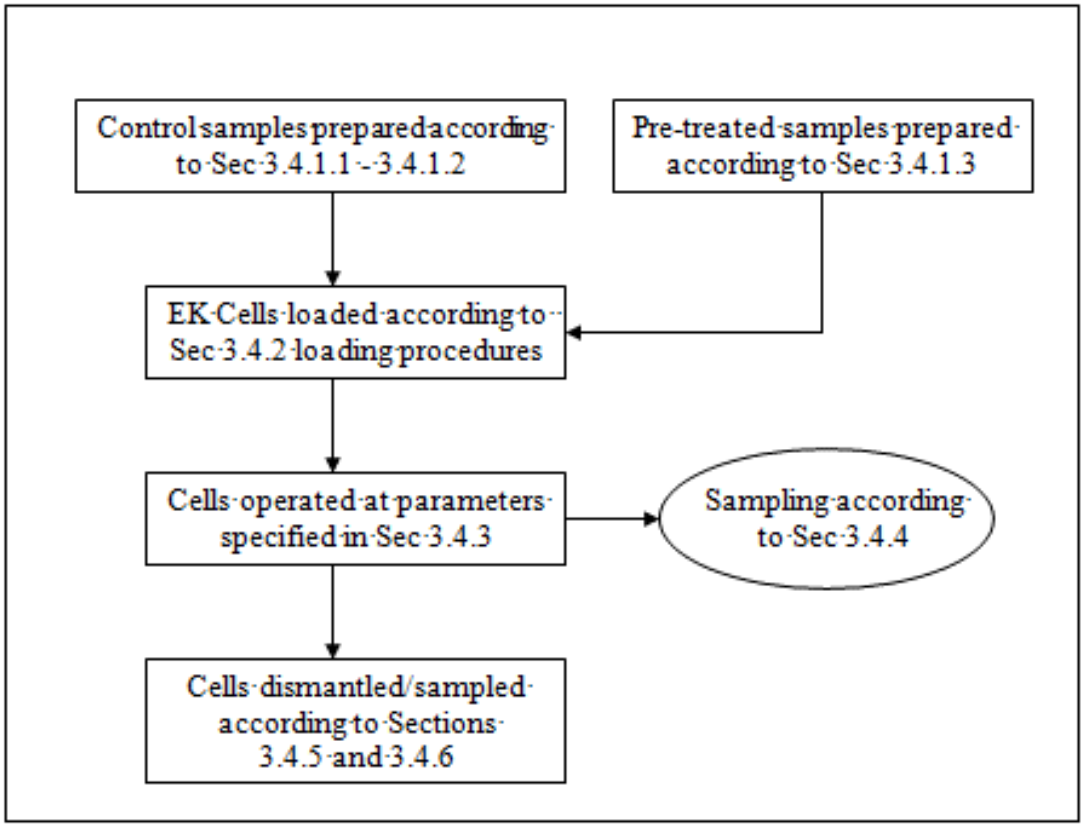

Figure 3.4 EK phase experimental setup

Figure 3.5 Photographs of sample wood particle size levels

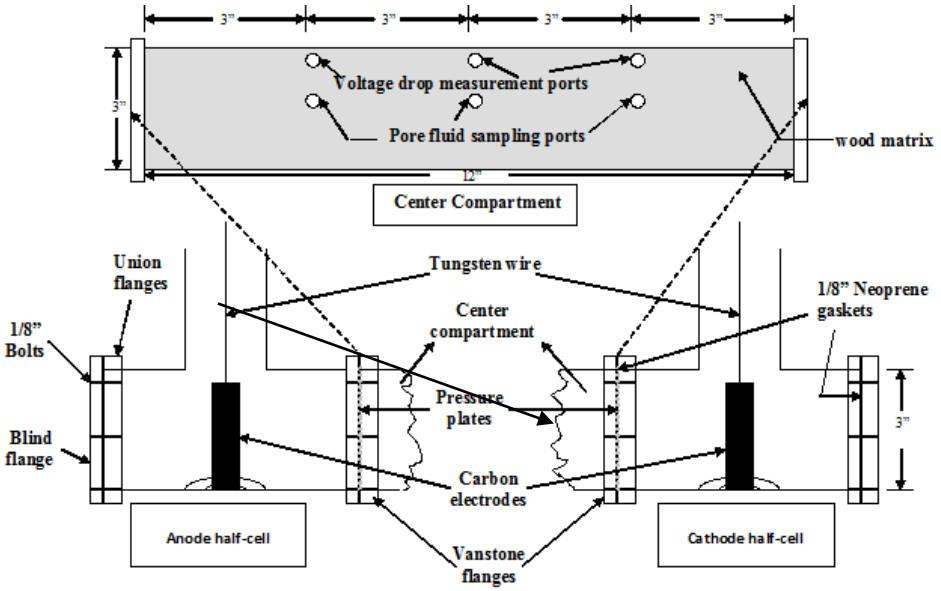

Figure 3.6 Schematic diagram of electrokinetic half cells and the center compartment

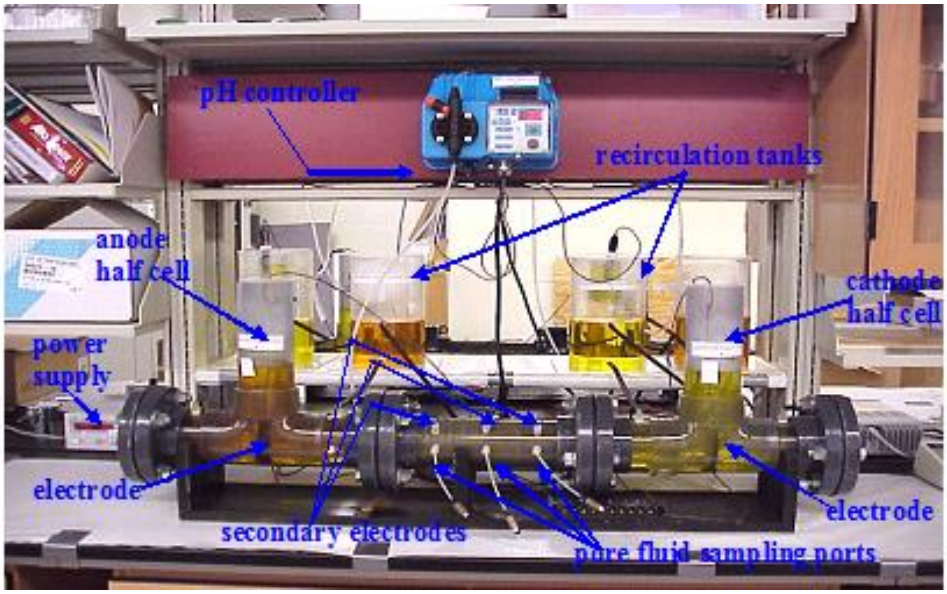

Figure 3.7 Photograph of a working EK cell

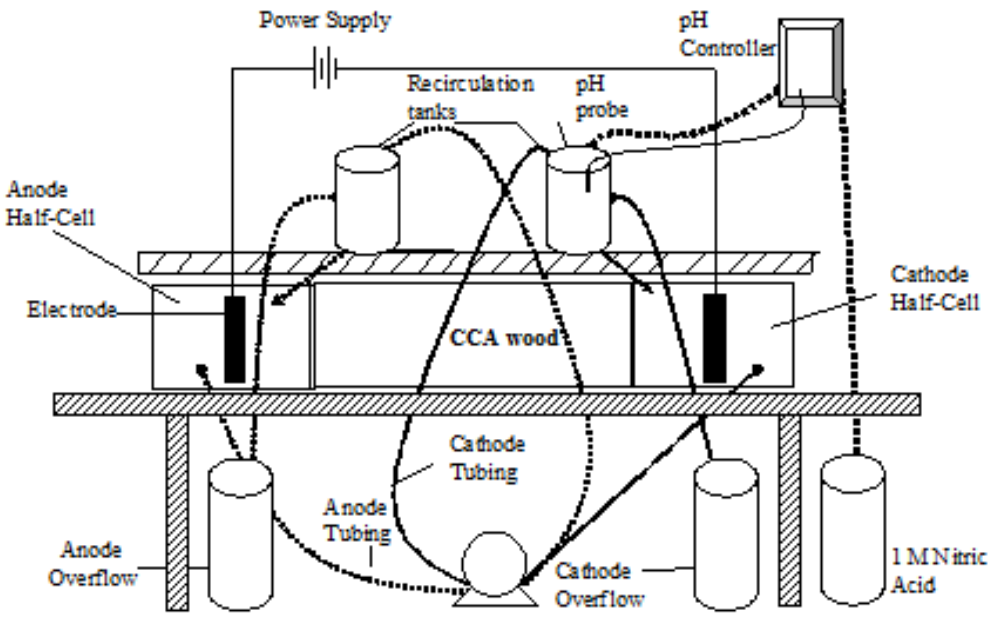

Figure 3.8 Schematic diagram of a fully assembled EK system during operation

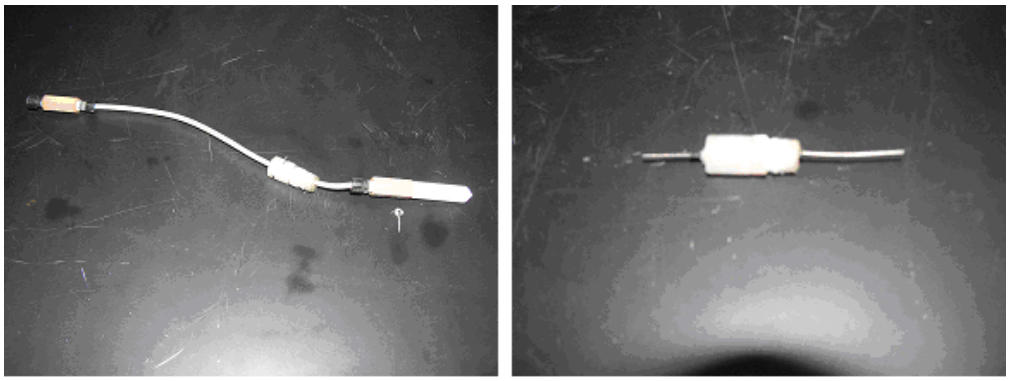

Figure 3.9 Photographs of a pore sampling device (left) and a secondary electrode (right)

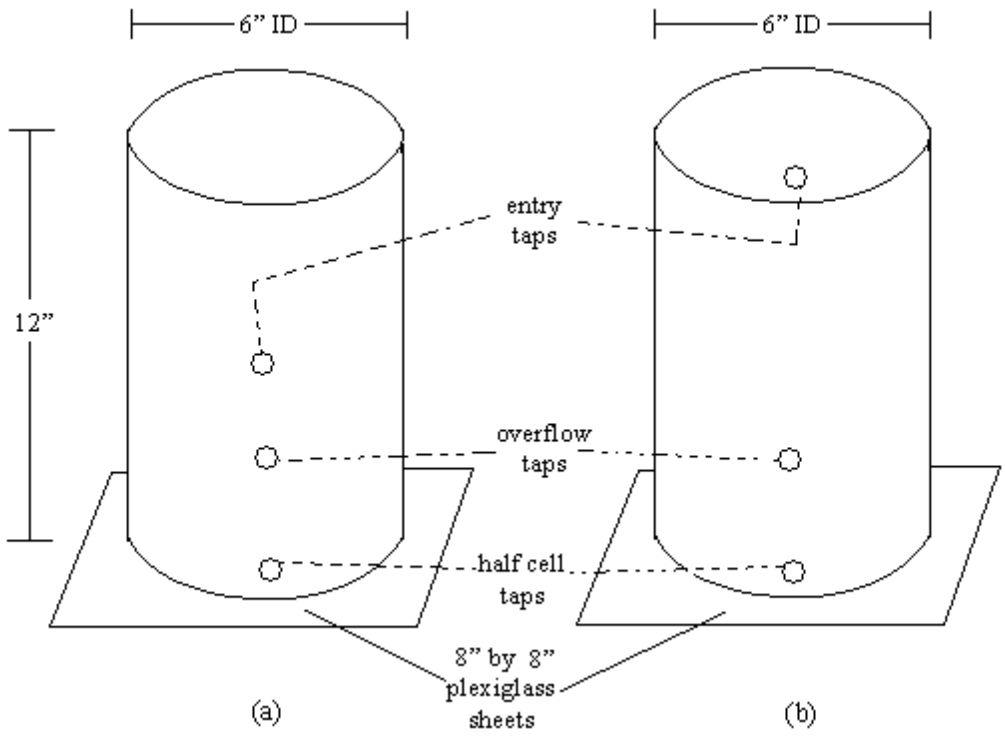

Figure 3.10 Schematic diagrams of an anode recirculation tank (a) and a cathode recirculation tank (b)

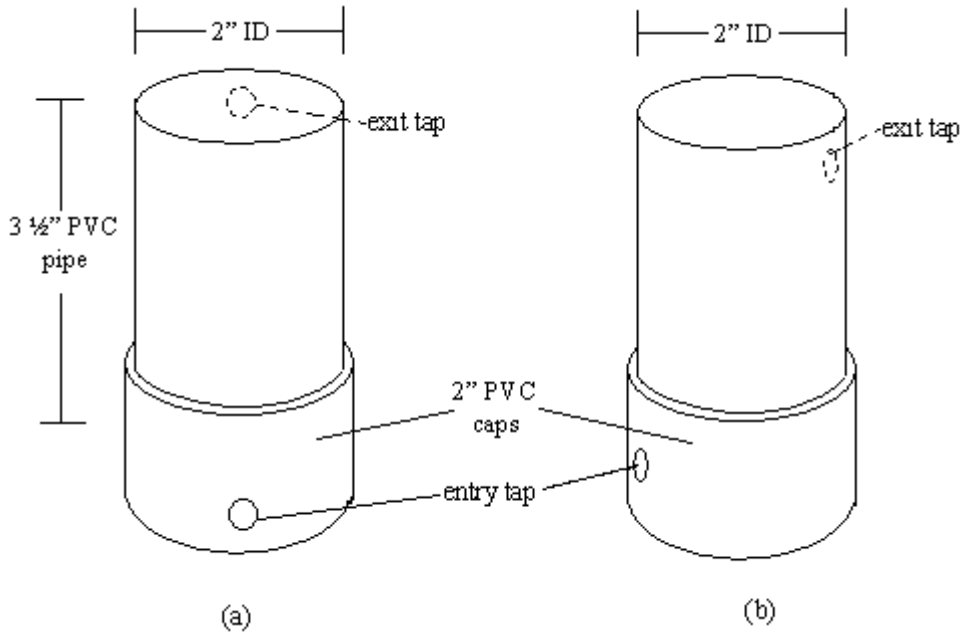

Figure 3.11 Schematic diagrams of pH control reservoirs where (a) indicates a front view and (b) indicates a side view

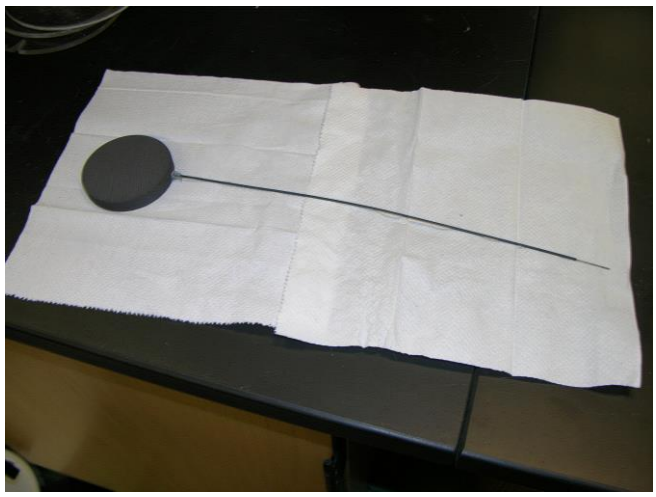

Figure 3.12 Photograph of a fabricated carbon electrode

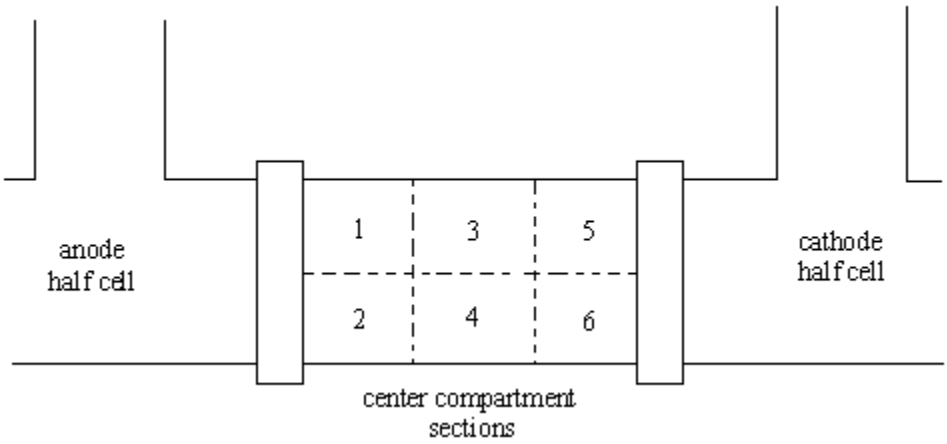

Figure 3.13 Schematic diagram of the center compartment sections of the EK cell

CHAPTER IV

RESULTS AND DISCUSSION

The main purpose of this experimental program was to examine the effect of oxidative chemical pre-treatment on the EK remediation of CCA wood waste. The results of the experiments have been divided into five sections. Arsenic, chromium, and copper ions are defined as the contaminants of concern (CoC). In the first section, results from the characterization of the CCA material used in the experiments are presented. In the second section, the chemical pre-treatment screening and optimization results are presented. In the third section, post EK results are presented. The post-EK results include: overall CoC removal efficiency, sectional CoC removal efficiencies, post-EK ionic mobility, and post-EK CoC distribution across the EK cell. In the fourth section, the results of the CoC accumulation/transport rate analyses are presented. In the fifth section, the EK cell power usage is presented as well as an interpretation of the pH and oxidation-reduction potential (Eh) sample data.

4.1 Phase I Experiments

4.1.1 Sample Collection and Preparation

The CCA specimen used in the experiments was donated for research to Mississippi State University by Starkville Electric Company. The specimen was a 16 foot long cylindrical utility pole with an average diameter of 14 inches. The utility pole was

placed into service in December 1990 and removed from service in May 2005. All of the experimental samples used in the study were generated from this specimen.

4.1.2 Evaluation of CoC Content of the Base Wood Specimen

Research done by Ribeiro indicates that CoC are leached from in-service CCA products over time and that leaching rates are typically higher in cases where the CCA product is either submerged or buried. The base of the CCA specimen used in this research was buried five feet into the ground and the remaining length was exposed to atmospheric conditions. To account for the possible difference in CoC content between the two portions of the utility pole, samples were generated, tested, and analyzed from each portion independently. Samples that were generated from the buried portion of the utility pole were labeled as "subsurface" and samples generated from the portion of the utility pole that was exposed to atmospheric conditions were labeled as "surface".

Six samples from each portion of the utility pole were digested and analyzed for CoC content according to methods described in Section 3.1.2. It was found that the surface portion contained higher concentrations of all three CoC than the subsurface portion (Figure 4.1). As a result, the decision was made to move forward with the study using samples generated from the surface portion of the utility pole only. This was done for three reasons:

- To ensure the homogeneity of CCA samples used in further experiments.
- So that results presented in this section would apply to the theoretical worse case of CCA contamination attainable in this study.
- On the basis of volume, the surface portion of the utility pole represents the larger fraction of CCA products that will be entering the waste stream.

4.1.3 Evaluation of Base Wood Specimen TCLP

The toxicity characteristic leaching procedure (TCLP) test was used to estimate the mobility of CoC in this study. Six samples were prepared for TCLP characterization and analyzed according to the methods described in Section 3.1.3. In the TCLP characterizations, copper was the most mobile ion by a significant margin with a TCLP concentration of 25.8 ppm; followed by arsenic at 7.5 ppm and then chromium at 3.3 ppm. The averaged results of the TCLP characterization analysis are displayed in the Figure 4.2. Supporting data may be viewed in Appendix A.

4.1.4 Evaluation of Base Wood Specimen Moisture Content

To assess the dry weight of wood material being handled in this study, moisture content experiments were performed on the raw CCA specimen. Samples were prepared and analyzed according to the methods described in Section 3.1.4. It was found that the specimen contained 6.94 % moisture on average. Supporting data may be viewed in Appendix A.

4.2 Phase II Experiments

4.2.1 Chemical Treatment Agent Selection: Stage One

Monobasic potassium phosphate (KH_2PO_4), sodium hypochlorite (NaOCl), and hydrogen peroxide (H_2O_2) were tested as possible pre-EK treatment chemicals. Pure deionized water (H_2O) was used as an experimental control. The objective of the phase II stage one experiments was to find which of these pre-EK chemical treatment agents was most effective at leaching CoC from wood mass. Experimental units were prepared by diluting the active leaching agent to between six and eight mass percent and combining

100 milliliters of the diluted solution with 4.00 grams of CCA wood fines in a 125 milliliter HDPE sample bottle. Tests were run as described in Section 3.2.1.

With respect to CoC removal efficiency, the NaOCl and H_2O_2 solutions performed much better than the KH_2PO_4 and deionized water solutions. The NaOCl solution was the most effective leaching agent by a large margin, removing 95% of arsenic, 89% of chromium, and 90% of copper. The H_2O_2 solution was able to remove 56% of arsenic, 26% of chromium, and 46% of copper. In the NaOCl and H_2O_2 experiments, the ranking of CoC removal percentages from highest to lowest was arsenic; followed by copper and then chromium. In the KH_2PO_4 and deionized water experiments, the CoC removal percentages were much lower. Also, the ranking of CoC removal percentages from highest to lowest was different; with copper being the easiest CoC to remove followed by arsenic and then chromium. An example of the effect of the different solutions on arsenic can be viewed in Figure 4.3. Other supporting data can be viewed in Appendix B.

Stage one experiments proved that the NaOCl and H_2O_2 treatments had a greater effect on CoC than the KH_2PO_4 and control treatments. However, their effect on CoC was accompanied by a significant amount of damage to the wood mass. The level of damage was such that recovery of the filtered solid material was impossible. So to measure the degree of degradation, samples were inspected visually as described in Section 3.2.1. There were no visual signs of degradation in the experiments where KH_2PO_4 and deionized water were used as pre-EK chemical treatment agents. Visual inspection did, however, reveal that high levels of degradation of woody mass occurred

in the experiments where NaOCl and H_2O_2 were used as pre-EK chemical treatment agents.

Stage one experiments resulted in the selection of NaOCl and H_2O_2 as possible pre-EK chemical treatment agents. The selection was based the ability of these chemicals to leach CoC from CCA impregnated wood. Since the enhanced removal of CoC was accompanied by an increase in the degradation of woody mass; it was decided that extra experimentation would be needed to optimize the solution strength of the chemical pre-treatment agent to a level where CoC can be effectively removed without causing as much damage to the woody mass.

4.2.2 Chemical Treatment Agent Selection: Stage Two

The objective of the phase II stage two experiments was to find chemical agent solution strength and the solid to liquid (S:L) ratio that would effectively solubilize the CoC without causing a dramatic loss of wood mass. Experimental units were prepared and analyzed as described in Section 3.2.2. The sample matrix for stage two can be viewed in Table 4.1.

This analysis revealed that higher CoC removals can be achieved by increasing solution strength and decreasing S:L ratio. NaOCl treatments were able to solubilize CoC more effectively than H_2O_2 treatments in every case examined in this study except at the 5g:60ml S:L ratio level. The analysis also reveals that H_2O_2 treatments cause more damage to the wood mass than NaOCl treatments. Based on this information, the following were eliminated as possible stage two selections:

- H_2O_2 treatments were eliminated due to their inability to remove CoC without damaging the wood mass (Figure 4.4).

- The 5g:60ml ratio level was eliminated because the degree of CoC solubilization obtainable at the high S:L ratio was significantly lower than at the 1g:60ml and 3g:60ml S:L ratio levels (Compare Figure 4.5 to Figure 4.6).

The remaining options at this point were NaOCl pre-treatment at a solution strength of 0.08%, 1.70%, 6.70%, or 16.7%; at a S:L ratio of either 1g:60ml or 3g:60ml. Of the remaining options, the following treatments were observed to be the most effective at solubilizing CoC:

- NaOCl at a solution strength of 16.7% and S:L ratio of 3g:60ml
- NaOCl at a solution strength of 6.70% and S:L ratio of 1g:60ml
- NaOCl at a solution strength of 16.7% and S:L ratio of 1g:60ml

The above listed treatments are presented in order ascending from less effective at solubilizing CoC to more effective at solubilizing CoC. Supporting data can be viewed in Appendix B.

The CoC removal efficiency is much higher in the 1g:60ml S:L ratio experiments than it is at the 3g:60ml S:L ratio experiment (Table 4.2). However, the improved CoC removals were accompanied by increases in the loss of total wood mass. To quantify this point, data was drawn from the analyses of the three experiments in question and rearranged to show the "total woody mass lost" versus "mass of CoC removed" and displayed in Table 4.3.

The 16.7% NaOCl treatment at a S:L of 3g:60ml was selected as the pre-EK chemical treatment method. The selection was made because of the three remaining treatments, the 16.7% NaOCl treatment at a S:L of 3g:60ml was able to solubilize a

portion of CoC into solution without causing as much damage to the wood sample as the other two pre-EK chemical treatment solutions.

4.3 EK Phase: Effects of Treatment Program on CoC

Three different particle size levels and two different chemical pretreatment levels were examined in EK experiments (Table 4.4). A total of twelve experimental units were assembled, prepared for EK experimentation, tested, sampled, and analyzed for CoC content according to the methods described in Sections 3.3 and 3.4.

4.3.1 Overall CoC Removal

Post-EK experimental samples were collected according to the methods described in Section 3.4.5. The contents of the center compartments were divided into six sections as shown in Figure 3.13 (at the end of Chapter 3). Two samples from each of the six sections were dried, digested, and analyzed for CoC content according to the methods described in Section 3.1.2. Mass removal percentages were calculated by dividing the post-EK CoC content into pre-EK CoC content of each of the six sections. The mass removal percentage of each experimental unit was calculated by averaging the six sectional removals. The overall mass removal percentages of duplicate cells were then averaged to generate the data presented in this section.

4.3.1.1 Mass Fraction Removal: Arsenic

Figure 4.7 shows that there is a particle size effect and a chemical pretreatment effect on arsenic removal. The particle size effect is present at each particle size level in both “control” and “pre-treat” experiments. The effect is demonstrated by a stable 5 % decrease in arsenic removal percentage as the particle size level increases from “fines” to

"plugs" within the "control" experiments. A 5 % decrease in arsenic removal percentage is also observed between the "fines" and "chips" particle size levels within the "pre-treat" experiments. The decrease in arsenic removal percentage increases to 10 % when particle size increases from the "chips" level to the "plugs" level within the "pre-treat" experiments.

A chemical pretreatment effect on arsenic removal is observed at the "fines" and "chips" particle size levels. When pretreatment is applied at the "fines" particle size level, a 4.8 % increase in arsenic removal percentage relative to the "control" is observed. When pretreatment is applied at the "chips" particle size level, a 3.9 % increase in arsenic removal percentage relative to the "control" is observed. Application of chemical pretreatment at the "plugs" particle size level results in a 1.4 % decrease in arsenic removal relative to the "control".

4.3.1.2 Mass Fraction Removal: Chromium

Figure 4.8 shows that there is a particle size effect and a chemical pretreatment effect on chromium removal. Within the "control" experiments, a particle size effect exists at the fines level only. Chromium removal is 5.6 % higher at the "fines" particle size level than it is at the "chips" and "plugs" particle size levels. Within the "pre-treat" experiments however, a particle size effect exists across all three particle size levels. A 3.7 % increase in chromium removal percentage is observed in the "fines / pre-treat" experiments relative to the "chips / pre-treat" experiments. A 9.4 % increase in chromium removal percentage is observed in the "chips / pre-treat" experiments relative to the "plugs / pre-treat" experiments.

A chemical pretreatment effect on chromium removal is observed at the "fines" and "chips" particle size levels. When pretreatment is applied at the "fines" particle size level, a 7.1% increase in chromium removal relative to the "control" is observed. When pretreatment is applied at the "chips" particle size level, a 9.0% increase in chromium removal relative to the "control" is observed. The application of chemical pretreatment results in a very small decrease in chromium removal percentages at the "plugs" particle size level.

4.3.1.3 Mass Fraction Removal: Copper

Copper removal does appear to be affected by the parameters examined in this study. The average mass removal percentage of copper across all conditions examined in this study is 95.3 % with a standard deviation of 0.57 %. These results are summarized in Figure 4.9.

4.3.1.4 Miscellaneous Observations

A point worth noting in this section is that the application of the chemical pretreatment at the "plugs" particle size level has little, if any effect on the post-EK CoC removal percentages. This is true for all three CoC. In Table 4.5, it is shown that chemical pretreatment successfully removes CoC from each particle size level before it is treated electrokinetically. At the "fines" and "chips" particle size levels the chemical pretreatment effect translates into an increase in overall post-EK CoC removal. At the "plugs" particle size level there is virtually no change to the post-EK CoC removal percentage.

The fact that the portion of CoC leached by chemical pretreatment had no effect on the overall post-EK CoC removal at the "plugs" particle size level suggests two things. First, that at the chemical pretreatment solution used in this study is not affecting CoC at the "plugs" particle size level. Second, that the chemical pretreatment solution may not be effective at removing a portion of the CoC that would be removed by the EK process alone at the "plugs" particle size level.

The first observation is supported by the experimental data presented in Table 4.5, which shows that the application of chemical pretreatment has less of an effect on CoC removal at the "plugs" particle size level than it does at the "fines" and "chips" particle size levels. The lack of effectiveness of the chemical pretreatment solution at removing CoC at the "plugs" particle size level may be due to the design of the phase II chemical treatment agent selection experiments. Stage two of the phase II experiments were conducted to improve the effectiveness of the chemical pretreatment solution by optimizing the strength of the solution. The experiments were performed using "fines" particle size level samples as the base material. Neither the "chips" nor the "plugs" particle size levels were considered during this phase of experiments. This means that pretreatment solution strength and S:L ratio were optimized at particle size level that is much smaller than the "plugs" samples. As a result, the effect of chemical pretreatment on the removal of CoC at the "plugs" particle size level may be negligible because the solution strength chosen could never be effective at the much larger "plugs" particle size level.

4.3.1.5 Summary of Findings

- Mass fraction removal of arsenic was affected by both particle size and chemical pretreatment. Of the three CoC arsenic consistently exhibited the second highest post-EK total mass fraction removal.
- Mass fraction removal of chromium was affected more strongly by chemical pretreatment than by particle size. Of the three CoC chromium consistently exhibited the lowest post-EK total mass fraction removal.
- Mass fraction removal of copper was not affected by particle size or chemical pretreatment. Of the three CoC copper consistently exhibited the highest post-EK total mass fraction removal.
- Application of chemical pretreatment at the "fines" and "chips" particle size levels results in an increase in overall removal of all three CoC.
- The chemical pretreatment solution used in this study does not enhance the overall post-EK removal of CoC at the "plugs" particle size level.

4.3.2 Sectional CoC Removal

A sectional CoC removal analysis was performed to examine whether or not the extractions were uniform along the entire length of the EK cell center compartment. Rather than analyzing the CoC removals of each of the six sections individually; the sectional removals were rearranged into three longitudinal slices in one analysis and into two vertical halves in the second analysis. The reworked data is displayed as bar charts so that comparisons between sectional CoC removals could be made.

4.3.2.1 Analysis of Longitudinal Slices

In this analysis the center compartment was divided into anodic, central, and cathodic zones as shown in Figure 4.10. This was done by averaging the sectional removals that fall into each longitudinal slice of the center compartment. For example, the anodic zone shown in Figure 4.10 is the average of sections 1 and 2 shown in Figure 3.13 (at the end of Chapter 3).

Figure 4.11 shows the mass fraction of arsenic removed as a function of longitudinal positioning. The bar chart shows that the difference between any two zones within an individual treatment is less than 2 % in all cases. A single exception exists at the "fines" particle size level.

In the "fines / control" experiments, the cathodic zone removal is approximately 7 % lower than the averaged anodic and central zone removals. In the "fines / pre-treat" experiments, the cathodic zone removal is approximately 2 % higher than the averaged anodic and central zone removals. The variance in cathodic zone accumulation between the "fines / control" and "fines / pre-treat" experiments suggest that applying chemical pretreatment at the "fines" particle size level may cause one or all of the following effects to take place:

- The diffusion or electromigration of arsenic through the cathodic zone is improved by the application of the chemical pretreatment.
- The chemical pretreatment causes a shift in arsenic speciation which results in the reaction of arsenic compounds that would normally accumulate in the cathodic region with other compounds that are able to migrate out of the cathodic region.

- The fraction of arsenic that would normally accumulate within the cathodic zone of the "fines / control" experiment is selectively removed during the chemical pretreatment stage.

Figure 4.12 shows the mass fraction of chromium removed as a function of longitudinal positioning. Similar to arsenic, there are few inconsistencies between sectional chromium removals within individual treatments except at the "fines" particle size level. In the "fines / control" experiments, the cathodic zone removal is approximately 13 % lower than cathodic zone removal in the "fines / pre-treat" experiments. In addition the anodic zone removal in the "fines / control" experiments is approximately 6 % higher than the anodic zone removal in the "fines / pre-treat" experiments. In the "fines / pre-treat" experiments, the cathodic zone removal is approximately 7 % higher than the averaged anodic and central zone removals. The findings in this case are mostly similar to the findings presented for arsenic. The variance in cathodic zone accumulation between the "fines / control" and "fines / pre-treat" experiments suggest that applying chemical pretreatment at the "fines" particle size level may cause one or all of the following effects to take place:

- The diffusion or electromigration of chromium through the cathodic zone is improved by the application of the chemical pretreatment and the diffusion or electromigration of chromium through the anodic zone is decreased by the application of the chemical pretreatment.
- The chemical pretreatment causes a shift in chromium speciation which results in the reaction of chromium compounds that would normally

accumulate in the cathodic region with other compounds that are able to migrate out of the cathodic region.

- Some of the same chromium containing compounds that were migrated out of the cathodic zone may be partially migrating towards the anodic half cell and concentrating in the areas between the cathodic zone and the anodic halve cell at the conclusion of the experiments.

Figure 4.13 shows the mass fraction of copper removed as a function of longitudinal positioning. The mass fraction removal of copper is stable across all of the longitudinal zones. There is no longitudinal positioning effect on the removal of copper.

4.3.2.2 Analysis of Vertical Halves

In this analysis the center compartment was divided into upper and lower zones as shown in Figure 4.14. This was done by averaging the sectional removals that fall into each vertical zone of the center compartment. For example, the upper zone shown in Figure 4.14 is the average of sections 1, 3, and 5 shown in Figure 3.13.

Figure 4.15 shows the mass fraction of arsenic removed as a function of vertical positioning. Arsenic removal is consistently greater in the lower zone than it is in the upper zone by an average margin of 2.5%. This is likely due to the design of the experiments. The inner diameter of the reactor was approximately 3.068" and the electrodes used in the experiments had a 2.750" diameter. This leaves 0.318" electrode coverage gap at the upper zone of the reactors. It is also worth noting that the lower zone removals are greater than the upper zone removals by margins ranging from 1.3% to 5.2% in all experiments except for those performed at the "fines / pre-treat" level. At the "fines / pre-treat" level the upper and lower zone removals are virtually equal.

Figure 4.16 shows the mass fraction of chromium removed as a function of vertical positioning. Chromium removal is consistently greater in the lower zone than it is in the upper zone by an average margin of 2.8%. This observation may be attributed to the same design characteristic mentioned in the analysis of vertical halves for arsenic.

Figure 4.17 shows the mass fraction of copper removed as a function of vertical positioning. The mass fraction removal of copper from the upper and lower zones appears to be stable across all levels of particle size and chemical pretreatment. The average difference between upper zone and lower zone removals is less than 1%. The effect of vertical positioning on the post-EK distribution of copper across the center compartment of the EK cell is negligible.

4.3.2.3 Summary of Findings

In the longitudinal sections analysis:

- The longitudinal positioning of wood sample within the center compartment of the EK cell does not affect the post-EK distribution of CoC except for at the "fines" particle size level.
- There is a chemical pretreatment effect on the post-EK distribution of arsenic across the center compartment at the "fines" particle size level only.
- There is a chemical pretreatment effect on the post-EK distribution of chromium across the center compartment at the "fines" particle size level only.
- There were no apparent effects on the post-EK distribution of copper across the center compartment.

In the vertical sections analysis:

- The vertical positioning of wood sample within the center compartment of the EK cell has an effect on the post-EK distribution of arsenic across the center compartment.
- The vertical positioning of wood sample within the center compartment of the EK cell has an effect on the post-EK distribution of chromium across the center compartment.
- The vertical positioning of wood sample within the center compartment of the EK cell does not have a significant effect on the post-EK distribution of copper across the center compartment.

4.3.3 Effect of Treatment Program on Ionic Mobility

Post-EK experimental samples were collected for TCLP characterization testing according to the methods described in Section 3.4.5. The contents of the center compartments were divided into six sections as shown in Figure 3.13. Two samples from each of the six sections were tested to examine the post-EK mobility of CoC in the treated wood. The results of the post-EK TCLP characterization of each CoC was averaged into an overall post-EK ionic mobility for each experimental condition and presented in Figure 4.18. The post-EK ionic mobilities of each CoC were also charted individually by CoC as a function of their sectional locations. These charts were generated in the same manner as the sectional CoC removals presented in Section 4.3.2 and they have been included in Appendix C. For reference, the results of the raw sample TCLP characterization tests are also shown in Appendix C.

4.3.3.1 Arsenic Mobility

According to Figure 4.18, the lowest post-EK ionic mobilities were found in the "fines / pre-treat" and "chips / pre-treat" experiments. These two treatment conditions were also responsible for the highest overall arsenic mass removals. The high arsenic removals coupled with the decrease in ionic mobility of arsenic suggest that the "fines / pre-treat" and "chips / pre-treat" experimental conditions were able to effectively solubilize arsenic ions into solution then mobilize those ions toward the EK half cells.

In comparison, the post-EK ionic mobilites of arsenic in the "fines / control" and "chips / control" experiments were among the highest achieved in this study. And the overall arsenic mass removals in the "fines / control" and "chips / control" experiments were lower than the overall mass removals achieved in the "fines / pre-treat" and "chips / pre-treat" experiments. The fact that higher ionic mobilities and lower arsenic removals were observed in these "control" experiments relative to their "pre-treat" experiments suggests that the EK process alone was effective in solubilizing arsenic ions, but less effective at mobilizing them towards the EK half cell electrodes. This demonstrates that the chemical pretreatment enhances the overall removal of arsenic from CCA wood at the "fines" and "chips" particle size levels while decreasing the mobility of the remaining ions in the post-EK wood product.

The third lowest ionic mobility was found in the "plugs / control" experiments. This experimental condition is responsible for the second lowest post-EK overall arsenic mass removal. In comparison, the ionic mobility of the "plugs / pre-treat" condition is among the highest. In Section 4.3.1.1 it was established that there was no significant difference between the post-EK overall CoC mass removal percentages of the "plugs /

control" and "plugs / pre-treat" experiments. The fact that chemical pretreatment causes an increase in the ionic mobility of arsenic but has no effect on the post-EK overall mass removal of arsenic suggests that the EK process is the limiting factor for arsenic removal at the "plugs" particle size level. The most obvious reason for this would be the increased density of solid mass in the center compartment of the "plugs" particle size experiments Figure 4.19.

The volume of the center compartments for all of the experiments conducted in this study is fixed. Therefore, it can be assumed that for any increase of solid mass density in the center compartment, there is a decrease in the volume of pore fluid that can be contained in the same space. Since pore fluid is the current carrying medium in the EK experiments, it stands to reason that a reduction in the volume of pore fluid in the center compartment would cause a decrease in the effectiveness of the EK process. In the case of the "plugs / control" experiments, the combination of low ionic mobility and low overall removal is likely due to the ineffectiveness of the EK process at mobilizing and removing arsenic. In the case of the "plugs / pre-treat" experiments, the combination of high ionic mobility and low overall treatment is likely due to the effectiveness of chemical pretreatment at partially solubilizing arsenic ions prior to EK treatment and the ineffectiveness of the EK process at mobilizing the solubilized ions towards one of the EK half cell electrodes.

Note that the mobility of arsenic ions in the cathodic zone of the "fines / control" experiment is significantly higher than the mobility of arsenic in the central and anodic zones (Figure 4.20). The mobility of arsenic in the cathodic zone of the "fines / control" experiment is also higher than the mobility of arsenic in the cathodic zones of the other

experimental conditions examined in this study. The increase in arsenic mobility in the cathodic zone relative to the anodic and central zones in the "fines / control" experiment is accompanied by a decrease in sectional arsenic removals of approximately 7 % (Figure 4.11). Arsenic ions are being solubilized effectively. However, there seems to be a barrier to arsenic ion migration through the cathodic zone of the EK cell center compartment in the "fines / control" experiments that does not exist in any of the other experimental conditions examined in this study.

4.3.3.2 Chromium Mobility

The trends of the post-EK ionic mobility of chromium are similar to those of arsenic. The three lowest ionic mobilities were found in the "fines / pre-treat", "chips / pre-treat", and "plugs / control" experiments. For the "fines / pre-treat" and "chips / pre-treat" experiments the low post-EK ionic mobilities are accompanied by improved post-EK chromium removal percentages. For the "plugs / control" experiment the low post-EK ionic mobility is accompanied by the lowest post-EK chromium removal percentage observed in this study. Since all of these observations are similar to the ones made for arsenic, the same findings reported in Section 4.3.3.1 can also be applied to chromium.

Within each experimental condition, the ionic mobility of chromium is relatively consistent across all of the center compartment sections. An exception to this statement is the "fines / control" experiments, where there is an increase in chromium mobility in the cathodic zone of the EK cell center compartment relative to the central and anodic zones. The increase in ionic mobility is accompanied by a decrease in sectional chromium removals of approximately 8 %. These observations are also similar to those made in the

post-EK mobility analysis of arsenic, and the same findings reported in Section 4.3.3.1 apply to chromium.

The similarities in the overall mass percentage removal and post-EK ionic mobilites between arsenic and chromium suggest that both ions are affected by common forces during the EK process. An example of data supporting this theory is shown in the CoC concentration curve in Figures 4.21 and 4.22. The arsenic and chromium cathodic concentration profiles for two EK experimental units are plotted on top of one another in Figures 4.21 and 4.22; and the cathodic concentration profile for arsenic is very much similar to the cathodic concentration profile for chromium.

4.3.3.3 Copper Mobility

Results of the post-EK copper mobility can be viewed in Appendix C. The graph is relatively featureless, showing copper mobilities of less than 0.60 for all sections under all treatment conditions. Given that the total removal of copper was greater than 94 % in all of the treatment conditions; it is likely that the small fraction of copper remaining in the wood exists as a chemical species that is strongly bound to the sample material in its post-EK state.

4.3.3.4 Summary of Findings

- For arsenic and chromium the lowest post-EK ionic mobilities were observed in the “fines / pre-treat”, “chips / pre-treat”, and “plugs / control” experiments. Since the highest removal efficiencies for arsenic and chromium are observed at the “fines / pre-treat” and the “chips / pre-treat” experiments levels; it seems likely that the low ionic mobilities observed for these experiments is

due to the lower availability arsenic and chromium in the EK cell center compartment after EK treatement. Since the lowest removal efficiencies for arsenic and chromium was observed at the "plugs / control" experiments level; it seems likely that the low ionic mobilities observed for these experiments is due to the relative ineffectiveness of the experimental program in solubilizing arsenic and chromium ions.

- For arsenic and chromium at the "plugs" particle size level, the application of chemical pretreatment prior to EK results in an increase in post-EK ionic mobility and had no effect on the overall mass removal. This suggests that the chemical pretreatment was able to partially solubilize arsenic and chromium ions prior to EK treatment; but that the EK process was ineffective at mobilizing/removing the solubilized ions. EK appears to be the limiting factor for arsenic and chromium removal at the "plugs" particle size level.
- Similarities exist between arsenic and chromium cathodic accumulation rates for all experimental conditions examined in this study. The similarities in the overall mass percentage removal and post-EK ionic mobilites between arsenic and chromium suggest that both ions are affected by common forces during the EK process.

4.3.4 Post-EK CoC distribution across the EK cell

The zones of the EK cell in which CoC may accumulate by the end of the experimental program are listed in Table 4.6. Samples from each of the accumulation zones were collected and analyzed for CoC according to the methods described in

Chapter 3. The results presented in this section were calculated on a post-EK zonal CoC accumulation basis. The zonal accumulation percentages were calculated as follows:

- For each individual EK cell, the post-EK CoC content of all of the accumulation zones was combined into a sum.
- Each zonal CoC accumulation was divided into its respective EK cell sum.
- Duplicate EK cell zonal accumulations were averaged.

Because the calculations were performed in a normalized manner the results within each experimental condition presented in this section are qualitative in nature.

4.3.4.1 EK Cell center compartment sectional accumulation of CoC

In general, the sectional accumulations of all three CoC are similar within each individual treatment. An example of this can be seen in Figure 4.23 where the accumulation percentages for arsenic, chromium, and copper are consistent across EK cell center compartment sections 1 through 6. Accumulation percentages for each individual CoC vary by less than 1 % across all six center compartment sections. This verifies that the CoC are distributed evenly across the length of the center compartment at the conclusion of the EK experiments. This is the case for all CoC in every experimental condition except for the "fines / control" condition (Figure 4.24). In the "fines / control" experiments there was an observable increase in the amount of CoC accumulated in EK cell center compartment sections five and six. This helps to confirm similar observations reported in Sections 4.3.2 and 4.3.3 for arsenic and chromium. The following observations were made regarding the accumulation of CoC in center compartment sections 5 and 6 of the "fines / control" experiments:

- An increase in the level of arsenic accumulation (1.6 %), chromium accumulation (2 %), and copper accumulation (6 %) was observed in EK cell center compartment sections 5 and 6 relative to sections 1 through 4 in the "fines / control" experiments
- Figure 4.25 reveals that in the "fines / pre-treat" experiments, CoC accumulation in the EK cell center compartment sections rises steadily, by no more than 1 percentage, as you move horizontally from section 6 to section 1.
- Application of chemical pretreatment to the "fines" particle size level causes an increase in the anodic accumulation percentage for all three CoC's (Tables 4.7- 4.9).

These results suggest that the application of chemical pretreatment at the "fines" particle size level causes an increase in the percentage of CoC that migrate toward the anodic half cell. This effect may be the result of a change in speciation of CoC ions caused by chemical pretreatment. The effect could also have been caused by the removal of the fraction of CoC prone to cathodic migration during chemical pretreatment. A high accuracy mass balance or a speciation study would have to be conducted to confirm which of these theories is more likely to be correct.

4.3.4.2 Anodic accumulation zone versus Cathodic accumulation zone

Once CoC are removed from the center compartment they may accumulate in one of eight zones. There are four accumulation zones on the anodic side of the EK cell and four accumulation zones on the cathodic side of the EK cell (Table 4.6). In this analysis, the four accumulation zones on the anodic end of the EK cell are combined into a single

"anodic accumulation" category, and the four accumulation zones on the cathodic end of the EK cell are combined into a single "cathodic accumulation" category.

According to Table 4.7; arsenic ions tend to accumulate more heavily on the anodic side of the EK cell than the cathodic side. One exception was observed at the "fines / control" particle size level where it was observed that arsenic accumulated in the cathodic side by 2.3 % more than in the anodic side. In the "control" experiments, anodic and cathodic zone accumulation percentages are relatively equal, with less than 5% difference between zonal accumulation percentages at all three particle size levels. The application of chemical pretreatment at the "fines" and "chips" particle size levels caused a rise in anodic accumulation. The same pretreatment effect was not observed at the "plugs" particle size level.

According to Table 4.8, chromium ions generally tend to accumulate more on the cathodic side of the EK cell than the anodic side. The cathodic zone accumulation percentage is greater than anodic zone accumulation percentage in all cases except for the "chips / pre-treat" experiments. In the "chips / pre-treat" experiments the anodic zone accumulation percentage is 6% greater than the cathodic zone accumulation percentage. In addition there is a large decrease in the cathodic zone accumulation percentage of chromium at the "chips" particle size level relative to the "fines" and "plugs" particle size levels. This is true in the "control" experiments and "pre-treat" experiments. A possible explanation of the phenomenon is contained in the following statement (Hunt and Garratt, 1967):

> … preservatives penetrate much more readily in the direction of the grain (longitudinally) than across it (radially or tangentially).

At the "fines" particle size level, the small size of the particles causes the alignment of the fines to be insignificant. At the "plugs" particle size level, the plugs were loaded into the center compartment in a way that guaranteed the wood sample would be longitudinally aligned, so that EK power would be applied in the direction of the wood grains. At the "chips" particle size level, the particles generated by the chipper-shredder were small in size, but oblong in shape. During EK cell loading, the shape and small size of the wood chips caused them to be packed into the center compartment in a randomly aligned manner. The difference in particle alignment may have had an effect on the migration of chromium species toward the cathodic accumulation zones in the "chips" particle size experiments.

According to Table 4.9, copper accumulates overwhelmingly in the cathodic zone. This is the case in all experiments except for the "chips / pre-treat" experiments. The trends of copper accumulation as a function of particle size are similar to the trends in chromium accumulation.

4.3.4.3 Summary of Findings

In the sectional CoC accumulation analysis:

- Within each center compartment, there was little variation between the post-EK sectional accumulations of CoC, suggesting a uniform overall treatment of CCA wood.
- An exception to the previous statement is the "fines / control" experiments where increased center compartment CoC accumulations are observed in the cathodic zone of the EK cell center compartment.

In the anodic versus cathodic CoC accumulation analysis:

- Arsenic generally tends to accumulate in the anodic zone.
- Chromium generally tends to accumulate in the cathodic zone.
- Copper generally tends to accumulate in the cathodic zone.
- The removal rate of chromium and copper towards the cathodic zone was much lower at the "chips" particle size level than it was at the "fines" or "plugs" particle size levels. The cause of this may be due to the process used for loading "chips" particle size level samples into the EK cell. The decrease in effectiveness of EK at the chips level may be due to inconsistent alignment of the chips in the EK cell center compartment.

4.4 CoC Accumulation and Transport Rate Modeling

During the experimental runs, fluid samples were collected from different sections of the EK cells and analyzed according to the methods described in Section 3.4.4. This data was used to generate CoC concentration curves for the anodic half cells, cathodic half cells, and pore fluid sampling zones of each experimental unit (concentration curves presented in Appendix G). "ACTIVESYNC" software was then used to model the concentration curves. Models for the CoC accumulation rate were then generated by taking the derivatives of the concentration curve models and making assumptions so that the parameters of the model could be directly associated with a physical mechanism of CoC accumulation or CoC transport. For all of the experimental conditions examined in this study, the concentration curve models behaved according to one of the two following equations.

The concentration (C_t) of arsenic and chromium in the anodic and cathodic half cells as a function of time can be modeled by a simple exponential decay equation:

$$C_t = A\ e^{-Rt} \tag{4.1}$$

where: C_t = CoC concentration (*ppm*)

t = time (*days*)

A = pre-exponential factor (*ppm*)

R = rate constant (day^{-1})

In these models the initial CoC concentration in the half cells can be assumed to be zero because the half cells were filled with tap water at the onset of the experimental run. The pre-exponential factor is a negative number for all of the cases examined in this study. This model describes the concentration of CoC into a control volume as increasing rapidly early in the experiment, then stabilizing at a theoretical maximum concentration as time progresses.

The concentration of copper in the anodic and cathodic half cells and the concentration of all three CoC in pore fluid zones can be modeled by the following equation:

$$C_t = A\left[1 - e^{-(k1)\,t} - \left(\frac{k_1}{k_1 + k_3}\right)\left(1 + \frac{k_1 e^{-(k1+k3)\,t} - (k_1 + k_3)e^{-(k2)\,t}}{-k_1 + k_2 + k_3}\right)\right] \tag{4.2}$$

where: C_t = CoC concentration (*ppm*)

t = time (*days*)

A = pre-exponential factor (*ppm*)

k_1, k_2 , and k_3 = rate constants (day^{-1})

This model is similar to the concentration curve of the reactive intermediate for a first order series reaction in which the reactant (X) is irreversibly converted to a reactive intermediate (Y). The reactive intermediate species (Y) then comes to an equilibrium with another product (Z). The reaction mechanism is shown in Equation 4.3.

$$X \xrightarrow{k1} Y \underset{k3}{\overset{k2}{\rightleftharpoons}} Z \tag{4.3}$$

Equation 4.3 may be used to interpret Equation 4.2 as a model of the concentration of component "Y" as a function of time with respect to parameters "k_1", "k_2", "k_3" and "A". This model describes the concentration of CoC into a control volume as increasing rapidly early in the experiment to a maximum observed concentration, then decreasing to a level below that of the maximum observed concentration before stabilizing at a lower concentration as time progresses.

4.4.1 CoC Accumulation Rates in Half Cells

4.4.1.1 Arsenic

The accumulation of arsenic in both half cells is modeled by Equation 4.1. The accumulation rate can be found by taking the derivative of Equation 4.1 with respect to time as shown in Equation 4.4.

$$\frac{d(C_t)}{dt} = -(AR)\, e^{-Rt} \tag{4.4}$$

In this series of experiments, the equilibrium point of the accumulation model is reached in less than 10 days with little or no activity occurring thereafter. Since this is the case, it will be assumed that the initial rate of arsenic accumulation at "t = 0 days" is

sustainable over the time period in which accumulation activity is observable. The product of the rate constant "R" and the pre-exponential factor "A" will be the basis for comparison between the different half cell arsenic accumulation rates.

The anodic half cell accumulation rate of arsenic at the "fines / control" level is approximately 65 ppm/day which is significantly higher than the accumulation rates of the other treatment level examined in this study that range from 13-26 ppm/day (Figure 4.26). The rate of arsenic accumulation in the anodic half cell is at least an order of magnitude higher than the rate of arsenic accumulation in the cathodic half cell in all of the treatments examined in this study. A particle size effect on the rate of arsenic accumulation in the anodic half cell was observed in Figure 4.26 as well. The rate of arsenic accumulation in the anodic half cells decreases as particle size increases. The strongest particle size effect is present in anodic accumulation rates at the "control" treatment levels. The same trend is present (but much less extreme) in the cathodic accumulation rates for the "pre-treat" experiments, the cathodic accumulation rates for the "control" experiments, and the anodic accumulation rates for the "pre-treat" experiments.

A pretreatment effect on the rate of arsenic accumulation in the anodic and cathodic half cells exists at all of the particle size levels examined in this study. For every particle size level, the application of chemical pretreatment causes a decrease in the rate of arsenic accumulation in the anodic and cathodic half cells. The pretreatment effect is strongest at the "fines" particle size level; followed by the "chips" and then the "plugs" particle size levels.

It was observed in section 4.3.1 that the application of pretreatment at the "fines" particle size level causes a 4.8 % increase in overall arsenic removal percentage and that application of pretreatment at the "chips" particle size level causes a 3.9 % increase in overall arsenic removal percentage. So the application of the chemical pretreatment resulted in an increase in the overall removal percentage of arsenic and a decrease in the initial rates of arsenic accumulation in the anodic half cell and in the cathodic half cell. A possible explanation for this is that the application of chemical pretreatment removed the same arsenic ions that would have been targeted by early EK, lowering the initial availability of arsenic in the EK cell center compartment, and negatively affecting the anodic and cathodic half cell accumulation rates for arsenic. It is also possible that the application of the chemical pretreatment resulted in a shift the speciation of arsenic that reduced the ability of EK to electromigrate arsenic ions to the anodic and cathodic half cells early in the EK experiments. In either case the end result was slower rates for arsenic accumulation when chemical pretreatment was applied.

4.4.1.2 Chromium

The accumulation of chromium in both half cells is modeled by Equation 4.1. The rate of accumulation will be quantified by taking the product of the rate constant "R" and the pre-exponential factor "A".

The anodic and cathodic half cell accumulation rates of chromium at the "fines / pretreat" level are significantly higher than the accumulation rates at any other treatment level examined in this study (Figure 4.27). The rate of chromium accumulation in the cathodic half cell is greater than the rate of chromium accumulation in the anodic half cell at all treatment levels except for the "chips / pretreat" level.

A particle size effect exists in anodic half cell accumulation rates. As the particle size increases the anodic accumulation rate decreases. The effect is present at both treatment levels, however the effect is more extreme at the "pretreat" level than it is at the "control" level. The same trend is observed for cathodic accumulation rates.

A pretreatment effect exists in both anodic and cathodic half cell chromium accumulation rates. The application of chemical pretreatment causes the rate of chromium accumulation to increase. This effect is strongest at the "fines" particle size level; followed by the "chips" and "plugs" particle size levels.

It was observed in section 4.3.1 that the application of pretreatment at the "fines" particle size level causes a 7.1 % increase in overall chromium removal percentage and that application of pretreatment at the "chips" particle size level causes a 9.0 % increase in overall chromium removal percentage. The application of the chemical pretreatment resulted in an increase in the overall removal percentage of chromium and an increase in the initial rates of chromium accumulation in the anodic half cell and in the cathodic half cell. So in addition to improving the overall removal efficiency of chromium; the application of chemical pretreatment also improves the initial accumulation rates of chromium in the anodic and cathodic half cells. This is a strong indication that the application of the chemical pretreatment results in a shift the speciation of chromium that improves the ability of EK to electromigrate chromium ions to the anodic and cathodic half cells early in the EK experiments.

4.4.1.3 Copper

In the copper concentration curves, the concentrations peak early in the experiments. The peak is followed by a slow, steady decrease in the concentration of

copper for the remainder of the experimental run. Therefore, Equation 4.2 was used to model the half cell accumulation rate of copper.

The decrease in the half cell concentration of copper is likely due to copper precipitating out of the half cell solutions and depositing on the electrodes and the side wall of the half cell. The precipitation of copper out of the half cell solutions was observed in all of the experiments. Copper precipitation was more extreme in the cathodic half cells, where the deposits became visible within the first week and continued to accumulate at the bottom of the half cell as the experiments progressed. A photo of this observation is included in Figure 4.28.

A schematic representation of the solid deposition effect can be viewed in Figure 4.29. In the figure, rate constants "k_1-k_3" are associated with physical mechanisms of copper ion transport as follows:

- k_1 is associated with the migraton of CoC into the half cell
- k_2 is associated with the precipitation of CoC out of the half cell solution
- k_3 is associated with the solubilization of precipitated CoC back into the half cell solution

The accumulation rate can be found by taking the derivative of Equation 4.2 with respect to time. The derivative is shown in Equation 4.5.

$$\frac{d(C_t)}{dt} = -\left(\frac{A k_1 e^{-(k1+k2+k3)t}}{k_1 - k_2 - k_3}\right)\left[k_2 e^{(k1)t} - (k_1 - k_3)\, e^{(k2+k3)t}\right] \tag{4.5}$$

It is difficult to make generalized comparisons between the copper accumulation rates of different treatments with Equation 4.5 because it contains four different

parameters. To simplify the Equation 4.5 model to a point where meaningful comparisons can be made between the different experiments, the model equation was interpreted in such a way that the rate constants "k_1-k_3" from Equation 4.3 are physically associated with transport/accumulation mechanisms. The following assumptions were made to simplify the model:

- The initial ionic mobility of copper is much greater than that of arsenic or chromium (Section 4.1.3); and the accumulation of copper in half cells occurs at a high initial rate.
- The accumulation of copper in half cells is irreversible; the drop in the half cell concentrations is likely due to the precipitation of a solid phase of copper out of the half cell solution; and the experimental setup was such that the weekly half cell samples could not account for the precipitated forms of copper (Figure 4.54).

If copper accumulates rapidly and irreversibly at high concentrations in the half cells, and the drop in the half cell concentrations of copper later in the experiments can be attributed to the precipitation of copper out of the solution; then it can be assumed that the initial rate of copper accumulation at "t = 0 days" is sustainable over the time period in which accumulation activity in the EK half cells occurs. Equation 4.6 is the result of applying the assumptions to Equation 4.5.

$$\frac{d(C_t)}{dt} = A k_1 \tag{4.6}$$

The basis for comparison between different half cell copper accumulation rates is the product of the pre-exponential factor "A" and the rate constant "k_1".

Figure 4.30 shows that the rate of copper accumulation in the cathodic half cell is greater than the rate of copper accumulation in the anodic half cell at all treatment levels except for the "plugs / pretreat" level.

A particle size effect on the half cell accumulation rates of copper was observed in all of the experiments examined in this study. In general, the highest accumulation rates were observed in the "plugs" particle size level, followed by the "fines" and then the "chips" particle size levels. This trend was present in the anodic and cathodic half cell accumulation rates of the "control" experiments and the anodic half cell accumulation rate of the "pre-treat" experiments. For the cathodic half cell accumulation rates in the "pre-treat" experiments, the highest accumulation rates were observed at the "fines" particle size level, followed by the "plugs" and then the "chips" particle size level. It is interesting to note that the lowest accumulation rates are observed at the intermediate "chips" particle size level instead of at one of the more extreme particle size levels. The effect is likely due to the particle size alignment issue that was presented in in detail back in Section 4.3.4.2.

A pretreatment effect exists in the anodic half cell copper accumulation rates. The application of chemical pretreatment causes a large increase in the rate of copper accumulation in the anodic half cell. This effect is strongest at the "plugs" particle size level; followed by the "chips" and "plugs" particle size levels. The same effect is not observed in the cathodic half cell accumulation rates; where the application of chemical pretreatment causes a decrease in the rates of copper accumulation at the "chips" and "plugs" particle size levels and a small increase in the rate of copper accumulation at the "fines" particle size level. This is a strong indication that the application of the chemical

pretreatment results in a shift the speciation of copper that improves the ability of EK to electromigrate copper ions as anions to the anodic half cells early in the EK experiments.

4.4.1.4 Summary of Findings

- Arsenic: The anodic accumulation rates are greater than cathodic accumulation rates for all of the experiments examined in this study.
- Arsenic: The highest accumulation rate was observed in the anodic half cell of the "fines / control" experiments.
- Arsenic: A strong particle size effect exists in the anodic half cell accumulation rates of the "control" experiments. As particle size decreases, accumulation rate increases.
- Arsenic: A strong pretreatment effect was observed in the anodic half cell accumulation at the "fines" particle size level. Application of pretreatment causes the accumulation rate to decrease significantly; especially at the "fines" particle size level.
- Chromium: The cathodic accumulation rates are greater than anodic accumulation rates for all of the experiments examined in this study with the exception of the "chips / pretreat" experiments.
- Chromium: The highest accumulation rates in both the anodic and the cathodic half cells were observed in the "fines / pretreat" experiments.
- Chromium: A strong particle size effect exists in the anodic and cathodic half cell accumulation rates of the "pre-treat" experiments. As particle size decreases, accumulation rates increase.

- Chromium: A strong pretreatment effect was observed in the anodic and cathodic half cell accumulation rates at the “fines” particle size level. Application of pretreatment causes the accumulation rate to increase significantly.
- Copper: The cathodic accumulation rates are greater than anodic accumulation rates for all of the experiments examined in this study with the exception of the “plugs / pretreat” experiments.
- Copper: The anodic and cathodic half cell accumulation rates are lowest at the “chips” particle size level for both “control” and “pretreat” experiments.
- Copper: A strong pretreatment effect was observed in the anodic half cell accumulaton rates at the “plugs” and “fines” particle size levels. Application of pretreatment caused an increase in the accumulation rate.

4.4.2 CoC Center Compartment Transport Rates

During EK experimental runs, pore fluid samples were collected from the three sampling ports on the center compartment on a weekly basis and analyzed for CoC content according to the methods described in Section 3.4.4. The results of the weekly sampling analyses were compiled into pore fluid concentration curves that are included in Appendix G. The objective of collecting these samples was to generate models that effectively describe the rate of CoC accumulation and deaccumulation in the pore fluid sampling zones of the EK cell center compartment.

The goal of these experiments is to effectively solubilize CoC in the center compartment; then to mobilize those CoC away from the pore fluid zones and toward the EK half cells. The accumulation of CoC in the pore fluid zones is desirable early in the

experiments because it is an indication of the conversion of CoC from the solid phase where the CoC is immobile into an ionic phase that can be affected by the EK process. As the experiment progresses, the deaccumulation of solubilized CoC ions from the pore fluid zones is desirable because it is an indication of effective transport of CoC ions out of the pore fluid zones.

The general trend in the pore fluid concentration curves is for the concentration of CoC to peak early in the experiment, then to slowly and steadily decrease for the remainder of the experimental run. Equation 4.2 was used to model the CoC concentrations as a function of time in the pore fluid sampling zones and Equation 4.5 was used to model the CoC accumulation rates within pore fluid sampling zones as a function of time.

It is difficult to make generalized comparisons between the CoC transport rates through pore fluid zones with Equation 4.5 because it contains four different parameters. In order to simplify the Equation 4.5 model to a point where meaningful comparisons can be made between the different experiments, the pore fluid transport model equations were interpreted in such a way that the rate constants "k_1-k_3" from Equation 4.2 are physically associated with transport/accumulation mechanisms.

A schematic representation of the physical model can be viewed in Figure 4.31. In the figure, rate constants "k_1-k_3" are shown associated with the mechanisms described in Equation 4.3 as follows:

- Rate constant "k_1" is associated with the generation of CoC in the pore fluid zone by solubilizing CoC from the contaminated wood into the pore fluid.

- Rate constant "k_2" is associated with the migration of CoC out of the pore fluid zone.
- Rate constant"k_3" is associated with the migration of CoC into the pore fluid zone.

It will be assumed that the initial increase of CoC in the pore fluid sampling zones is the result of the rapid, irreversible solubilization of CoC from the contaminated wood into the pore fluid combined with the relatively slower rate of CoC transport out of the pore fluid zones (ie: "k_1" is the dominant rate constant early in the experiments) . It will also be assumed that the initial solubilization reaction is sustainable over the span of the first 1-2 weeks and the CoC accumulation rate at "t = 0" will be taken as the basis for comparison between initial CoC solubilization rates. The application of these assumptions to Equation 4.5 results in Equation 4.6. Equation 4.6 describes the basis for comparison between different initial CoC solubization rates as the product of the pre-exponential factor "A" and the rate constant "k_1". A good EK treatment would be characterized by a high "$A \times k_1$" value; which would indicate that CoC were effectively solubilized from the contaminated wood into the pore fluid zones within the first two weeks of the experimental run.

Since there is a finite amount of contaminated wood in each experimental unit, it is logical to assume that the initial solubilization reactions cannot be sustained for more than 2 weeks. Therefore it will be assumed that after 2 weeks, the "$A \times k_1$" term will decrease to a much slower rate and the "k_2" and "k_3" rate constants will dominate the model. Equation 4.7 is the result of applying this assumption to Equation 4.3.

$$Y \underset{k3}{\overset{k2}{\rightleftharpoons}} Z \tag{4.7}$$

Equation 4.7 is an elementary first order reversible reaction. The ratio of product to reactant at the time when equilibrium is reached may be quantified by taking the equilibrium constant, which is shown below.

$$k_{EQUIL} = \frac{k_3}{k_2} \tag{4.8}$$

Equation 4.8 shows the basis for comparison between different pore fluid zone transport rates as being the quotient of the rate constant "k_3" and the rate constant "k_2". A good EK treatment would be characterized by a low k_{EQUIL} value; which would indicate that there is a lower concentration of solubilized CoC (*Y* species) remaining in the pore fluid of the EK cell center compartment as the EK experiment comes to its conclusion. In the terms of equation 4.7, the equilibrium concentrations of CoC would be shifted to the right towards the "*Z*" species when the k_{EQUIL} value is low.

At this point it must be made clear that a high "$A \times k_1$" value, by itself, does not necessarily correspond to an effective EK experiment. A high "$A \times k_1$" value specifically means that the concentration of CoC in a pore fluid sampling zone is increasing rapidly at the start of an experimental run due primarily to the solubilization of CoC from the solids contained in the center compartment into the pore fluid. High "$A \times k_1$" values can be misleading when comparing between different levels examined in this study due to the fact that the mass of CoC in the center compartment at the onset of the experiments is not a fixed number for all of the particle sizes. For example, the mass of dry solids contained in the center compartment of an EK experimental unit at the "fines" particle size level is,

on average, 50 grams more than the mass of dry solids contained in the center compartment of an EK experimental unit at the "chips" particle size level. And although the mass of dry solids contained in the center compartment of the "fines / control" experiments and the "fines / pre-treat" experiments are similar; in the "pre-treat" experiments CoC were removed from the contaminated wood prior to EK treatment. In both of these situations, the availability of CoC in the EK cell center compartment is inconsistent at the start of the EK experiments. It is expected that this would have an effect on the initial CoC solubilization rate (ie: reduced availability of CoC in the "chips / pretreat" experiment could cause the initial CoC solubilization rate to be much less than that of the "fines / control" experiment).

Low k_{EQUIL} values can be misleading also. A low k_{EQUIL} value specifically means that there is a low concentration of CoC in a pore fluid zone at the conclusion of an EK experiment. A low k_{EQUIL} value does not verify an all-around high rate of CoC mobilization; it only verifies that the solubilized forms of CoC that became available in a pore fluid zone at some point during the EK experiment were effectively mobilized away from the pore fluid zone. The k_{EQUIL} value does not account for the unsolubilized portion of CoC remaining in the solid component of the pore fluid zone. As a result, a low k_{EQUIL} value can just as well be attributed to a high rate of CoC mobility through a pore fluid zone as it can to a lack of solubilized CoC available in a pore fluid zone.

The data presented in this section should not be used to make inferences about how much more effective the EK process was at solubilizing one CoC relative to another CoC. The model may be used to make a qualitative comparison between the rates of the

accumulation of CoC into a pore fluid zone, and the subsequent deaccumulation of that portion of solubilized CoC from the pore fluid zone.

4.4.2.1 Arsenic

The results of the initial CoC solubization rate analysis are presented in Figure 4.32. The initial pore fluid zone accumulation rates at the "fines / control" level were much higher than in the rest of the experiments. In the "fines / control" experiments, the initial arsenic accumulation rates were 209.5 ppm/day in the port 1 sampling zone, 177.6 ppm/day in the port 2 sampling zone, and 255.5 ppm/day in the port 3 sampling zone. In comparison, the initial pore fluid accumulation rates for arsenic in experiments other than the "fines / control" experiments were consistently lower, with arsenic accumulation rates of 61.2 ± 23.9 ppm/ day in the port 1 sampling zone, 64.4 ± 31.4 ppm/ day in the port 2 sampling zone, and 35.9 ± 8.9 ppm/ day in the port 3 sampling zone. This effect could be due to the combination of the initial availability of arsenic in the non-pretreated wood sample and the effectiveness of EK at removing arsenic at the fines particle size level as observed in section 4.3.1.1.

The results of the k_{EQUIL} analysis are presented in Figure 4.33. Figure 4.33 shows that the lowest k_{EQUIL} value occurred in the "fines / pre-treat" experiments. This k_{EQUIL} value is significantly less than the k_{EQUIL} value observed in the "fines / control" experiments. This is an indication that a pretreatment effect exists at the "fines" particle size level where application of pretreatment causes an increase in the rate of transport of mobilized arsenic ions through the pore fluid sampling zones. Chemical pretreatment has the opposite effect at the "chips" and "plugs" particle size levels; and that effect is much more extreme in the port 3 sampling zones where the k_{EQUIL} values are twice as high in

the “chips / pre-treat” experiments than they are in the “chips / control” experiments; and approximately four times as high in the “plugs / pre-treat” experiments than they are in the “plugs / control” experiments.

At this point it should be noted that a trend exists in all except for the “fines / pretreat” experiments. The trend is for the k_{EQUIL} values in the port 1 and 2 sampling zones to be similar to one another and for there to be a spike in the k_{EQUIL} value at the port 3 sampling zone. This finding suggests that there could either be a barrier to arsenic ion migration through the port 3 sampling zone; or that the solubilization rate of arsenic in the port 3 sampling zone has been slowed down to the point that arsenic ions are still being solubilized into the pore fluid zone 50-60 days into the EK experimental run.

4.4.2.2 Chromium

The results of the initial CoC solubization rate analysis are presented in Figure 4.34. The initial pore fluid accumulation rates are much higher in the “fines / control” and “fines / pretreat” experiments than in the other experiments examined in this study. However, the magnitudes of the accumulation rates are distributed across the pore fluid zones differently. At the “fines / pretreat” level, the initial chromium accumulation rate is approximately 24.1 ppm/day in the port 1 sampling zone; approximately 59.5 ppm/day in the port 2 sampling zone; approximately 77.6 ppm/day in the port 3 sampling zone; and the average chromium accumulation rate across all three pore fluid zones is approximately 53.7 ppm/day. At the “fines / control” level, the initial chromium accumulation rate is approximately 58.8 ppm/day in the port 1 sampling zone; approximately 76.0 ppm/day in the port 2 sampling zone; approximately 52.7 ppm/day in the port 3 sampling zone; and the average chromium accumulation rate across all three

pore fluid zones is approximately 62.5 ppm/day. This indicates that for the "fines" particle size experiments; the level of chromium mobilization is higher on average and more consistent across the center compartment of the EK cell when no pretreatment is applied. When pretreatment is applied, the average pore fluid accumulation rate is lower and chromium is accumulating to a higher degree in the pore fluid zones adjacent to the cathodic half cell.

The results of the k_{EQUIL} analysis are presented in Figure 4.45. Figure 4.45 shows that on average, the lowest k_{EQUIL} values occur in the "fines / control" and "fines / pre-treat" experiments. This is encouraging because it means that the two experimental units with the highest initial chromium accumulation rates also have the highest diffusion rates later in the experiments. At this point it should be noted that the distribution of k_{EQUIL} values across the pore fluid zones of the "fines / control" and "fines / pretreat" experiments are not consistent. The application of pretreatment to "fines" causes there to be a dip in the k_{EQUIL} value in the port 1 and 2 sampling zones and a spike in the k_{EQUIL} value in the port 3 sampling zone. This indicates that the application of chemical pretreatment improves the diffusion rate of chromium through the pore fluid zones closest to the anodic half cell and decreases the diffusion rate of chromium through the pore fluid zone adjacent to the cathodic half cell; but this occurs at the "fines" particle size level only. The same trend does not exist at the "chips" particle size level or at the "plugs" particle size level. As a matter of fact, the application of chemical pretreatment affects each of the particle size levels differently. At the "chips" particle size level, the application of chemical pretreatment causes a decrease in the rate of chromium ion diffusion through the port 1 sampling zone and no significant change in the rate of

chromium ion diffusion through the port 2 and 3 sampling zones. At the "plugs" particle size level, the application of chemical pretreatment causes an decrease in the rate of chromium ion diffusion through the port 1 sampling zone, an increase in the rate of chromium ion diffusion through the port 2 sampling zone, and no significant change in the rate of chromium ion diffusion through the port 3 sampling zone.

The trends in center compartment transport rates of chromium ions are vague at best. One trend that is relatively consistent is that pore fluid zones having high initial chromium solubilization rates tend to have lower chromium diffusion rates. This could mean that the assumption that chromium ion solubilization occurs primarily at the start of the experiment may not be accurate; and that the chromium ion transportation rates in each pore fluid zone are indeed affected by latent chromium ion solubilization that is still occurring 50-60 days into the experiment.

4.4.2.3 Copper

The results of the initial CoC solubization rate analysis are presented in Figure 4.36. The initial pore fluid accumulation rates of copper do not vary by much between the treatments examined in this study. The rates are slightly higher in the "fines / control" and "plugs / pretreat" experiments; but not overwhelmingly so.

The basis for comparison between the different pore fluid copper accumulation rates later in the experiments is the k_{EQUIL} value described in equation 4.8. The results of this analysis are presented in Figure 4.37. Figure 4.37 shows that the k_{EQUIL} values do not vary by much between the treatments examined in this study. The k_{EQUIL} values are lower in the "fines / control" and "plugs / pretreat" experiments; but not overwhelmingly so.

The fact that there are not any obvious trends in the initial rate of copper accumulation or in the latter-experiment diffusion rate of copper is not surprising considering that the average mass removal percentage of copper across all of the experiments performed in this study was 95.3 % with a standard deviation of 0.57 %. The results of this analysis are further proof that the different levels of particle size and chemical pretreatment that were examined as a part of this study have little effect on the overall removal of copper, or on the removal rates of copper. However, there is one trend that was observed in this analysis that is interesting to note. The pore fluid zones having high initial copper solubilization rates tend to have higher latter-experiment copper diffusion rates (relative to the copper diffusion rates of other pore fluid zones). This is opposite of the trend observed in chromium removal rates, where pore fluid zones having high initial chromium solubilization rates were observed to have lower chromium diffusion rates later in the experiments. This could be an indication that copper is both rapidly mobilized at the start of the experiment and rapidly diffused through the pore fluid zones as the experiments progresses.

4.4.2.4 Summary of Findings

- Arsenic: The highest initial pore fluid accumulation rates occurred in the "fines / control" experiments.
- Arsenic: The highest pore fluid transport rates occurred in the "fines / pretreat" experiments.
- Arsenic: At the "fines" particle size level; application of chemical pretreatment causes an increase in all three of the pore fluid transport rates.

- Chromium: The highest initial pore fluid accumulation rates occurred at the "fines / control" experiment, followed closely by the "fines / pretreat" experiment. All other experiments had much lower initial pore fluid accumulation rates.
- Chromium: The highest pore fluid transport rates occurred in the "fines / control" experiments, followed by the "fines / pretreat"experiments.
- Chromium: At the "fines" particle size level; application of chemical pretreatment causes a decrease in in port 1 and port 2 initial pore fluid accumulation rates and a decrease in port 3 initial pore fluid accumulation rates.
- Chromium: At the "fines" particle size level; application of chemical pretreatment causes an increase in port 1 and port 2 pore fluid transport rates and a decrease in port 3 pore fluid transport rates.
- Copper: Initial pore fluid accumulation rates and pore fluid transport rates do not vary significantly with respect to the different experimental conditions examined in this study. The "fines / control" experiments and the "plugs / pretreat" experiments have slightly higher initial accumulation rates and pore fluid diffusion rates than the rest of the experimental units.
- Copper: A correlation exists between initial accumulation rates and pore fluid transport rates. Experimental units with higher initial accumulation rates also had higher pore fluid transport rates.

4.5 Daily and Weekly Sampling Data Reporting

As indicated in Section 3.4.4, the following measurements were recorded on a daily basis during EK experimental runs: potential difference across the cell, current flow through the cell, potential difference between the anode and each secondary electrode, volume of anode and cathode overflows, volume of tap water added to the anode and cathode half cells for the maintenance of zero hydraulic head pressure, and the volume of one molar nitric acid consumed for the purpose of pH control. These parameters were recorded on a daily basis to generate the power curves presented in Appendix E and to identify any gaps in the general performance of the EK cells relative to one another (ie: does one experiment consume a much higher amount of utilities than another?).

4.5.1 Consumption of Power

The power usage of each EK experiment was calculated by multiplying the potential difference across the EK cell by the amount of current flowing through the EK cell. The value was calculated for every day from day 0 of the experiment to day 50 of the experiment. The data was used to generate curves illustrating the power consumed as a function of time for all 12 of the experimental units. The power curves for individual experimental units are shown in Appendix E.

"ACTIVESYNC" software was used to create a model equation for each of the experimental units. The power curves were modeled according to equation 4.9:

$$P_t = a\left[1 - e^{(-b(t-f))} - \left(\frac{c}{c+d}\right)\left(1 + \frac{b\, e^{(-(c+d)(t-f))} - (c+d)\, e^{(-b(t-f))}}{-b+c+d}\right)\right] \tag{4.9}$$

where: P_t = power being consumed by the EK process at a given time (10^{-6} Watts)

t = time (days)

a, b, c, d, f = model equation constants

The Equation 4.9 model constants and the goodness of fit values are listed in Appendix E.

In addition to modeling the experimental units individually, models were developed on the basis of treatment level as well. This was done by averaging the power levels of duplicate experimental units (ie: EK Cell 1 and EK Cell 2 power levels were averaged together and plotted against time as the "fines / chips" treatment level). The averaged treatment level power curves are included with the individual experimental unit power curves in Appendix E. The average power consumed by an EK experiment was then calculated by integrating the model equations over a range of 0-50 days.

The amount of EK power consumed over the course of the experiments was calculated by taking the integral of equation 4.9 (see equation 4.10) and then calculating the integrals for each of the treatment levels over a fifty day time period using the rate constants tabulated in Appendix E.

$$P_t = 2.4*10^{-8}\left[\frac{-ac}{(c+d)}t + a\frac{\left(bte^{bt}+e^{bf}\right)\left(e^{-bt}\right)}{b} + \frac{(ac)\,e^{bf-bt}}{b(b-c-d)} - \frac{(abc)\,e^{(-ct-dt+cf+df)}}{(b-c-d)(c+d)^2}\right] \quad (4.10)$$

where P_t = power being consumed by the EK process at a given time (microwatts)

t = time (days)

a, b, c, d, f = model equation constants

$2.4*10^{-8}$ = unit conversion from microwatt-days to kilowatt-hours

4.5.1.1 Power Consumed by EK at Each Treatment Level

Figure 4.38 and Table 4.10 show that the size of wood particles treated has a significant effect on the amount of EK power consumed at each treatment level. While the amount of power consumed at the "fines" and "chips" particle size levels are on the order of 10^{-8} kWh; the amount of power consumed at the "plugs" particle size levels is on the order of 10^{-9} kWh for the "plugs / control" treatment level and 10^{-10} kWh for the "plugs / pretreat" treatment level.

The application of chemical pretreatment causes a small decrease in the amount of EK power consumed at the "fines" and "plugs" particle size levels; and a significant increase in the amount of EK power consumed at the "chips" particle size level. The amount of EK power consumed at the "chips / pretreat" treatment level is approximately 5 times larger than the amount of EK power consumed at the "chips / control" treatment level.

4.5.1.2 CoC Removed by EK at Each Treatment Level

Figure 4.39 and Table 4.11 show that the mass of CoC removed through EK is affected by the size of the wood particles in the center compartment of the EK cell. At both chemical pretreatment levels, the most CoC were removed at the "plugs" level, followed by the "fines" level, and then finally the "chips" level. This particle size effect trend is not consistent with the particle size effect trend on the amount of power consumed during the EK experimental run. This means that improving the consumption of power during the EK experiments does not necessarily improve the removal of CoC.

A chemical pretreatment effect on the mass of CoC removed through EK also exists. The mass of CoC removed by EK from "pretreat" wood is consistently less than

the mass of CoC removed by EK from "control" wood. This was expected since there was less availability for CoC in the "pretreat" experiments to begin with due to the removal of a percentage of the CoC during the chemical pretreatment process.

4.5.1.3 EK Power Efficiency

The EK power efficiency was calculated for each experimental level by dividing the power consumed by EK over the course of the experiment by the mass of CoC removed by EK over the course of the experiment. These results are shown in Figure 4.40 and Table 4.12. The highest EK power efficiency was observed in the "plugs / pretreat" experiments; which were an order of magnitude more efficient than the next best treatment. The second most efficient treatment was observed in the "plugs / control" experiments; which were also an order of magnitude more efficient than the next best treatments. The "plugs / control" experiments were followed by the "fines / control", the "chips / control", and the "fines / pretreat" experiments; which all had similar EK power efficiencies. The "chips / pretreat" experiments were the least efficient of the treatment levels examined in this study.

4.5.1.4 Overall Power Efficiency

In the previous three sections, the power consumption and efficiency of the EK process alone was evaluated. It is important to note, however, that the EK process is not the only area of this study where power was consumed. The work involving particle size reduction and chemical pretreatment also consumed power. In fact the power consumed during particle size reduction and chemical pretreatment is significantly more than the power consumed by the EK process. This is in part due to the execution method of

particle size reduction and chemical pretreatment. These methods are described in Chapter 3.

The power consumed during chemical pretreatment was calculated by assuming that the "tumbler" described in Chapter 3 was run for a period of 18 hours where it drew 5.5 amps from a 115 VAC motor at a power factor of 0.85. This puts power consumed by the tumbling of samples for the purpose of chemical pretreatment at 23.8 kWh; which is approximately 10^8 times the amount of power that the EK process consumed on average. The total power consumed, the total mass CoC removed, and the total power efficiency are shown in Appendix E.

The conclusion of this analysis is that the application of chemical pretreatment removes a small amount of CoC prior to EK and it appears to improve the EK removal efficiencies slightly. However, these positive effects come at the cost of raising the overall power consumption of the experiments by a factor of at least 10^8.

4.5.1.5 Effect of EK Center Compartment Density on EK Efficiency

It is interesting to note that the EK efficiency of an experiment is directly proportional to density of solids contained in the center compartment of the EK cell. If the average EK efficiencies are calculated by dividing the average CoC removed according to particle size by the average EK power consumed according to particle size as they are presented in Section 4.5.1.4; the EK efficiencies in descending order are as follows:

- "plugs" at $2.02*10^{12}$ mg CoC per kWh
- "fines" at $2.09*10^{11}$ mg CoC per kWh
- "chips" at $5.41*10^{10}$ mg CoC per kWh

If the average density of solids in the center compartment of the EK cell at the start of an experiment is taken according to particle size; the average density of solids contained in center compartment at the start of an experiment in descending order is as follows:

- "plugs" at 7.19 g / in^3
- "fines" at 5.63 g / in^3
- "chips" at 4.84 g / in^3

Higher EK efficiencies can be achieved when the center compartment of the EK cell is more densely packed because the increase in EK center compartment density results in an increase in resistance to the flow of EK current. The additional resistance in the center compartment slows the migration of ions across the EK cell, limiting activity at the electrodes, and results in a net decrease in the total amount of power consumed by EK. Also, the alignment of the particles in the "plugs" and "fines" particle size level treatments may selectively encourage the movement of CoC towards electrode half cells due to the particle size alignment issue explained in detail in Section 4.3.4.2.

Another more simple explanation to the observation that higher EK efficiencies can be achieved when the center compartment of the EK cell is more densely packed is because there are more CoC available for removal. Since the volume of the center compartment is fixed, the different center compartment densities correspond to different mass of contaminated sample loaded into the center compartment at the start of the experiment. On average, the mass of contaminated sample contained in an EK center compartment at the start of an experiment according to the particle size of the sample is as follows:

- "plugs" treatments contain approximately 451 grams of contaminated sample
- "fines" treatments contain approximately 347 grams of contaminated sample
- "chips" treatments contain approximately 294 grams of contaminated sample

The difference in mass of contaminated sample contained in the center compartment at the start of an experiment between the "plugs" and "chips" particle size levels is approximately 203 grams. By multiplying the difference in mass by the concentrations of CoC per gram of sample as they are defined in Appendix A, it can be shown that those 203 grams of wood sample contain 3,008 milligrams of CoC. This number is significant considering that the average mass of CoC removed by EK treatment observed in this study was 3,906 ± 1313 milligrams.

4.5.1.6 Summary of Findings

- The amount of power consumed during an EK experiment is affected by particle size. With respect to particle size, the amount of power consumed in descending order was "chips", "fines", then "plugs".
- The application of chemical pretreatment causes a slight decrease in the amount of power consumed during EK.
- The mass of CoC removed during an EK experiment is affected by particle size. With respect to particle size, the mass of CoC removed in descending order was "plugs", "fines", then "chips".
- The application of chemical pretreatment causes a slight decrease in the mass of CoC removed during EK.

- The power efficiency of an EK experiment is affected by particle size. With respect to particle size, the power efficiency of EK in descending order was “plugs”, “fines”, then “chips”.
- The application of chemical pretreatment causes a slight increase in the power efficiency of an EK experiment.
- The overall power efficiency of an experiment is affected by particle size. With respect to particle size, the overall power efficiency in descending order was “plugs”, “chips”, then “fines”.
- Regarding the overall power efficiency, “pretreat” experiments consume at least 10^8 more kWh than control experiments.

4.5.2 Chemical Environments

4.5.2.1 pH

Fluid samples were taken from the anodic half cell, the cathodic half cell, and ports 1-3 in the EK cell center compartment on a weekly basis during each of the EK experimental runs. The pH of each of these samples was evaluated. The results are charted in Appendix F. In general, all of the EK cells behaved similarly with respect to pH.

The pH of the anodic half cell at the beginning of the EK experiments is close to that of tap water (ie: ~6.5). By the end of the first week the pH has decreased to a value of 1.62 ± 0.14 where it remains stable until the end of the experimental run. The pH of ports 1-3 samples behave similarly but the pH values stabilize at 1.73 ± 0.14, which is slightly higher than the pH in the anodic half cell.

The pH of the cathodic half cell at the beginning of the EK experiments is close to that of tap water. As soon as the experiment begins the cathodic half cell is dosed with 1 molar nitric acid. This is part of the design of the experiment that is meant to keep the pH of the cathodic half at level below 3.0. The reason for doing this is to limit the hydrolysis reactions at the cathode and to encourage the system to "complete the electrical loop" between the working electrodes of the EK cells by electromigrating CoC through the center compartment of the EK cell by electromigration instead of by electrolysing water molecules at the electrodes. The method is effective in all cases and by the third week, all of the cathodic half cells are stable at a pH of 2.80 ± 0.48.

4.5.2.2 Oxidation-Reduction Potential

The same fluid samples that were analyzed for pH were also analyzed for oxidation reduction potential (Eh). In general, the Eh values were erratic for a short period after the start of the experiments, but they became stabilized after a period of three weeks. The magnitudes of the Eh values relative to one another were as expected. The highest potential for oxidation reactions was expected in the anodic half cell. The highest potential for reduction reactions was expected in the cathodic half cell and the lowest Eh values were observed in the cathodic half cell. The magnitudes of the pore fluid Eh values were in between the values observed in the anodic half cell and the cathodic half cell. Supporting data is included in Appendix F.

4.5.2.3 Nitric Acid consumed for pH regulation at the Cathodic Half Cell

The pH of the cathodic half cell was controlled to a value less than or equal to 3 throughout the EK experimental run by injecting 1 molar nitric acid into the cathodic half

cell when the pH of the half cell rose above 3.0. The main purpose of pH regulation during the experiments was to keep the reduced chemical species generated at the cathode from migrating back towards the anodic half cell. If the pH were not regulated then a "base front" of chemical species produced by reduction reactions at the cathode could migrate back toward the anodic half cell as ions. This would result in inconsistencies in the chemical environment across the center compartment of the EK cell and would likely result in the accumulation of precipitated ions at the interface of the base front to the EK cell center compartment.

The overall volume of 1 molar nitric acid consumed by the cathodic half cell during the EK experiments is shown in Figure 4.41. A particle size effect was observed on the volume of nitric acid consumed. The most nitric acid is consumed at the "fines" particle size level; followed by the "chips" particle size level and then the "plugs" particle size level. A slight chemical pretreatment effect also exists. The application of chemical pretreatment results in a rise in nitric acid consumed at the cathodic half cell.

4.5.2.4 Cathodic activity in the EK Cell

Every reaction at the cathode produces a reduced chemical species, which increases the pH of the cathodic half cell. Monitoring the volume of nitric acid consumed by the cathodic half cell during an EK experiment provides a general indication of how much reduced species are being generated in the cathodic half cell over the course of the experiment. This information can be used to estimate the activity of the cathode.

The fact that one of the highest EK power efficiencies and one of the lowest levels of nitric acid consumption was observed at the "plugs / pretreat" level suggests that EK power was spent efficiently to remove CoC with low activity at the cathode. It is an

indication that the EK power that was used in the "plugs / pretreat" experiments resulted in ions being electromigrated towards half cells and not on side reactions at the cathode such as reduction of water or non-CoC containing ions. In this way the consumption of nitric acid at the cathodic half cell can be used to quantify the ability of an EK experiment to electromigrate CoC to EK half cells as the primary mechanism of current transfer through the EK cell, which would be indicated by a high CoC mass removal coupled with a low consumption of nitric acid; versus the tendency of an EK experiment to support side reactions at electrodes instead of electromigrating CoC, which would be indicated by a low CoC mass removal coupled with a high consumption of nitric acid. The ability of an EK treatment to electromigrate CoC to EK half cells as a primary mechanism of current transfer through the EK cell will be referred to as "selectivity" in the following paragraphs.

Figure 4.42 shows the amount of CoC removed by EK per unit volume of nitric acid consumed during an experimental run. The graph shows that there is a particle size effect on the EK cell selectivity. The "plugs" particle size level is the most selective towards CoC followed by the "chips" and then the "fines" particle size levels. There is also a chemical pretreatment effect on the EK cell selectivity. The application of chemical pretreatment causes a decrease in EK cell selectivity towards CoC.

The particle size effect on EK cell selectivity can be explained by considering the stability and/or availability of CoC in the wood matrices at the different particle size levels. At the "plugs" particle size level, the surface area of the woody material in the center compartment is nearly equal to that of the native wood sample and the center compartments were loaded in a way that guaranteed that EK would be applied in the

direction of the wood grain. With the wood sample loaded this way, compounds containing CoC would be the least stable of all compounds contained in the center compartment and therefore would be expected to be more responsive to EK than the natural woody mass compounds.

At the "fines" particle size level the surface area of the woody material in the center compartment was exponentially higher than the other particle size levels which made the loading of the EK center compartment irrelevant to the alignment of wood grains. The lower particle size of the wood and the exponential increase in the surface area of the wood resulted in a decrease in the stability of all ionic species contained in the wood. The net result was a relative increase in the response of non-CoC containing ionic species to the EK treatment and a decrease in the selectivity of EK towards CoC containing ionic species.

At the "chips" particle size level the surface area of the wood sample was intermediate and the EK cell center compartment was loaded in a way that the chips were aligned in a random manner with no control over the general direction of the wood grain. The result was a CoC selectivity similar to that of the "plugs" particle size level with a delay in the rate of CoC migration towards the half cells due to the random alignment of the wood grains in the EK cell center compartment.

4.5.2.5 Summary of Findings

- In each zone of the EK cell, the pH stabilizes after a 3 day period. There were no observable trends in pH.
- In each zone of the EK cell, the Eh stabilizes after a three week period. There were no observable trends in Eh.

- The volume of nitric acid consumed during an EK experimental run is a function of the surface area of the solid sample loaded into the EK cell center compartment. With respect to particle size, the volume of nitric acid consumed in descending order was “fines”, “chips”, then “plugs”.
- The selectivity of EK towards CoC is a function of the surface area of the solid sample loaded into the EK cell center compartment. With respect to particle size, the EK selectivity towards CoC in descending order was “plugs”, “chips”, then “fines”.

4.5.3 Half Cell Overflow and Maintenance of Hydraulic Head

No trends in EK half cell overflow or EK half cell refilling were observed according to treatment level in this study. For this reason the half cell overflow / refill results were analyzed on the basis of individual EK cells instead of according to treatment level. Data involving the half cell overflow and the volume of water added to maintain zero hydraulic head across the EK cells is included in Appendix F.

In general, it was observed that overflow volumes in the anodic half cells were much greater than the overflow volumes in the cathodic half cells. Also the volume of tap water added to the cathodic half cell was much greater than the volume of tap water added to the anodic half cell. These trends were observed in all experimental units except in the case of EK cell number 4; where the exact opposite effect was observed.

The fact that a higher volume of overflow is being observed at the anodic half cell while a higher volume of tap water is being added to the cathodic half cell indicates that there is a net flow of water away from the cathodic half cell and towards the anodic half cell.

Table 4.1 Chemical pre-treatment selection: Stage II. Experimental unit matrix

chemical agent	solid:liquid ratio	liquid solution strength by volume %			
	1 g: 60 ml	0.08 %	1.70 %	6.70 %	16.7 %
NaOCl	3 g: 60 ml	0.08 %	1.70 %	6.70 %	16.7 %
	5 g: 60 ml	0.08 %	1.70 %	6.70 %	16.7 %
	1 g: 60 ml	0.08 %	1.70 %	6.70 %	16.7 %
H_2O_2	3 g: 60 ml	0.08 %	1.70 %	6.70 %	16.7 %
	5 g: 60 ml	0.08 %	1.70 %	6.70 %	16.7 %

Table 4.2 Chemical Treatment Selection: Stage II. CoC removal percentages for the 16.7% NaOCl chemical pre-treatment experiments at S:L ratios of 3g:60ml and 1g:60ml

	solid to liquid ratio	
CoC	**3g:60ml**	**1g:60ml**
Arsenic	9.6 %	47.8 %
Chromium	18.8 %	63.1 %
Copper	6.8 %	25.1 %

Table 4.3 Chemical Treatment Selection: Stage II. Mass of CoC solubilized per mg of solid treated versus the total mass lost per mg of solid treated in the NaOCl chemical pre-treatment experiments

S:L ratio	Solution strength	CoC solubilized per gram of wood sample	total mass lost per gram of wood sample	Amount of mass lost per mg of CoC solubilized
3g : 60ml	**16.7%**	1.91 mg	11.5 mg	6.02 mg
1g : 60ml	**6.70%**	2.80 mg	80.1 mg	28.6 mg
1g : 60ml	**16.7%**	7.31 mg	63.1 mg	8.63 mg

Table 4.4 Experimental unit matrix for EK experiments.

EK cell number	particle size level	chemical pre-treat level
1	fines	control
2	fines	control
3	chips	control
4	chips	control
5	plugs	control
6	plugs	control
7	fines	pre-treat
8	fines	pre-treat
9	chips	pre-treat
10	chips	pre-treat
11	plugs	pre-treat
12	plugs	pre-treat

Table 4.5 Average CoC removed during chemical pretreatment in units of milligrams of CoC per kilogram of solid treated.

EK CELL TYPE	CoC		
	Arsenic	***Chromium***	***Copper***
fines / pre-treat	470	896	301
chips / pre-treat	969	820	447
plugs / pre-treat	305	306	111

Table 4.6 EK Cell CoC Accumulation Zones

1	Pre-EK Chemical Treatment	
2	Anodic Overflow	Anodic Accumulation
3	Anodic Recirculation	
4	Anodic Half Cell	
5	Anodic Pressure Plate	
6	Section 1	Sectional Accumulation
7	Section 2	
8	Section 3	
9	Section 4	
10	Section 5	
11	Section 6	
12	Cathodic Pressure Plate	Cathodic Accumulation
13	Cathodic Half Cell	
14	Cathodic Recirculation	
15	Cathodic Overflow	

Table 4.7 Anodic Accumulation versus Cathodic Accumulation: Arsenic

EK CELL TYPE	*Anodic accumulation % "A"*	*Cathodic accumulation % "B"*	*Difference between anodic and cathodic accumulation % "A-B"*	*Combined overall anodic and cathodic accumulation % "A+B"*
fines / control	40.7	43.0	-2.3	83.7
chips / control	40.1	35.6	4.5	75.7
plugs / control	38.7	35.3	3.4	74.0
fines / pre-treat	48.7	31.3	17.4	80.0
chips / pre-treat	45.4	27.3	18.1	72.7
plugs / pre-treat	40.4	34.6	5.8	75.0

Table 4.8 Anodic Accumulation versus Cathodic Accumulation: Chromium

EK CELL TYPE	*Anodic accumulation % "A"*	*Cathodic accumulation % "B"*	*Difference between anodic and cathodic accumulation % "A-B"*	*Combined overall anodic and cathodic accumulation % "A+B"*
fines / control	13.6	38.2	-24.6	51.8
chips / control	16.1	18.7	-2.6	34.8
plugs / control	15.7	26.4	-10.7	42.1
fines / pre-treat	17.5	36.5	-19.0	54.0
chips / pre-treat	22.9	16.9	6.0	39.8
plugs / pre-treat	18.5	22.0	-3.5	40.5

Table 4.9 Anodic Accumulation versus Cathodic Accumulation: Copper

EK CELL TYPE	*Anodic accumulation % "A"*	*Cathodic accumulation % "B"*	*Difference between anodic and cathodic accumulation % "A-B"*	*Combined overall anodic and cathodic accumulation % "A+B"*
fines / control	19.3	59.6	-40.3	78.9
chips / control	28.3	48.5	-20.2	76.8
plugs / control	25.5	57.1	-31.6	82.6
fines / pre-treat	27.0	42.0	-15.0	69.0
chips / pre-treat	37.1	18.7	18.4	55.8
plugs / pre-treat	26.2	53.2	-27.0	79.4

Table 4.10 Power Consumed by each Treatment Level Examined in this Study

EK cell type	*Power consumed by EK (kWh)*	*Power consumed by Pre-treatment (kWh)*	*Total Power Consumed (kWh)*
fines / control	2.45064×10^{-8}	0	2.45064×10^{-8}
chips / control	1.81476×10^{-8}	0	1.81476×10^{-8}
plugs / control	4.89360×10^{-9}	0	4.89360×10^{-9}
fines / pre-treat	1.17912×10^{-8}	23.8	$2.38000 \times 10^{+1}$
chips / pre-treat	8.84952×10^{-8}	23.8	$2.38000 \times 10^{+1}$
plugs / pre-treat	1.12627×10^{-10}	23.8	$2.38000 \times 10^{+1}$

Table 4.11 Mass of CoC removed by each treatment level examined in this study

EK cell type	*Mass of CoC removed by EK (mg)*	*Mass of CoC removed by Pre-treatment (mg)*	*Total mass of CoC removed (mg)*
fines / control	4762.133	0	4762.133
chips / control	3756.941	0	3756.941
plugs / control	5521.699	0	5521.699
fines / pre-treat	2813.040	546.954	3359.994
chips / pre-treat	2004.144	733.635	2737.779
plugs / pre-treat	4578.424	236.886	4815.309

Table 4.12 CoC removal efficiencies at each treatment level examined in this study

EK cell type	*EK Power Efficiency (mg /kWh)*	*Pre-treatment Power Efficiency (mg /kWh)*	*Total Power Efficiency (mg /kWh)*
fines / control	$1.94322 \times 10^{+11}$	N/A	$1.94322 \times 10^{+11}$
chips / control	$2.07301 \times 10^{+11}$	N/A	$2.07031 \times 10^{+11}$
plugs / control	$1.12835 \times 10^{+12}$	N/A	$1.12835 \times 10^{+11}$
fines / pre-treat	$2.38571 \times 10^{+11}$	$2.29813 \times 10^{+1}$	$1.41176 \times 10^{+2}$
chips / pre-treat	$2.26469 \times 10^{+10}$	$3.08250 \times 10^{+1}$	$1.15033 \times 10^{+2}$
plugs / pre-treat	$4.06513 \times 10^{+13}$	$9.95319 \times 10^{+0}$	$2.02324 \times 10^{+2}$

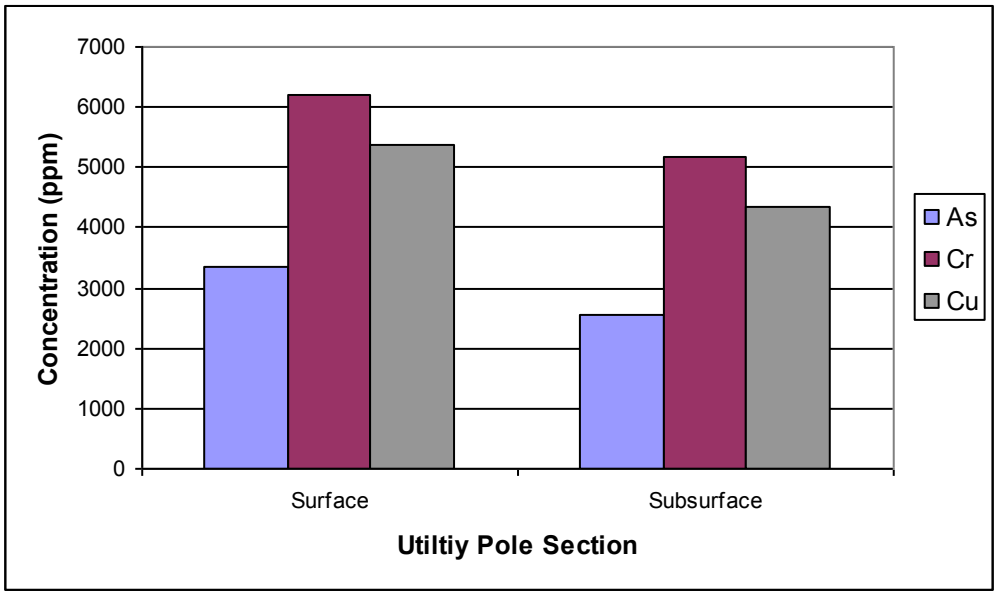

Figure 4.1 Average CoC content of the raw CCA wood specimen at the "Surface" and Subsurface" levels of the utility pole.

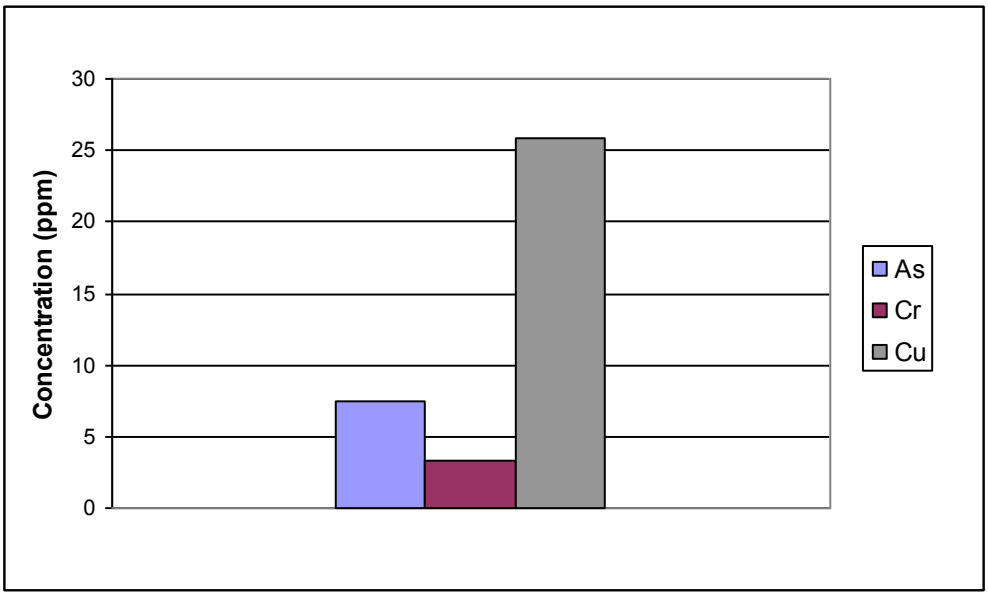

Figure 4.2 Average TCLP concentrations of the raw CCA wood specimen.

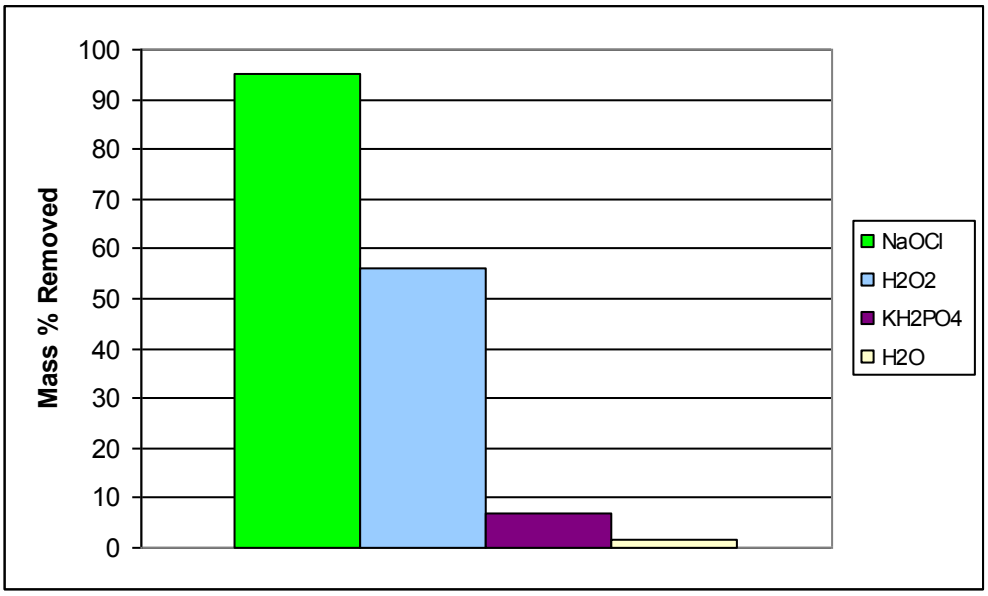

Figure 4.3 Chemical pre-treatment selection: Stage I. Plot of arsenic mass percentage removed versus chemical pre-treatment agent type

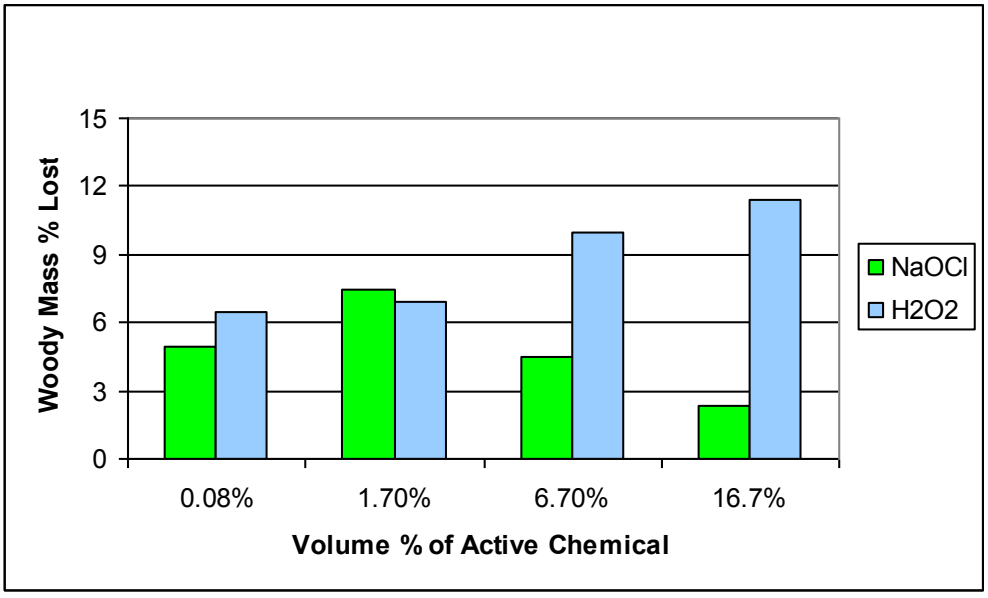

Figure 4.4 Chemical pre-treatment selection: Stage II. Plot of percentage of woody mass lost versus chemical pre-treatment agent solution strength at 5.00 grams of solid per experimental unit

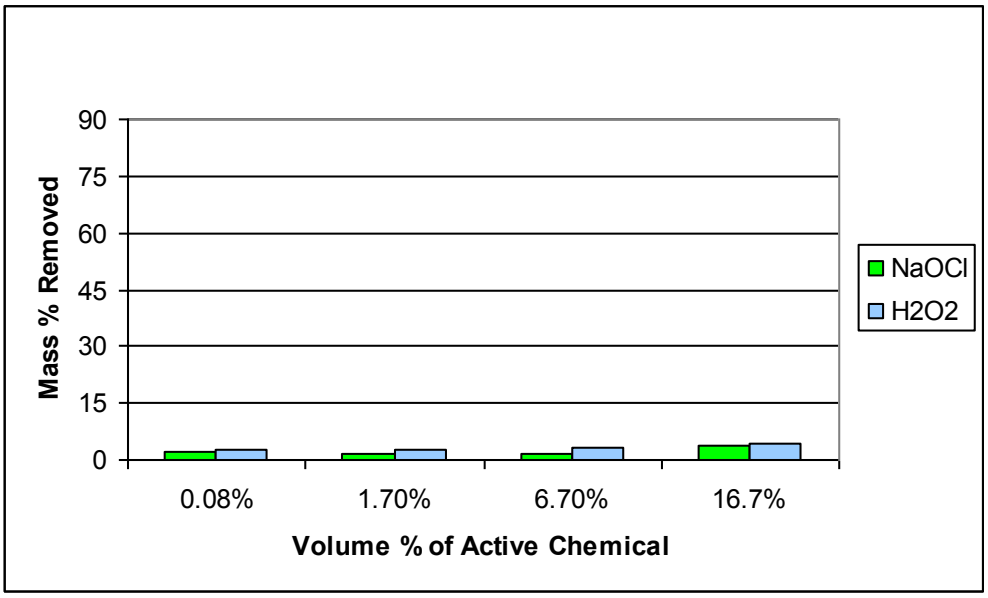

Figure 4.5 Chemical pre-treatment selection: Stage II. Plot of arsenic mass percentage removed versus chemical pre-treatment agent solution strength at 5.00 grams of solid per experimental unit

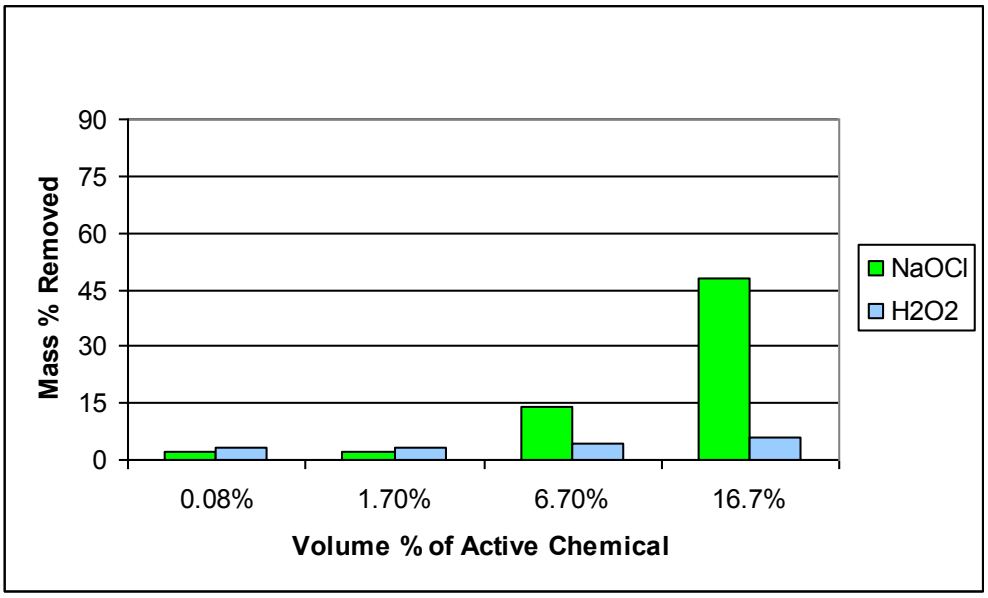

Figure 4.6 Chemical pre-treatment selection: Stage II. Plot of arsenic mass percentage removed versus chemical pre-treatment agent solution strength at 1.00 grams of solid per experimental unit

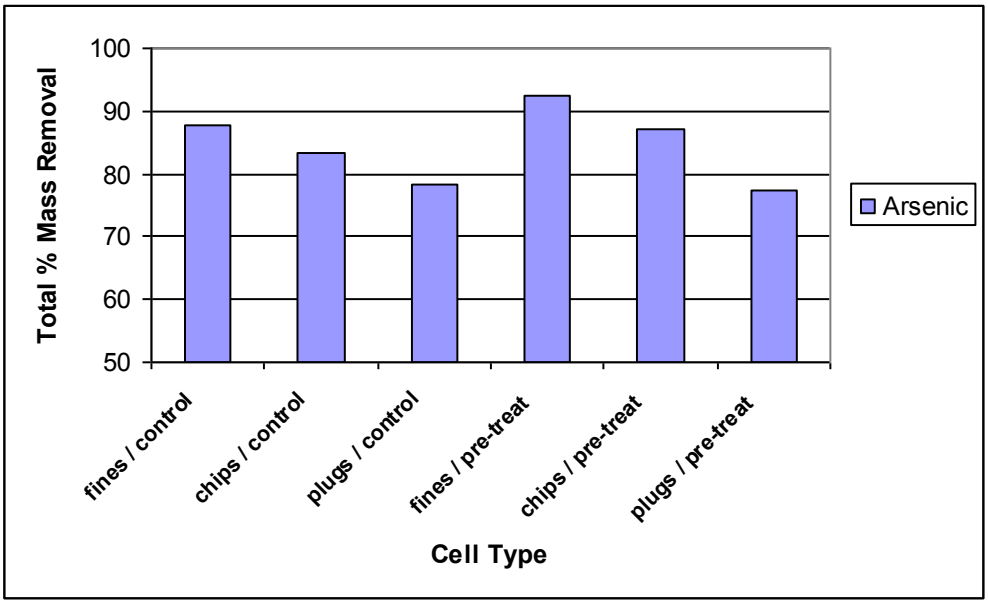

Figure 4.7 Overall post-EK mass removal percentage for arsenic

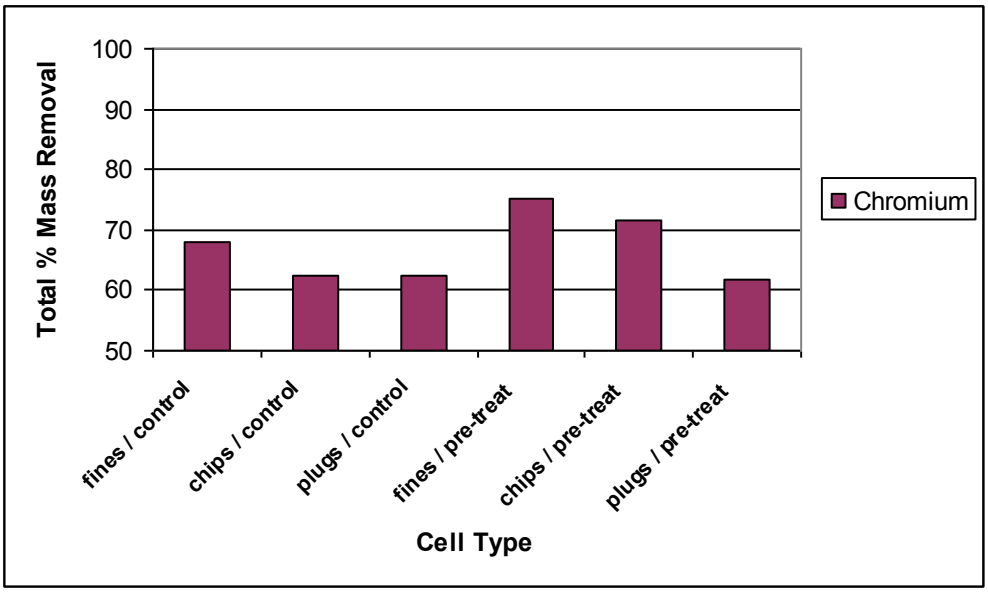

Figure 4.8 Overall post-EK mass removal percentage for chromium

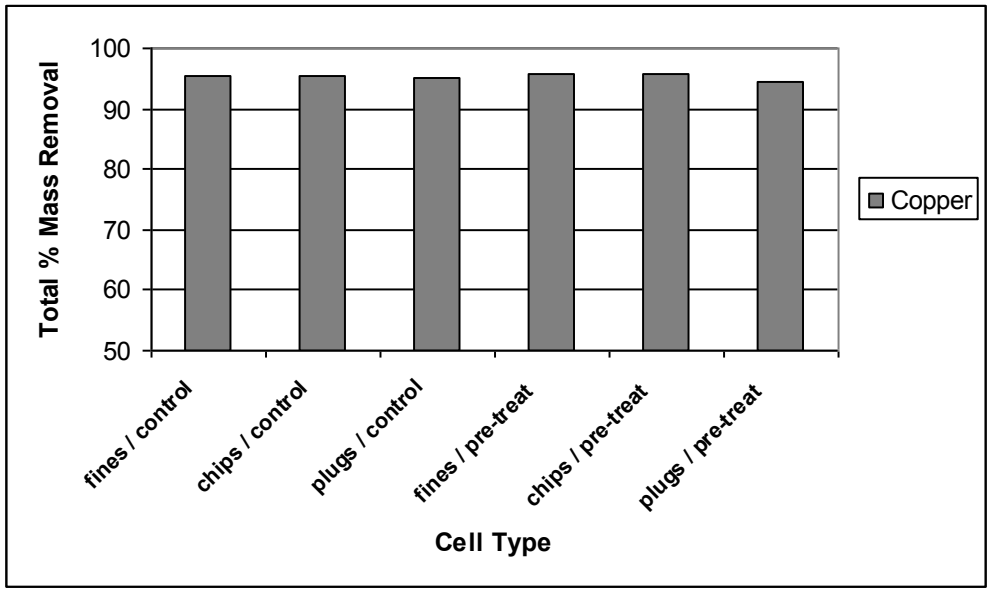

Figure 4.9 Overall post-EK mass removal percentage for copper

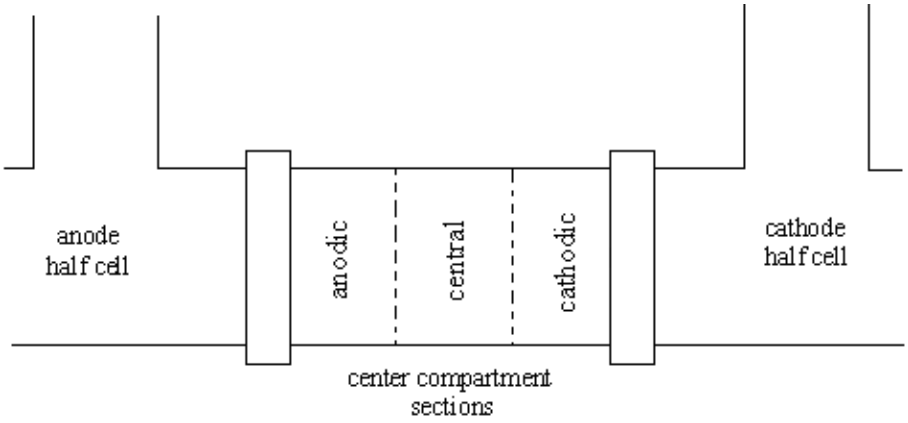

Figure 4.10 Longitudinal zone divisions of the center compartment

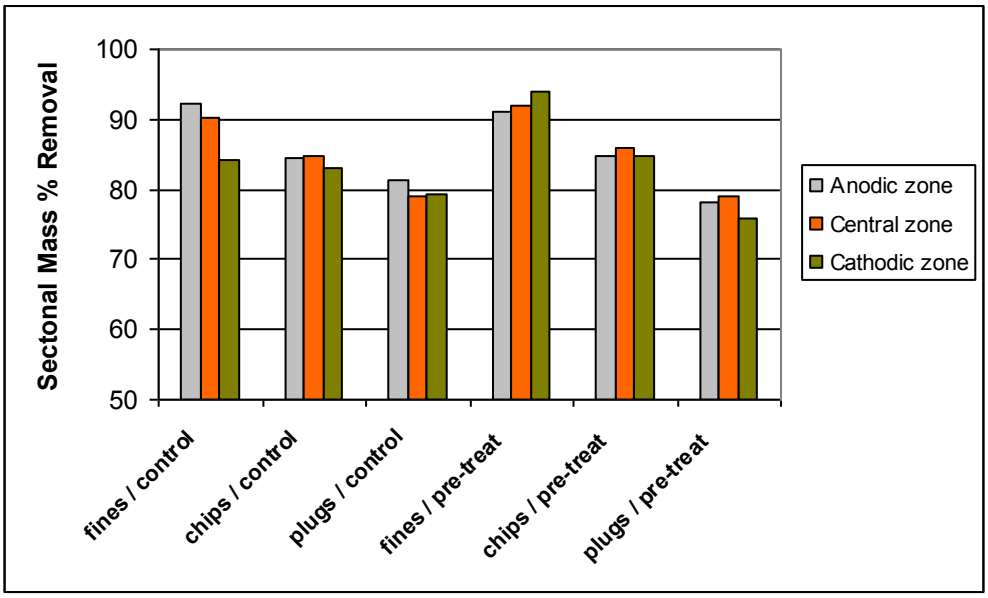

Figure 4.11 Sectional post-EK mass removal percentage for arsenic with the EK cell center compartment divided into longitudinal sections.

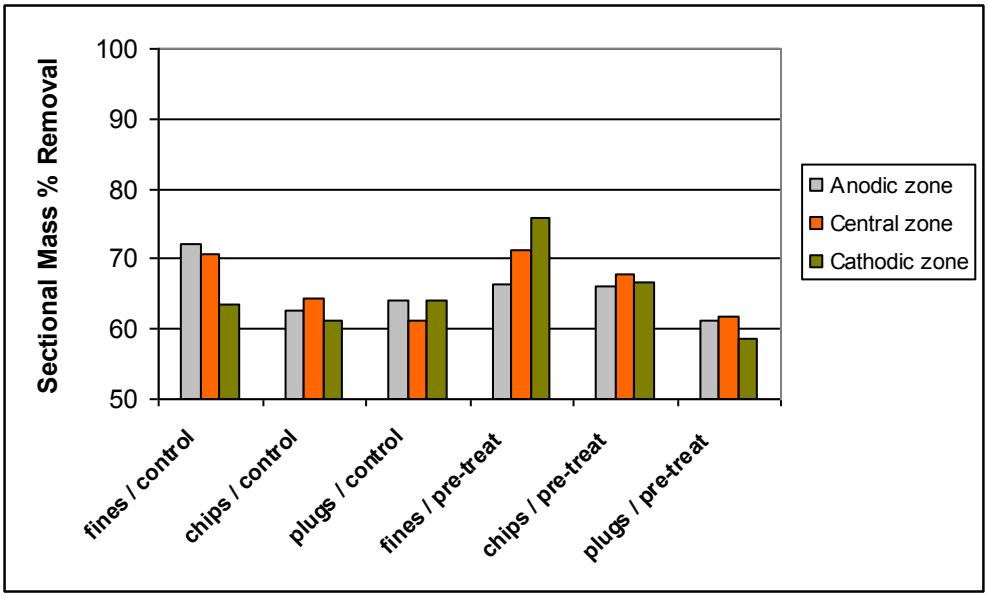

Figure 4.12 Sectional post-EK mass removal percentage for chromium with the EK cell center compartment divided into longitudinal sections

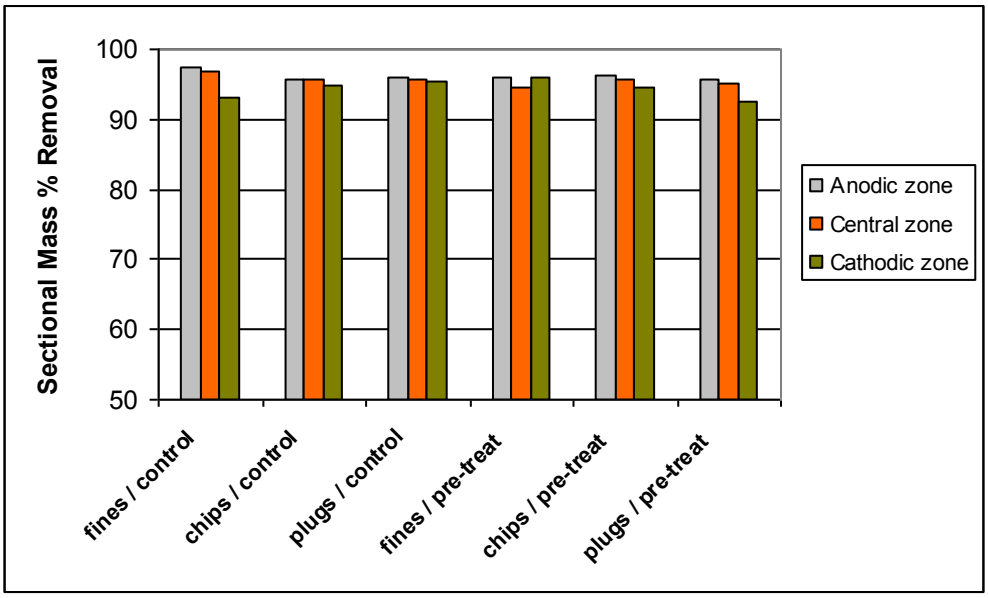

Figure 4.13 Sectional post-EK mass removal percentage for copper with the EK cell center compartment divided into longitudinal sections

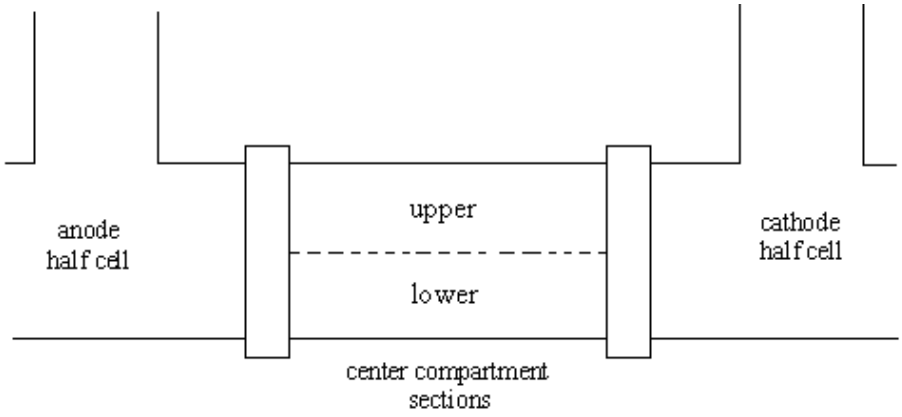

Figure 4.14 Vertical zone divisions of the center compartment

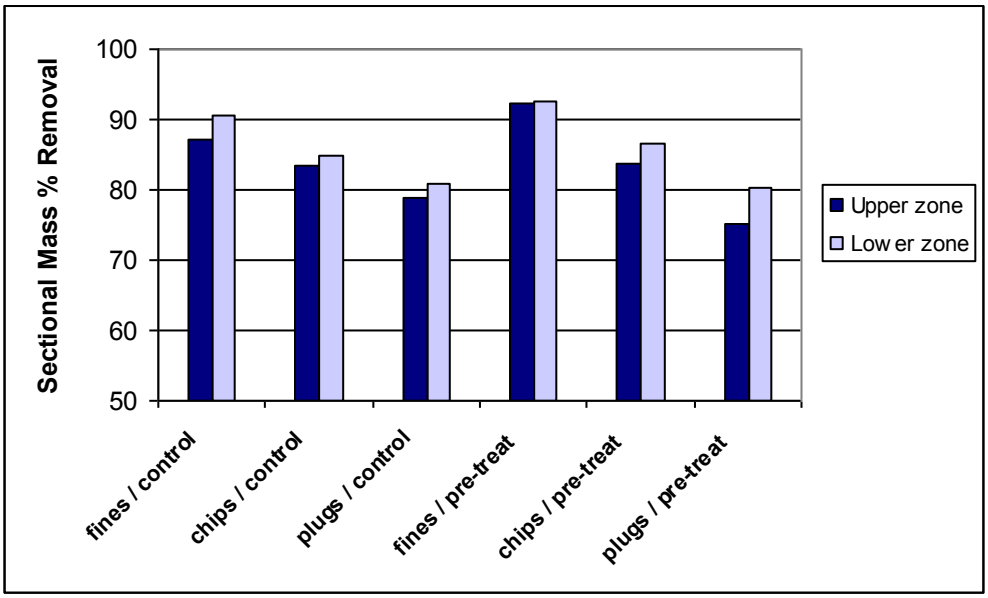

Figure 4.15 Sectional post-EK mass removal percentage for arsenic with the EK cell center compartment divided into vertical sections

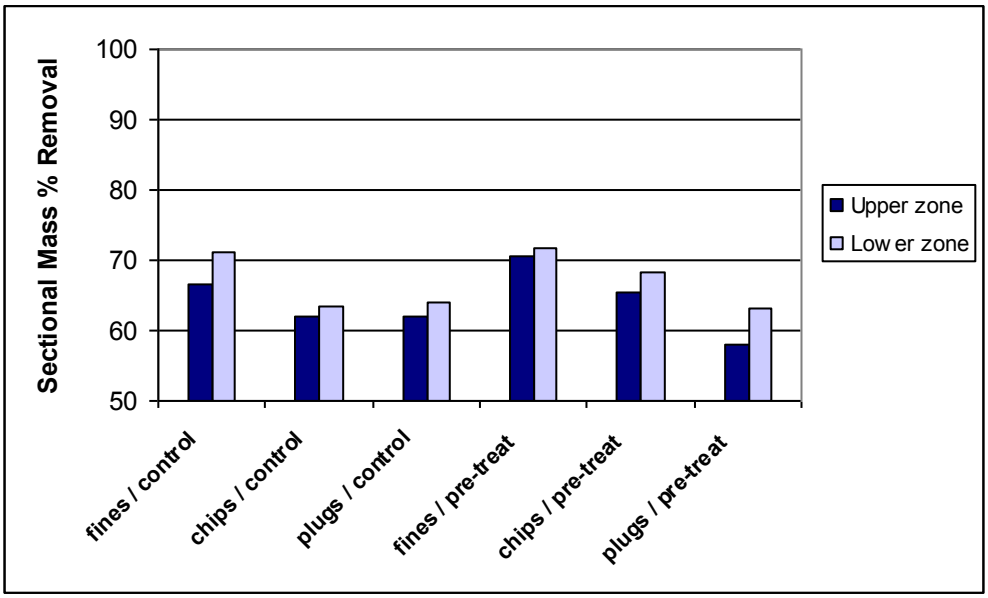

Figure 4.16 Sectional post-EK mass removal percentage for chromium with the EK cell compartment divided into vertical sections

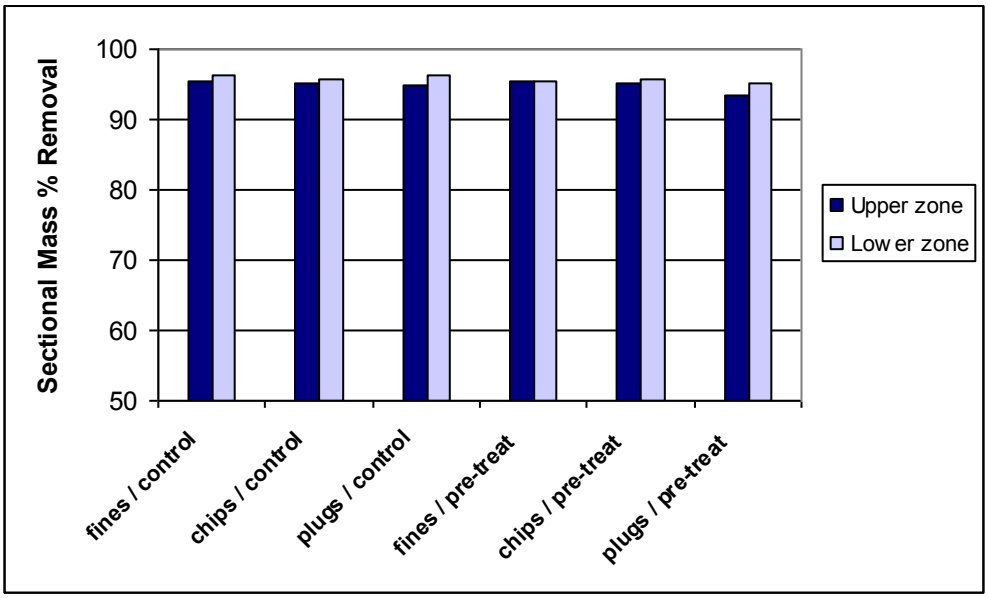

Figure 4.17 Sectional post-EK mass removal percentage for copper with the EK cell center compartment divided into vertical sections

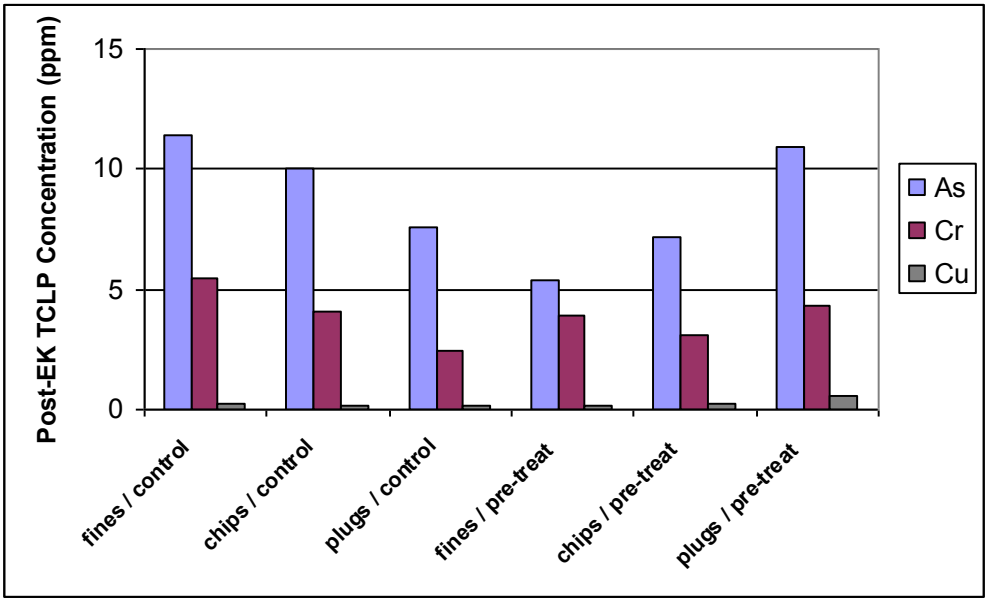

Figure 4.18 Overall post-EK TCLP concentration for arsenic, chromium, and copper

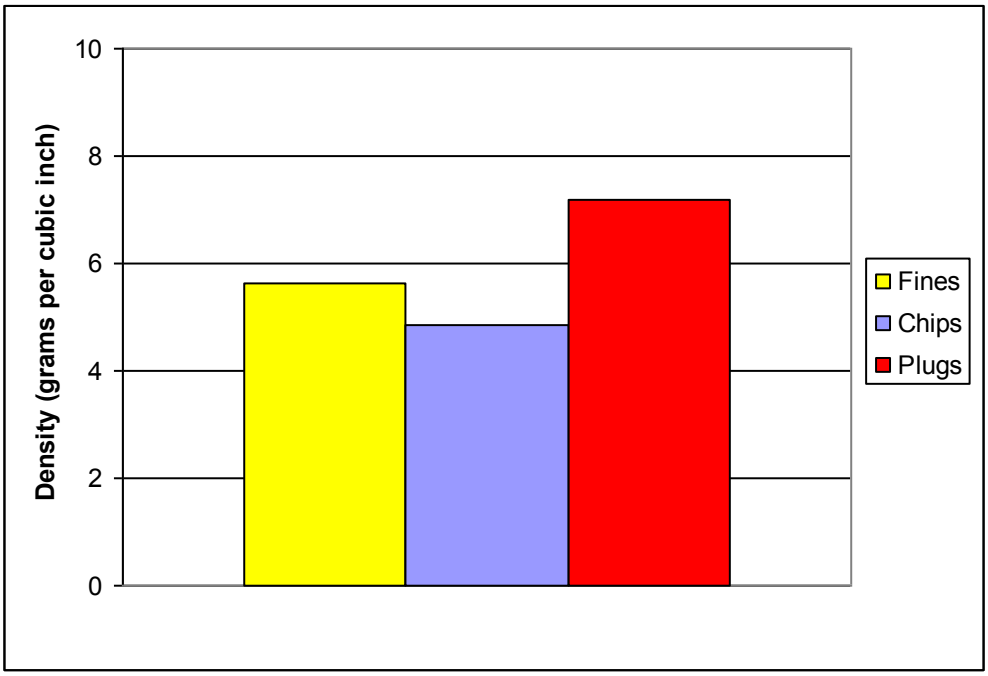

Figure 4.19 Average density of solid materials in the EK cell center compartments according to the particle sizes of the wood

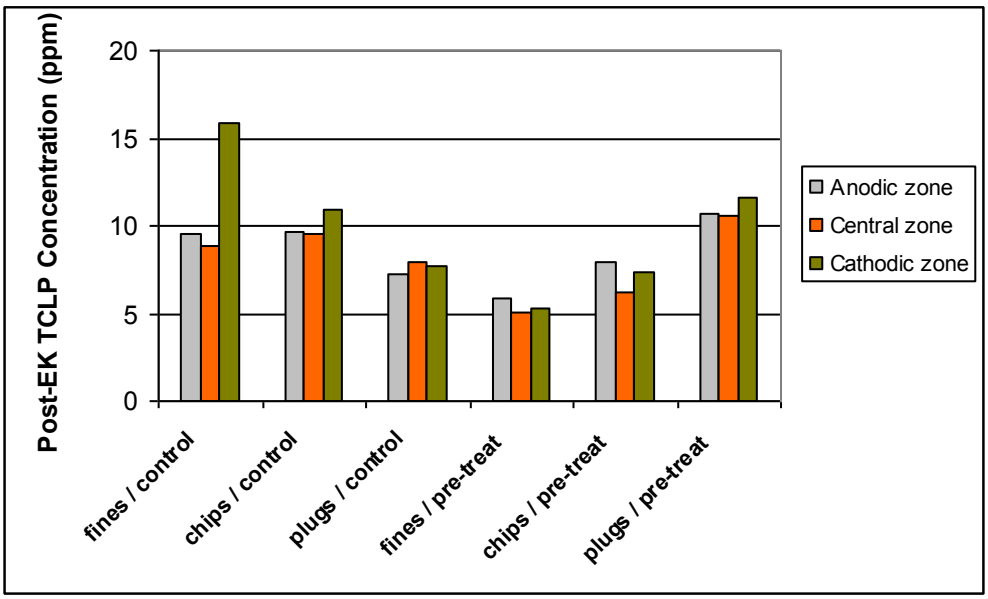

Figure 4.20 Sectional post-EK TCLP concentrations for arsenic with the EK Cell center compartment divided into longitudinal sections

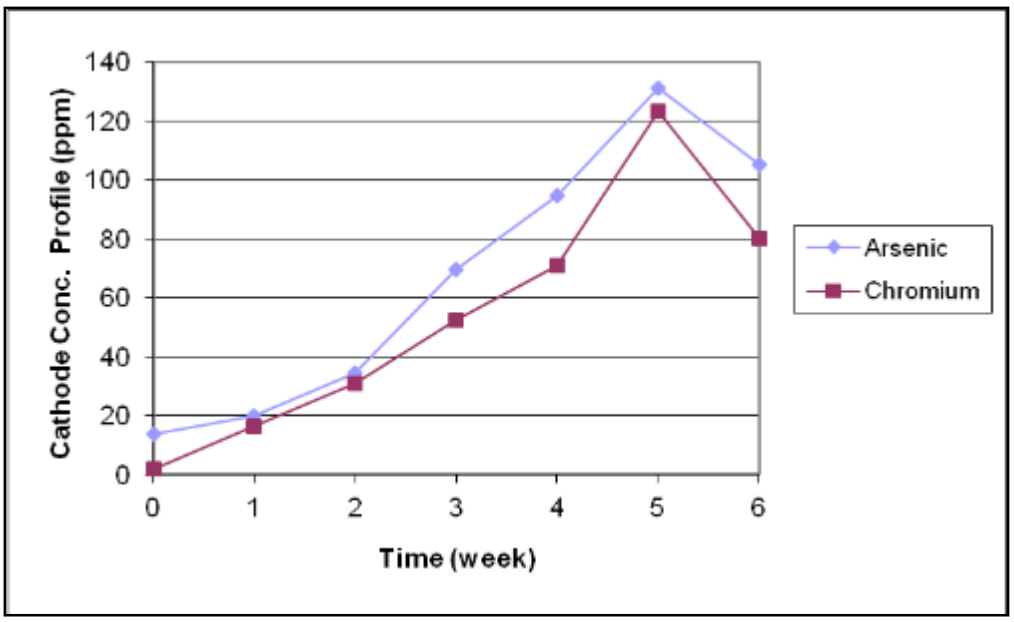

Figure 4.21 EK Cell 5: Concentration curves for the accumulation of arsenic and chromium in cathodic half cell

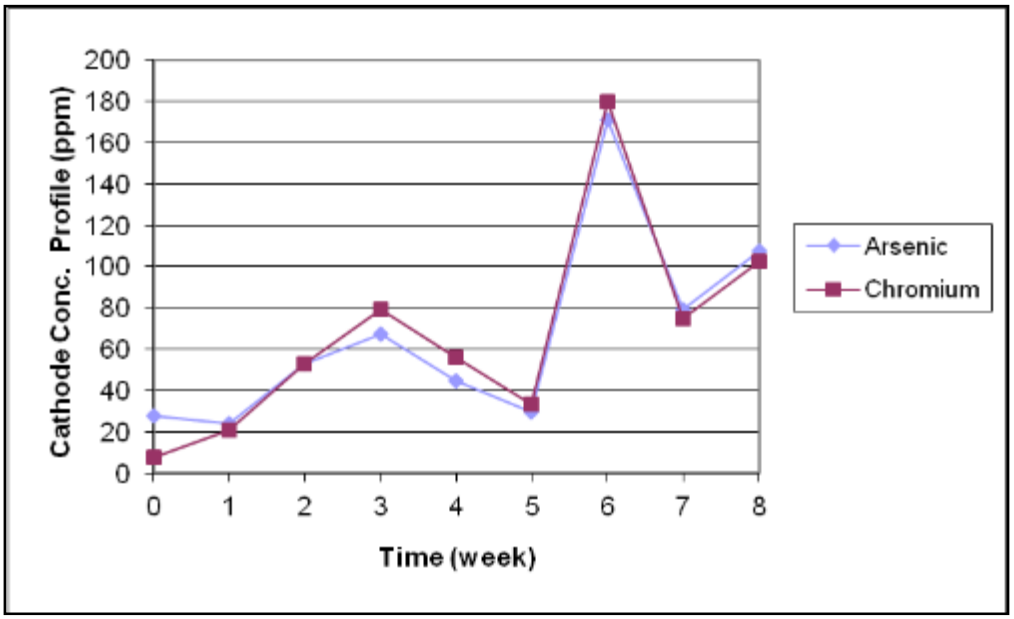

Figure 4.22 EK Cell 2: Concentration curves for the accumulation of arsenic and chromium in cathodic half cell

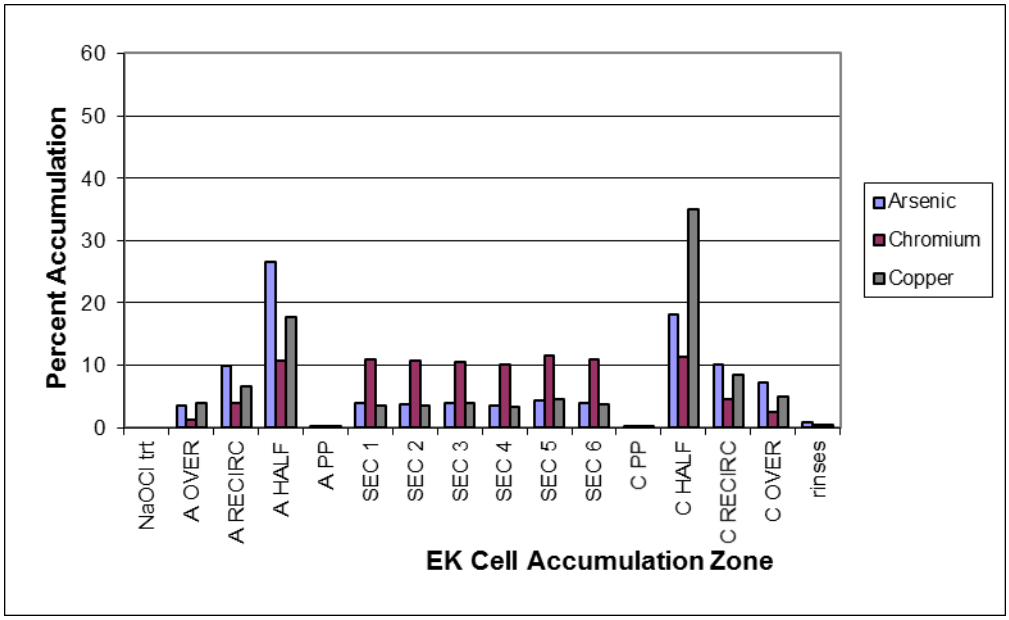

Figure 4.23 Averaged Post EK distribution of CoC across the EK cell for the "chips / control" experimental units

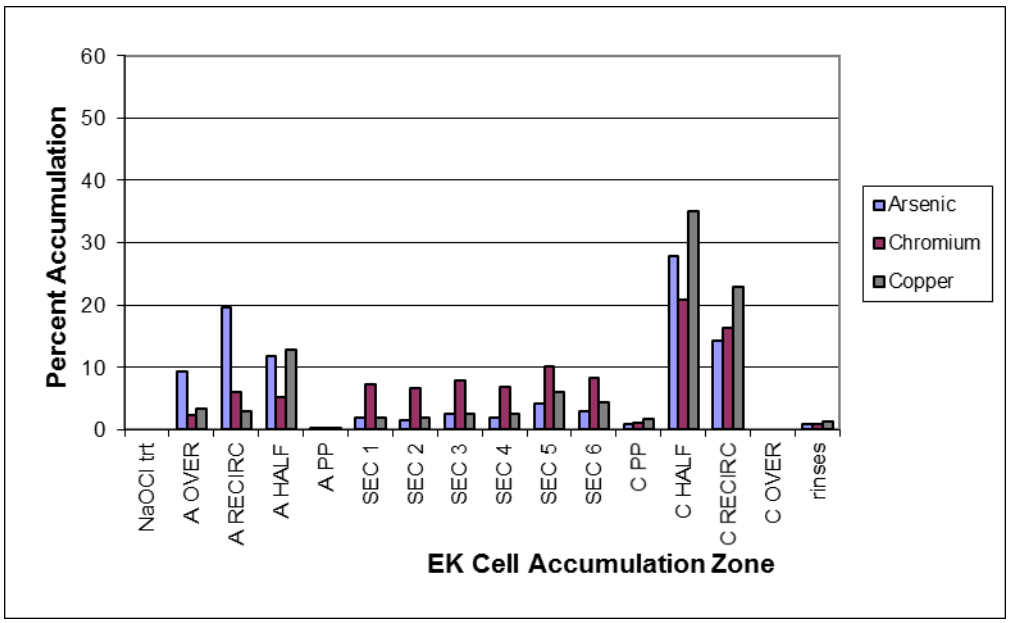

Figure 4.24 Averaged Post EK distribution of CoC across the EK cell for the "fines / control" experimental units

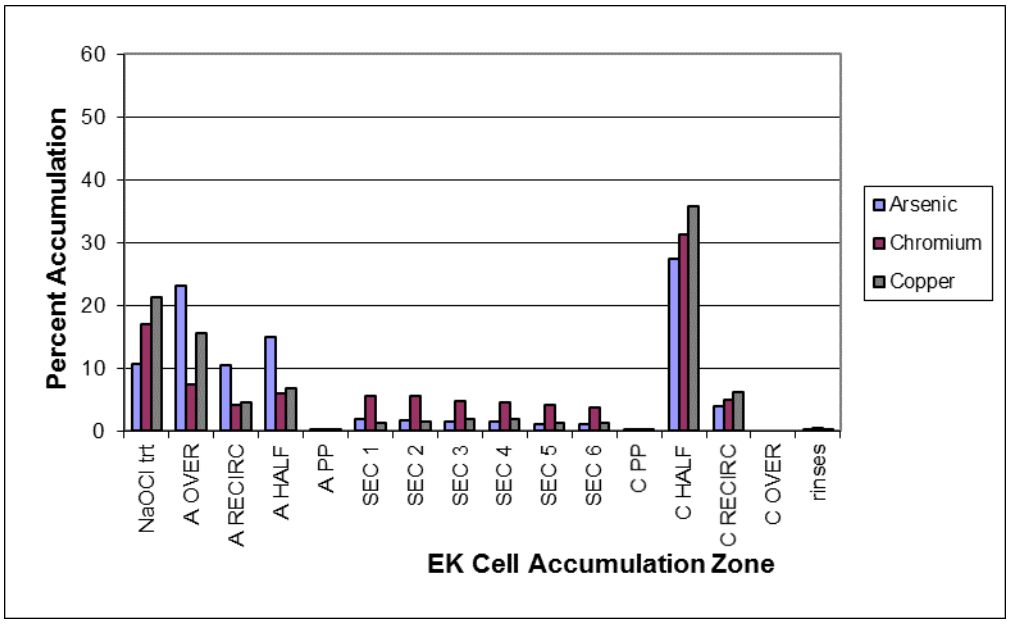

Figure 4.25 Averaged Post EK distribution of CoC across the EK cell for the "fines / pre-treat" experimental units.

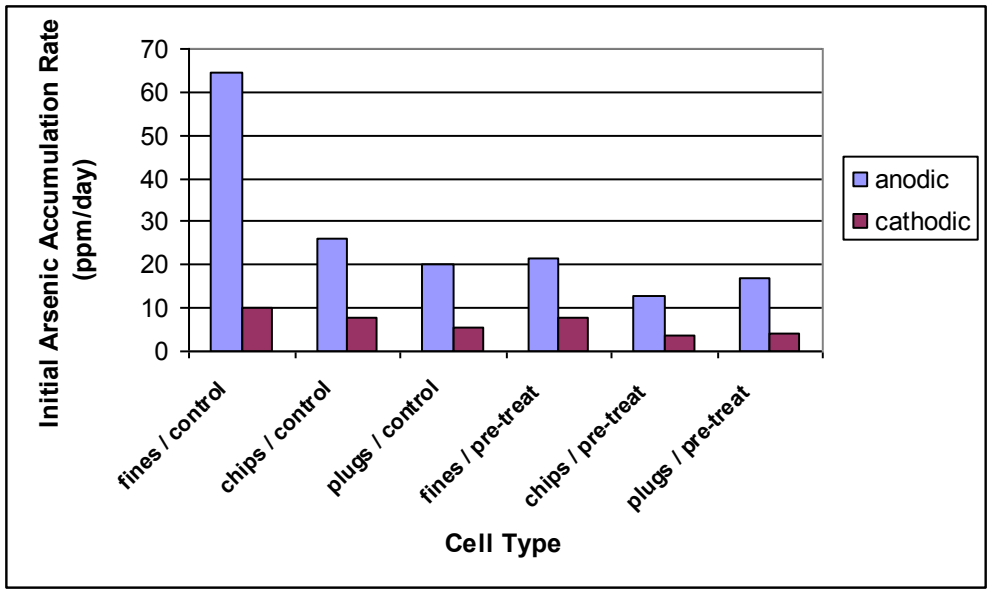

Figure 4.26 Initial accumulation rate "A×R" for the arsenic half cell accumulation rate model

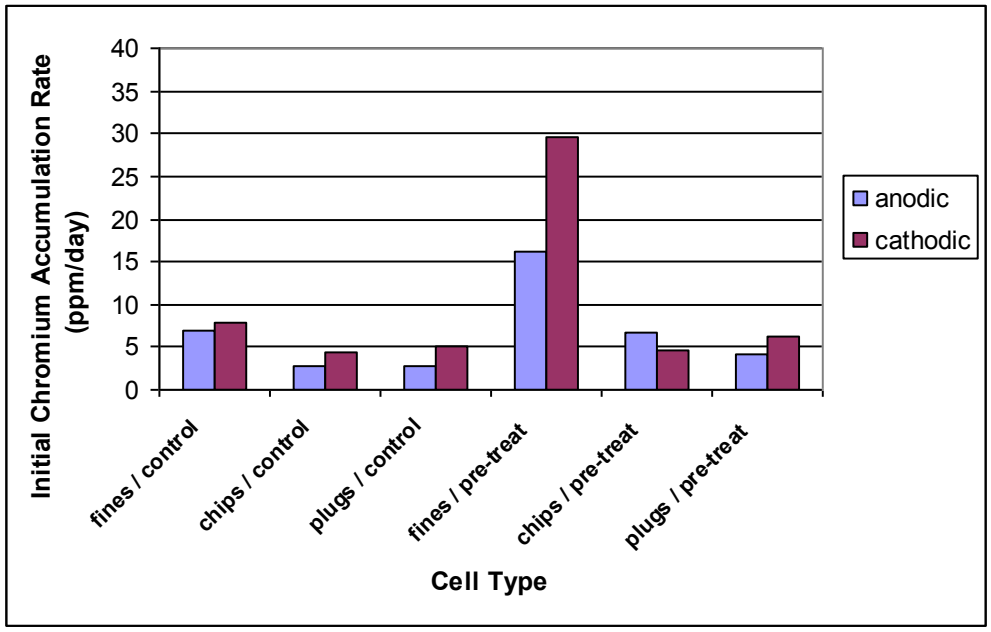

Figure 4.27 Initial removal rate "A×R" for the chromium half cell accumulation rate model

Figure 4.28 Photograph of the solid deposit observed on the electrodes during the EK experimental runs

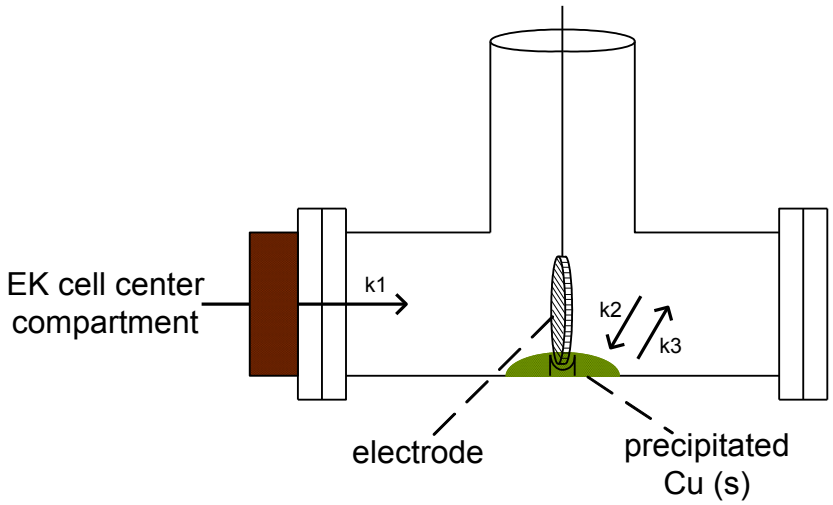

Figure 4.29 Schematic representation of the mechanism of copper ion accumulation in an EK half cell during the EK experiments.

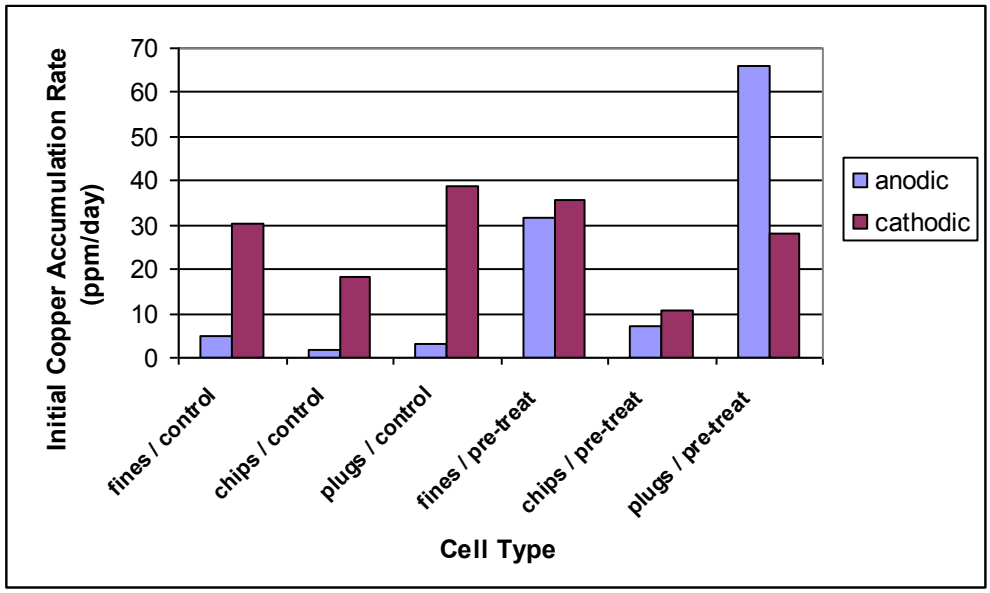

Figure 4.30 Initial removal rate "$A \times K_1$" for the copper half cell accumulation rate model

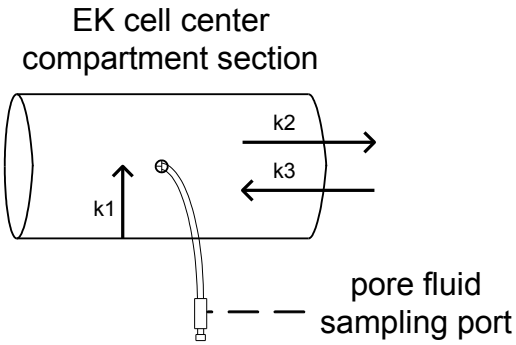

Figure 4.31 Schematic representation of the movement of CoC through a pore fluid sampling zone during the EK experiments

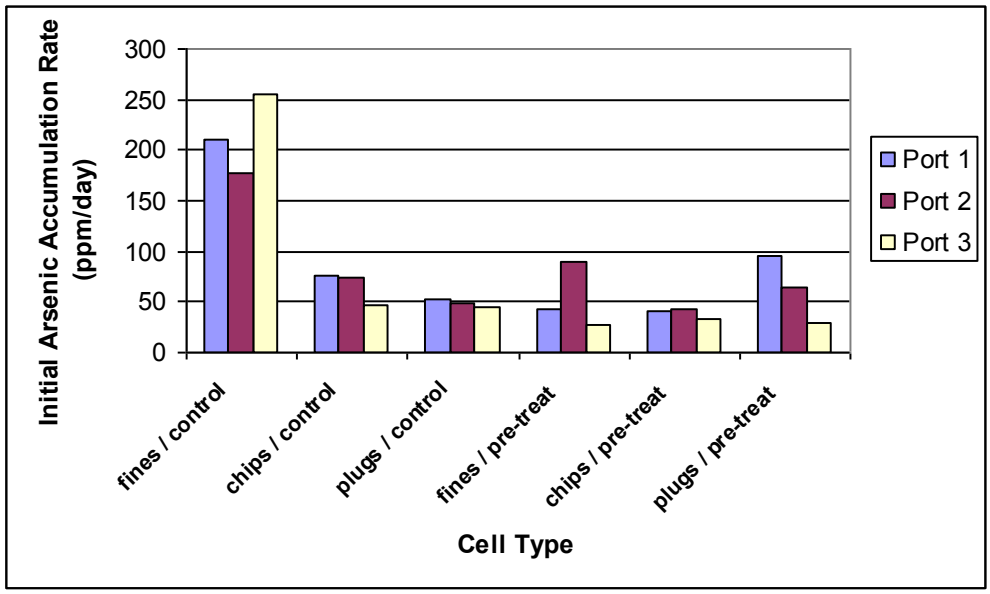

Figure 4.32 Initial arsenic accumulation rates "$A \times K_1$" in the pore fluid zones of the EK cell central compartment

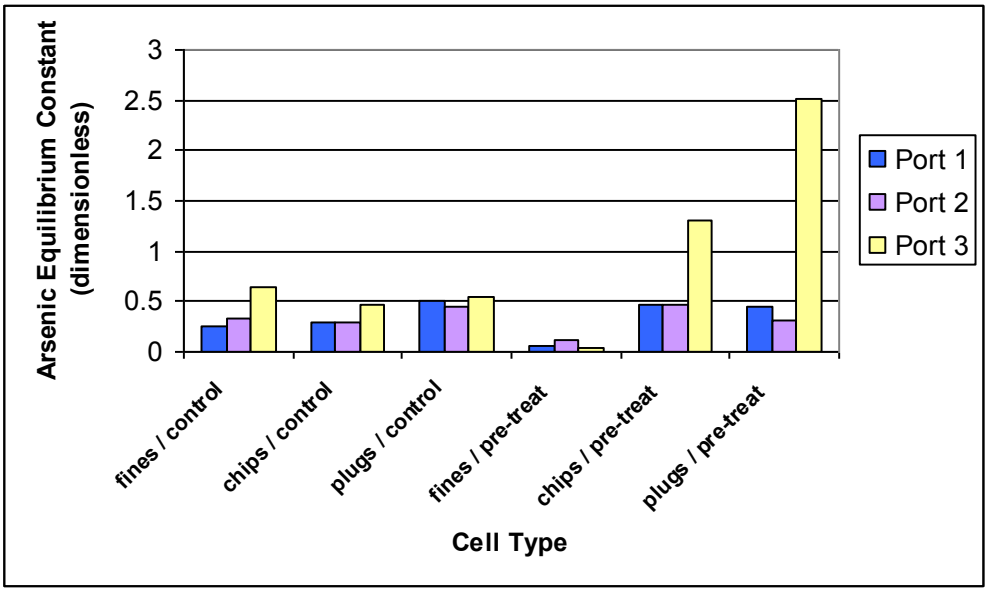

Figure 4.33 Arsenic equilibrium constant "k_{EQUIL}" in the pore fluid zones of the EK cell central compartment

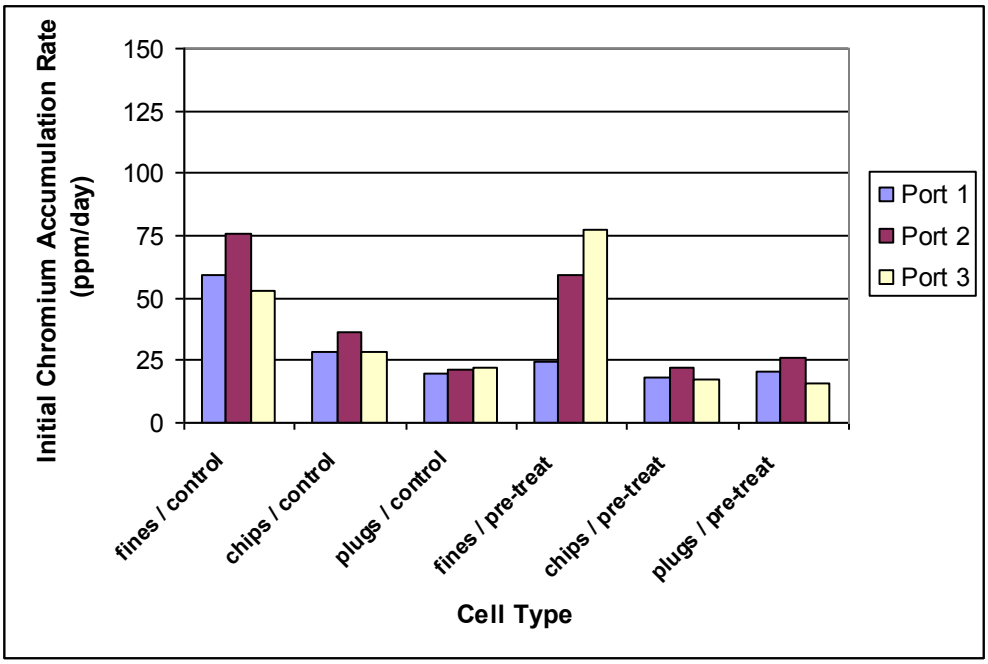

Figure 4.34 Initial chromium accumulation rates "$A \times K_1$" in the pore fluid zones of the EK cell central compartment

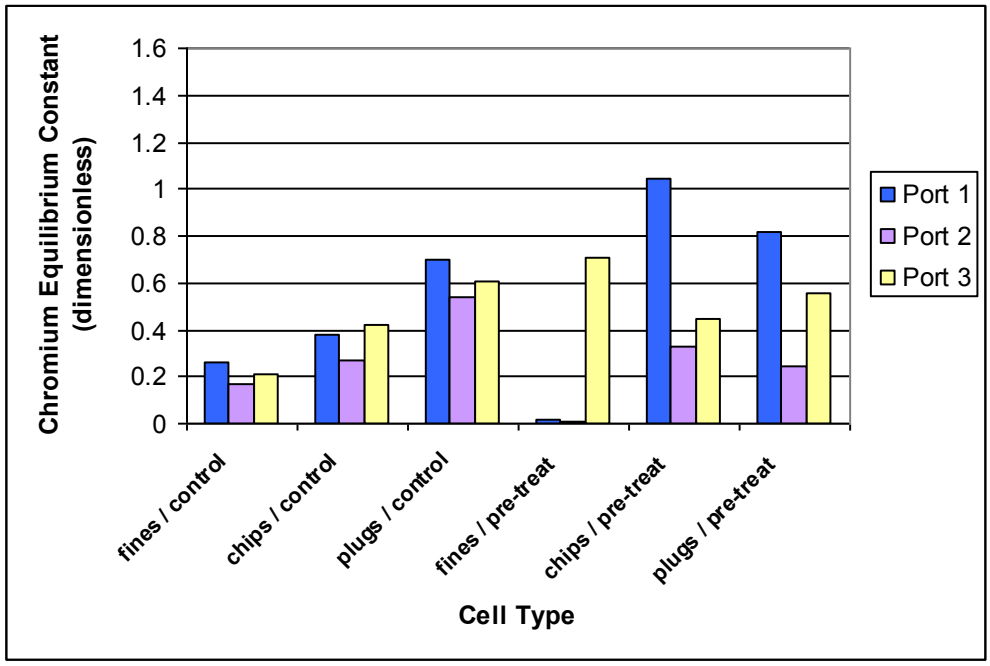

Figure 4.35 Chromium equilibrium constant "k_{EQUIL}" in the pore fluid zones of the EK cell central compartment

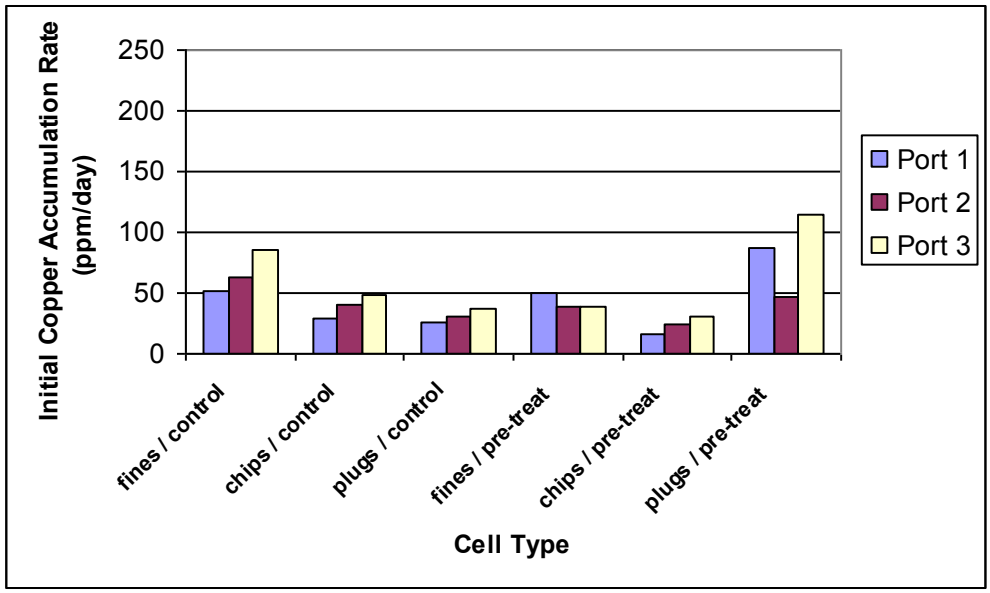

Figure 4.36 Initial copper accumulation rates "$A \times K_1$" in the pore fluid zones of the EK cell central compartment

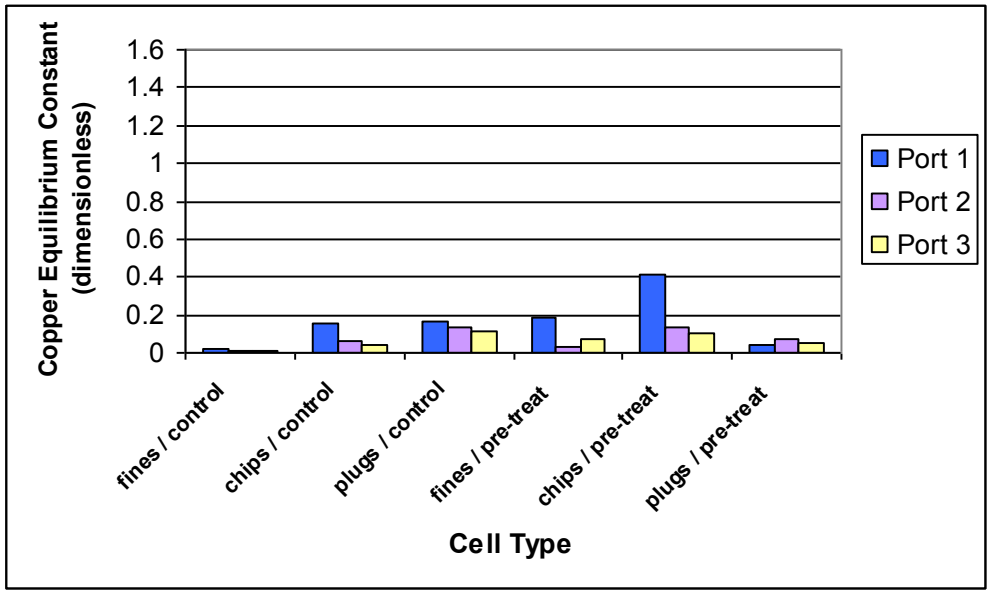

Figure 4.37 Copper equilibrium constant "k_{EQUIL}" in the pore fluid zones of the EK cell central compartment

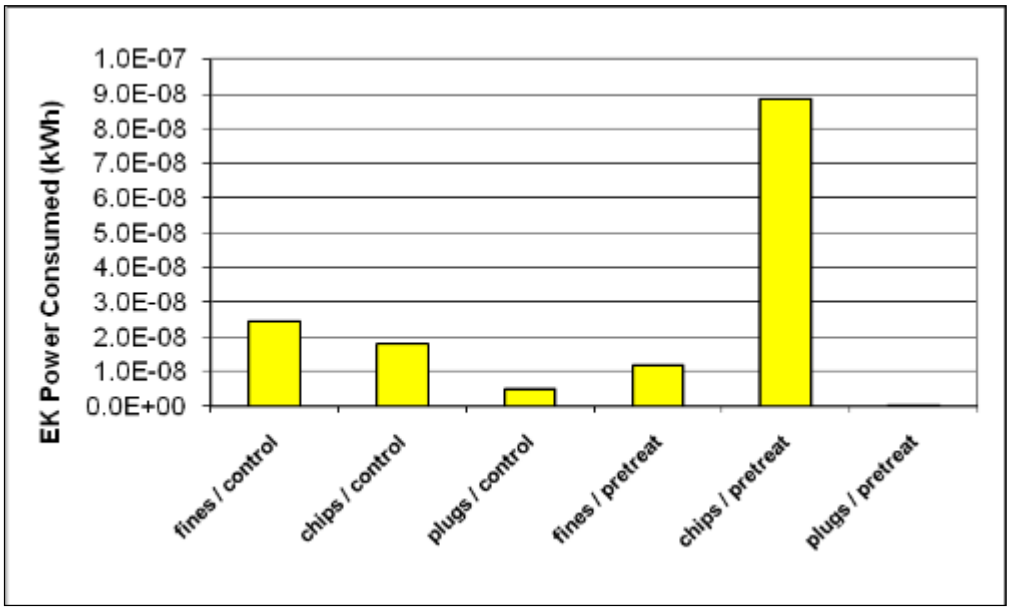

Figure 4.38 Power consumed by EK for the first 50 days of the experimental runs at each treatment level

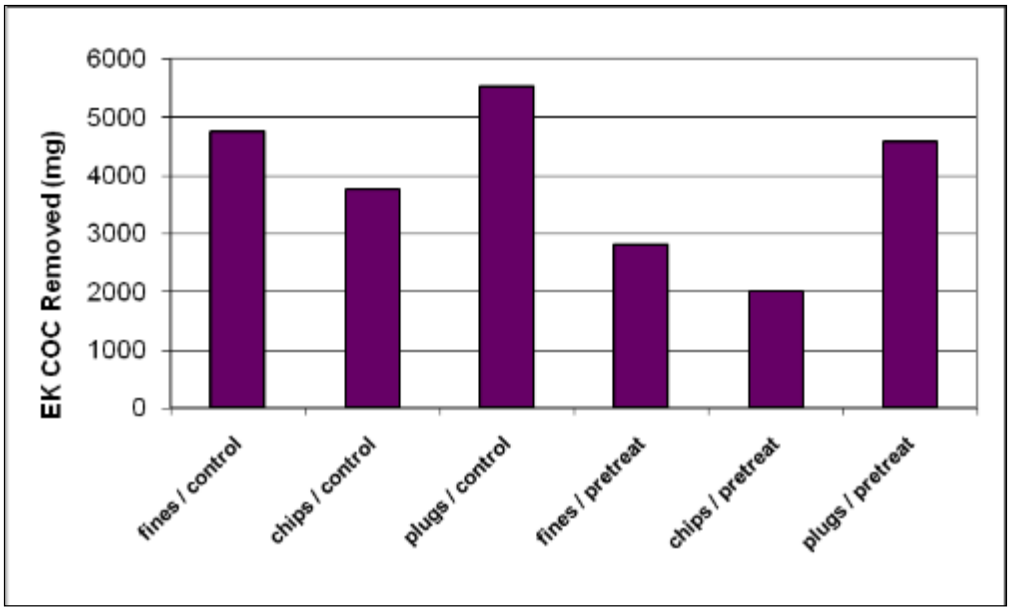

Figure 4.39 Mass of CoC removed during EK for the first 50 days of the experimental runs at each treatment level

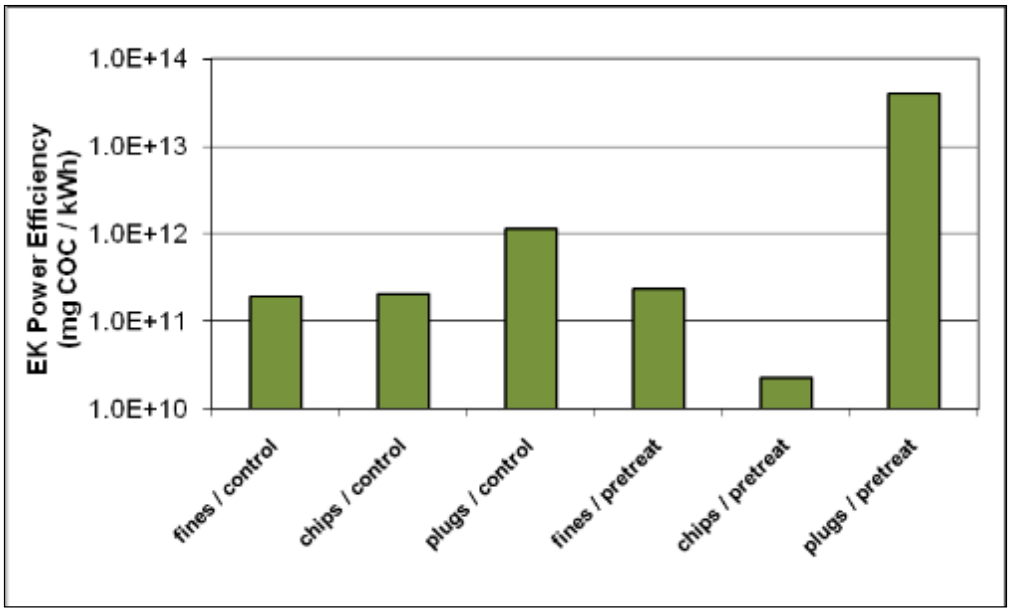

Figure 4.40 CoC removed per kilowatt-hour consumed by EK for the first 50 days of the experimental runs at each treatment level.

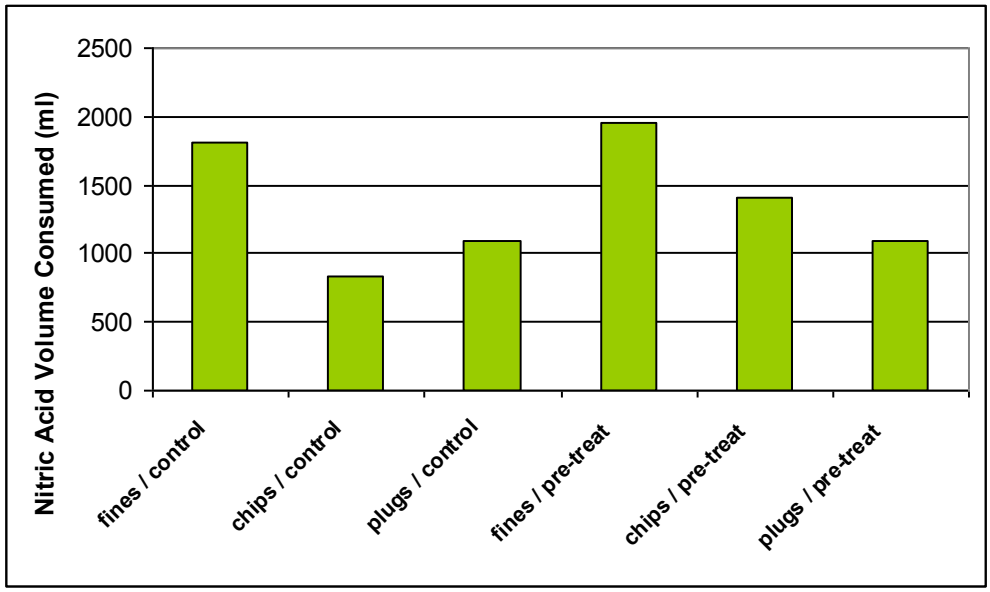

Figure 4.41 Overall volume of 1 Molar nitric acid consumed in the cathodic half cell during the EK experiments

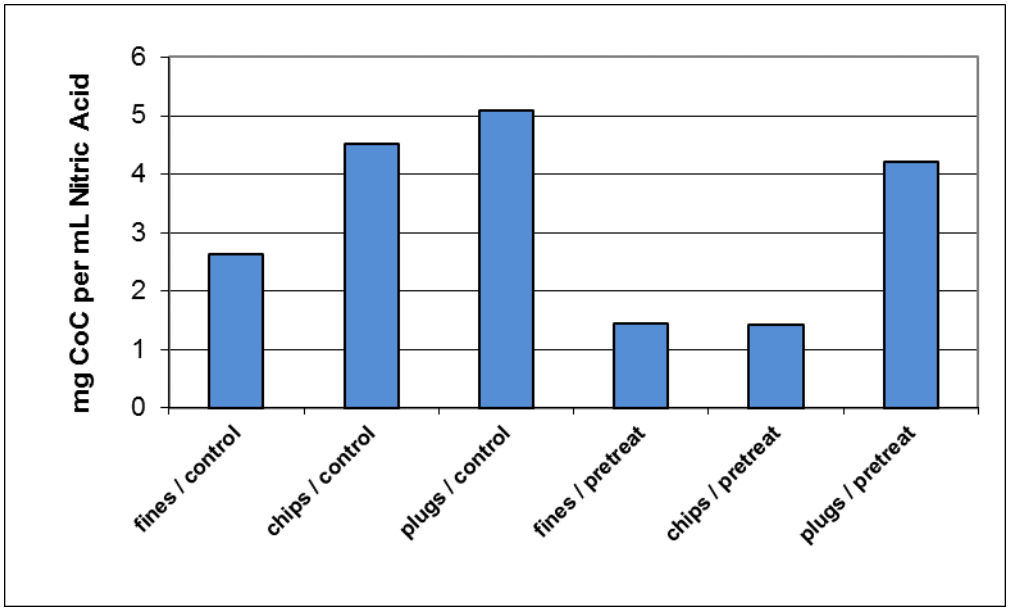

Figure 4.42 EK CoC removed per unit volume of nitric acid consumed at the cathode

CHAPTER V

CONCLUSIONS

The overall goal of this study was to determine if EK technologolies could be effective at removing the target contaminants of concern arsenic, chromium, and copper (CoC) from pressure treated CCA wood. The effects of pre-treamtent techniques such as pre-EK chemical treatment, and particle size reduction by chipping and grinding were also investigated. From the results of this study it appears that EK technologies are very effective for treating raw CCA wood and that pretreatment results in a small increase in the overall removal efficiencies of the target metals. Based on the data generated during this study the following conclusion can be made:

- EK treatment is effective at removing large percentages of arsenic, chromium, and copper from CCA treated wood at a constant current density of 0.92 milliampere/cm^2 (2.75" OD electrode area and 140 milliampere direct current continuously applied) and using acid neutralization at the cathode.
- EK is most effective at removing copper with an average of over 95% (by weight) of the initial content being removed. EK was also effective at removing up to 88 % of the initial content of arsenic and up to 68 % of the initial content of chromium. The effectiveness of EK at removing each CoC was as follows:

Cu (95%) > As (88%) > Cr (68%)

- Of the pre-EK chemical treatment solutions evaluated in this study NaOCl appears to be the most effective chemical evaluated. NaOCl at a concentration of 16.7 % (by volume) and at a solid:liquid ratio of approximately 3 grams to 60 milliliters was used as the pre-EK chemical treatment in this study.
- By applying pre-EK chemical treatment to the particle size levels described above, the removal of copper was improved to 96 % (by weight) of the initial copper content of the base wood sample. The removal of arsenic was improved to 92 % and the removal of chromium was improved to 75 %. The level of improvement of CoC removal relative to EK without pre-EK chemical treatment was as follows:
- Copper: + 1 %
- Arsenic: + 4 %
- Chromium: + 7%
- As expected the reduction of the particle size of CCA wood by grinding or chipping in general enhances the overall CoC removal percentage. The level of improvement of CoC removal by EK between the largest particle size and the smallest particle size was as follows:
    - Copper: < 0.5 %
    - Arsenic: 6 %
    - Chromium: 9 %

When pre-EK chemical treatment was applied to the wood samples the level of improvement of CoC removal by EK between the largest particle size and the smallest particle size was as follows:

- Copper: 1 %
- Arsenic: 13 %
- Chromium: 15 %

- In this study the duration of the EK treatment was 8 weeks on average. It appears the majority of the CoC removal occurred during the first 2-3 weeks of treatment for the smaller particle sized material. It appears the majority of the CoC removal occurred during the first 3-4 weeks for the larger particle sized material.
- Although most of the CoC are removed by EK treatment, the ionic mobility of the contaminants remaining in the post EK treated CCA wood are increased in the cases of arsenic and chromium. So EK treated CCA woods are more likely to be classified as hazardous according to the TCLP. On average the concentration of arsenic and chromium in the TCLP extract is increased as follows:
  - Arsenic:
    - Raw sample TCLP: 7.5 ppm
    - Post-EK treated TCLP: 9.0 ppm
  - Chromium:
    - Raw sample TCLP: 3.3 ppm
    - Post-EK treated TCLP: 4.0 ppm

- In general CoC are ionically complexed into positively charged ions under EK conditions and migrate towards the cathode as cations. When the CCA wood is subjected to pre-EK chemical treatment there is a chemical speication shift that causes a portion of each of the CoC to migrate towards the anode as anions. The shift is the most dramatic for copper, where an additional 15 % of is removed to the anodic half cell. The shift is also present for arsenic (8 %) and for chromium (9 %).
- For all of the experimental units in this study the pH at the center of the EK cell center compartment stabilied to a value of 1.7 in approximately 3 days. Thus, it is relatively easy to control the pH of the CCA wood during EK treatment.
- For non pre-EK chemically treated EK experiments the oxidation reduction potential at the center of the EK cell center compartment stabilied to a value of 387 mV in approximately three days. When pre-EK chemical treatment was applied to the wood samples the oxidation reduction potential at the center of the EK cell center compartment stabilied to a value of 464 mV in approximately three days.
- The model used to interpret the half cell accumulation rates of arsenic and chromium were very useful and fit the data reasonably well. The average "goodness of fit" values of the models were as follows:
    - Arsenic half cell accumulation: 0.86
    - Chromium half cell accumulation: 0.86

- The model used to interpret the half cell accumulation rates of copper and the accumulation/deaccumulation rates of CoC in the EK cell center compartment pore fluid accumulation zones were very useful and fit the data reasonably well. The average "goodness of fit" values of the models were as follows:
    - Copper half cell accumulation: 0.86
    - Copper pore fluid accumulation/deaccumulation: 0.91
    - Arsenic pore fluid accumulation/deaccumulation: 0.95
    - Chromium pore fluid accumulation/deaccumulation: 0.91
- The most economical method for removing CoC mass from CCA-contaminated wood waste in this study appears to be the EK treatment of the CCA plug material without pre-EK chemical treatment.

The following recommendations are included as suggestions for the improvement of similar research in the future. The recommendations were either identified by research technicians over the course of this research, received as feedback from colleagues at conference proceedings, or mentioned in passing during the defense of the thesis. Based on this study the following recommendations are provided:

- Additional EK studies using shorter treatment periods and more frequent sampling should be conducted. This would allow for quicker turnaround on experimental results and more accurate concentration curves.
- The post-EK wood samples need to be de-acidified o enhance the TCLP performance of the wood. This could be done by washing the wood, reversing of the electrode polarity for a brief period, or increasing the pH control limit.

This could possibly raise the pH of the post-EK wood, and possibly decrease the mobility of the CoC that remain in the treated wood.

- The carbon electrodes used in the EK cells experienced significant degradation over the course of the experiment. Plated electrodes would help with mass balance accuracy and improve the overall consistency of the electrical performance of the EK cell.
- Detailed economic evaluations of the EK treatment process for CCA wood should be conducted.
- If the economics studies prove that EK is a cost effective method, this process should be scaled-up and pilot studies of the process should be conducted.

REFERENCES

Barnhart, J., "Chromium Chemistry and Implications for Environmental Fate and Toxicity," *Journal of Soil Contamination*, 6 (6), 561-568, 1997.

Breslin, V. T., Adler-Ivanbrook, L., "Release of Copper, Chromium and Arsenic from CCA-C Treated Lumber in Estuaries," *Estuarine, Coastal and Shelf Science*, 46, 111-125, 1998.

Bricka, R.M., Parker A.M., "Laboratory-scale fast pyrolysis of cca-treated wood waste," 2008 AIChe Annual Meeting, Philadelphia, PA, 83913, 2008.

Christensen, I. V., Pedersen, A. J., Ottosen, L. M., Ribeiro, A. B., "Electrodialytic remediation of CCA-treated waste wood in a 2 cubic meter pilot plant," *Science of the Total Environment*, 364, 45-54, 2006.

Clausen, C. A., "Enhanced removal of CCA from treated wood by Bacillus licheniformis in continuous culture," 28th Annual Meeting of the International Research Group on Wood Preservation Section 5 Environmental Aspects, Whistler, British Columbia, Canada, 25-30 May 1997.

Clausen, C. A., "Improving the two step remediation process for CCA-treated wood: Part II. Evaluating bacterial nutrient sources," *Waste Management*, 24, 407-411, 2004.

Clausen, C. A., Smith, R. L., "CCA removal from treated wood by chemical, mechanical, and microbial processing," Proceedings of the 4th International Wood Preservation Symposium the Challenge-Safety Environment," Cannes-Mandelieu, France, 2-3 February 1998.

Cooper, P. A., "Leaching of CCA from treated wood: pH effects," *Forest Products Journal*, 41 (1), 30-32, 1991.

Cooper, P. A., Jeremic, D., Taylor, J. L., "Residual CCA Levels in CCA-Treated Poles Removed From Service," Forest Products Journal, 51 (10), 58-62, 2001.

Cooper, P. A., Jeremic, D., Ung Y. T., "Effectiveness of CCA fixation to avoid hexavalent chromium leaching," Forest Products Journal, 54 (3), 56-58, 2004.

Freeman, M. H., Shupe, T. F., Vlosky, R. P., Barnes, H.M., "Past Present and Future of the Wood Preservation Industry," *Forest Products Journal*, 53 (10), 8-14, 2003.

Gezer, E. D., Yildiz, U., Yildiz, S., Dizman, E., Temiz, A., "Removal copper, chromium, and arsenic from CCA-treated yellow pine by oleic acid," *Building and Environment*, 41, 380-385, 2006.

Helsen, L., Van den Bulck, E., "Review of disposal technologies for chromated copper arsenate (CCA) treated wood waste, with detailed analyses of thermochemical conversion processes," *Environmental Pollution*, 134, 301-314, 2005.

Helsen, L., Van den Bulck, E., Hery, J.S., "Total recycling of CCA treated wood waste by low-temperature pyrolysis," *Waste Management*, 18, 571-578, 1998.

Hingston, J. A., Collins, C. D., Murphy, R. J., Lester, J. N., "Leaching of chromated copper arsenate wood preservatives: a review," *Environmental Pollution*, 111, 53-66, 2001.

Hunt, Garratt, Wood Preservation, Third Edition, McGraw Hill, New York, 1967.

Issosari, P., Marjavaara, P., Lehmus, E., "Sequential electrokinetic treatment and oxalic acid extraction for the removal of Cu, Cr and As from wood," Journal of Hazardous Materials, 182(1-3), 869-876, 2010.

Kakitani, T., Hata, T., Kajimoto, T., Imamura, Y., "A Novel Extractant for Removal of Hazardous Metals from Preservative-Treated Wood Waste," *Journal of Environmental Quality*, 35, 912-917, 2006.

Kakitani, T., Toshimitsu, H., Takeshi, K., Imamura, Y., "Designing a purificaiton process for chromium-, coppper-, and arsenic-contaminated wood," *Waste Management*, 26, 453-458, 2006.

Kakitani, T., Toshimitsu, H., Takeshi, K., Imamura, Y., "Effect of pyrolysis on solvent extractability of toxic metals from chromated copper arsenate (CCA)-treated wood," *Journal of Hazardous Materials B*, 109, 53-57, 2004.

Kazi, F. K. M., Cooper, P. A., "Method to recover and reuse chromated copper arsenate wood preservative from spent treated wood," *Waste Management*, 26, 182-188, 2006.

Kazi, F. K. M., Cooper, P. A., "Rapic-extraction oxidation process to recover and reuse copper chromium and arsenic from industrial wood preservative sludge," *Waste Management*, 22, 293-301, 2002.

Kazi, F. K. M., Cooper, P. A., Chen, J., "Kinetic Model of CCA Fixation in Wood. Part II. The Main Reaction Zone," *Wood and Fiber Science*, 32(4), 442-449, 2000.

Lebow, S. T., Foster, D. O., Lebow, P. K., "Release of Copper, Chromium, and Arsenic From Treated Southern Pine Exposed in Seawater and Freshwater," Forest Products Journal, 49 (7/8), 80-89, 1999.

Lebow, S., Brooks, K., Simonsen, J., "Environmental Impact of Treated Wood in Service," Enhancing the Durability of Lumber and Engineered Wood Products, Kissimmee, FL, 11-13 February 2002.

McMahon, C. K., Bush, P. B., Woolson, E. A., "Release of Copper, Chromium, and Arsenic from Burning Wood Treated With Preservatives," 78th Annual Meeting of the Air Pollution Control Association, Detroit, MI., 16-21 June, 1985.

Moreira, E. E., Ribeiro, A. B., Mateus, E. P., Mexia J. T., Ottosen, L. M., "Regressional modeling of electrodialytic removal of Cu, Cr and As from CCA treated timber waste: application to sawdust," *Wood Science Technology*, 39, 291-309, 2005.

Nico, P. S., Fendorf, S. E., Lowney, Y. W., Holm, S. E., Ruby, M. V., "Chemical Structure of Arsenic and Chromium in CCA-Treated Wood: Implications of Environmental Weathering," *Environmental Science and Technology*, 38, 5253-5260, 2004.

Ottosen, L. M., Kristensen, I. V., Pedersen, A. J., Hansen, H. K., Villumsen, A., Ribeiro, A. B., "Electrodialytic Removal of Heavy Metals from Different Solid Waste Products," *Separation Science and Technology*, 38(6), 1269-1289, 2003.

Ottosen, L. M., Pedersen, A. J., Christensen, I. V., "Characterization of Residues From Thermal Treatment of CCA Impregnated Wood. Chemical and Electrochemical Extraction of Cu, Cr, As and Zn," Wood Science and Technology, 39(2), 87-98, 2005.

Pedersen, A. J., Kristensen, I. V., Ottosen, L. M., Ribeiro, A. B., Villumsen, A., "Electrodialytic remediation of CCA-treated wasted wood in pilot scale," *Engineering Geology*, 77, 331-338, 2005.

Pedersen, A. J., Ottosen, L.M., "Elemental analysis of ash residue from combustion of CCA treated wood waste before and after electrodialytic extraction," *Chemosphere*, 65, 110-116, 2006.

Pizzi, A., "The Chemistry and Kinetic Behavior of Cu-Cr-As/B Wood Preservatives. IV. Fixation of CCA to Wood," *Journal of Polymer Science*, 20, 739-764, 1982.

Ribeiro, A. B., Mateus, E. P., Ottosen L. M., Bech-Nielsen, G., "Electrodialytic Removal of Cu, Cr, and As from Chromated Copper Arsenate-Treated Timber Waste," *Environmental Science and Technology*, 34, 784-788, 2000.

Ribeiro, A. B., Rodriguez-Maroto, J. M., Mateus, E. P., Velizarova, E., Ottosen, L. M., "Modeling of electrodialytic and dialytic removal of Cr, Cu, and As from CCA-treated wood chips," *Chemosphere*, 66, 1716-1726, 2007.

Richardson, B. A., Wood Preservation, First Edition, E. & F.N. Spon, New York, 1993.

Sarahney, H.,Wang, J., Alshawabkeh, A., “Electrokinetic Process for Removing Cu, Cr, and As from CCA-Treated Wood,” *Environmental Engineering Science*, 22, 642-650, 2005.

Saxe, J. K., Wannamaker, E. J., Conklin, S. W., Shupe, T. F., Beck, B. D., "Evaluating landfill disposal of chromated copper arsenate (CCA) treated wood and potential effects on groundwater: Evidence from Florida," *Chemosphere*, 66, 496-504, 2007.

Solo-Gabriele, H., Townsend, T., "Disposal practices and management alternatives for CCA-treated wood waste," *Waste Management and Research*, 378-389, 1999.

Stook, K., Tolaymat, T., Ward, M., Dubey, B., Townsend, T., Solo-Gabriele, H., Bitton, G., "Relative Leachingand Aquatic Toxicity of Pressure-Treated Wood Products Using Batch Leaching Tests," *Environmental Science and Technology*, 39, 155-163, 2005.

Townsend, T., Thalbet, T., Solo-Gabriele, H., Dubey, B., Stook, K., Wadanambi, L., "Leaching of CCA-treated wood: implications for waste disposal," *Journal of Hazardous Materials B*, 14, 75-91, 2004.

Velizarova, E., Ribeiro, A. B., Mateus, E., Ottosen, L. M., "Effect of different extracting solutions on the electrodialytic remediation of CCA-treated wood waste Part I. Behavior of Cu and Cr," *Journal of Hazardous Materials B*, 107, 103-113, 2004.

Velizarova, E., Ribeiro, A. B., Ottosen, L. M., "A comparative study on Cu, Cr and As removal from CCA-treated wood waste by dialytic and electrodialytic processes," *Journal of Hazardous Materials B*, 94, 147-160, 2002.

Virkutyte, J., Velizarova, E., Ribeiro A. B., Sillanpaa, M., "Copper and Chromium Electrodialytic Migration in CCA-Treated Timber Waste," *Water, Air, and Soil Pollution*, 160, 27-39, 2005.

Weber, W. J., Jang, Y., Townsend, T. G., Laux, S., "Leachate from Land Disposed Residential Construction Waste," *Journal of Environmental Engineering*, 128 (3), 237-245, 2002.

APPENDIX A

PHASE I EXPERIMENTAL RESULTS FOR CHARACTERIZATION OF THE RAW CCA WOOD SAMPLE

Table A.1 Sample data and calculated averages of the CoC content raw wood specimen at the “Surface” level

	sample number	As (ppm)	Cr (ppm)	Cu (ppm)
	1	5225.2	6122.4	3283.0
	2	5205.9	6007.1	3232.2
	3	5307.5	6187.6	3287.7
	4	5418.4	6315.8	3335.5
	5	5441.5	6195.5	3464.4
	6	5575.0	6369.1	3403.2
average 1 - 6		5362.3	6199.6	3334.3
standard deviaion		142.1	130.7	85.9

Table A.2 Sample data and calculated averages of the CoC content raw wood specimen at the “Subsurface” level

	sample number	As (ppm)	Cr (ppm)	Cu (ppm)
	1	4393.03	5232.81	2591.12
	2	4195.73	5001.79	2507.71
	3	4245.78	5069.82	2511.76
	4	4413.46	5260.78	2584.14
	5	4393.56	5238.31	2581.45
	6	4343.85	5181.56	2555.26
average 1 - 6		4330.9	5164.2	2555.2
standard deviaion		89.8	105.0	37.3

Table A.3 Sample data and calculated averages of the TCLP concentrations of the raw wood specimen at the "Surface" level

	sample number	As (ppm)	Cr (ppm)	Cu (ppm)
	1	6.71	2.83	20.26
	2	8.55	3.68	29.07
	3	8.40	3.65	28.55
	4	8.34	3.62	29.08
	5	7.81	3.30	26.98
	6	5.34	2.47	20.86
average 1 - 6		7.53	3.26	25.8
standard deviaion		1.26	0.50	4.13

Table A.4 Sample data and calculated averages of the moisture content of the raw wood specimen at the "Surface" level

	sample number	moisture content (% total weight)
	1	6.65
	2	6.69
	3	7.22
	4	7.22
	5	7.11
	6	6.78
average 1 - 6		6.94
standard deviation		0.27

APPENDIX B

PHASE II EXPERIMENTAL RESULTS FOR THE SELCTION OF THE PRE-EK CHEMICAL TREATMENT AGENT

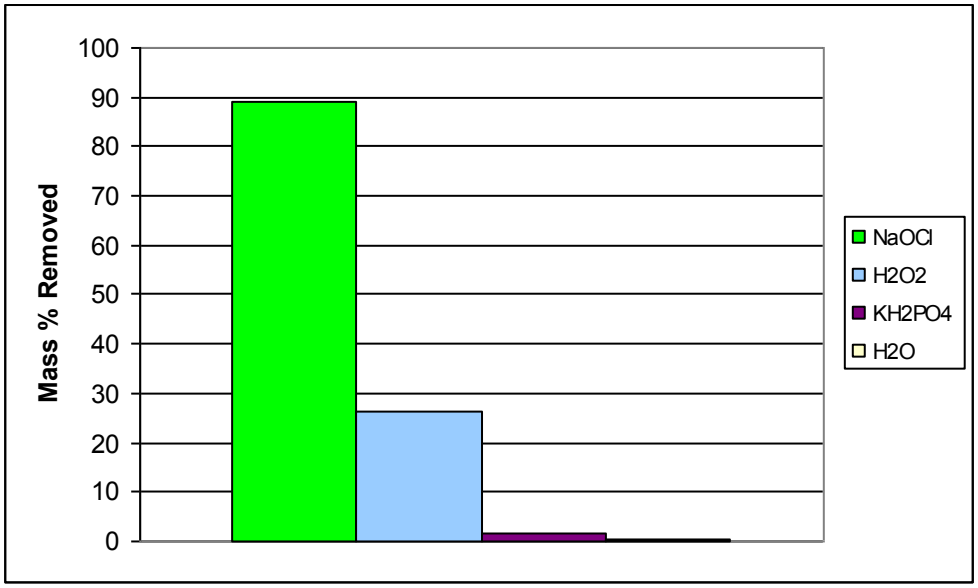

Figure B.1 Chemical pre-treatment selection: Stage I. Plot of chromium mass percentage removed versus chemical pre-treatment agent type

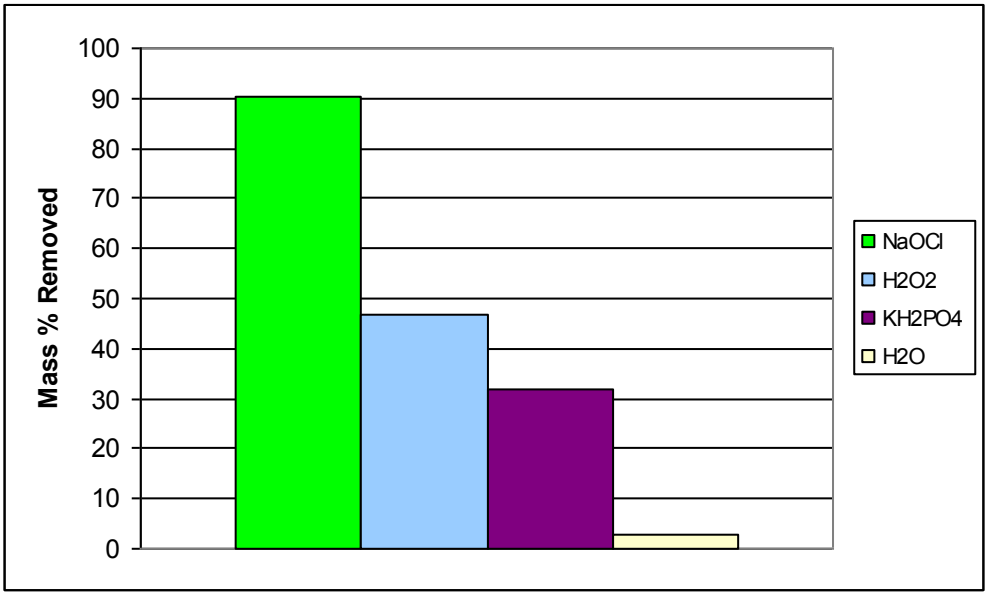

Figure B.2 Chemical pre-treatment selection: Stage I. Plot of copper mass percentage removed versus chemical pre-treatment agent type

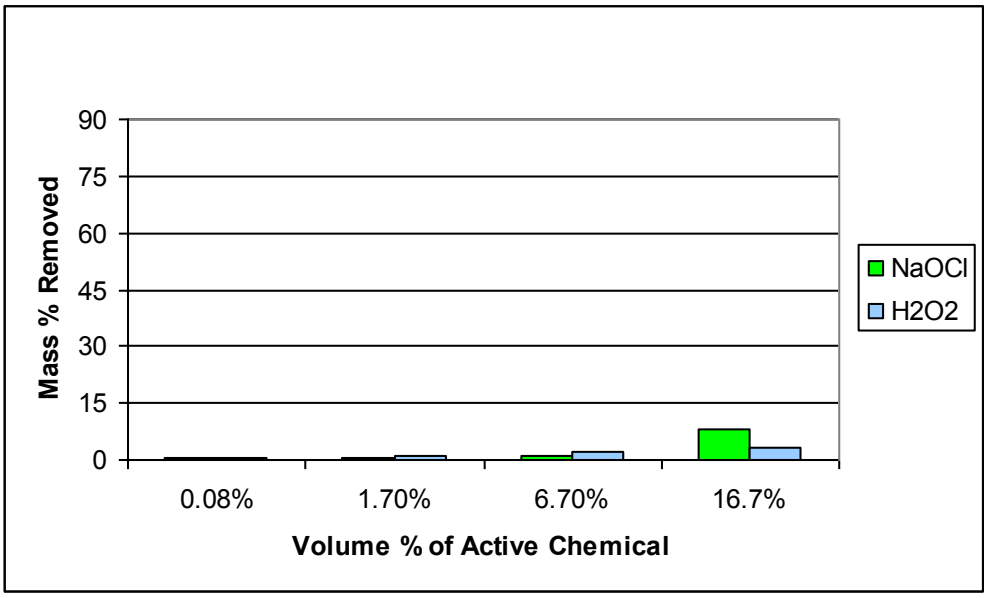

Figure B.3 Chemical pre-treatment selection: Stage II. Plot of chromium mass percentage removed versus chemical pre-treatment agent solution strength at 5.00 grams of solid per experimental unit

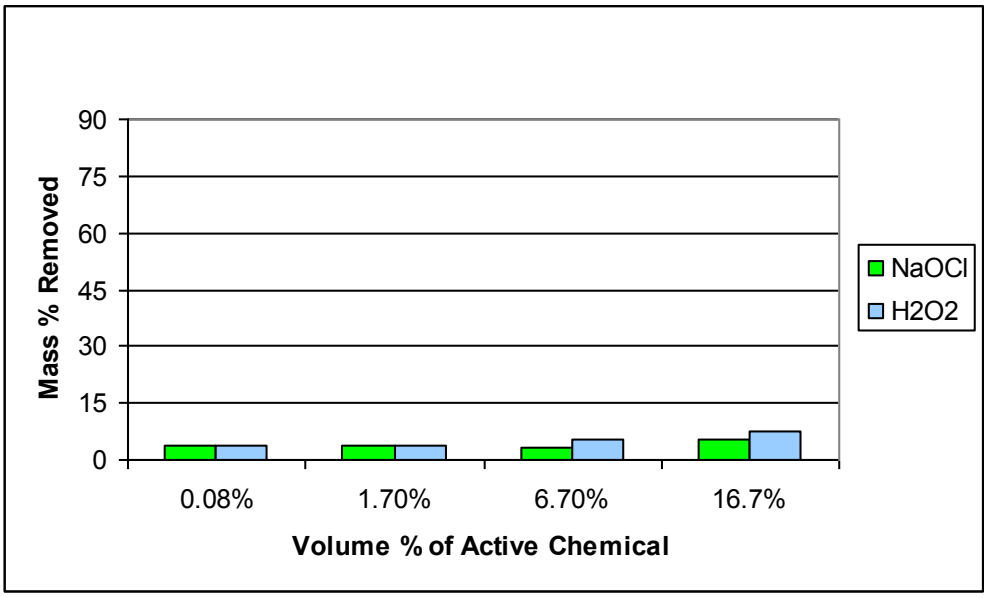

Figure B.4 Chemical pre-treatment selection: Stage II. Plot of copper mass percentage removed versus chemical pre-treatment agent solution strength at 5.00 grams of solid per experimental unit

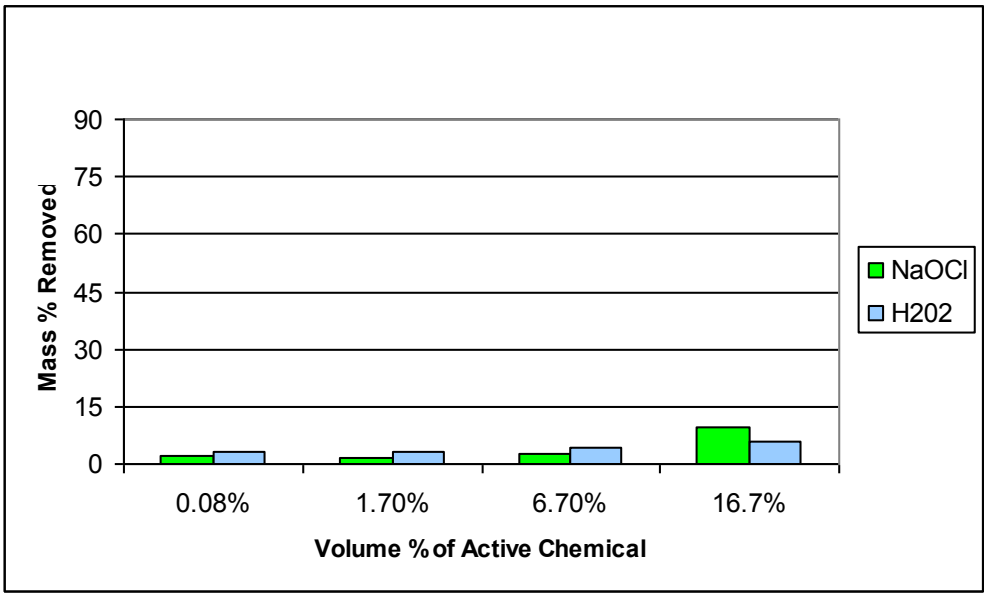

Figure B.5 Chemical pre-treatment selection: Stage II. Plot of arsenic mass percentage removed versus chemical pre-treatment agent solution strength at 3.00 grams of solid per experimental unit

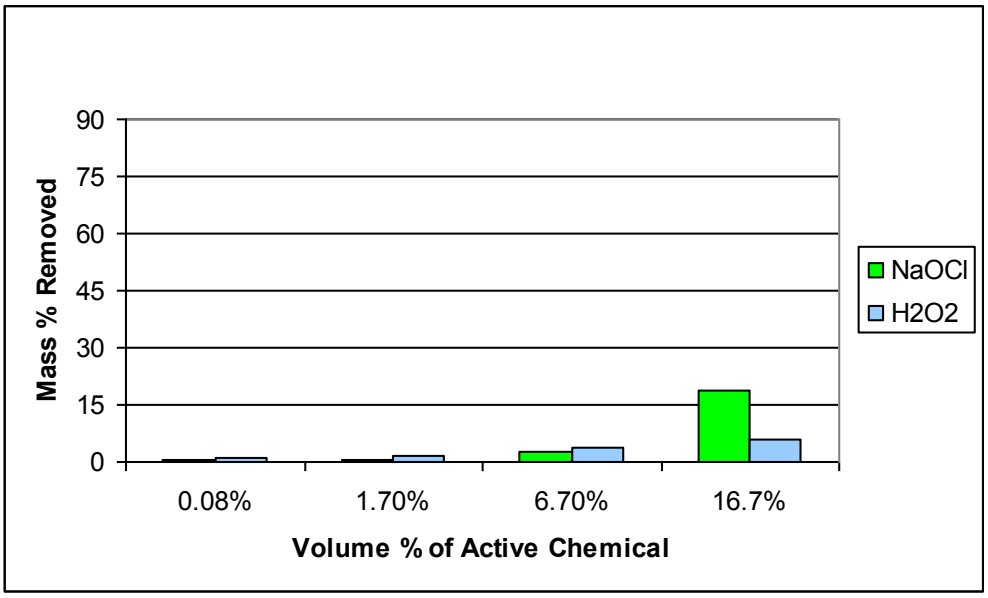

Figure B.6 Chemical pre-treatment selection: Stage II. Plot of chromium mass percentage removed versus chemical pre-treatment agent solution strength at 3.00 grams of solid per experimental unit

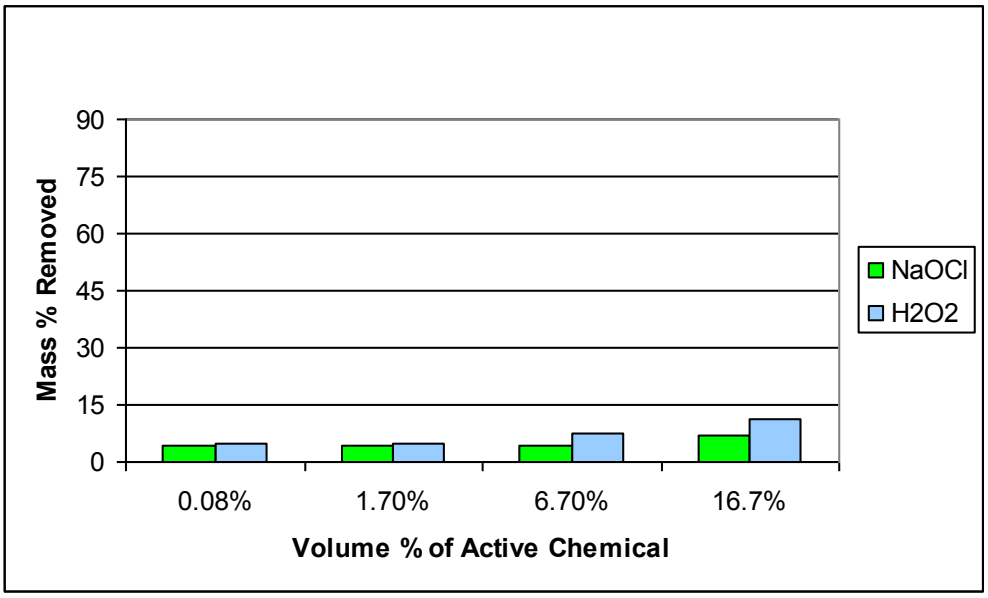

Figure B.7 Chemical pre-treatment selection: Stage II. Plot of copper mass percentage removed versus chemical pre-treatment agent solution strength at 3.00 grams of solid per experimental unit

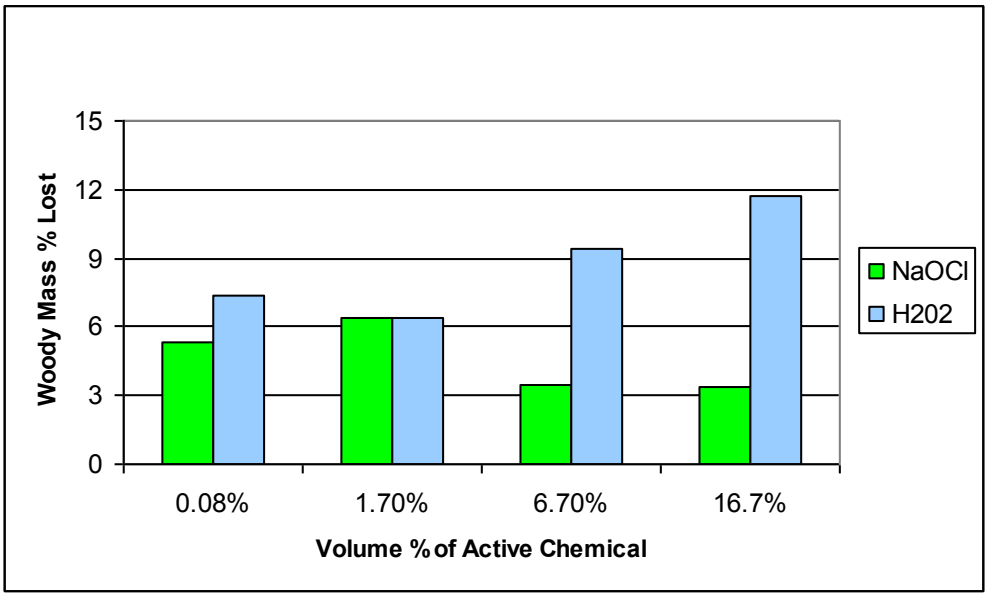

Figure B.8 Chemical pre-treatment selection: Stage II. Plot of percentage of woody mass lost versus chemical pre-treatment agent solution strength at 3.00 grams of solid per experimental unit

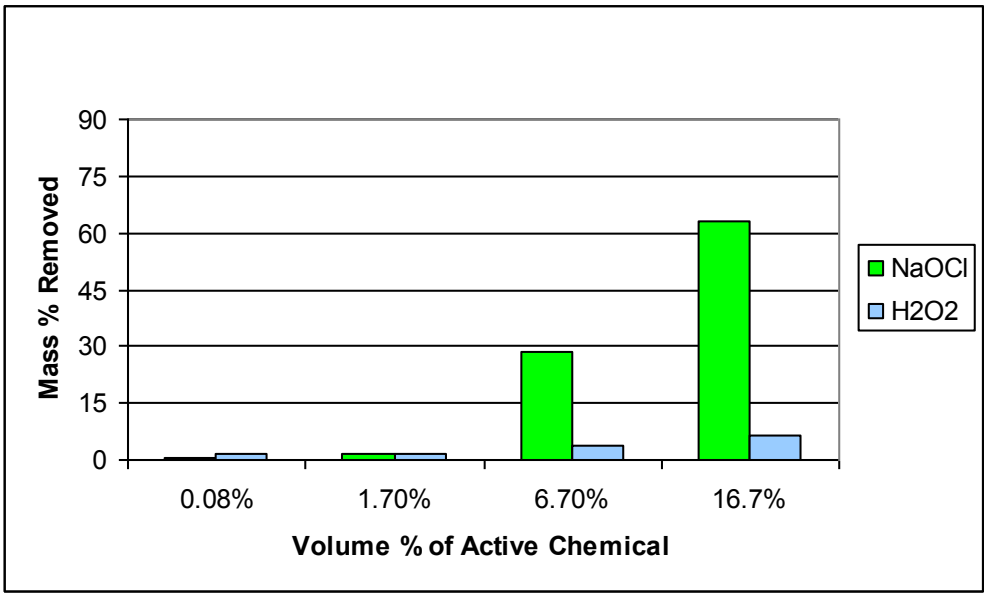

Figure B.9 Chemical pre-treatment selection: Stage II. Plot of chromium mass percentage removed versus chemical pre-treatment agent solution strength at 1.00 grams of solid per experimental unit

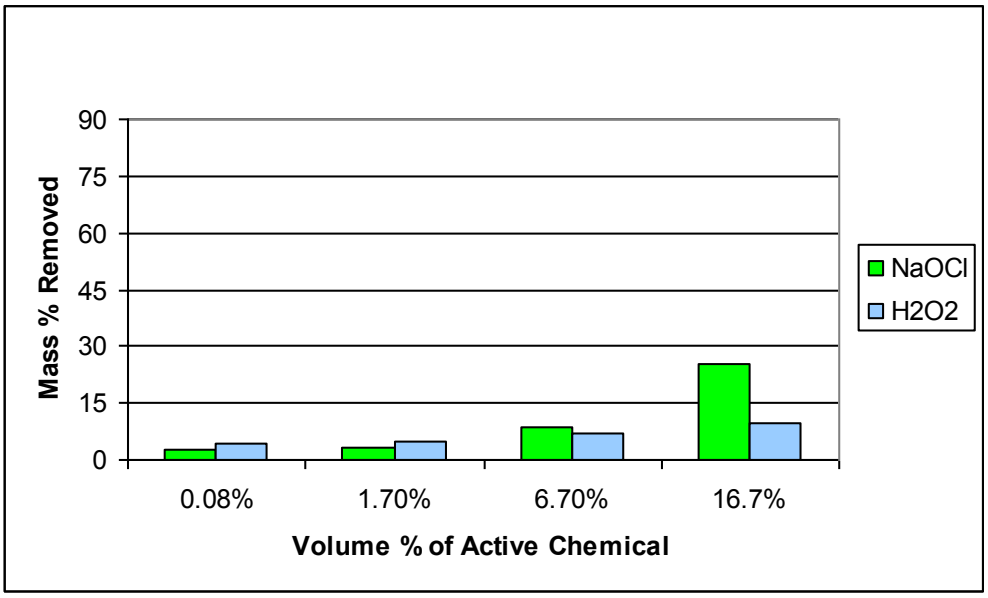

Figure B.10 Chemical pre-treatment selection: Stage II. Plot of copper mass percentage removed versus chemical pre-treatment agent solution strength at 1.00 grams of solid per experimental unit

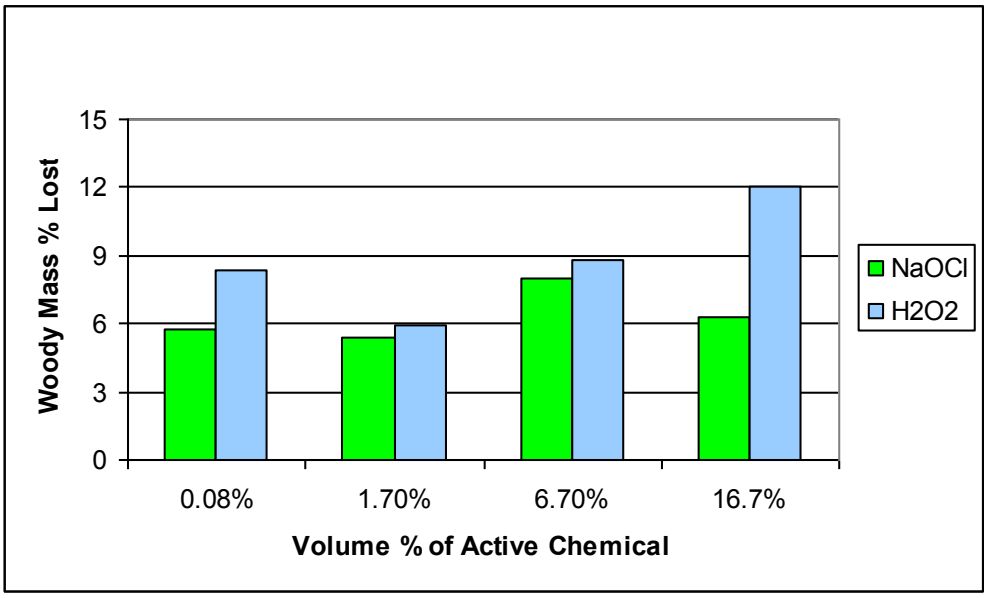

Figure B.11 Chemical pre-treatment selection: Stage II. Plot of percentage of woody mass lost versus chemical pre-treatment agent solution strength at 1.00 grams of solid per experimental unit

APPENDIX C

POST ELECTROKINETIC EXPERIMENT RESULTS FOR REMOVAL PERCENTAGES, IONIC MOBILITIES, AND METAL DISTRIBUTIONS

Table C.1 Average TCLP concentration of the source wood sample

	CoC		
	Arsenic	***Chromium***	***Copper***
average concentration (ppm)	7.32	3.25	25.8
standard deviation (ppm)	1.26	0.50	4.13

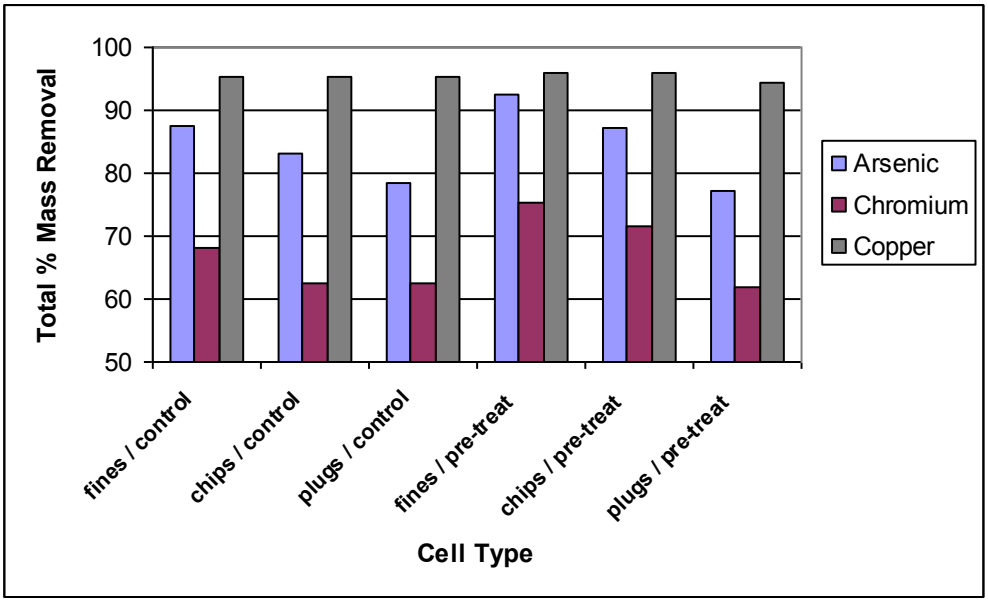

Figure C.1 Overall post-EK mass removal percentage for all CoC.

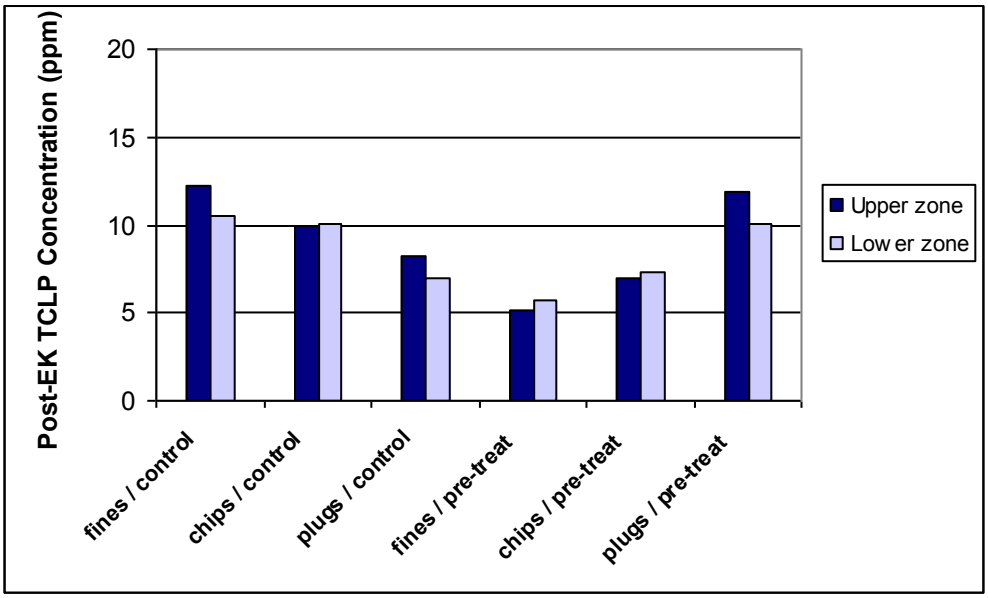

Figure C.2 Sectional post-EK TCLP concentrations for arsenic with EK cell center compartment divided into vertical sections

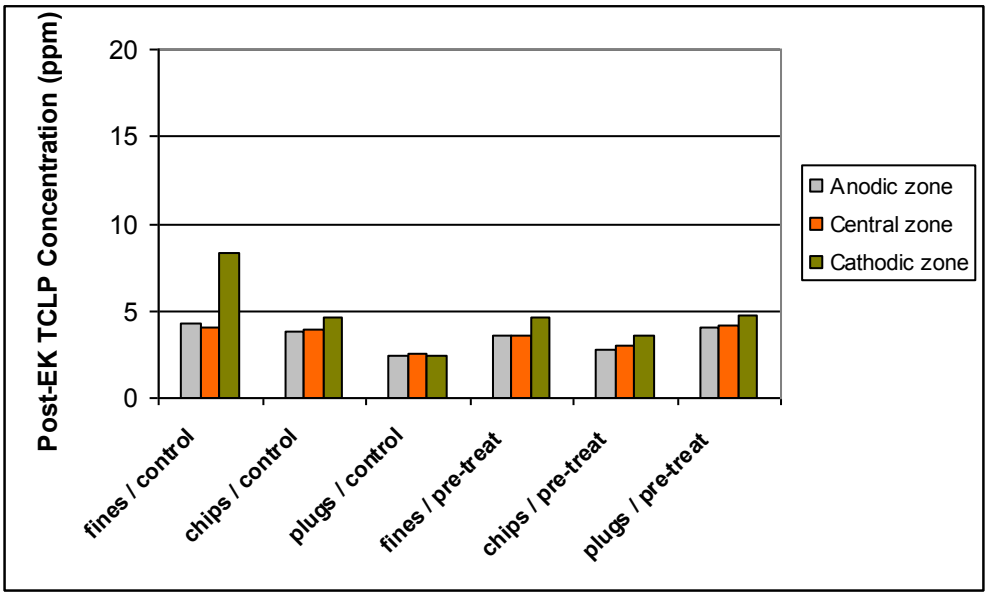

Figure C.3 Sectional post-EK TCLP concentrations for chromium with EK cell center compartment divided into longitudinal sections

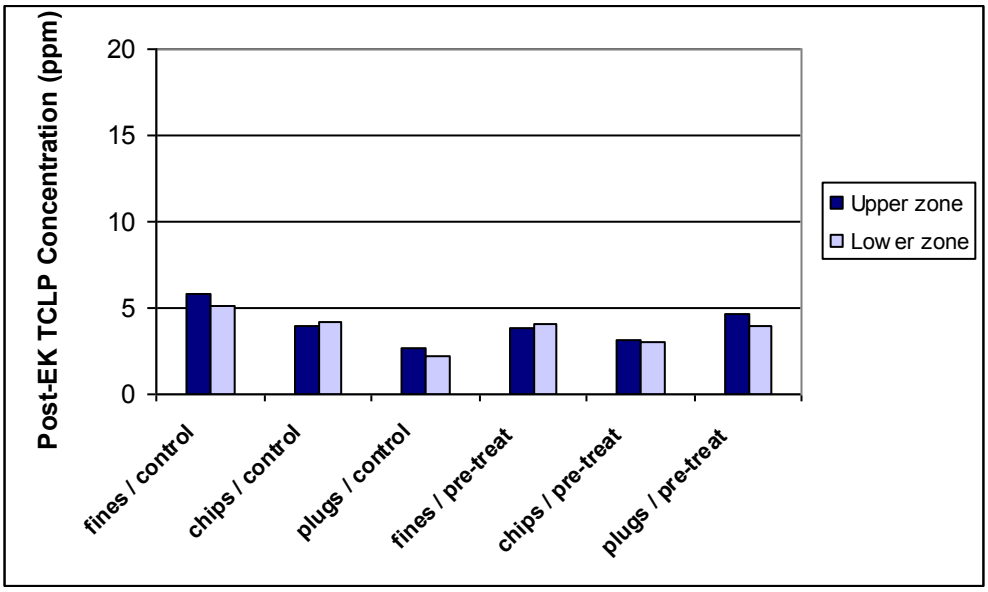

Figure C.4 Sectional post-EK TCLP concentrations for chromium with EK cell center compartment divided into vertical sections

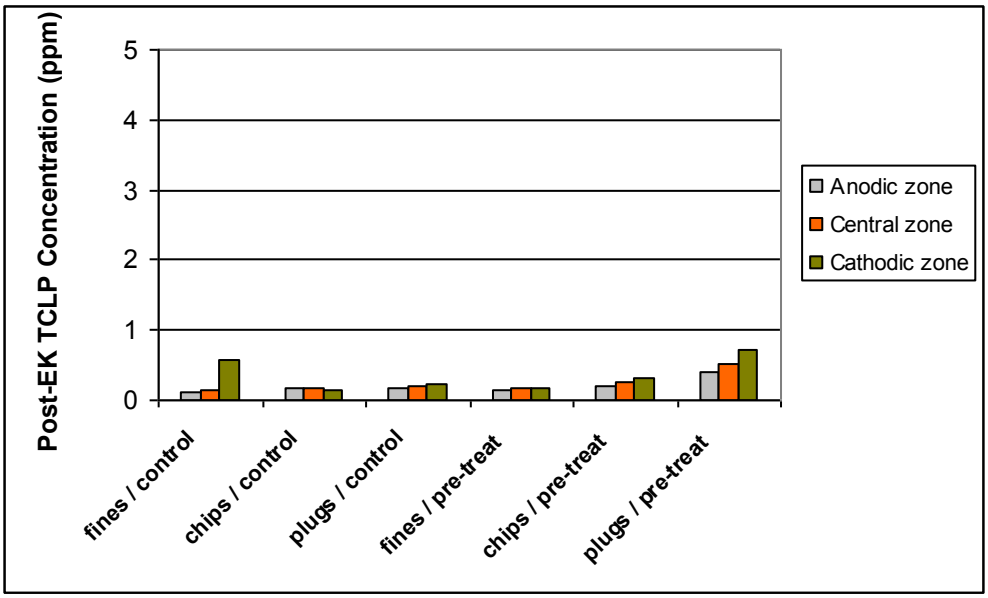

Figure C.5 Sectional post-EK TCLP concentrations for copper with EK cell center compartment divided into longitudinal sections

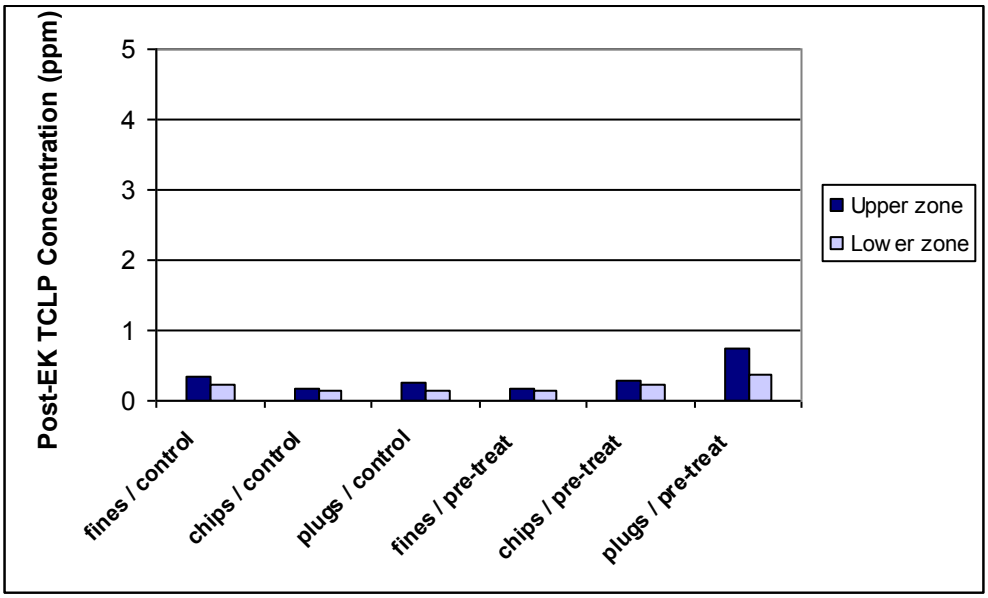

Figure C.6 Sectional post-EK TCLP concentrations for copper with EK cell center compartment divided into vertical sections

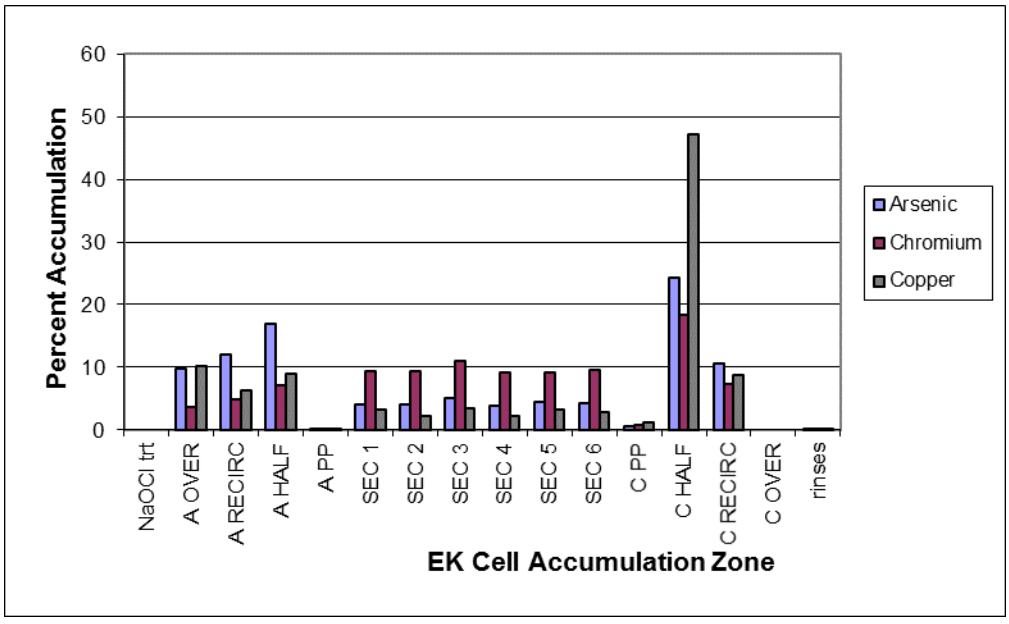

Figure C.7 Averaged Post EK distribution of CoC across the EK cell for the "plugs / control" experimental units

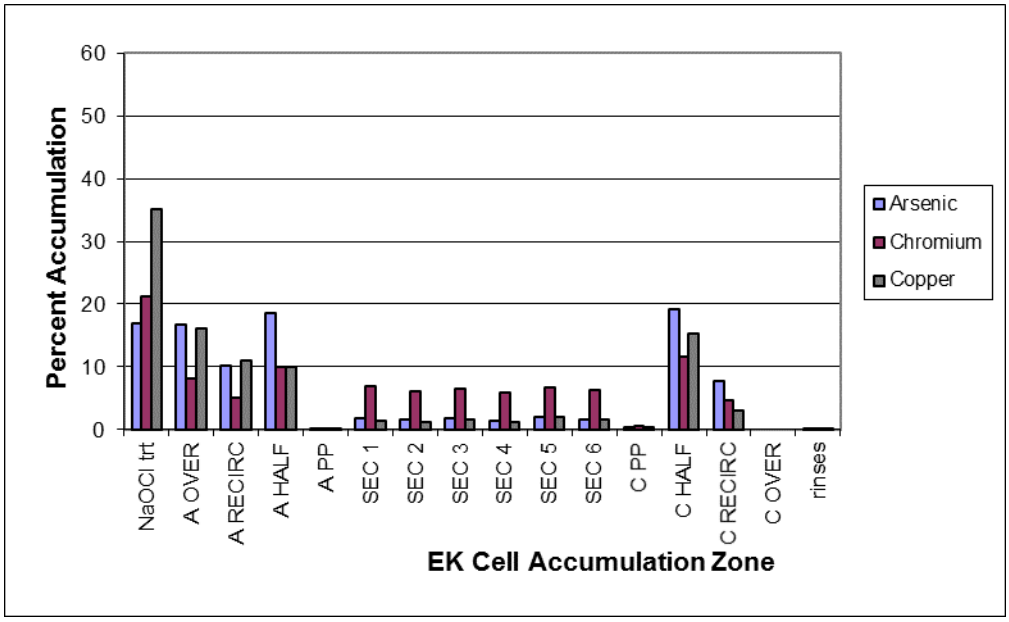

Figure C.8 Averaged Post EK distribution of CoC across the EK cell for the "chips / pre-treat" experimental units

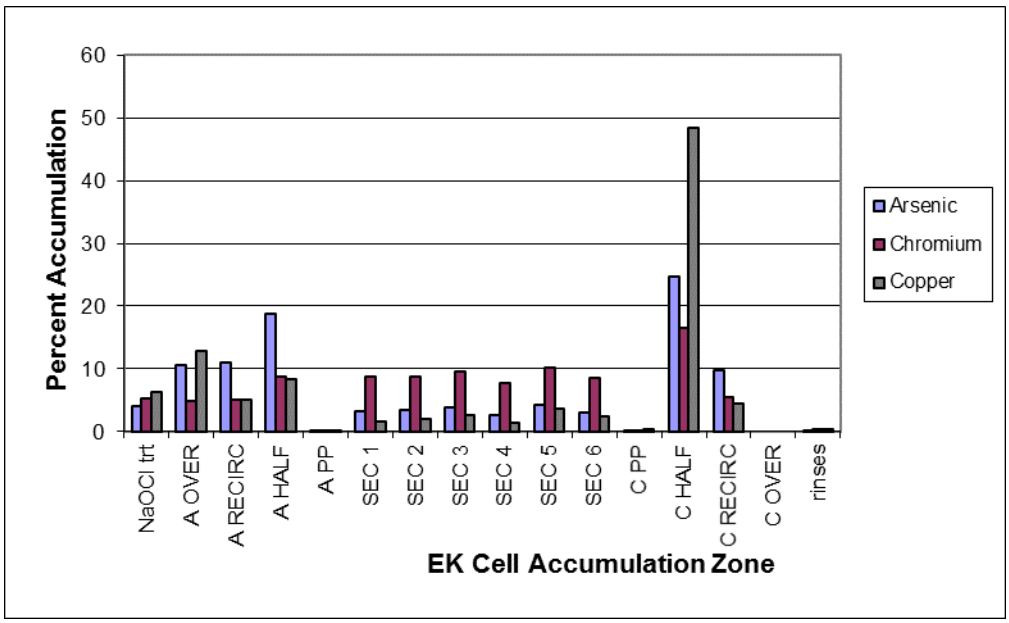

Figure C.9 Averaged Post EK distribution of CoC across the EK cell for the "plugs / pre-treat" experimental units

APPENDIX D

ADDITIONAL RATE MODELING DATA

Table D.1 Anodic and cathodic CoC accumulation rate model constants for arsenic

EK CELL TYPE	ANODE		CATHODE	
	Pre-exponential	*Rate Constant*	*Pre-exponential*	*Rate Constant*
	Factor "A"	*"R"*	*Factor "A"*	*"R"*
fines / control	173.4	0.3730	120.9	0.0822
chips / control	95.7	0.2730	111.1	0.0693
plugs / control	109.8	0.1816	109.0	0.0515
fines / pre-treat	147.4	0.1451	150.5	0.0513
chips / pre-treat	91.2	0.1421	82.8	0.0434
plugs / pre-treat	124.1	0.1348	120.8	0.0328

Table D.2 Anodic and cathodic CoC accumulation rate model constants for chromium

EK CELL TYPE	ANODE		CATHODE	
	Pre-exponential	*Rate Constant*	*Pre-exponential*	*Rate Constant*
	Factor "A"	*"R"*	*Factor "A"*	*"R"*
fines / control	47.3	0.1485	146.3	0.05339
chips / control	37.6	0.0762	73.0	0.06154
plugs / control	44.1	0.0623	87.3	0.05879
fines / pre-treat	54.1	0.2983	167.8	0.1764
chips / pre-treat	34.6	0.1918	50.8	0.09040
plugs / pre-treat	48.7	0.0843	62.1	0.1016

Table D.3 Anodic and cathodic CoC accumulation rate model constants for copper

EK CELL TYPE	ANODE		CATHODE	
	Pre-exponential	*Rate Constant*	*Pre-exponential*	*Rate Constant*
	Factor "A"	*"K1"*	*Factor "A"*	*"K1"*
fines / control	24.7	0.2049	273.4	0.1102
chips / control	24.8	0.07055	242.2	0.07625
plugs / control	69.1	0.04200	259.7	0.1501
fines / pre-treat	131.8	0.2411	250.1	0.1431
chips / pre-treat	76.5	0.09445	158.7	0.06805
plugs / pre-treat	85.5	0.7723	242.1	0.1163

Table D.4 EK cell center compartment CoC transport rate model constants for arsenic

EK CELL TYPE	PORT 1				PORT 2				PORT 3			
	"A"	*"K1"*	*"K2"*	*"K3"*	*"A"*	*"K1"*	*"K2"*	*"K3"*	*"A"*	*"K1"*	*"K2"*	*"K3"*
fines / control	614.6	0.3410	0.05829	0.01515	601.0	0.2956	0.1003	0.0336	399.9	0.6388	0.07538	0.04901
chips / control	419.3	0.1792	0.1388	0.0403	417.1	0.1797	0.1383	0.04135	223.7	0.2076	0.05068	0.02358
plugs / control	334.3	0.1547	0.1069	0.0532	357.7	0.1358	0.09290	0.0425	312.6	0.1414	0.08871	0.04862
fines / pre-treat	480.0	0.08766	0.01919	0.001	612.7	0.1472	0.05538	0.00598	228.9	0.1179	0.1139	0.00335
chips / pre-treat	265.7	0.1546	0.1050	0.0491	265.7	0.1621	0.1092	0.05205	153.9	0.2125	0.09147	0.1193
plugs / pre-treat	244.5	0.3935	0.3197	0.1459	322.3	0.2025	0.08553	0.02585	163.1	0.1785	0.1429	0.3582

Table D.5 EK cell center compartment CoC transport rate model constants for chromium

EK CELL TYPE	PORT 1				PORT 2				PORT 3			
	"A"	*"K1"*	*"K2"*	*"K3"*	*"A"*	*"K1"*	*"K2"*	*"K3"*	*"A"*	*"K1"*	*"K2"*	*"K3"*
fines / control	387.6	0.1518	0.1201	0.03175	521.4	0.1457	0.1251	0.02064	354.1	0.1488	0.07818	0.0162
chips / control	155.5	0.1811	0.1314	0.04965	191.1	0.1898	0.1489	0.04042	155.7	0.1817	0.1276	0.05350
plugs / control	124.4	0.1602	0.05939	0.04130	128.5	0.1683	0.05674	0.03040	159.0	0.1372	0.08586	0.05185
fines / pre-treat	332.6	0.07255	0.03506	0.0005	593.6	0.1002	0.04408	0.0005	716.7	0.1083	0.09991	0.07082
chips / pre-treat	119.1	0.1541	0.07623	0.07980	163.2	0.1378	0.1038	0.03380	124	0.1425	0.09851	0.04390
plugs / pre-treat	147.7	0.1403	0.07093	0.05805	193.5	0.1351	0.08859	0.02165	141.8	0.1137	0.06502	0.03630

Table D.6 EK cell center compartment CoC transport rate model constants for copper

EK CELL TYPE	PORT 1				PORT 2				PORT 3			
	"A"	*"K1"*	*"K2"*	*"K3"*	*"A"*	*"K1"*	*"K2"*	*"K3"*	*"A"*	*"K1"*	*"K2"*	*"K3"*
fines / control	208.2	0.2444	0.2380	0.00575	334.4	0.1897	0.1885	0.00109	435.0	0.1973	0.1956	0.00131
chips / control	121.0	0.2398	0.1312	0.02060	208.3	0.1964	0.1851	0.01165	257.2	0.1881	0.1797	0.00794
plugs / control	179.3	0.1442	0.1236	0.02020	210.2	0.1464	0.1298	0.01715	233.1	0.1559	0.1404	0.01602
fines / pre-treat	212.9	0.2351	0.08232	0.01531	369.7	0.1057	0.08873	0.00287	337.9	0.1145	0.1079	0.0074
chips / pre-treat	102.1	0.1649	0.1183	0.04875	163.8	0.1516	0.1333	0.01840	202.3	0.1493	0.1348	0.01383
plugs / pre-treat	163.9	0.5299	0.06524	0.00270	304.9	0.1508	0.1402	0.01050	188.7	0.6052	0.07171	0.00345

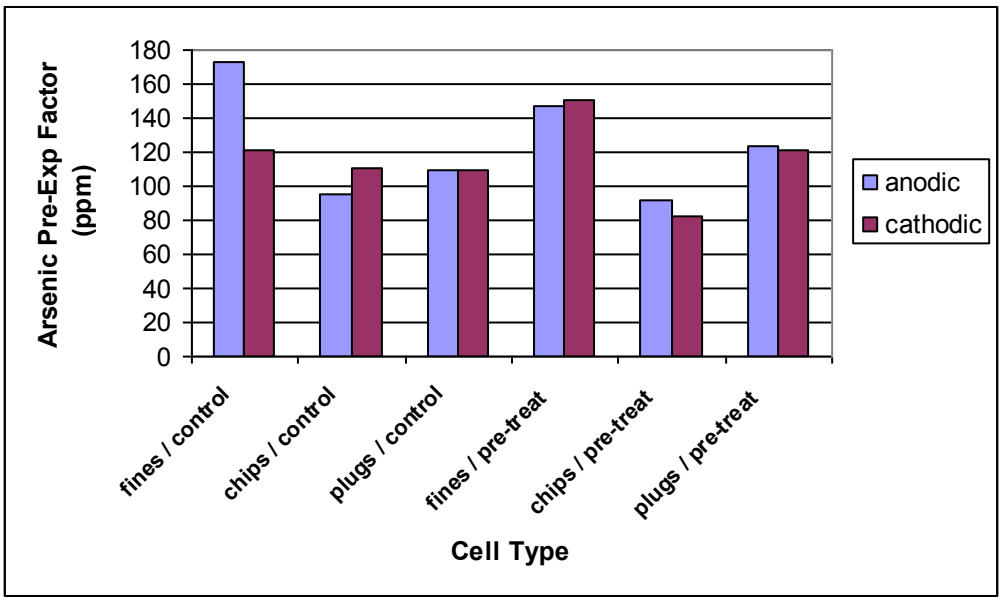

Figure D.1 Pre-exponential factor "A" for the arsenic half cell accumulation rate model

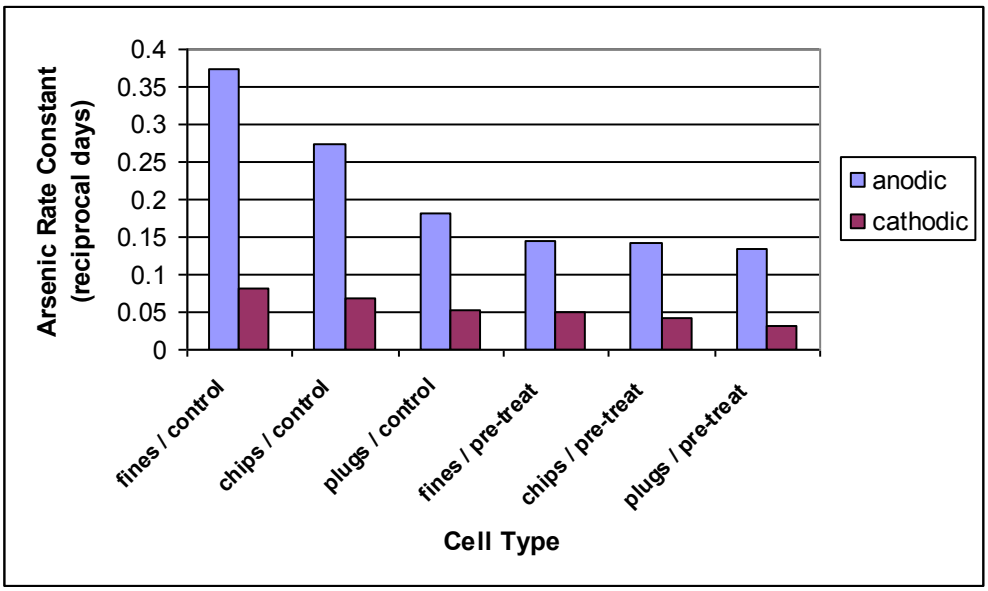

Figure D.2 Rate constant "R" for the arsenic half cell accumulation rate model

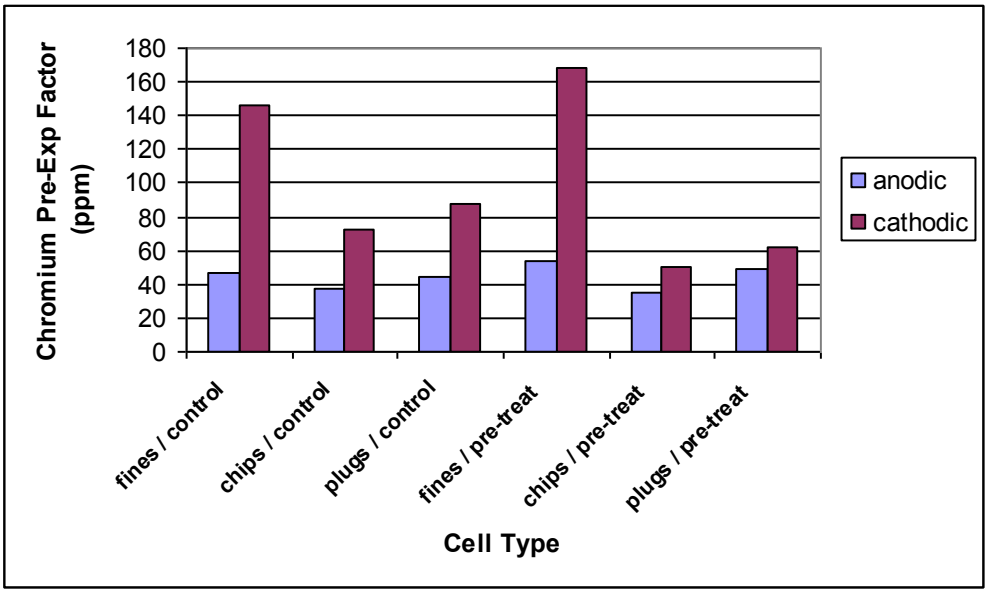

Figure D.3 Pre-exponential factor "A" for the chromium half cell accumulation rate model

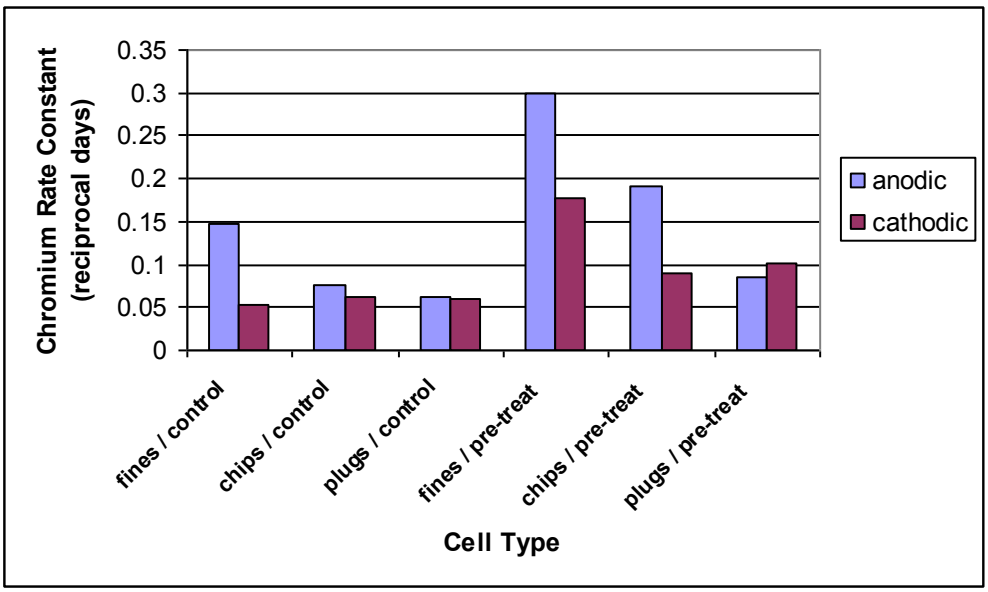

Figure D.4 Rate constant "R" for the chromium half cell accumulation rate model

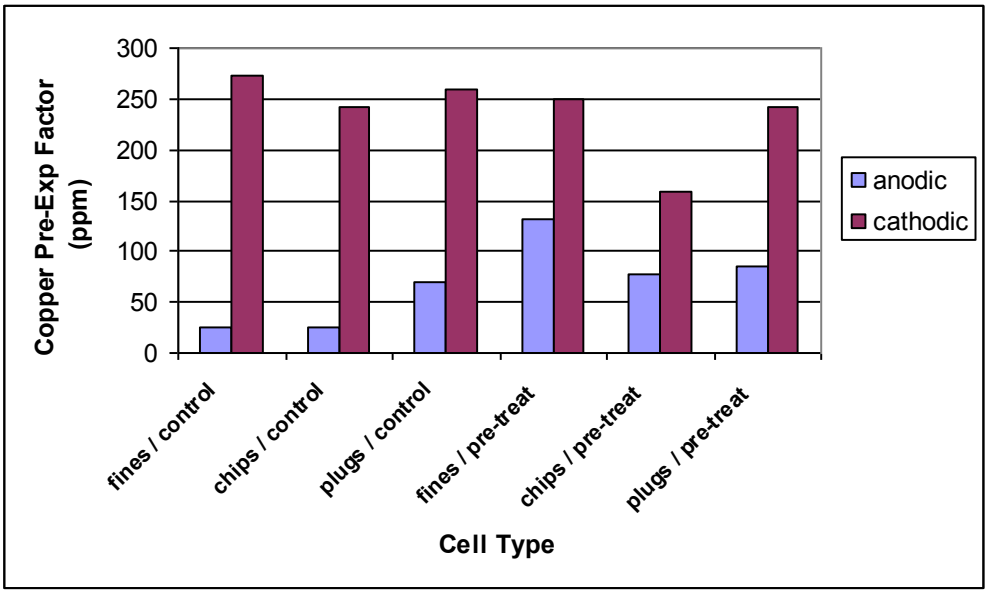

Figure D.5 Pre-exponential factor "A" for the copper half cell accumulation rate model

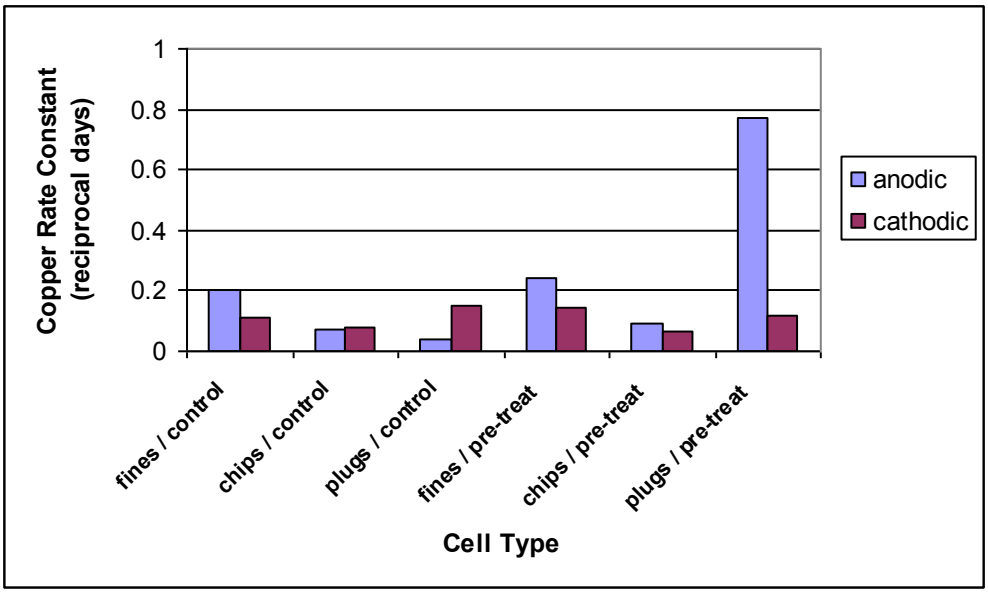

Figure D.6 Rate constant "K1" for the copper half cell accumulation rate model

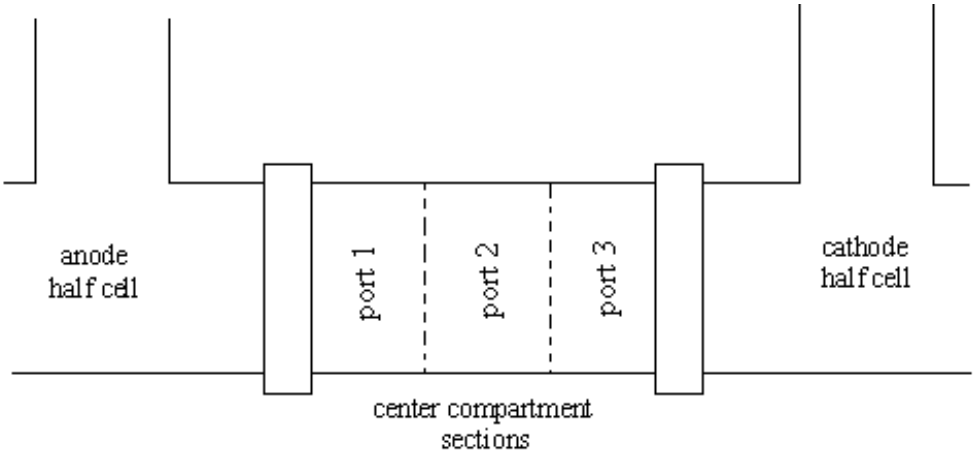

Figure D.7 Pore fluid sampling zones of the EK cell center compartment

APPENDIX E

POWER CONSUMPTION DATA

Table E.1 Equation 4.9 power curve model constants and goodness of fit values

EK CELL TYPE	*Rate Constant "a"*	*Rate Constant "b"*	*Rate Constant "c"*	*Rate Constant "d"*	*Rate Constant "f"*	*Goodness of Fit "R^2"*
fines / control	0.2733000	6.9227160	0.3502955	0.02958430	0.00515864	0.8767
chips / control	0.3011012	7.0780910	0.4252234	0.02390730	1×10^{-12}	0.9287
plugs / control	0.3475936	15.0229400	24.715837	0.17401064	0.05733383	0.9667
fines / pre-treat	0.5724705	5.0275537	8.7119912	0.06827703	0.11533493	0.9371
chips / pre-treat	0.2762500	16.8786220	0.7025447	0.26141892	0.07294500	0.9420
plugs / pre-treat	0.0002217	17.1588920	0.4692943	0.35510004	0.10713146	0.8499

Table E.2 Mass of CoC removed by EK treatment at the “control” levels compared to mass of CoC removed by chemical pretreatment at the “pretreat” levels

Particle size	Additional mass of removed by ek at "control" level relative to "pretreat" level (mg)	Additional mass of removed by pretreatment in the "pretreat" experiments (mg)
fines	1859	547
chips	1752	734
plugs	943	237

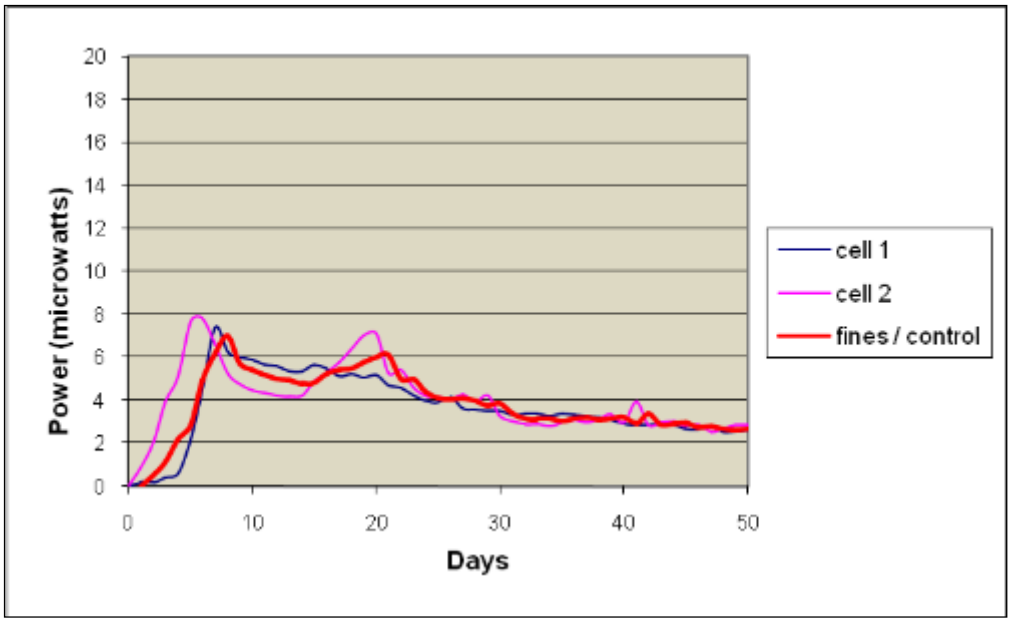

Figure E.1 Power curves describing the amount of power consumed during EK treatment as a function of time: EK Cells 1-2 and "fines / control"

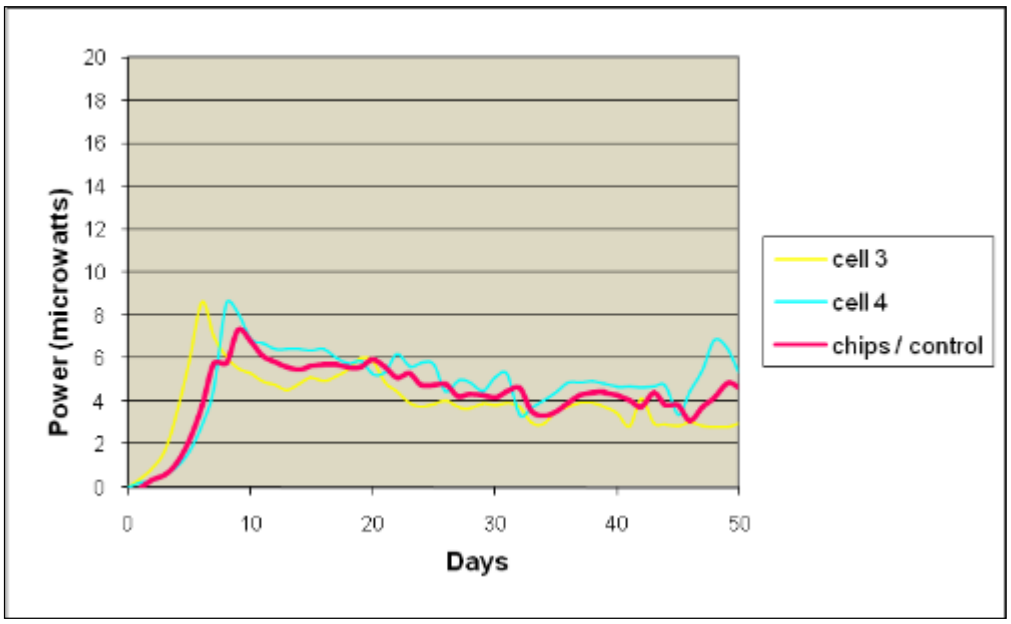

Figure E.2 Power curves describing the amount of power consumed during EK treatment as a function of time: EK Cells 3-4 and "chips / control"

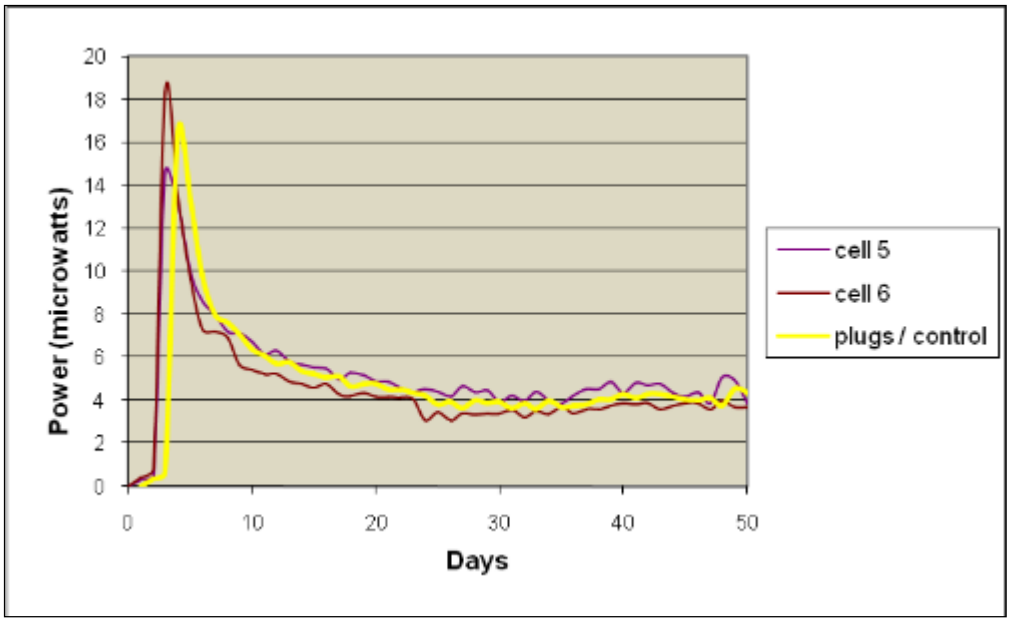

Figure E.3 Power curves describing the amount of power consumed during EK treatment as a function of: EK Cells 5- 6 and "plugs / control"

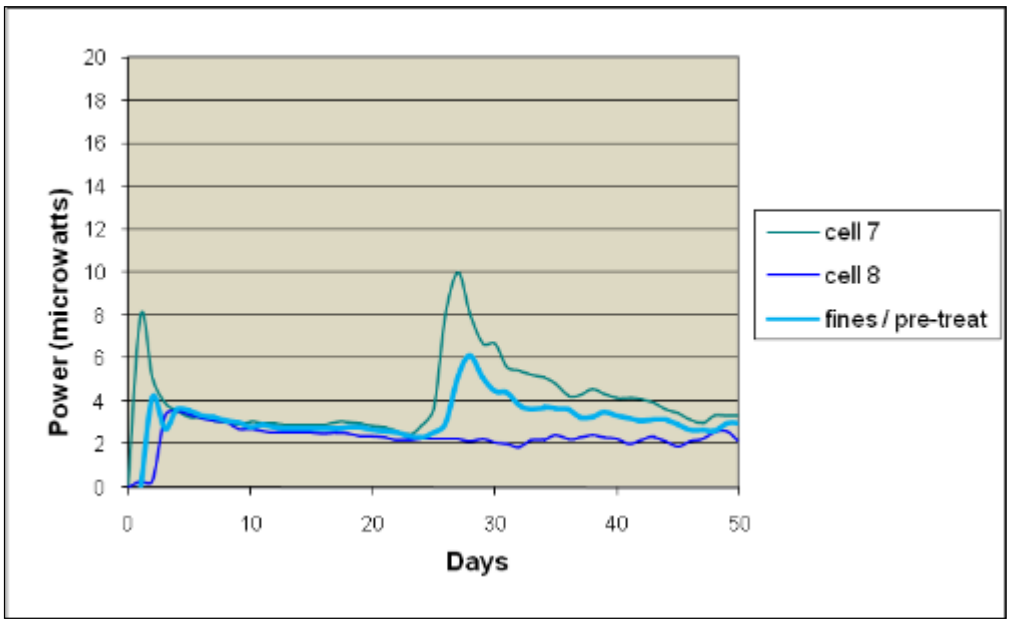

Figure E.4 Power curves describing the amount of power consumed during EK treatment as a function of time: EK Cells 7-8 and "fines / pre-treat"

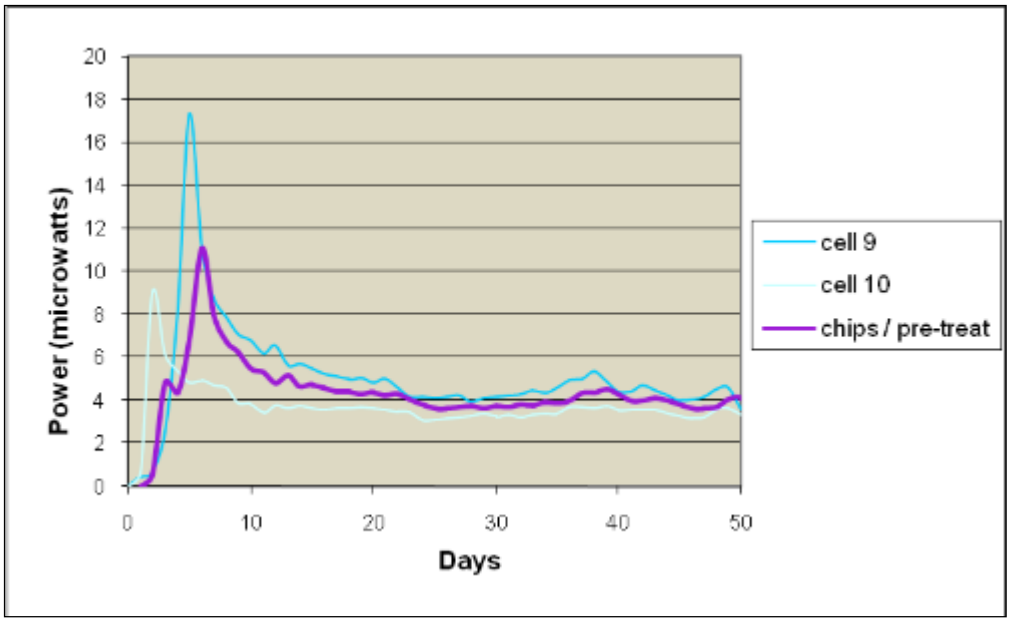

Figure E.5 Power curves describing the amount of power consumed during EK treatment as a function of time: EK Cells 9-10 and "chips / pre-treat"

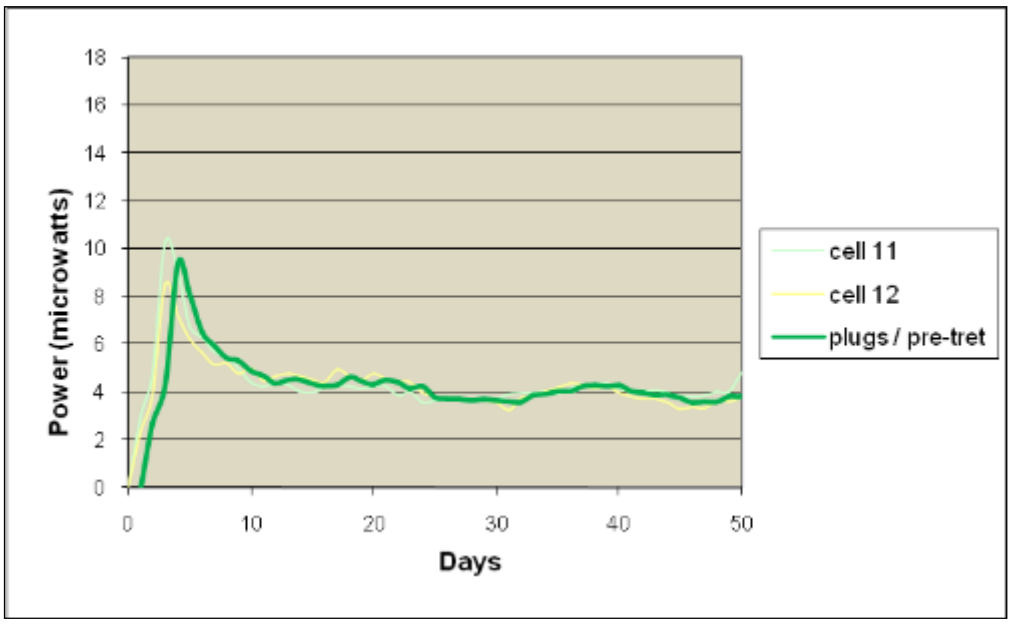

Figure E.6 Power curves describing the amount of power consumed during EK treatment as a function of time: EK Cells 11-12 and "fines / pre-treat"

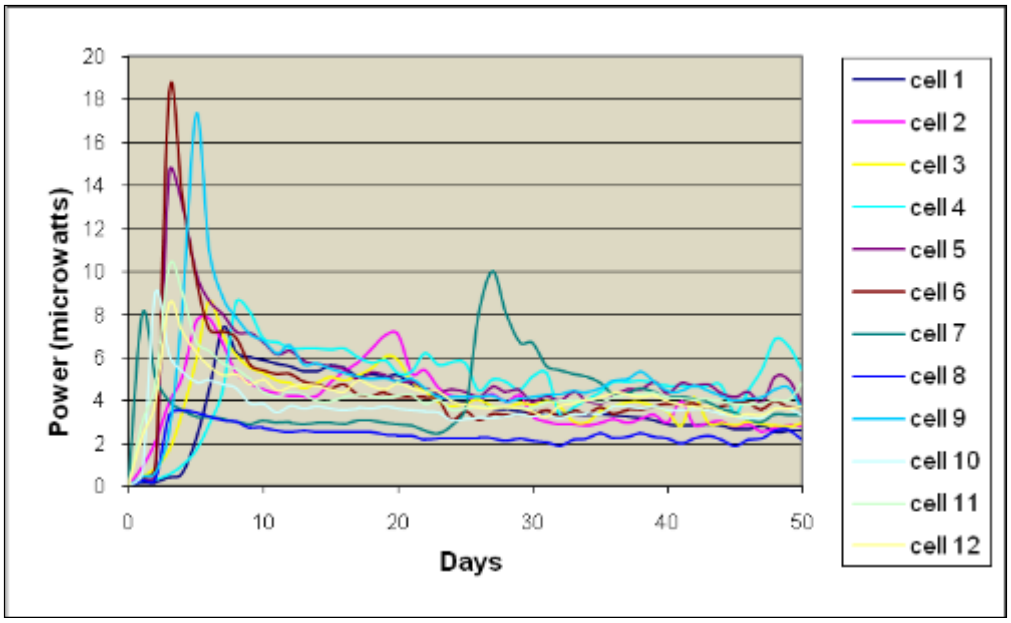

Figure E.7 Power curves describing the amount of power consumed during EK treatment as a function of time: Individual EK Cells

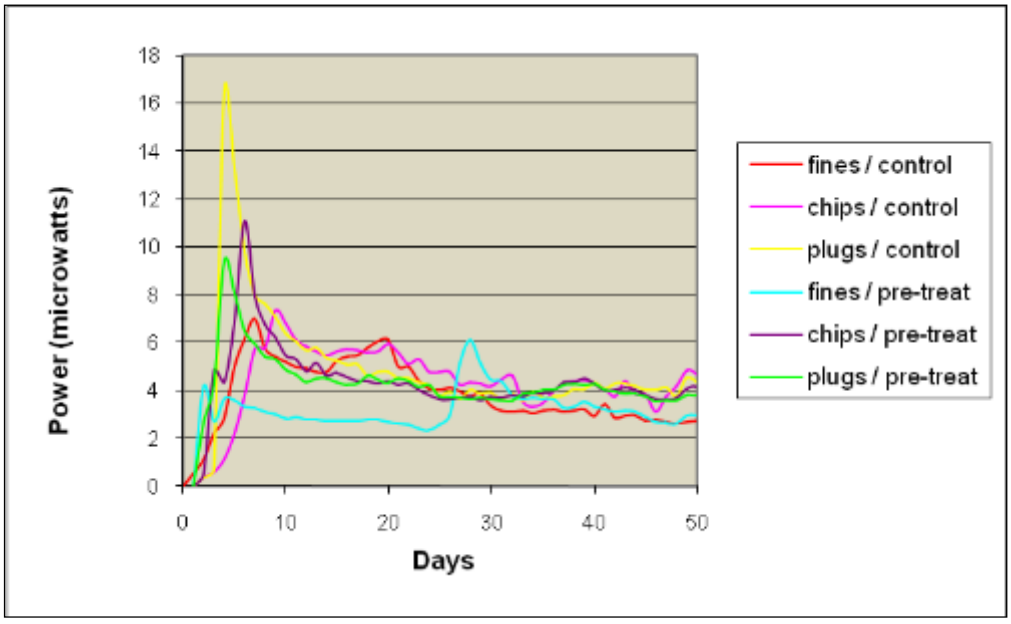

Figure E.8 Power curves describing the amount of power consumed during EK treatment as a function of time: averaged by treatment levels

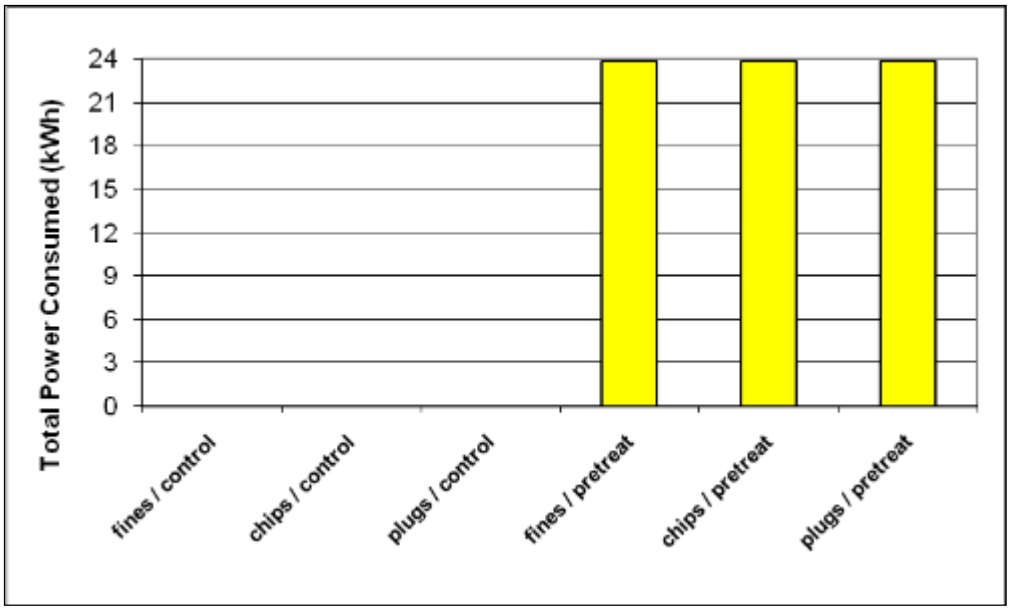

Figure E.9 Total power consumed by combined chemical pretreatment and EK for the first 50 days of the experimental runs at each treatment level

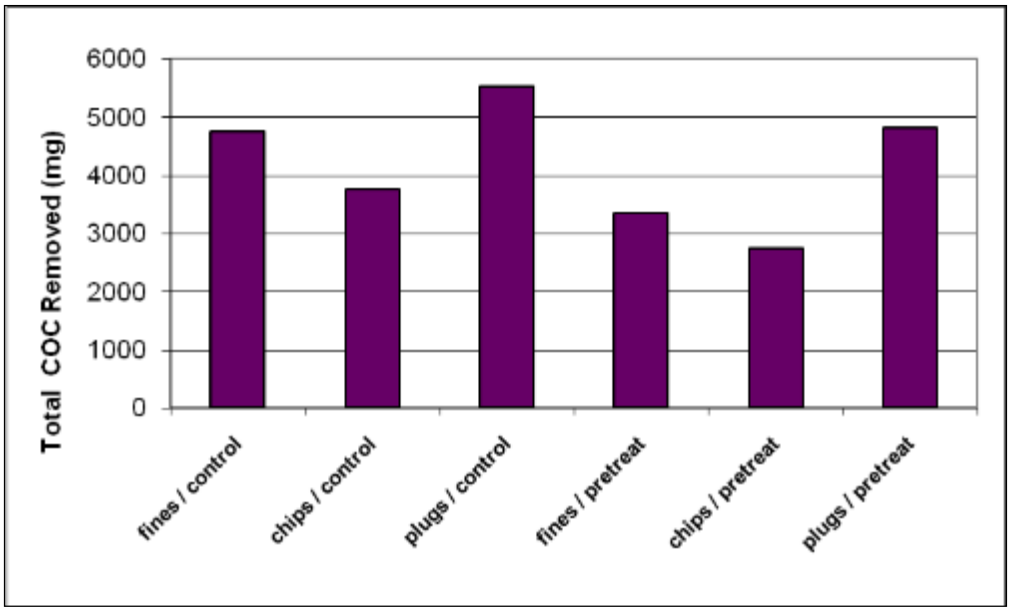

Figure E.10 Total CoC removed by combined chemical pretreatment and EK for the first 50 days of the experimental runs at each treatment level

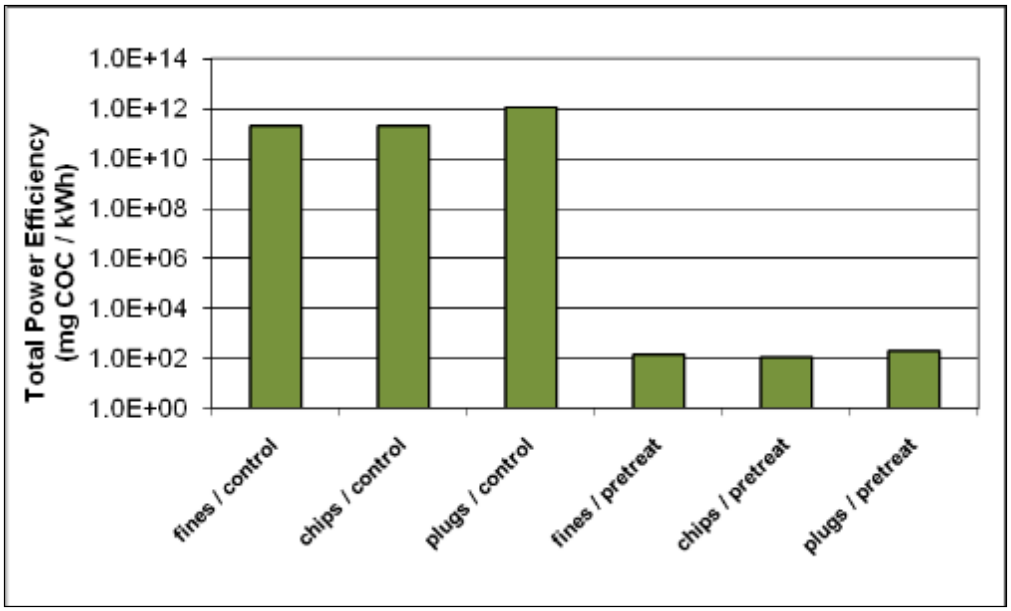

Figure E.11 Total CoC removed per kilowatt-hour by combined chemical pre-treatment and EK for the first 50 days of the experimental runs at each treatment level

APPENDIX F

DAILY SAMPLING DATA

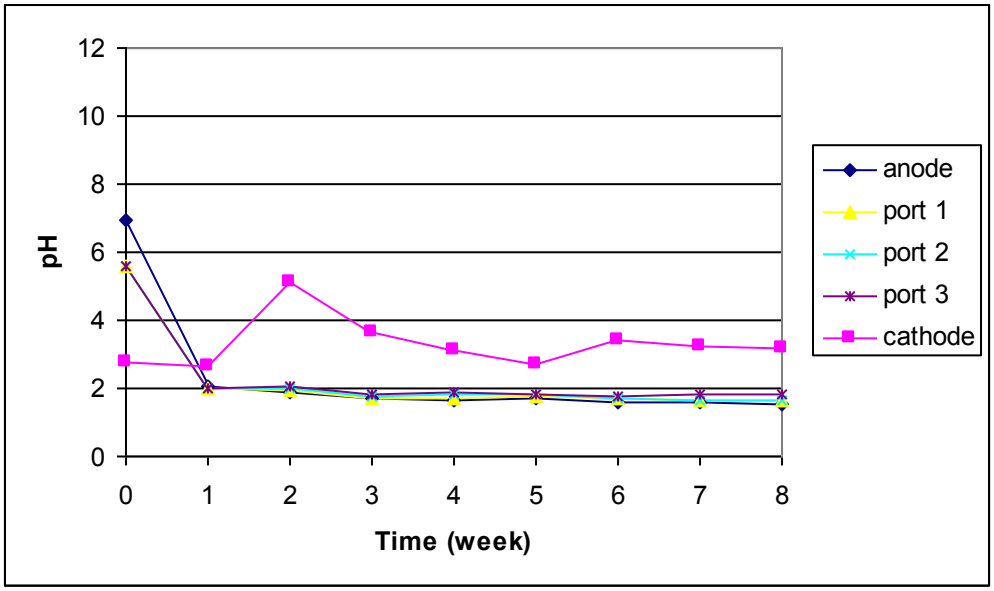

Figure F.1 EK Cell 1: pH profile

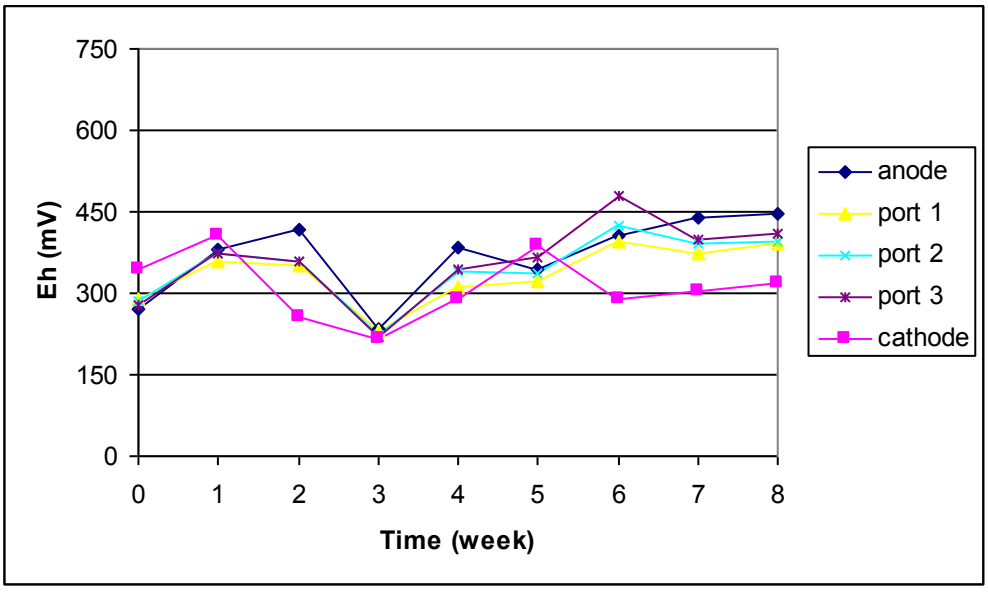

Figure F.2 EK Cell 1: Oxidation Reduction Potential profile

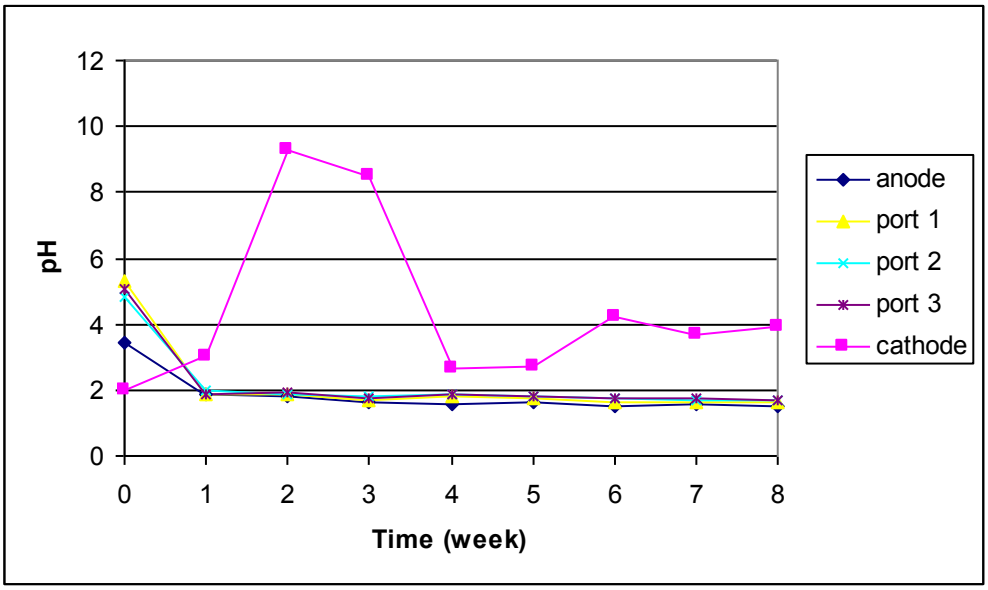

Figure F.3 EK Cell 2: pH profile

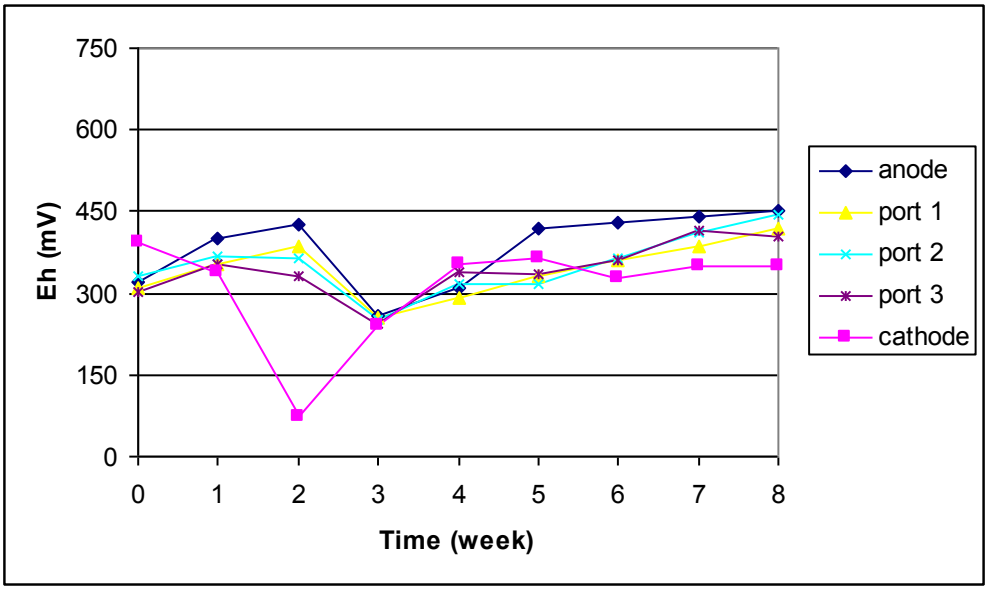

Figure F.4 EK Cell 2: Oxidation Reduction Potential profile

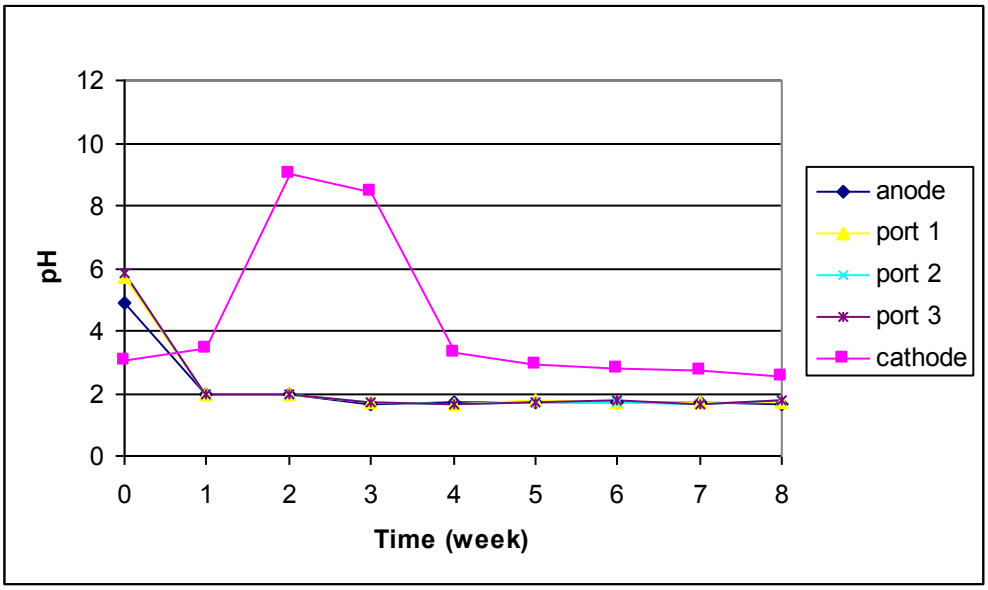

Figure F.5 EK Cell 3: pH profile

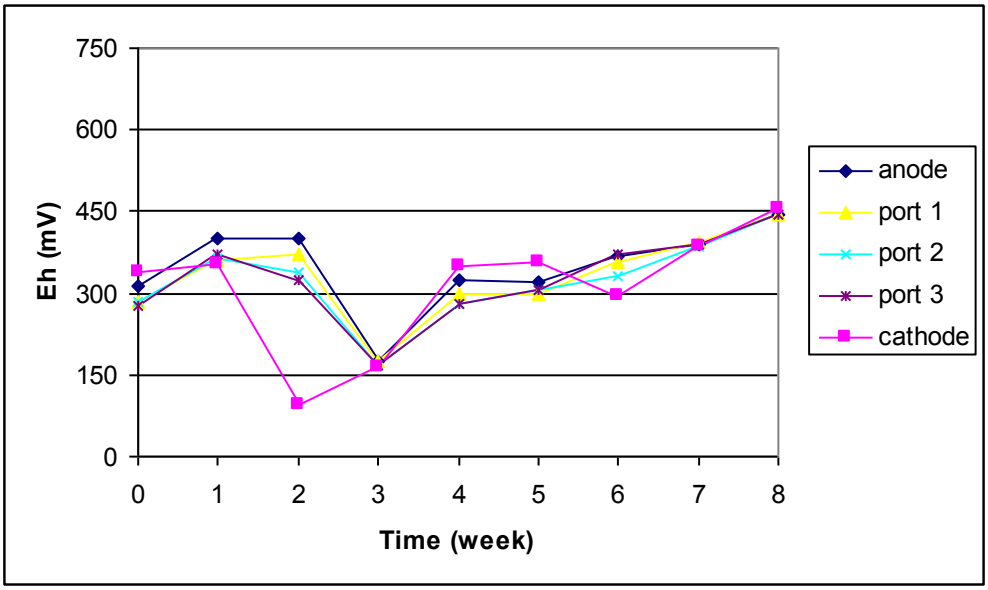

Figure F.6 EK Cell 3: Oxidation Reduction Potential profile

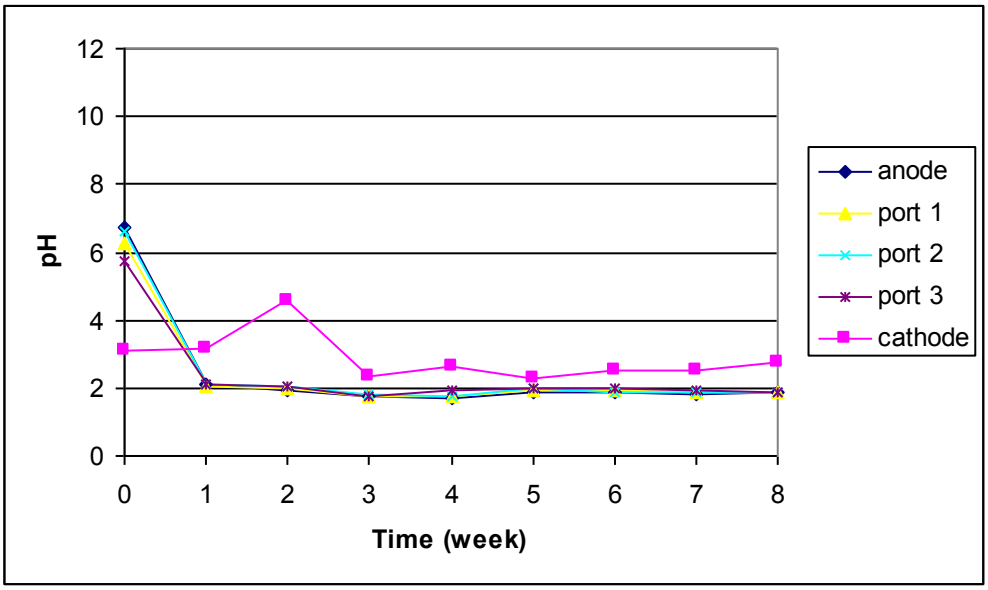

Figure F.7 EK Cell 4: pH profile

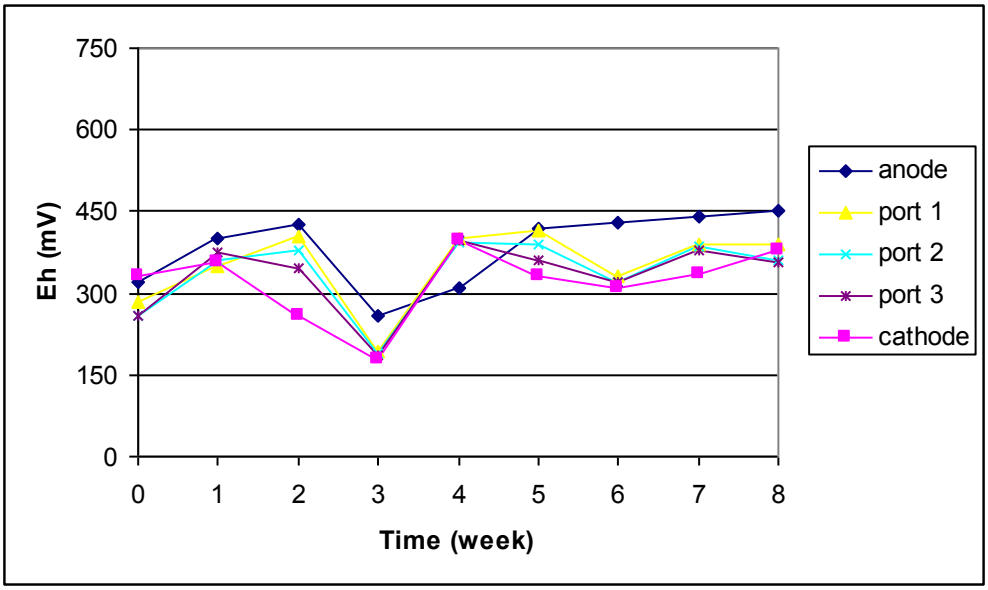

Figure F.8 EK Cell 4: Oxidation Reduction Potential profile

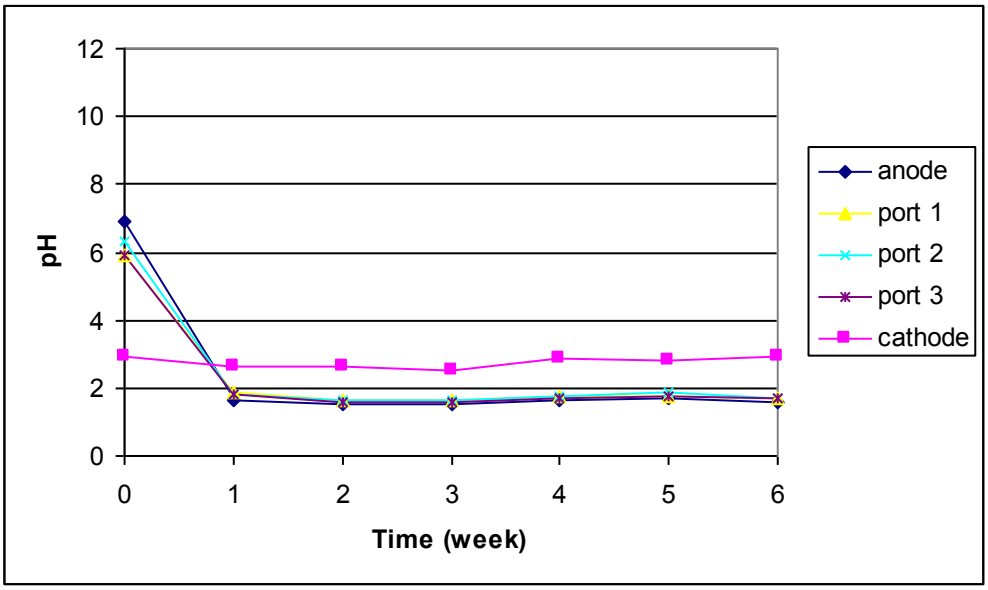

Figure F.9 EK Cell 5: pH profile

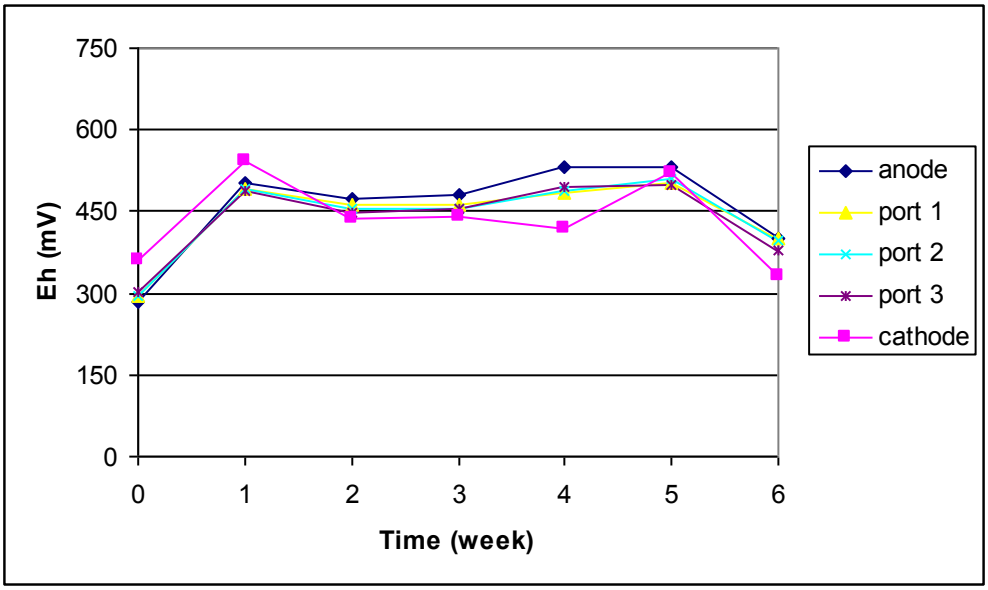

Figure F.10 EK Cell 5: Oxidation Reduction Potential profile

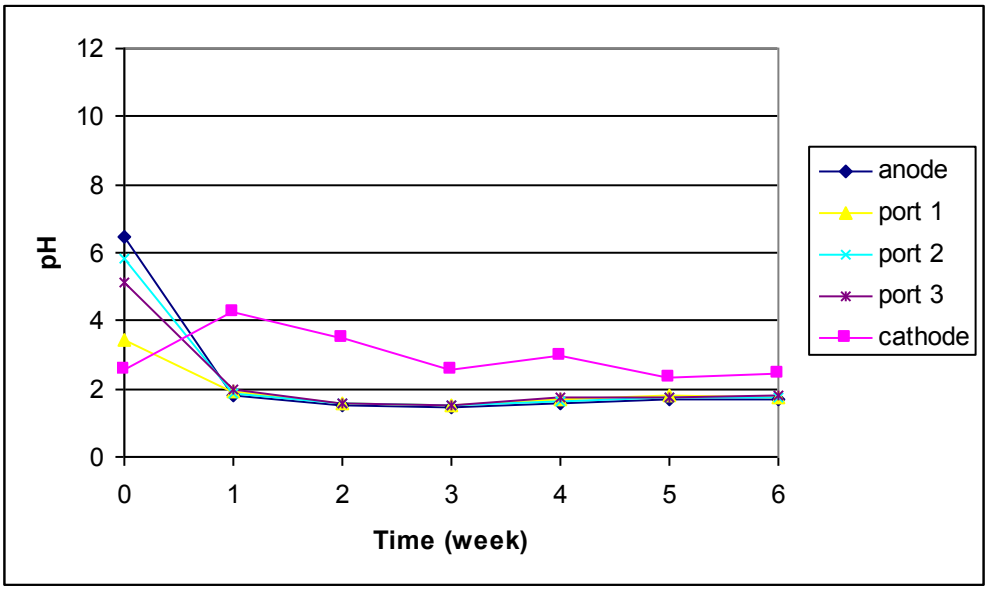

Figure F.11 EK Cell 6: pH profile

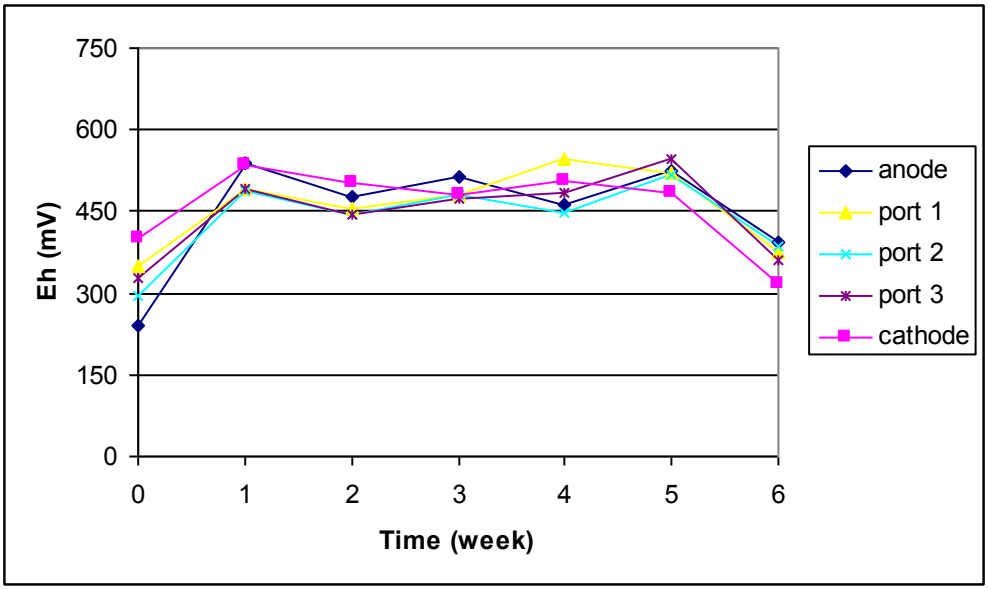

Figure F.12 EK Cell 6: Oxidation Reduction Potential profile

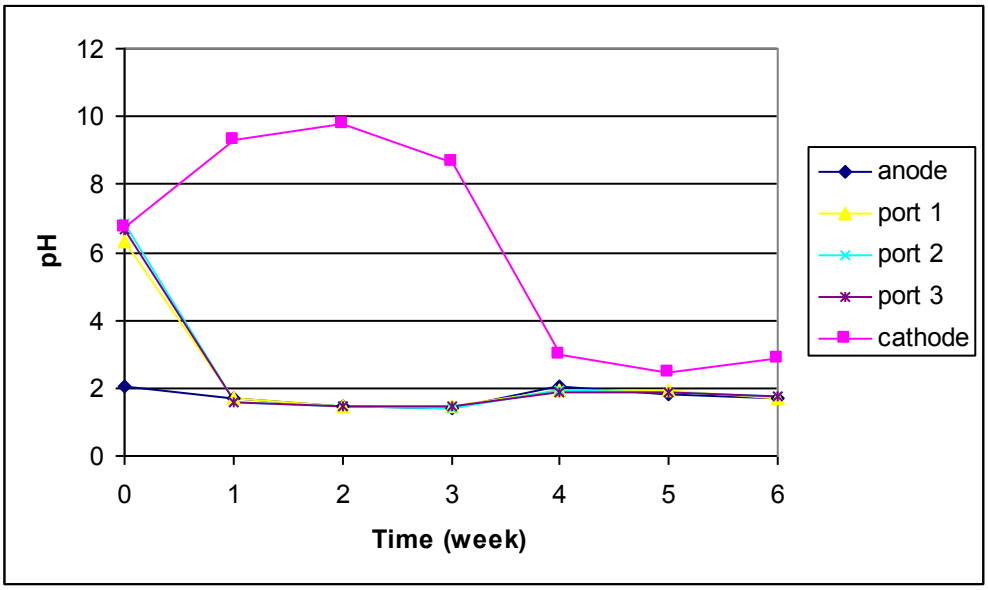

Figure F.13 EK Cell 7: pH profile

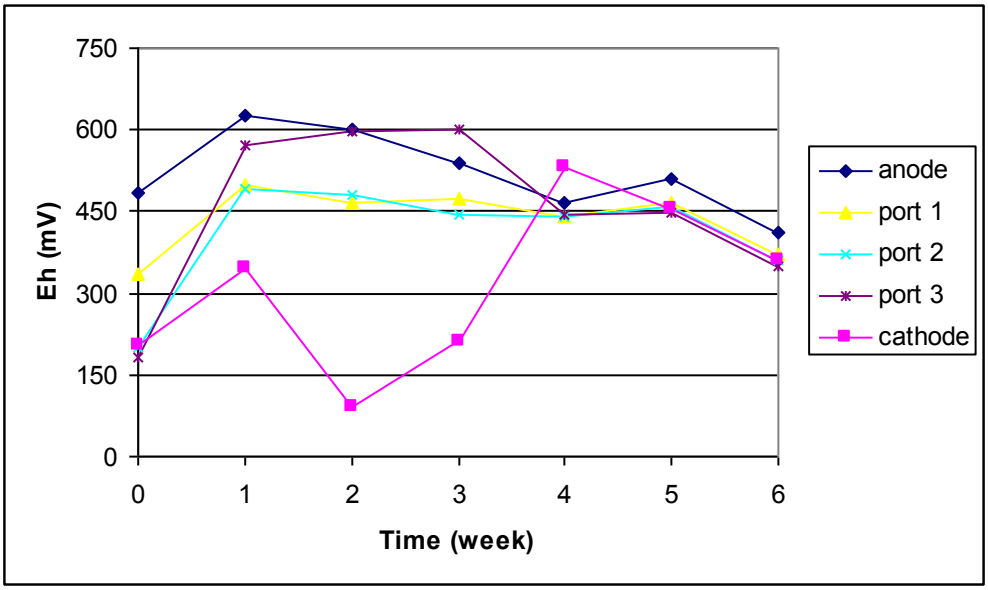

Figure F.14 EK Cell 7: Oxidation Reduction Potential profile

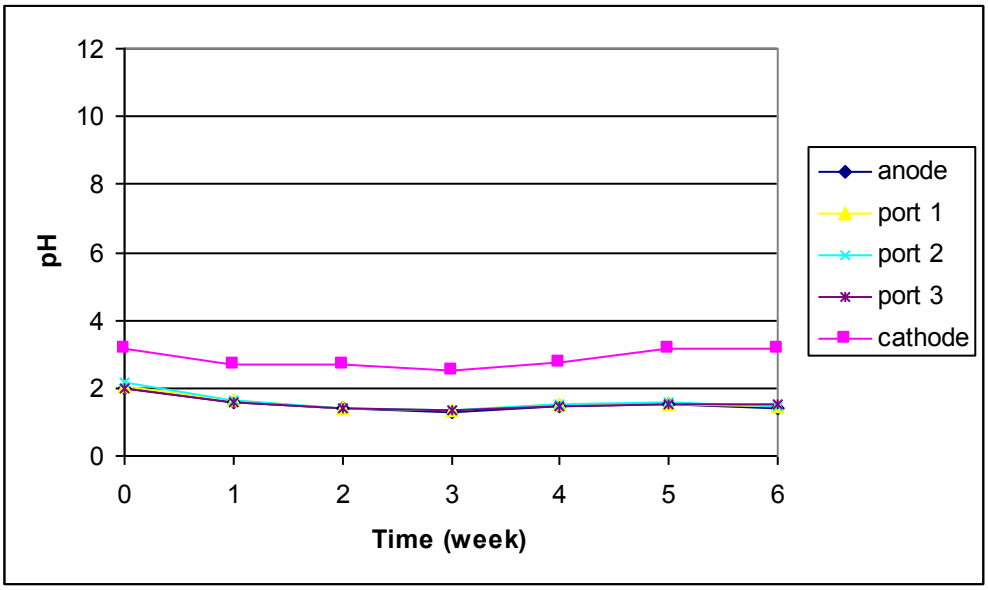

Figure F.15 EK Cell 8: pH profile

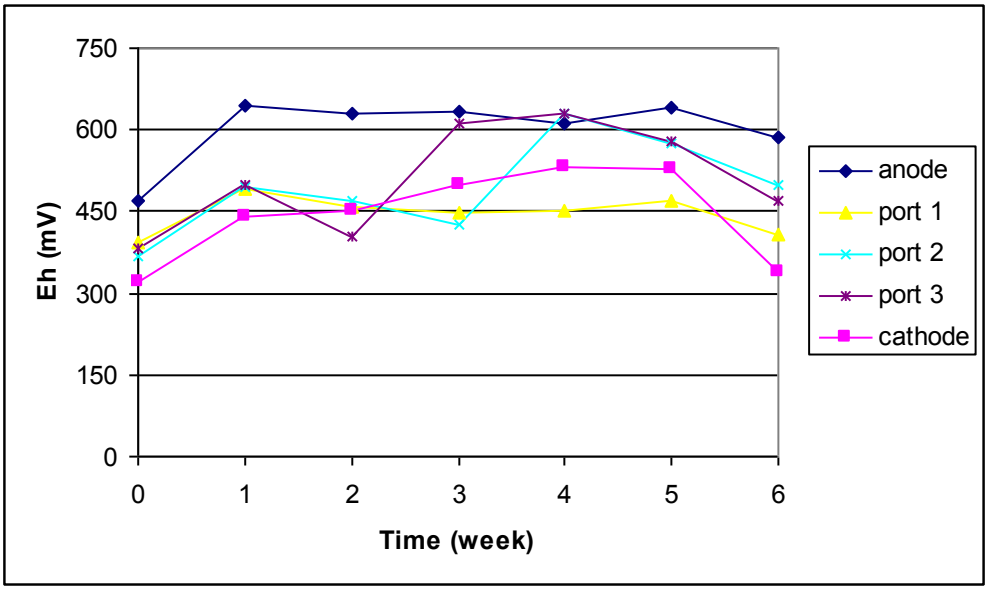

Figure F.16 EK Cell 8: Oxidation Reduction Potential profile

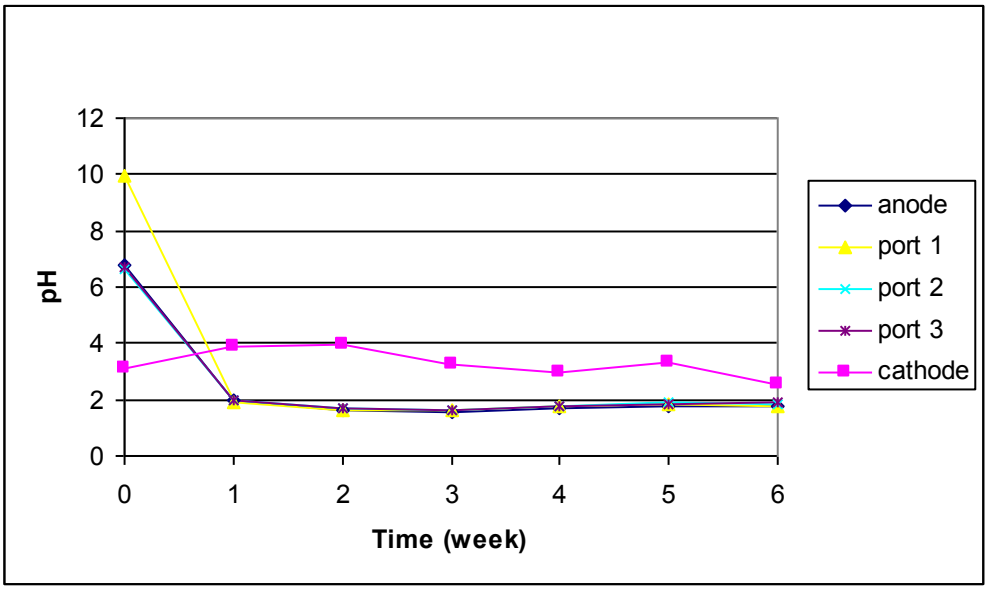

Figure F.17 EK Cell 9: pH profile

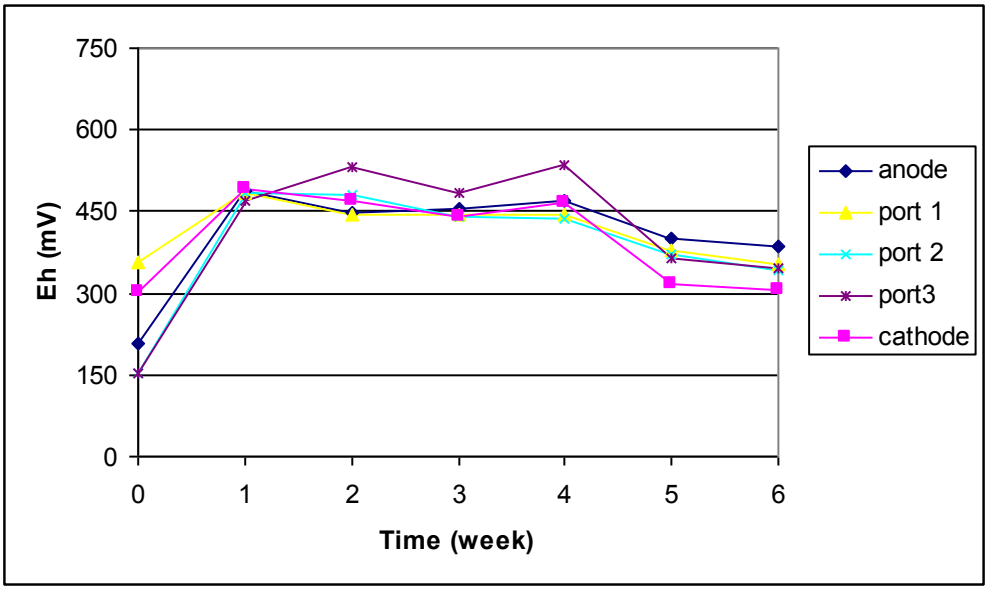

Figure F.18 EK Cell 9: Oxidation Reduction Potential profile

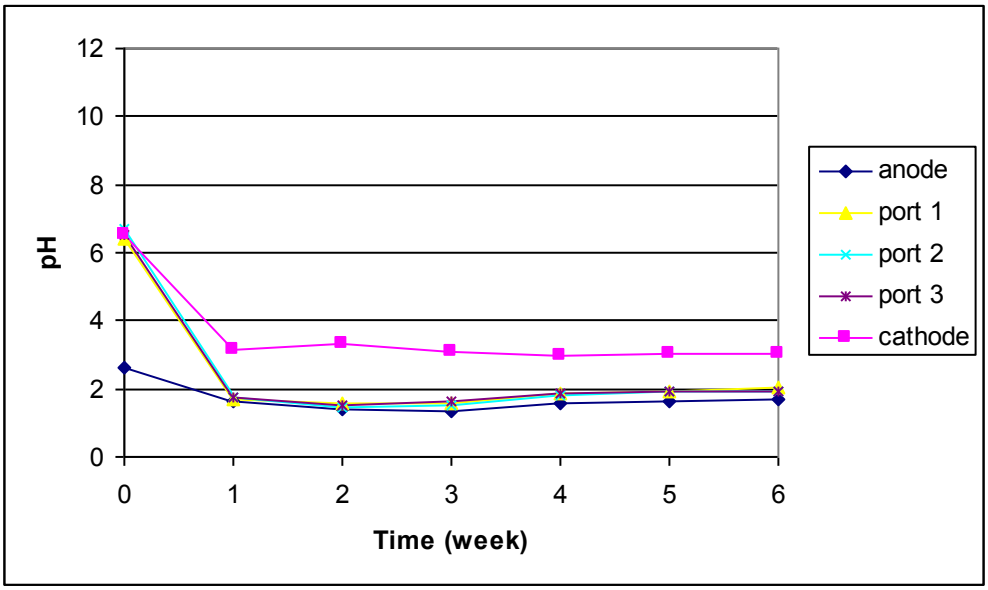

Figure F.19 EK Cell 10: pH profile

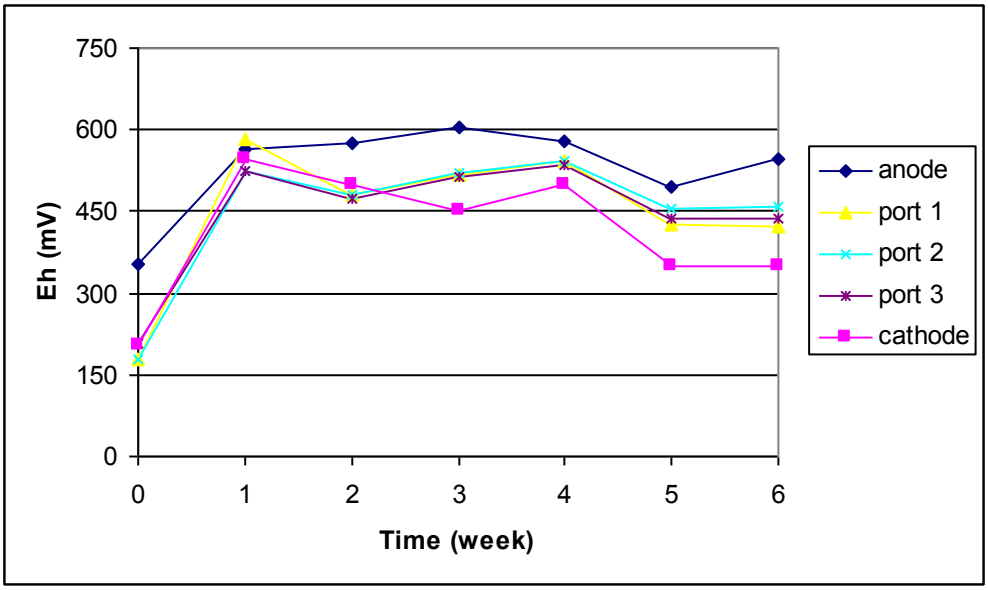

Figure F.20 EK Cell 10: Oxidation Reduction Potential profile

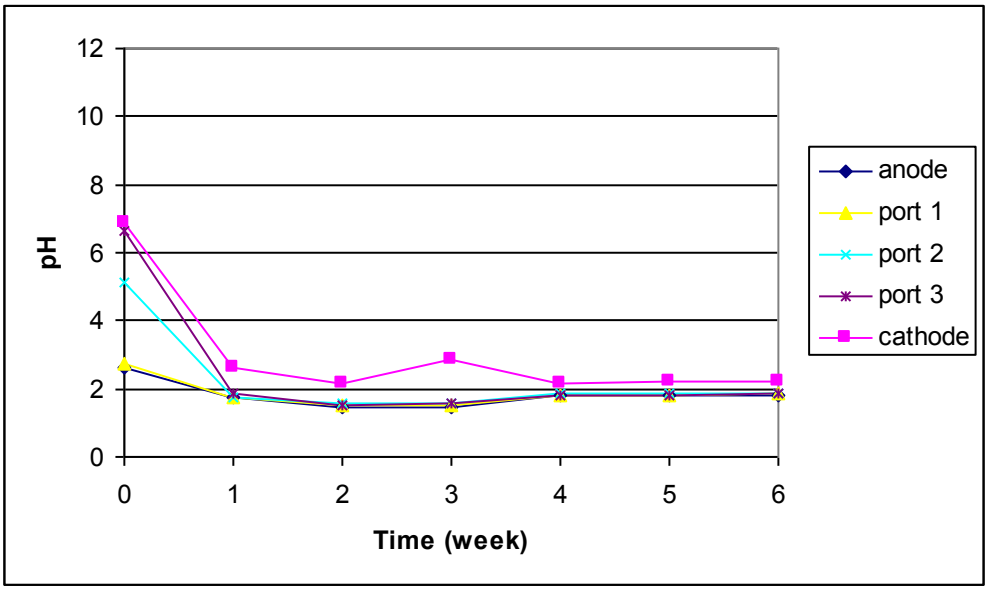

Figure F.21 EK Cell 11: pH profile

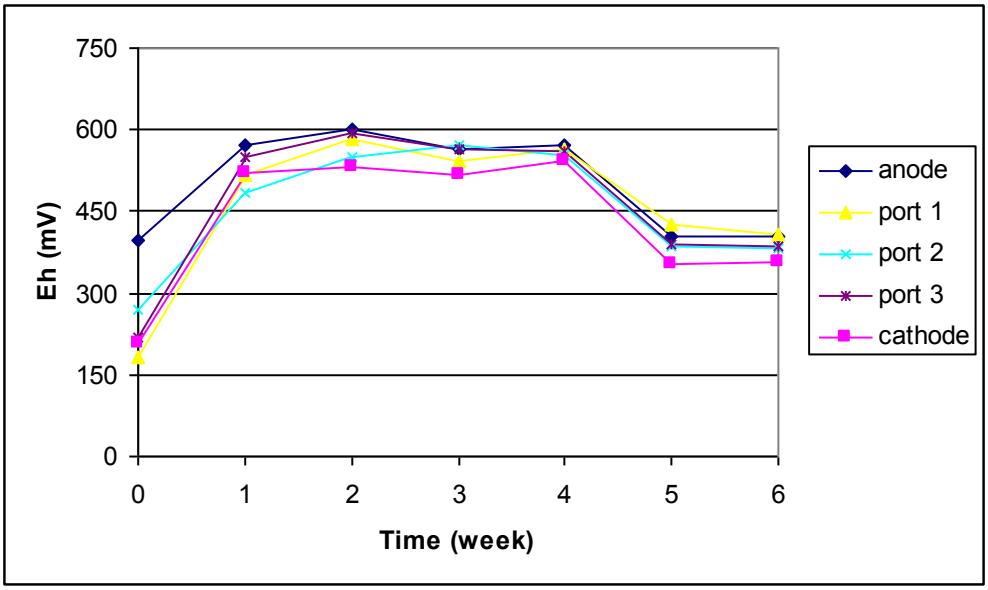

Figure F.22 EK Cell 11: Oxidation Reduction Potential profile

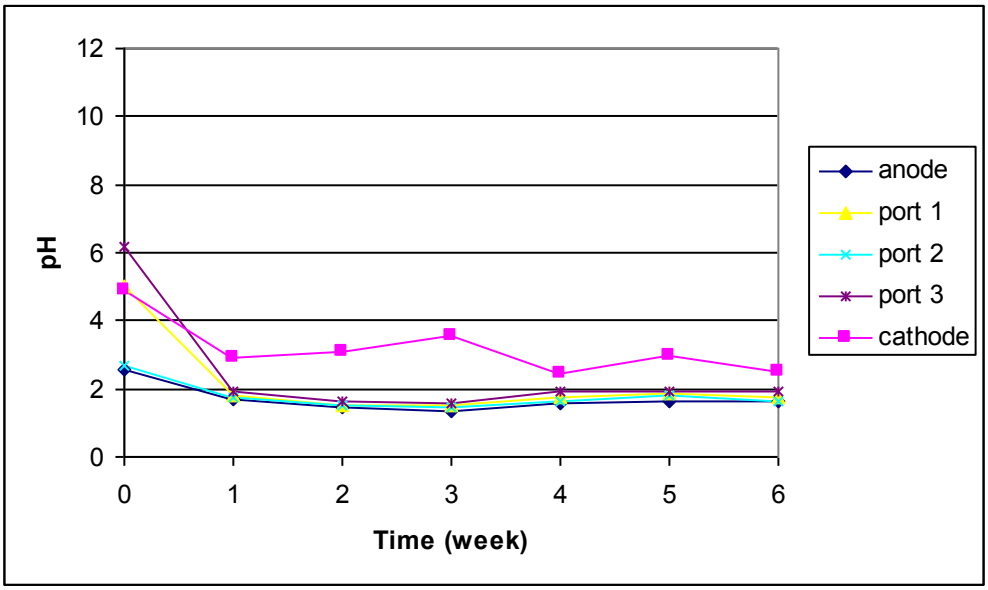

Figure F.23 EK Cell 12: pH profile

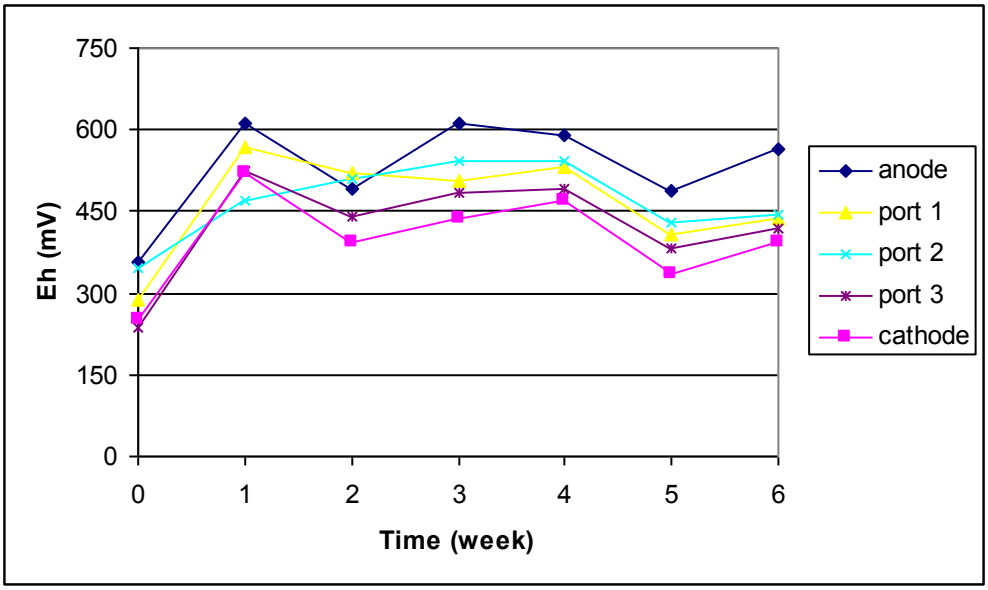

Figure F.24 EK Cell 12: Oxidation Reduction Potential profile

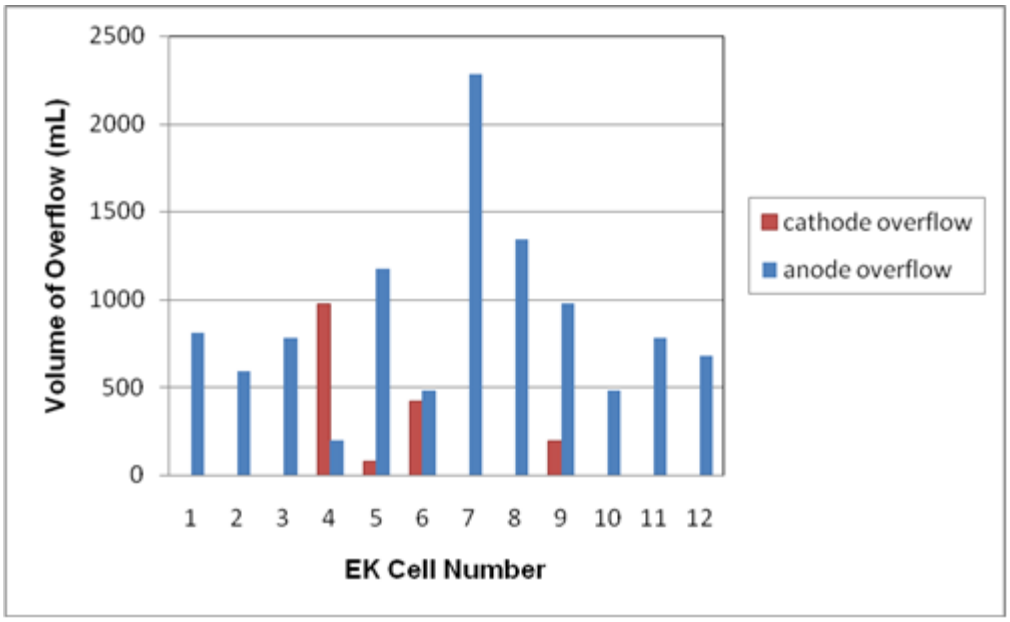

Figure F.25 Total accumulated overflow volumes observed in the anodic and cathodic EK half cells at the conclusion of the experimental run

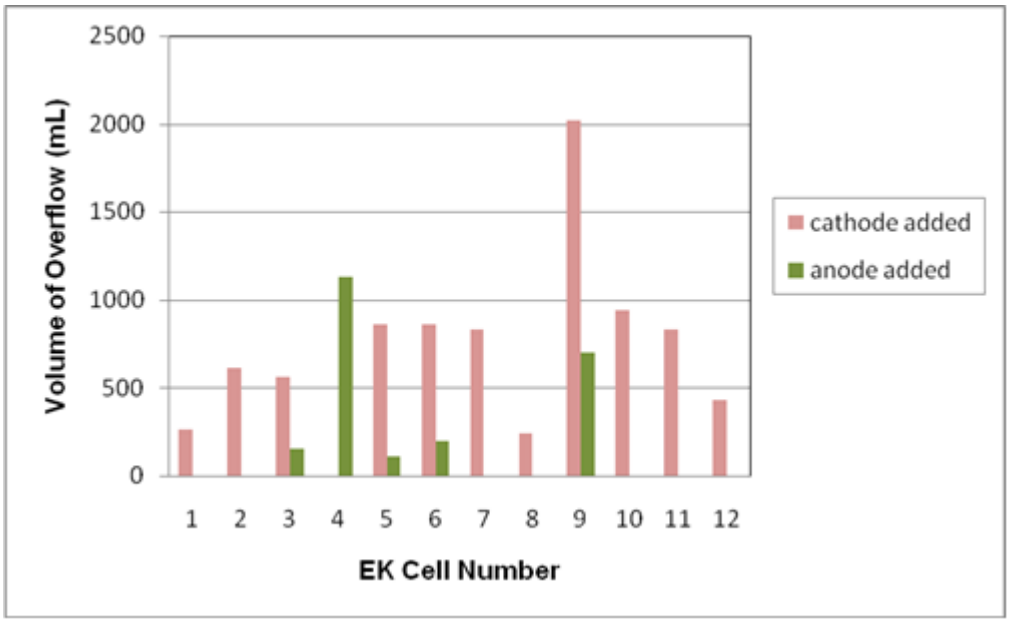

Figure F.26 Total accumulated volume of tap water added to the anodic and cathodic EK half cells at the conclusion of the experimental run

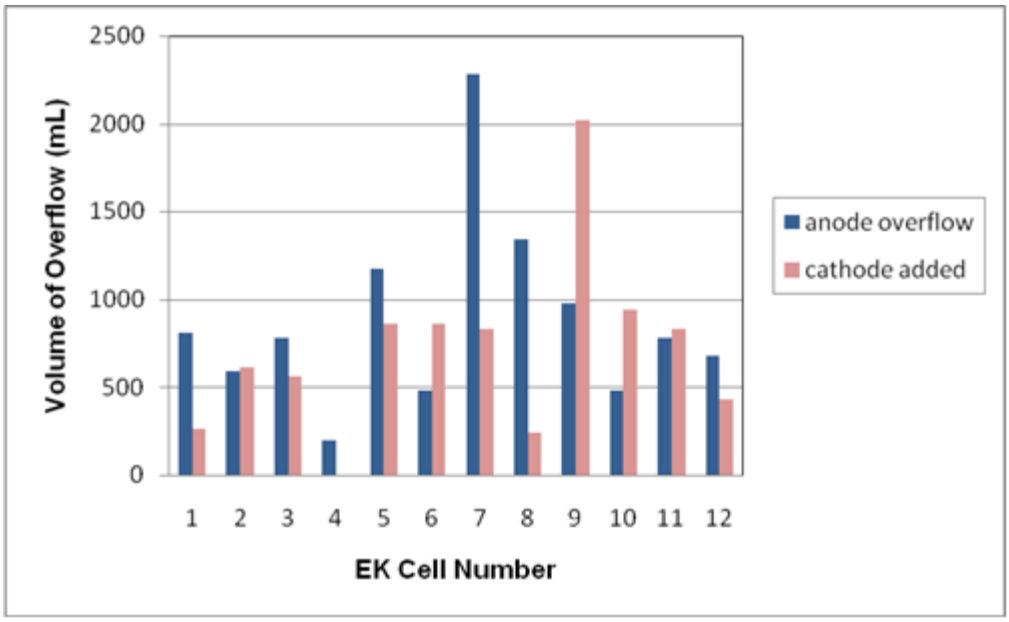

Figure F.27 Total accumulated volume of anodic EK half cell overflow and total accumulated volume of tap water added to the cathodic EK half cell at the conclusion of the experimental run

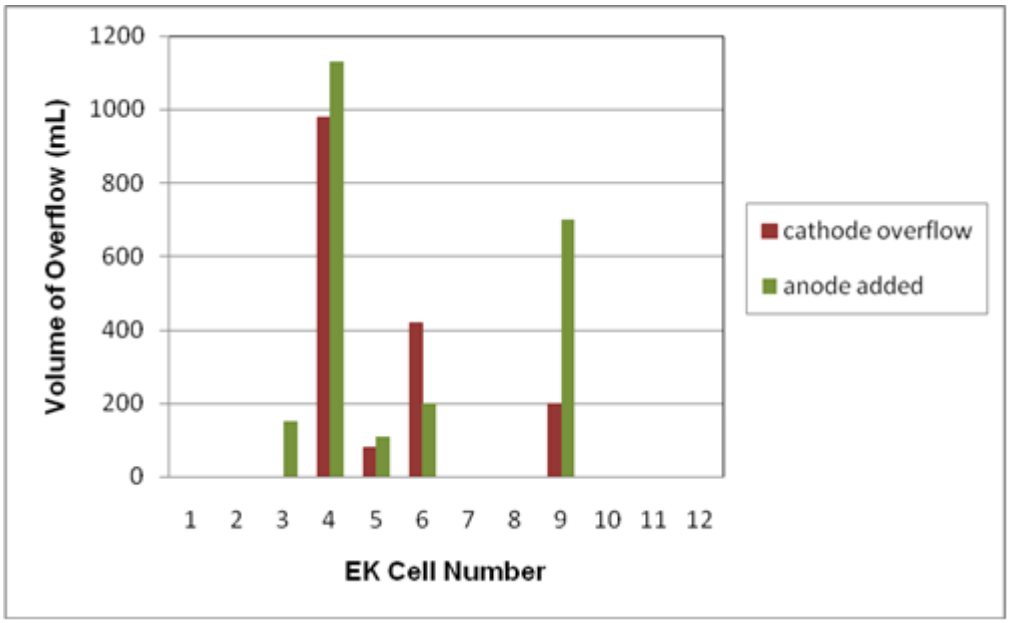

Figure F.28 Total accumulated volume of cathodic EK half cell overflow and total accumulated volume of tap water added to the anodic EK half cell at the conclusion of the experimental run

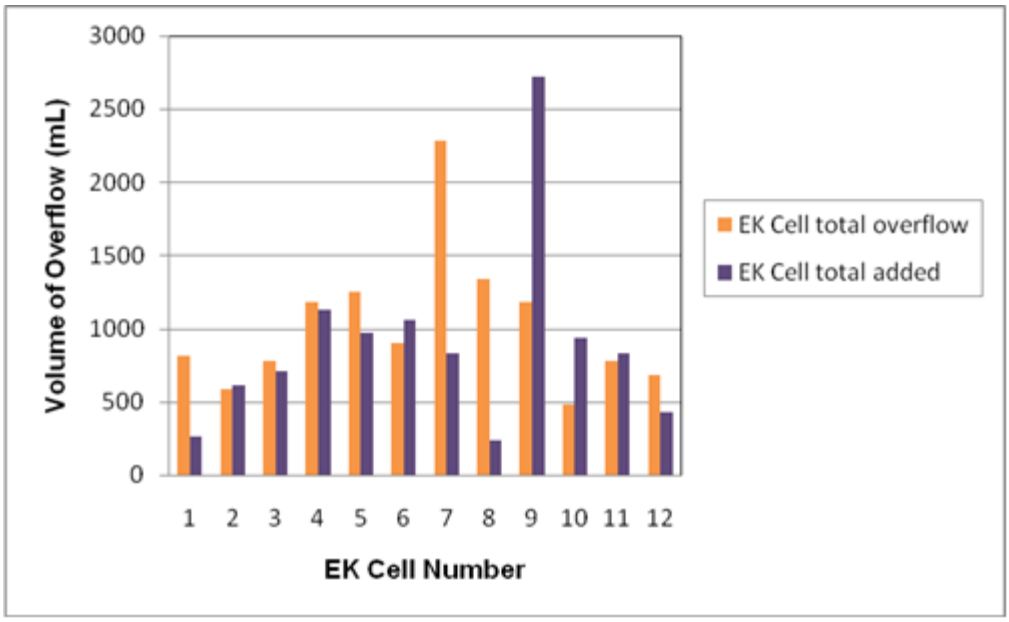

Figure F.29 Total accumulated volume of EK half cell overflow and total accumulated volume of tap water added to each EK half cell at the conclusion of the experimental run

APPENDIX G

CONCENTRATION CURVES

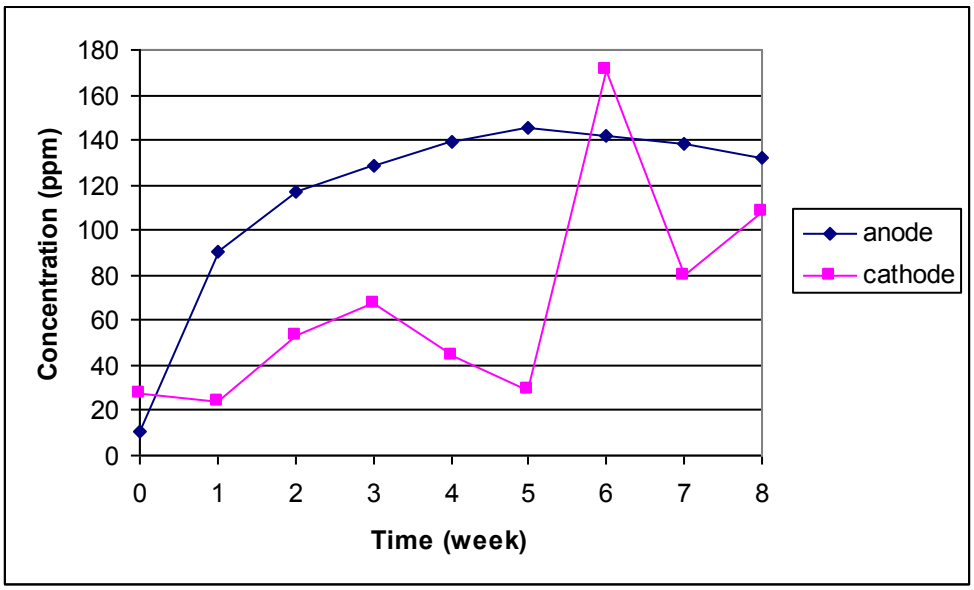

Figure G.1 EK Cell 1: Concentration curves describing the accumulation of arsenic in the anodic and cathodic half cells

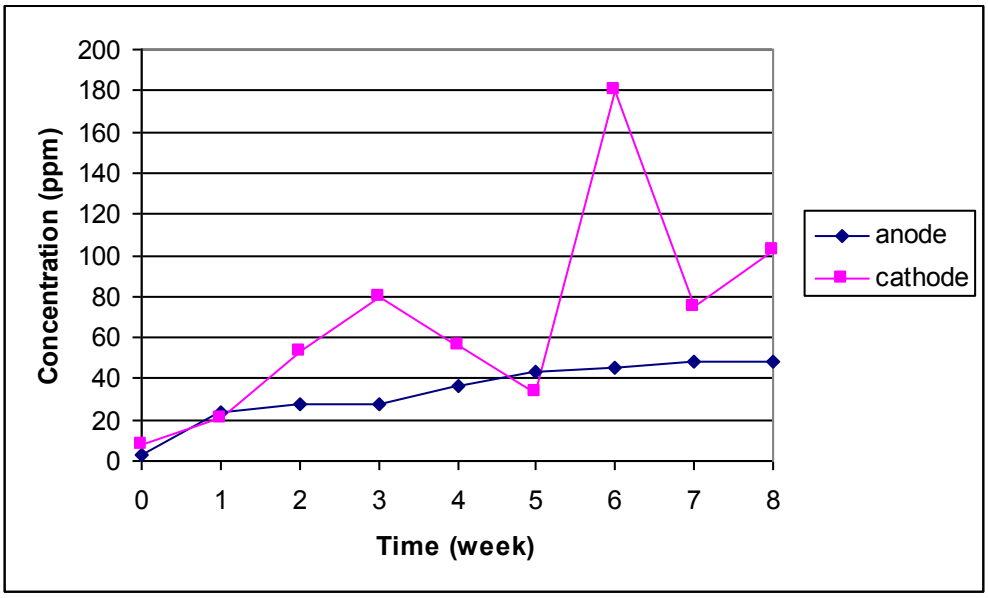

Figure G.2 EK Cell 1: Concentration curves describing the accumulation of chromium in the anodic and cathodic half cells

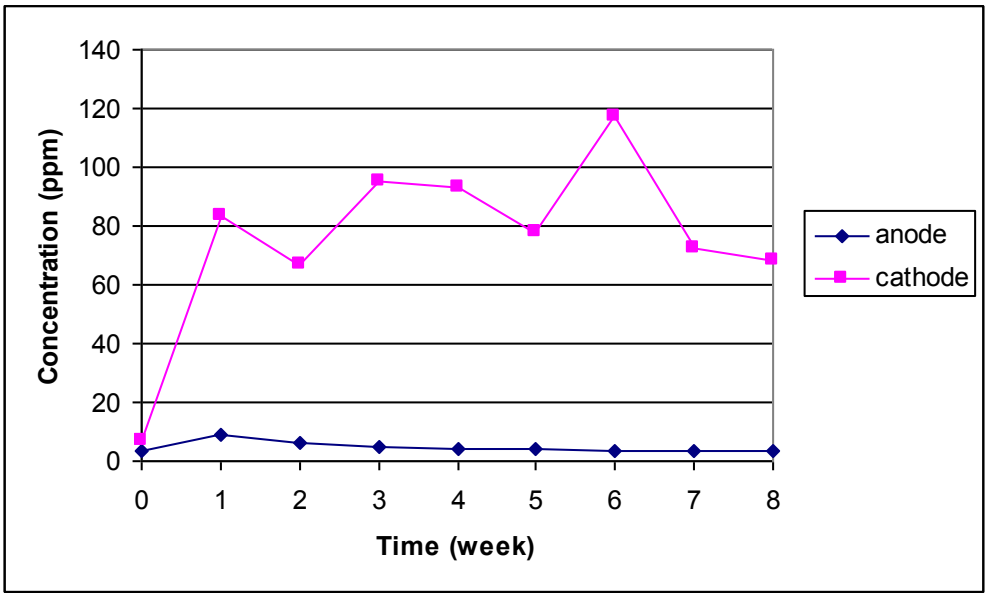

Figure G.3 EK Cell 1: Concentration curves describing the accumulation of copper in the anodic and cathodic half cells

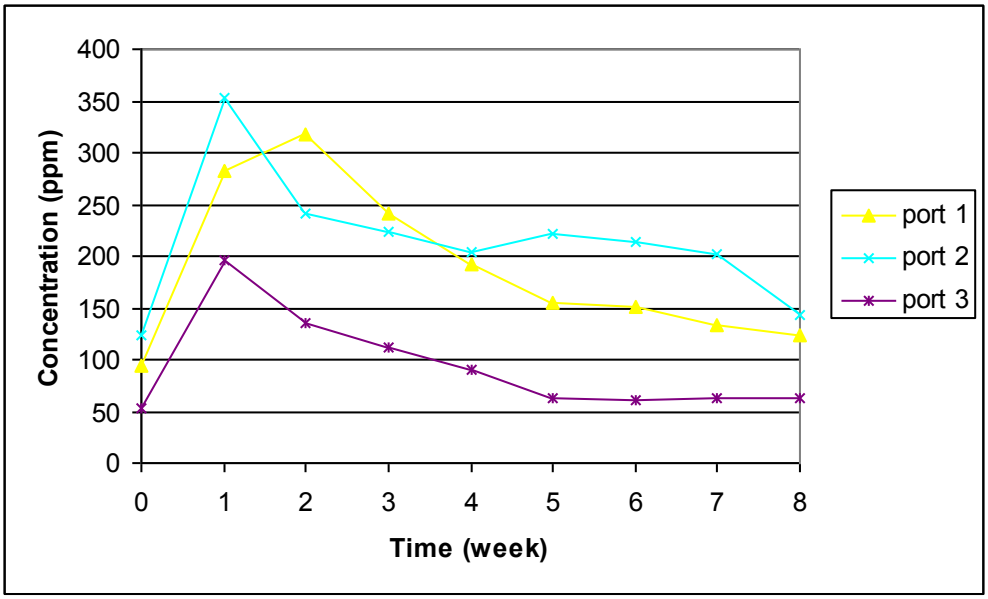

Figure G.4 EK Cell 1: Concentration curves describing the accumulation of arsenic in the pore fluid sampling zones of the EK cell center compartment

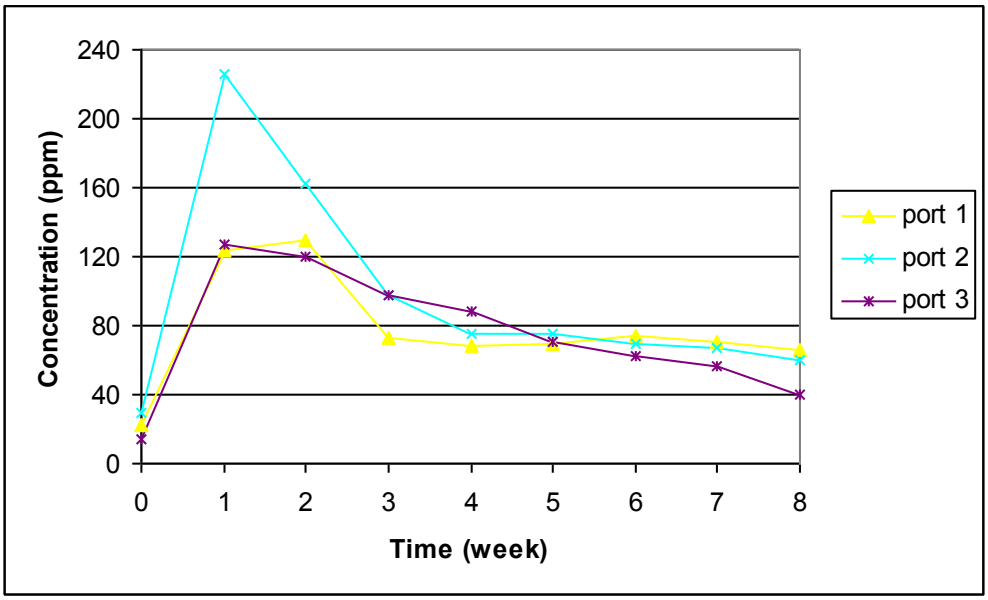

Figure G.5 EK Cell 1: Concentration curves describing the accumulation of chromium in the pore fluid sampling zones of the EK cell center compartment

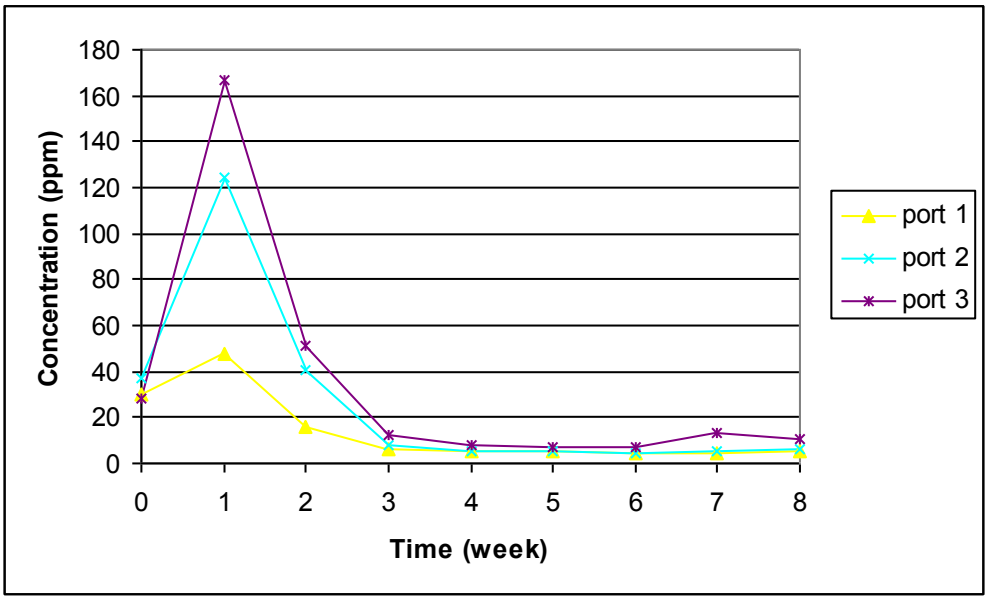

Figure G.6 EK Cell 1: Concentration curves describing the accumulation of copper in the pore fluid sampling zones of the EK cell center compartment

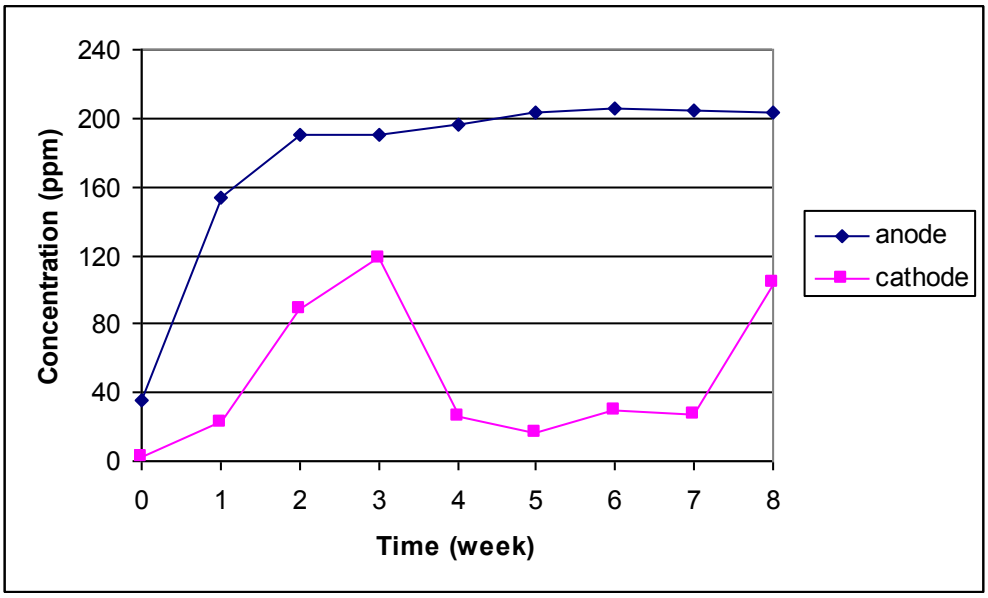

Figure G.7 EK Cell 2: Concentration curves describing the accumulation of arsenic in the anodic and cathodic half cells

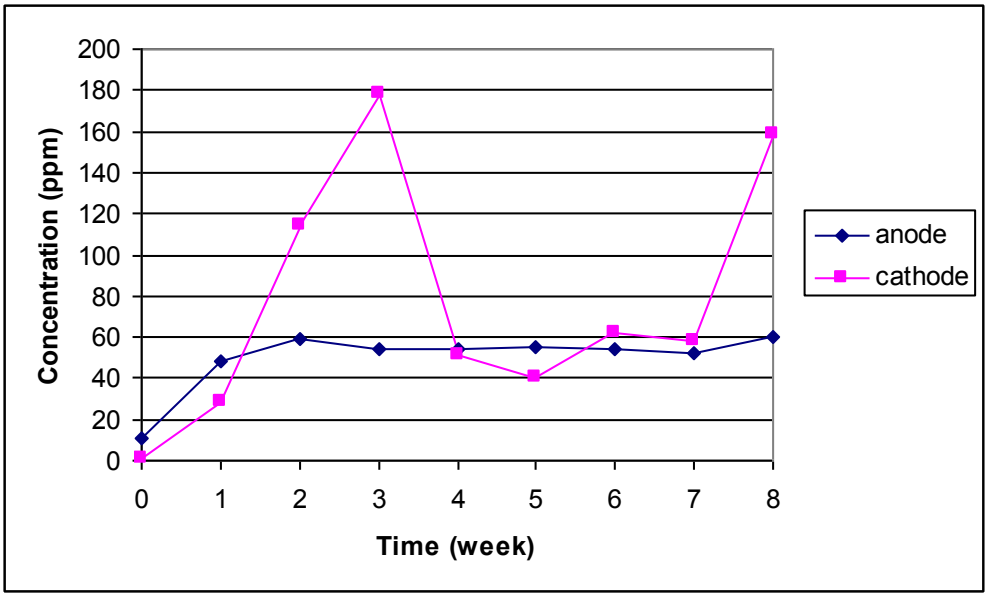

Figure G.8 EK Cell 2: Concentration curves describing the accumulation of chromium in the anodic and cathodic half cells

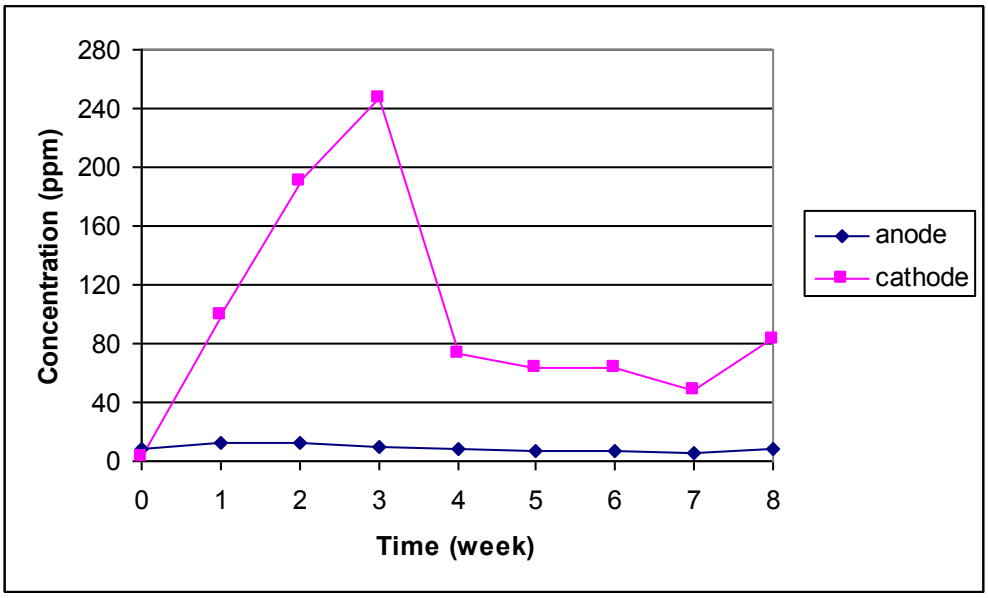

Figure G.9 EK Cell 2: Concentration curves describing the accumulation of copper in the anodic and cathodic half cells

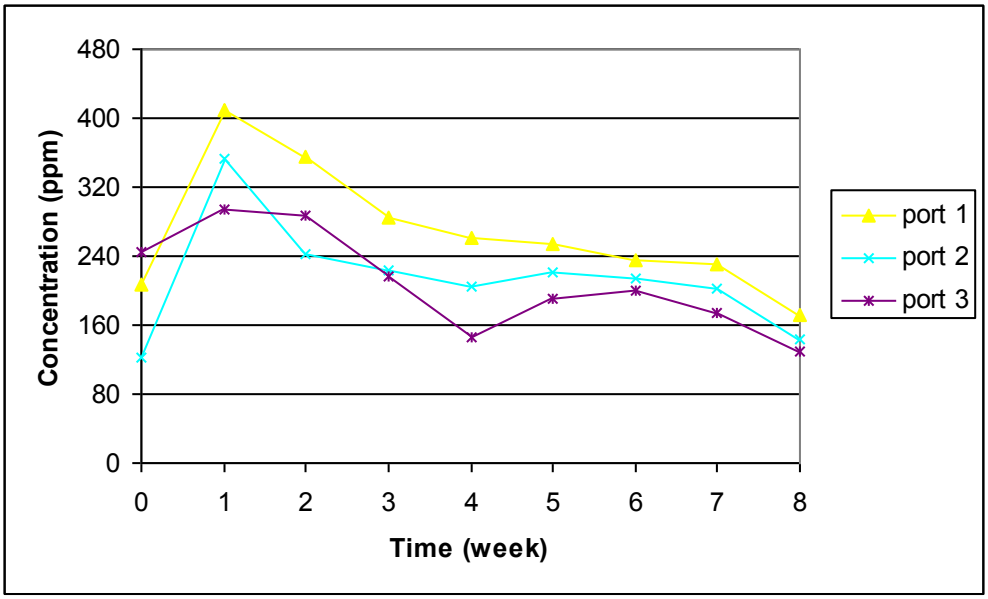

Figure G.10 EK Cell 2: Concentration curves describing the accumulation of arsenic in the pore fluid sampling zones of the EK cell center compartment

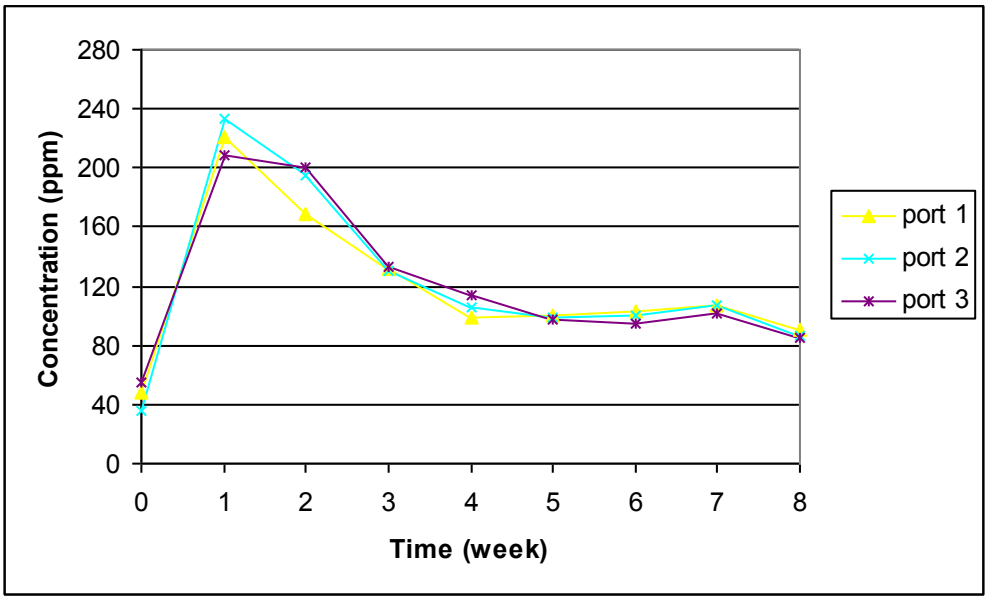

Figure G.11 EK Cell 2: Concentration curves describing the accumulation of chromium in the pore fluid sampling zones of the EK cell center compartment

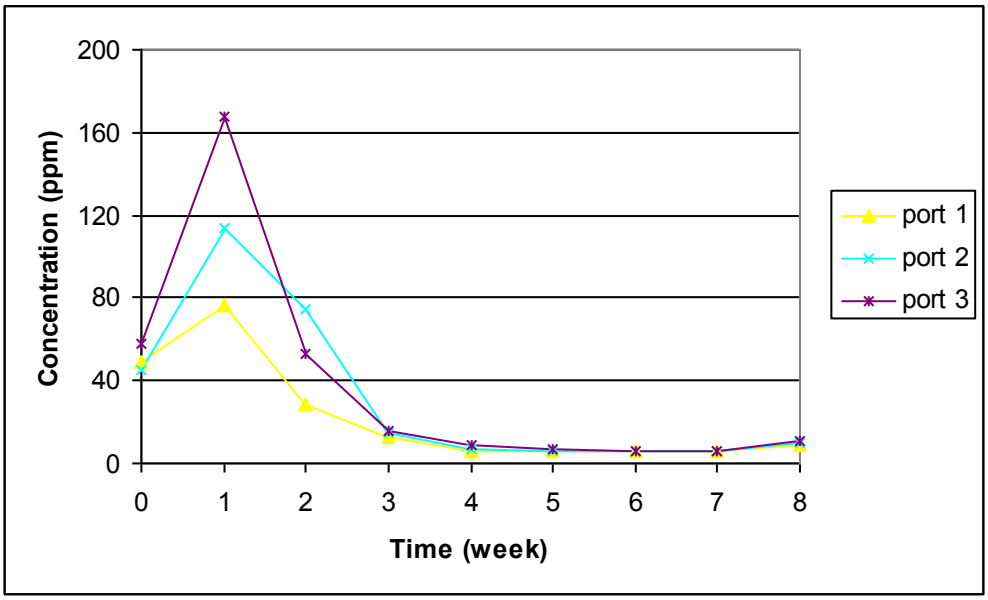

Figure G.12 EK Cell 2: Concentration curves describing the accumulation of copper in the pore fluid sampling zones of the EK cell center compartment

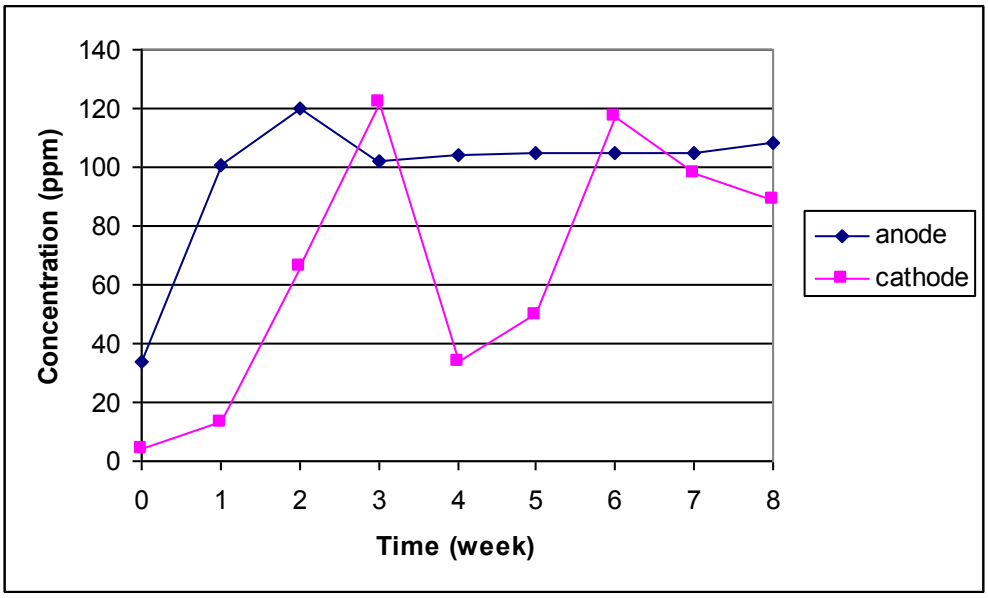

Figure G.13 EK Cell 3: Concentration curves describing the accumulation of arsenic in the anodic and cathodic half cells

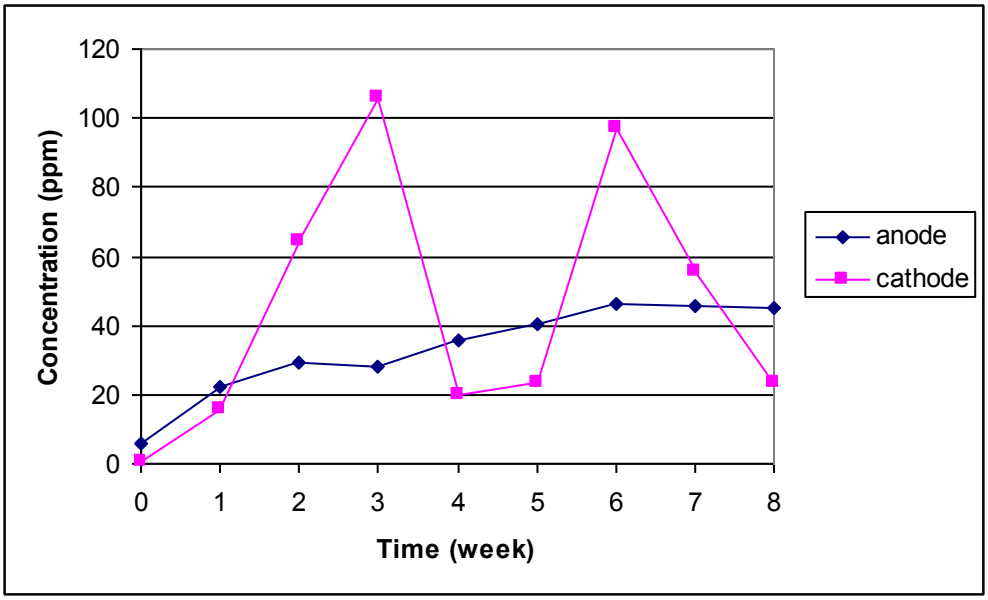

Figure G.14 EK Cell 3: Concentration curves describing the accumulation of chromium in the anodic and cathodic half cells

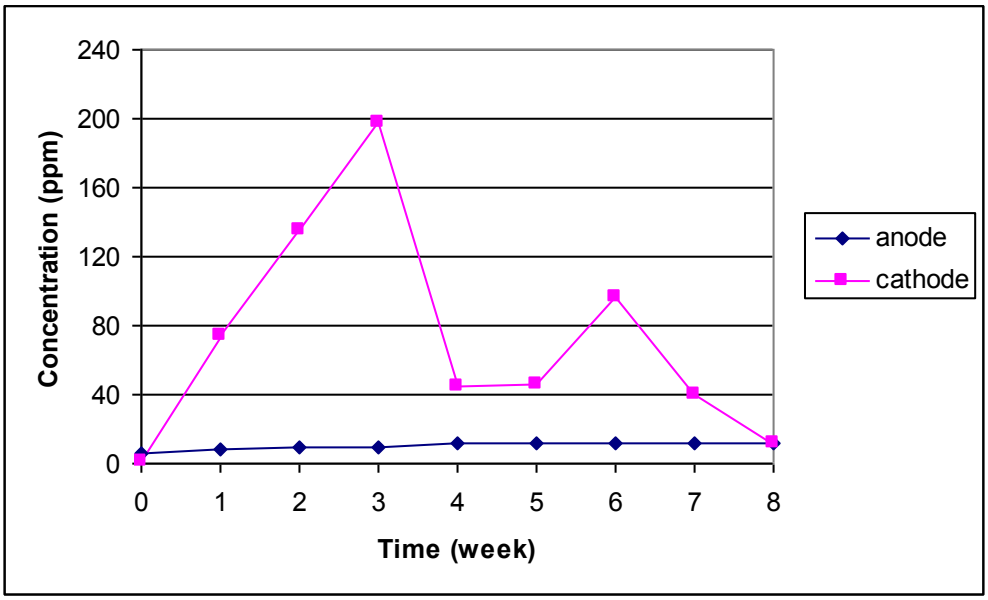

Figure G.15 EK Cell 3: Concentration curves describing the accumulation of copper in the anodic and cathodic half cells

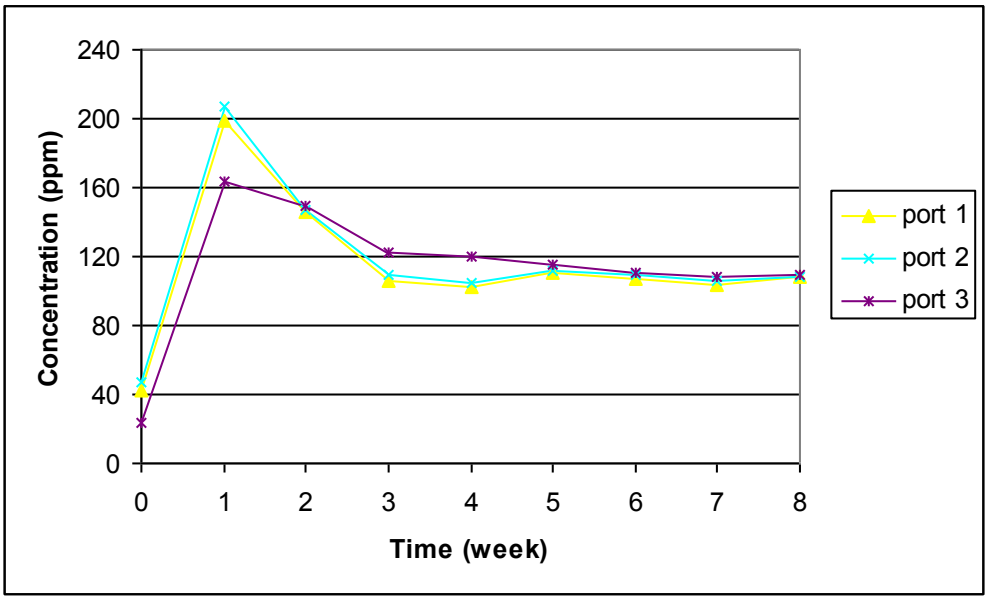

Figure G.16 EK Cell 3: Concentration curves describing the accumulation of arsenic in the pore fluid sampling zones of the EK cell center compartment

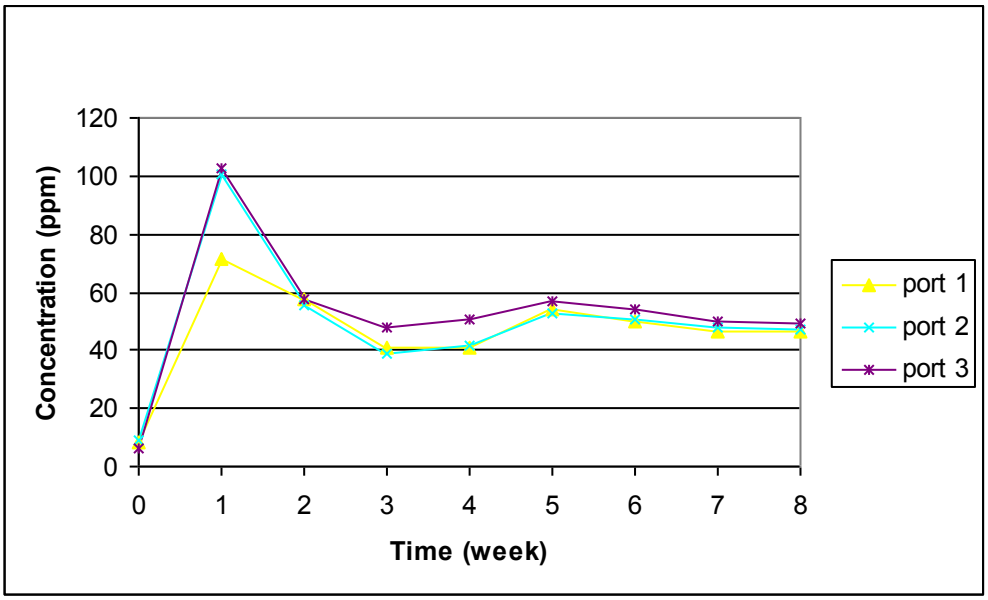

Figure G.17 EK Cell 3: Concentration curves describing the accumulation of chromium in the pore fluid sampling zones of the EK cell center compartment

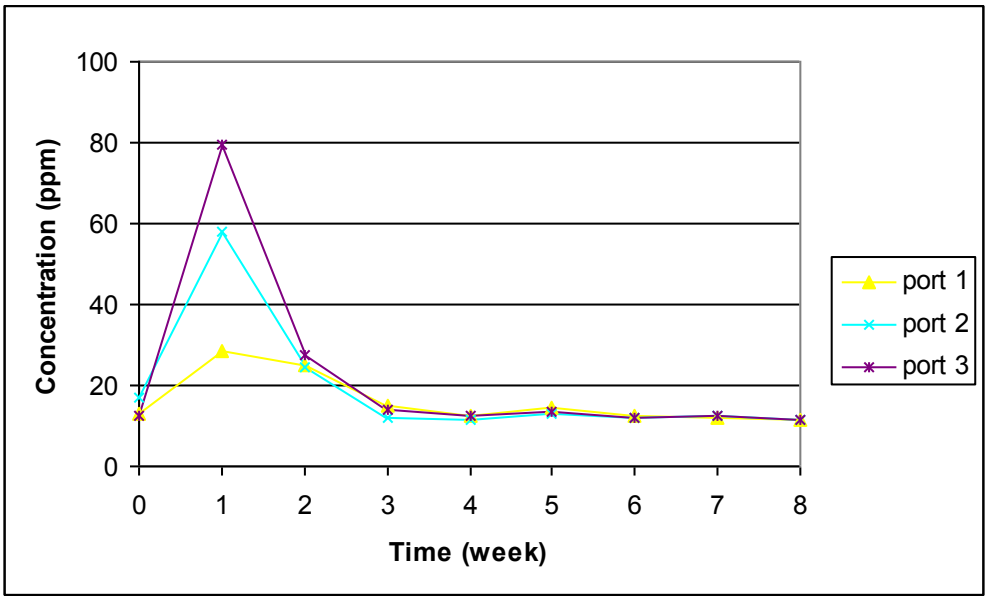

Figure G.18 EK Cell 3: Concentration curves describing the accumulation of copper in the pore fluid sampling zones of the EK cell center compartment

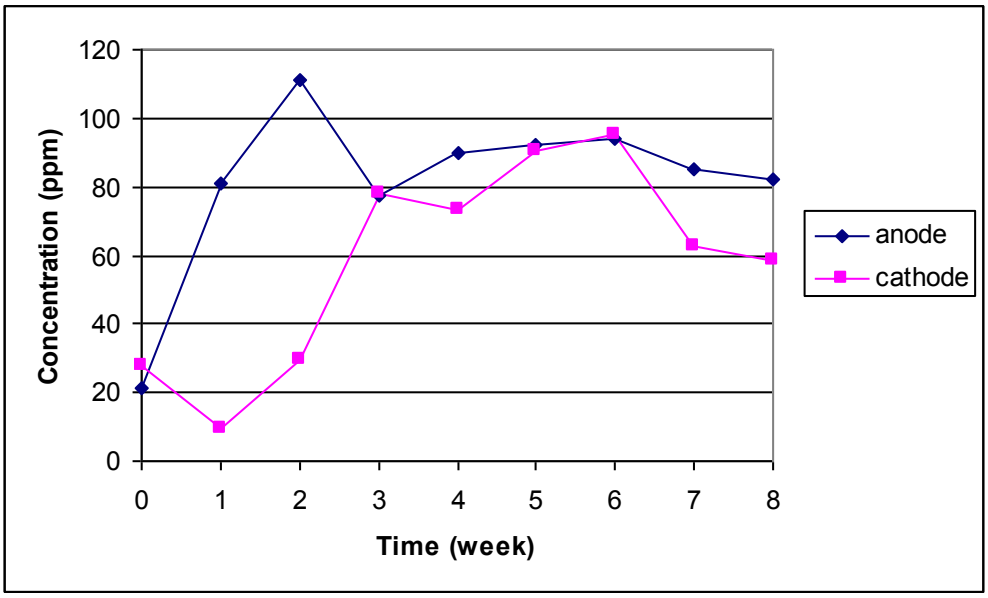

Figure G.19 EK Cell 4: Concentration curves describing the accumulation of arsenic in the anodic and cathodic half cells

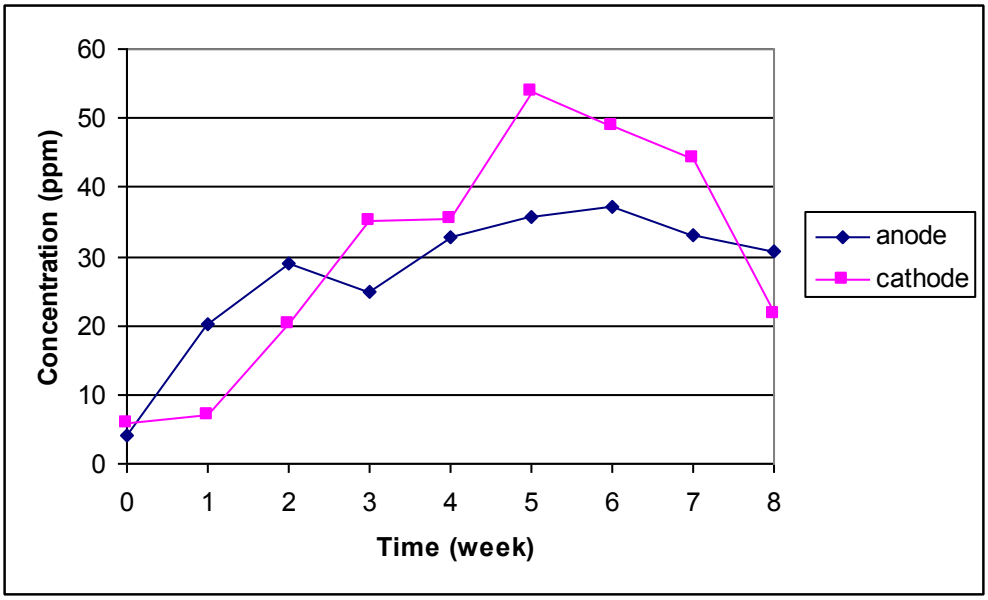

Figure G.20 EK Cell 4: Concentration curves describing the accumulation of chromium in the anodic and cathodic half cells

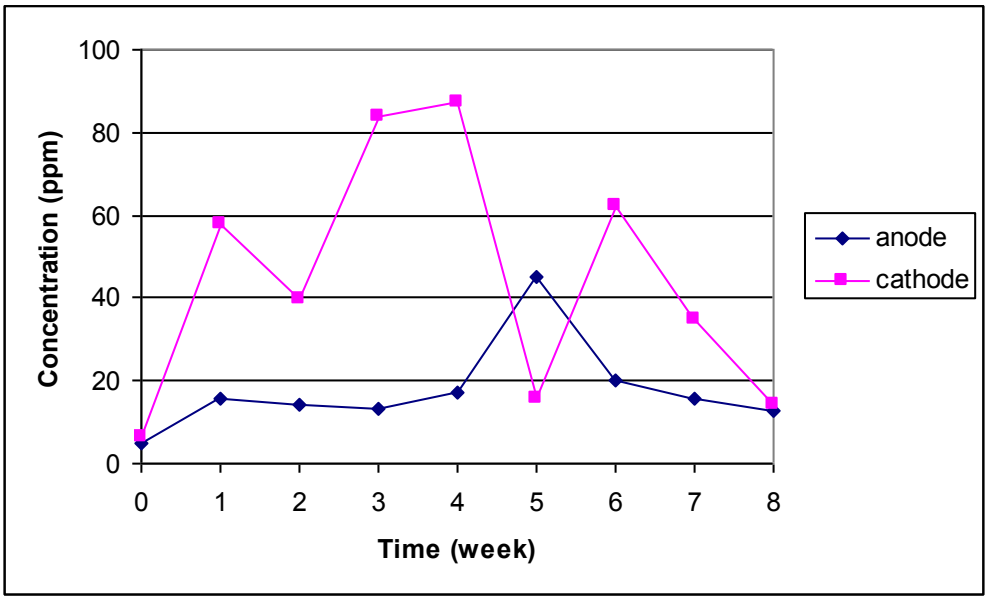

Figure G.21 EK Cell 4: Concentration curves describing the accumulation of copper in the anodic and cathodic half cells

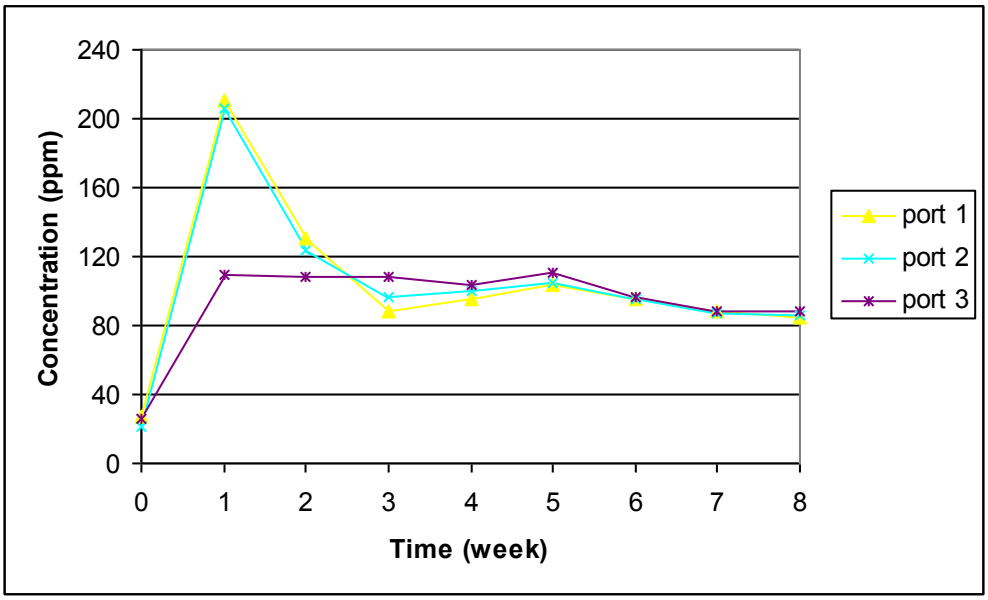

Figure G.22 EK Cell 4: Concentration curves describing the accumulation of arsenic in the pore fluid sampling zones of the EK cell center compartment

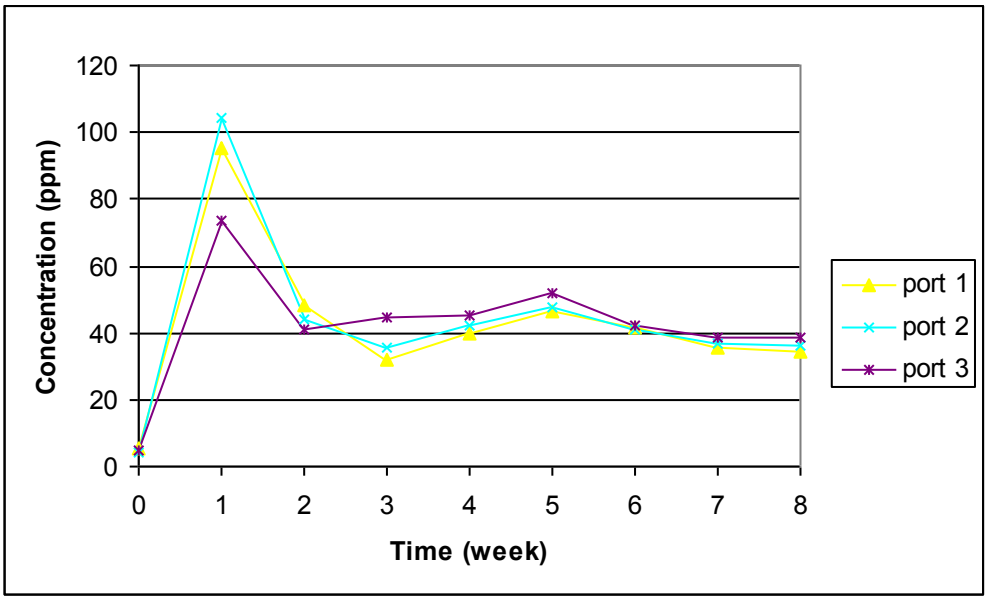

Figure G.23 EK Cell 4: Concentration curves describing the accumulation of chromium in the pore fluid sampling zones of the EK cell center compartment

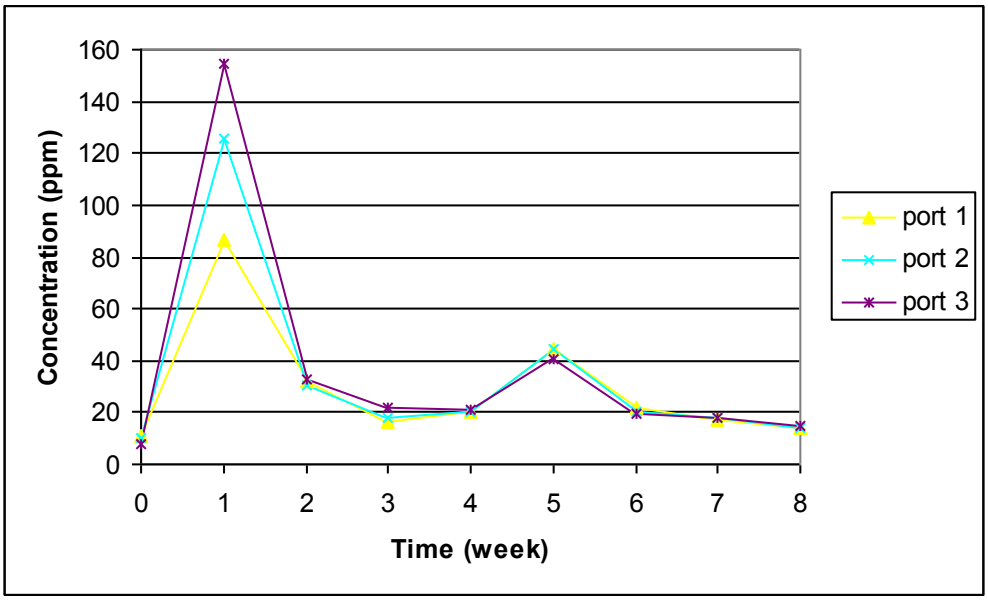

Figure G.24 EK Cell 4: Concentration curves describing the accumulation of copper in the pore fluid sampling zones of the EK cell center compartment

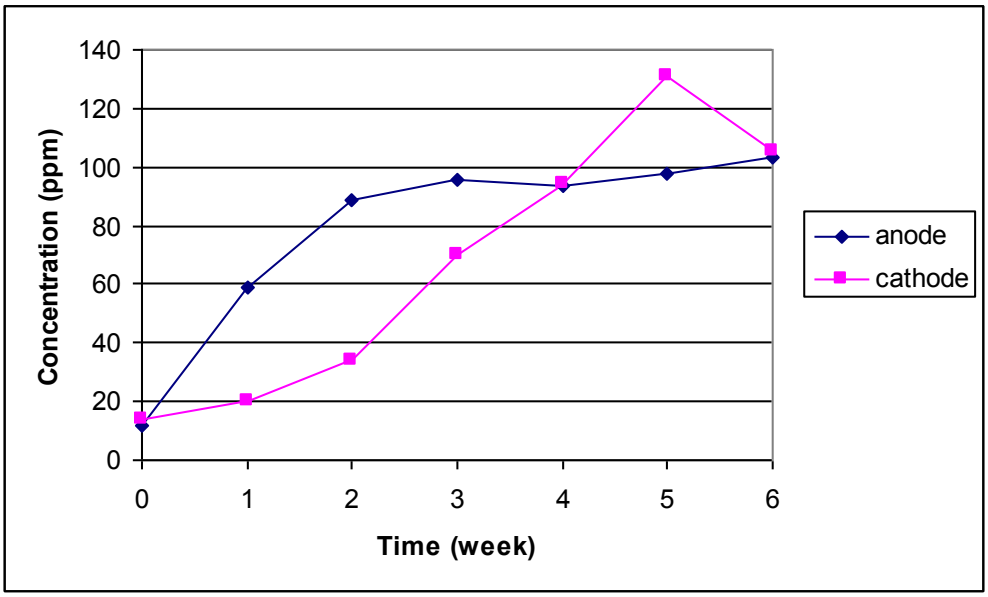

Figure G.25 EK Cell 5: Concentration curves describing the accumulation of arsenic in the anodic and cathodic half cells

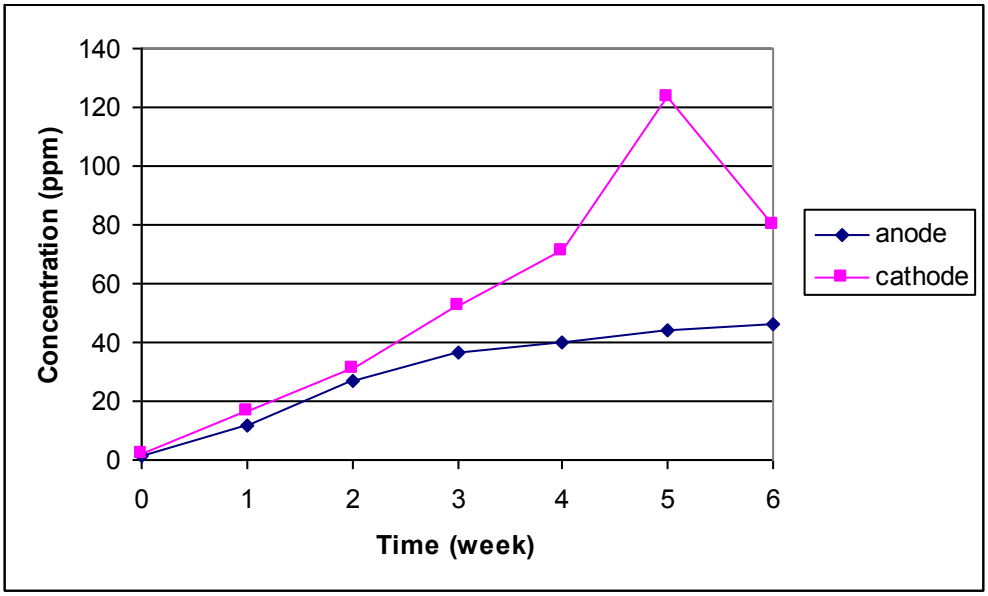

Figure G.26 EK Cell 5: Concentration curves describing the accumulation of chromium in the anodic and cathodic half cells

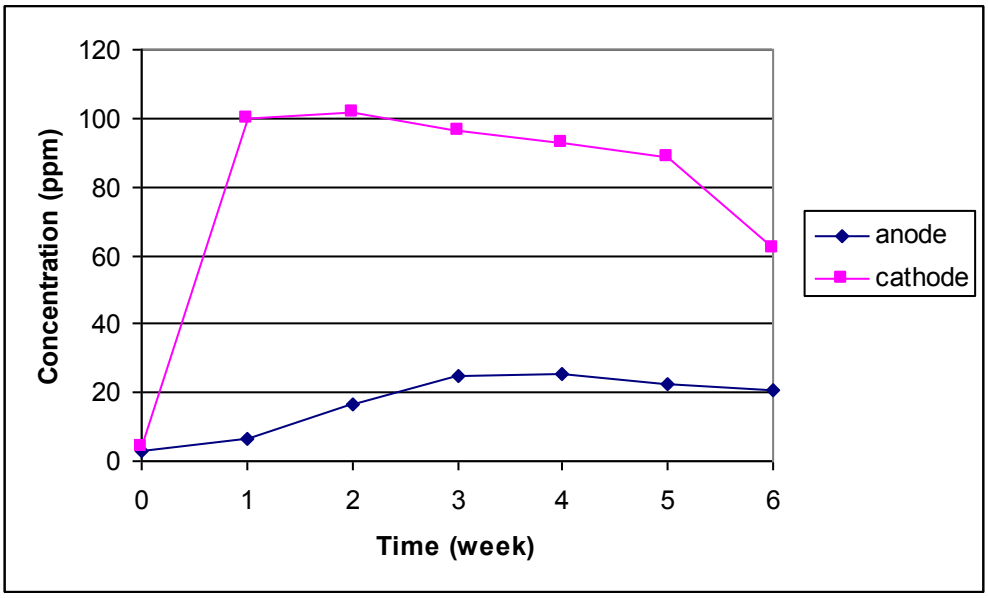

Figure G.27 EK Cell 5: Concentration curves describing the accumulation of copper in the anodic and cathodic half cells

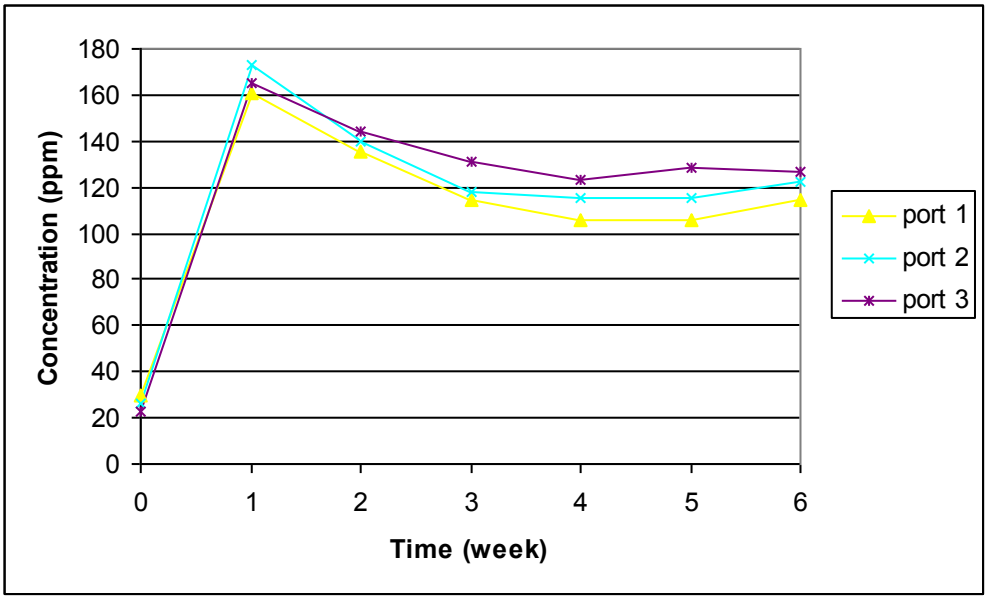

Figure G.28 EK Cell 5: Concentration curves describing the accumulation of arsenic in the pore fluid sampling zones of the EK cell center compartment

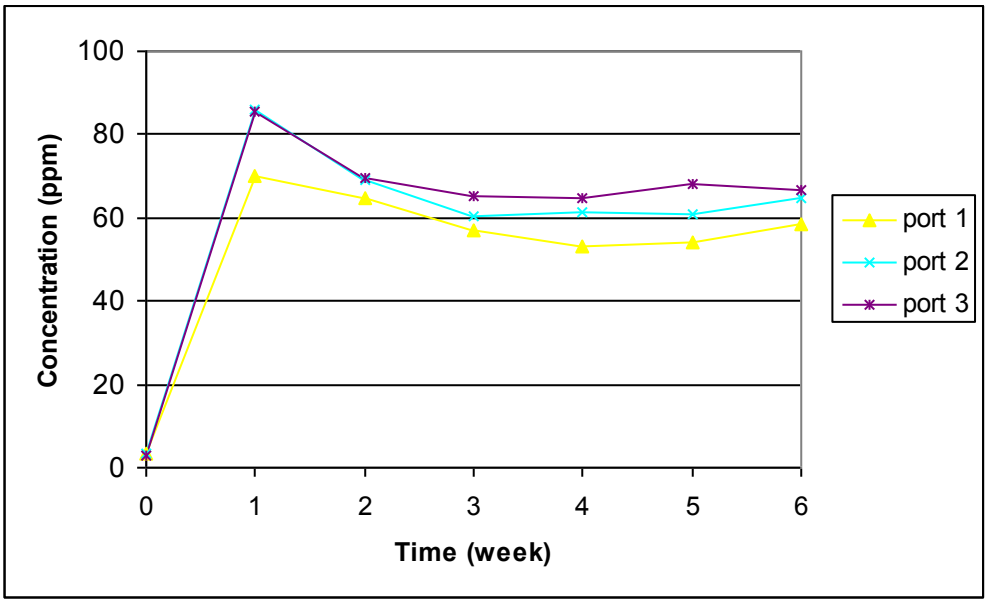

Figure G.29 EK Cell 5: Concentration curves describing the accumulation of chromium in the pore fluid sampling zones of the EK cell center compartment

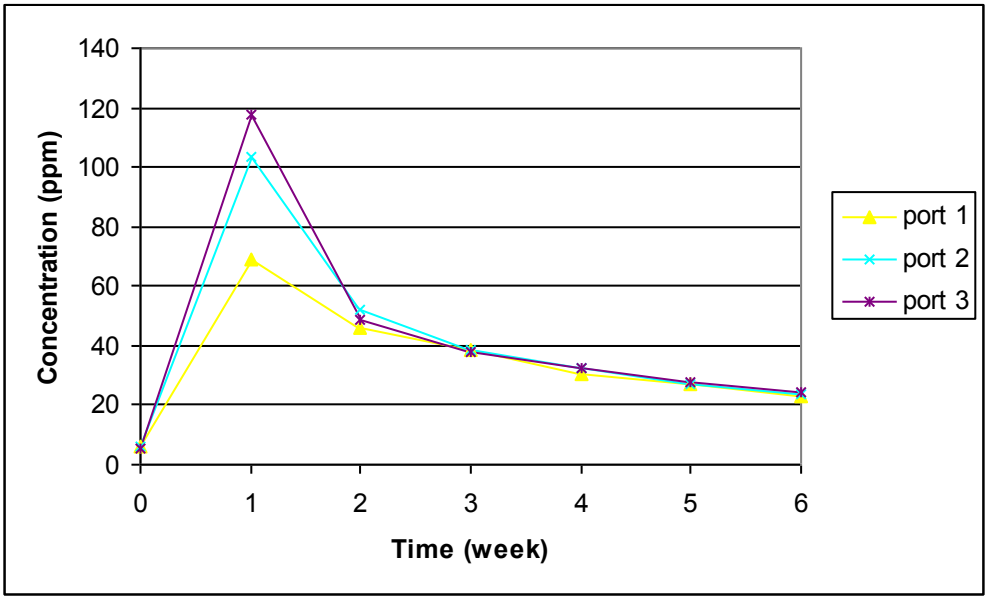

Figure G.30 EK Cell 5: Concentration curves describing the accumulation of copper in the pore fluid sampling zones of the EK cell center compartment

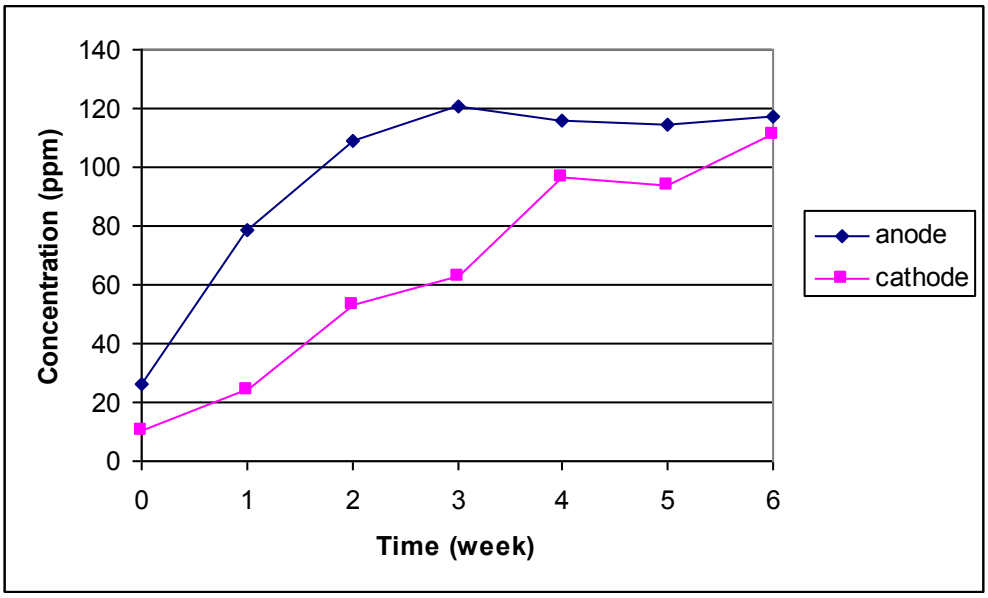

Figure G.31 EK Cell 6: Concentration curves describing the accumulation of arsenic in the anodic and cathodic half cells

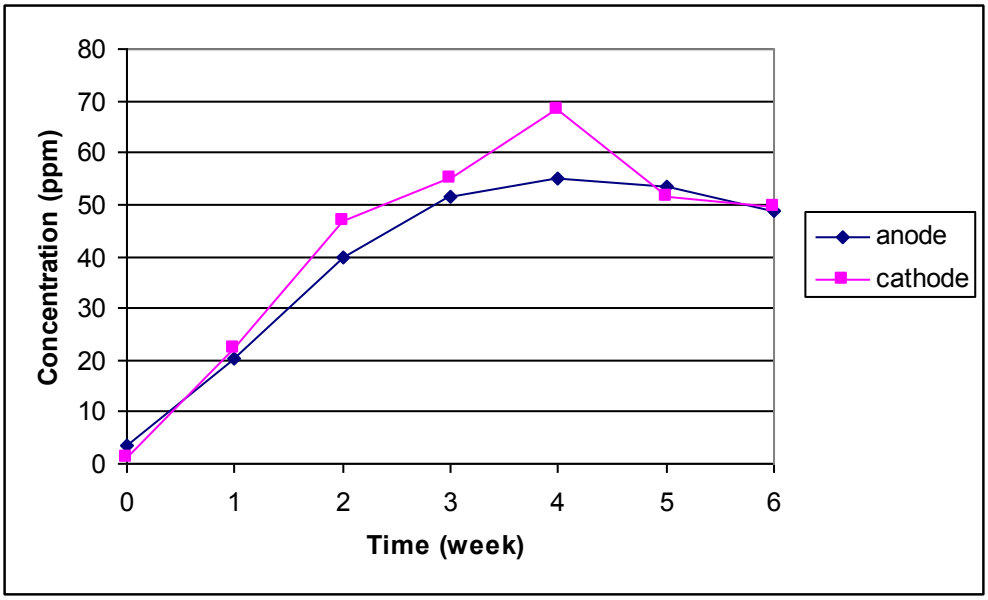

Figure G.32 EK Cell 6: Concentration curves describing the accumulation of chromium in the anodic and cathodic half cells

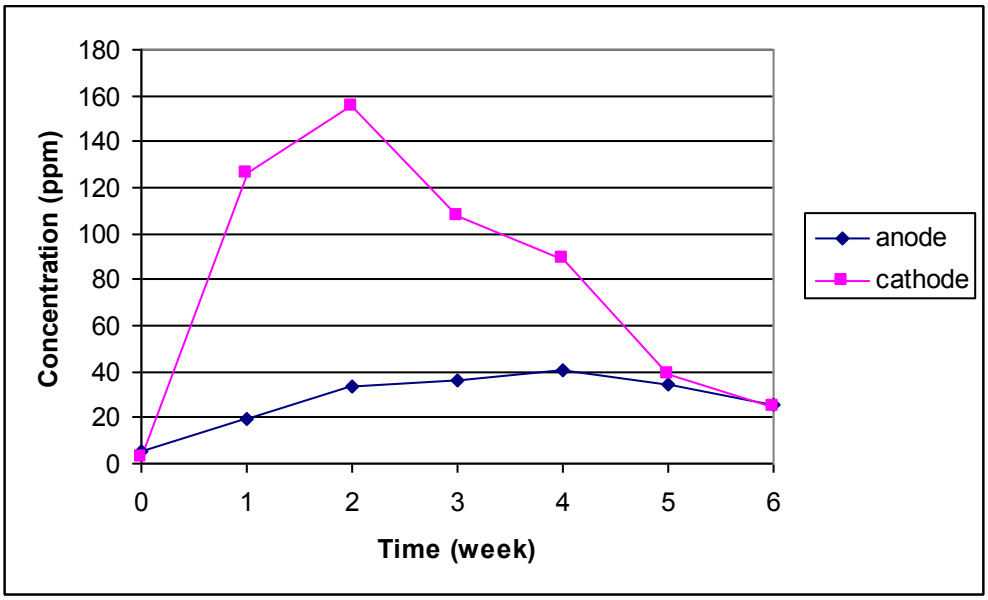

Figure G.33 EK Cell 6: Concentration curves describing the accumulation of copper in the anodic and cathodic half cells

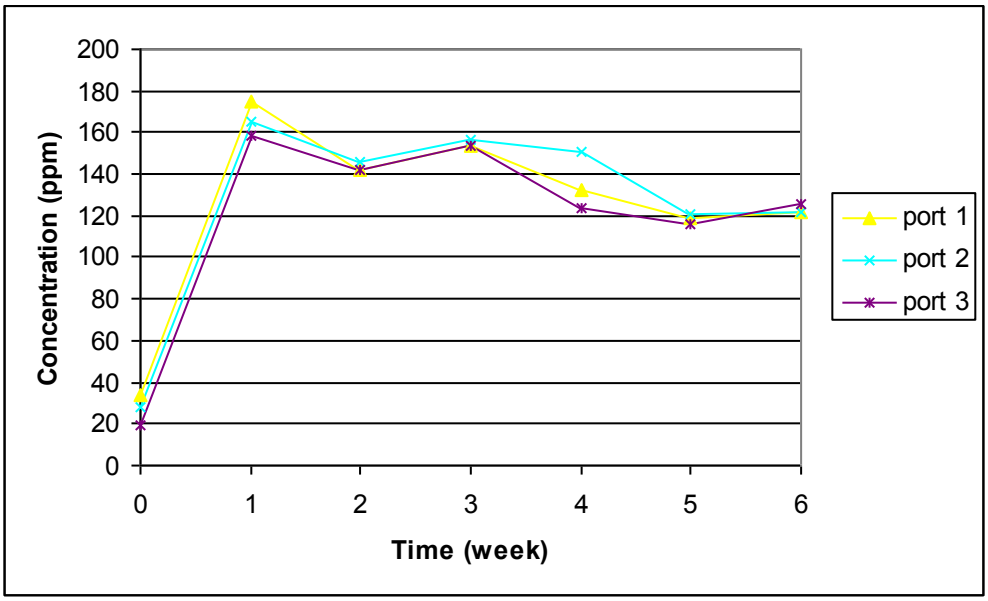

Figure G.34 EK Cell 6: Concentration curves describing the accumulation of arsenic in the pore fluid sampling zones of the EK cell center compartment

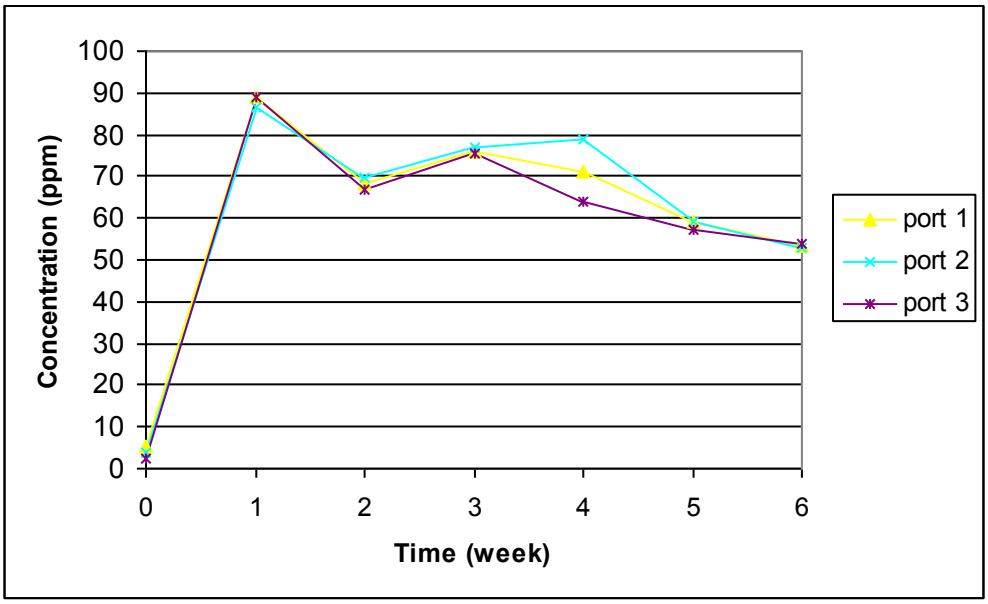

Figure G.35 EK Cell 6: Concentration curves describing the accumulation of chromium in the pore fluid sampling zones of the EK cell center compartment

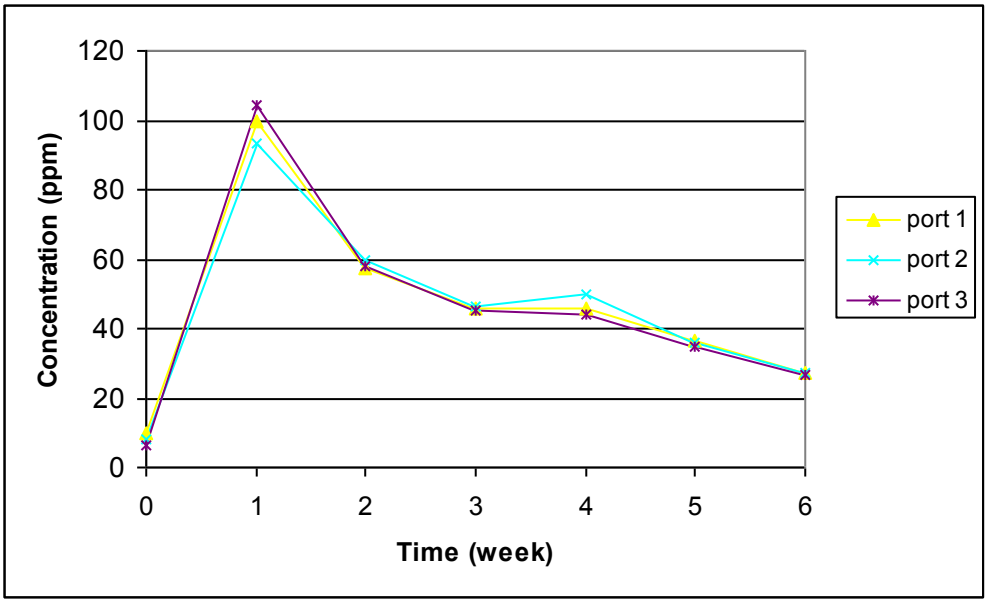

Figure G.36 EK Cell 6: Concentration curves describing the accumulation of copper in the pore fluid sampling zones of the EK cell center compartment

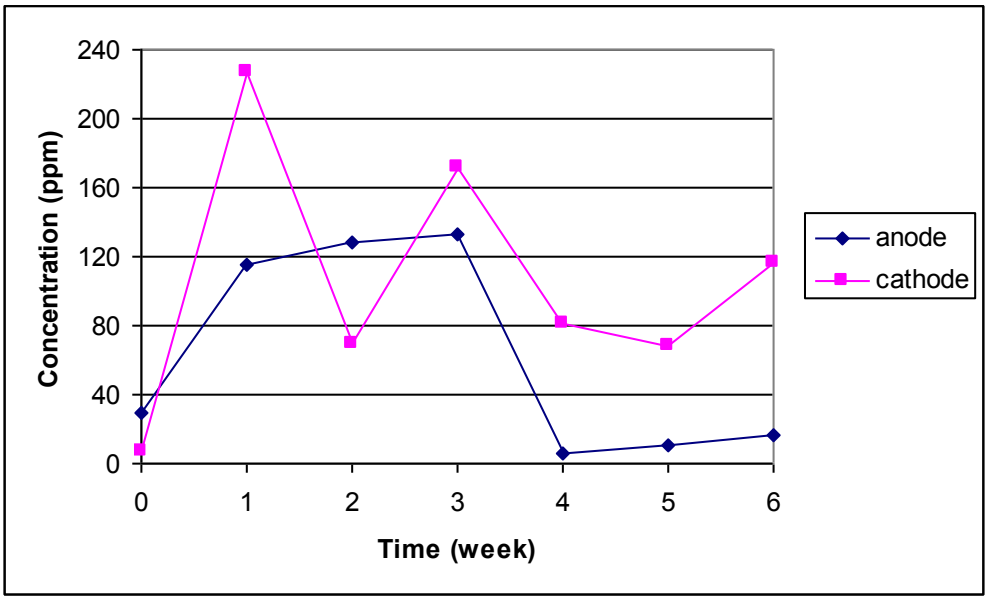

Figure G.37 EK Cell 7: Concentration curves describing the accumulation of arsenic in the anodic and cathodic half cells

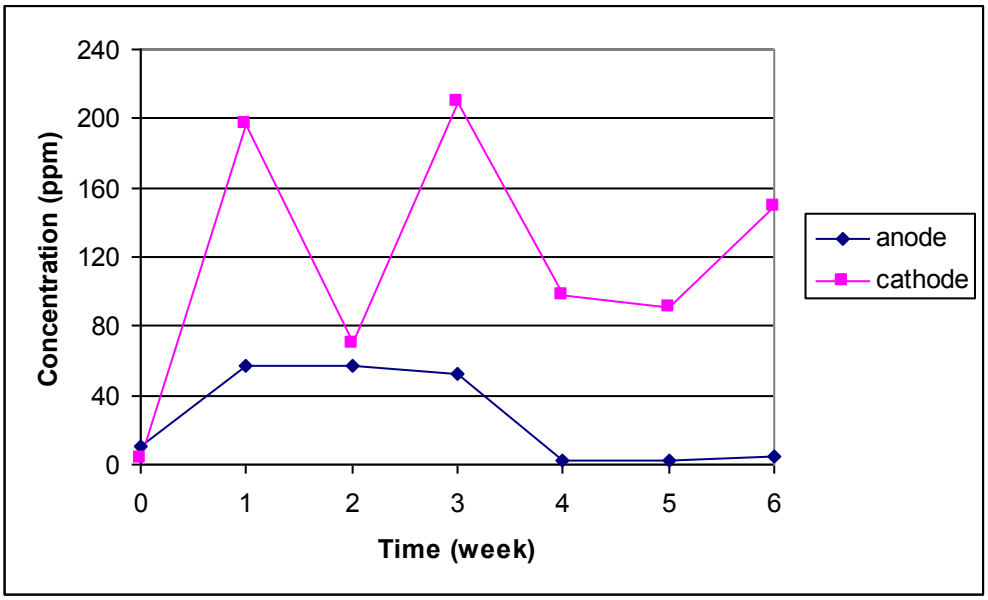

Figure G.38 EK Cell 7: Concentration curves describing the accumulation of chromium in the anodic and cathodic half cells

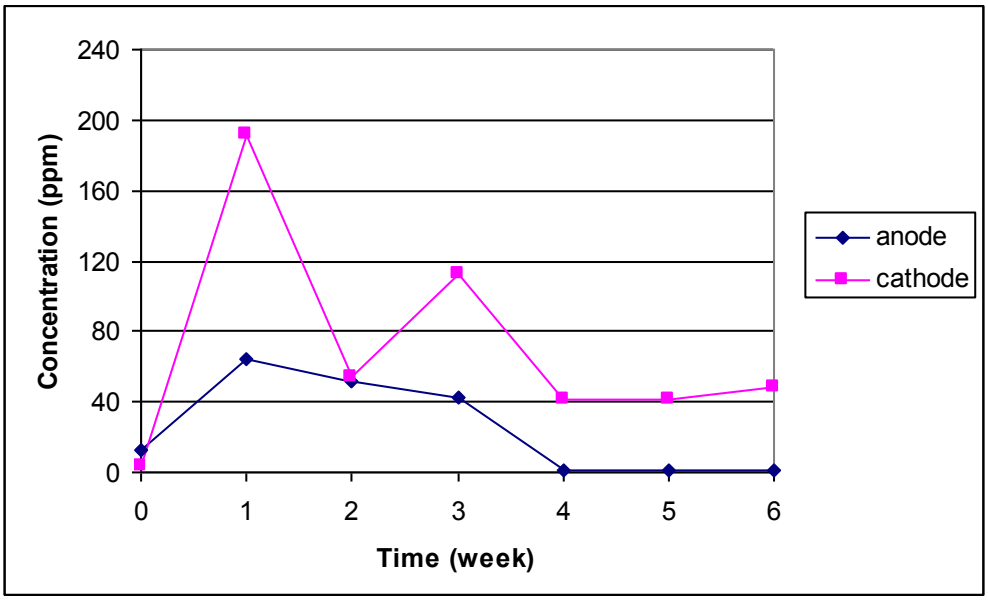

Figure G.39 EK Cell 7: Concentration curves describing the accumulation of copper in the anodic and cathodic half cells

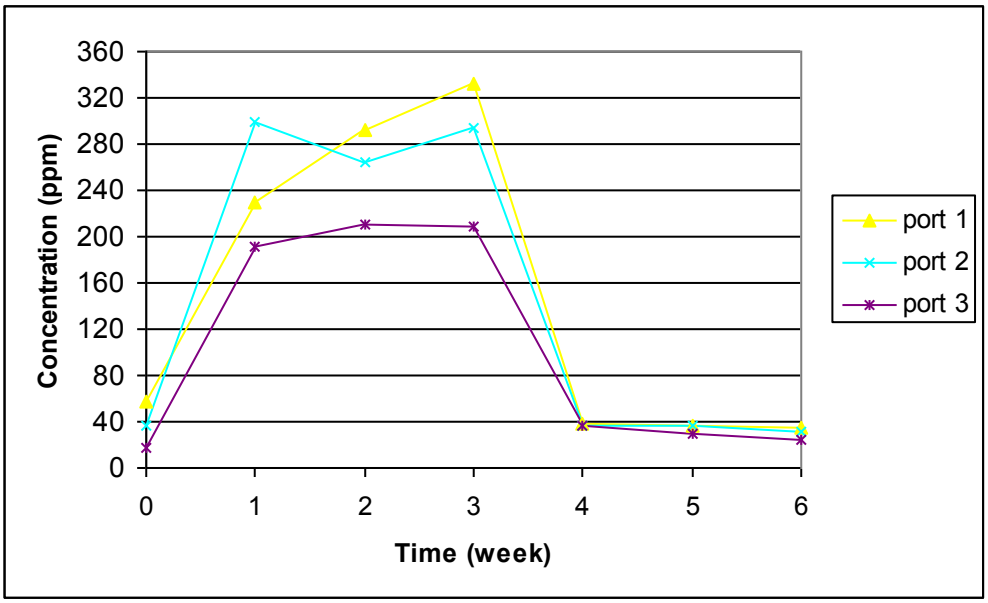

Figure G.40 EK Cell 7: Concentration curves describing the accumulation of arsenic in the pore fluid sampling zones of the EK cell center compartment

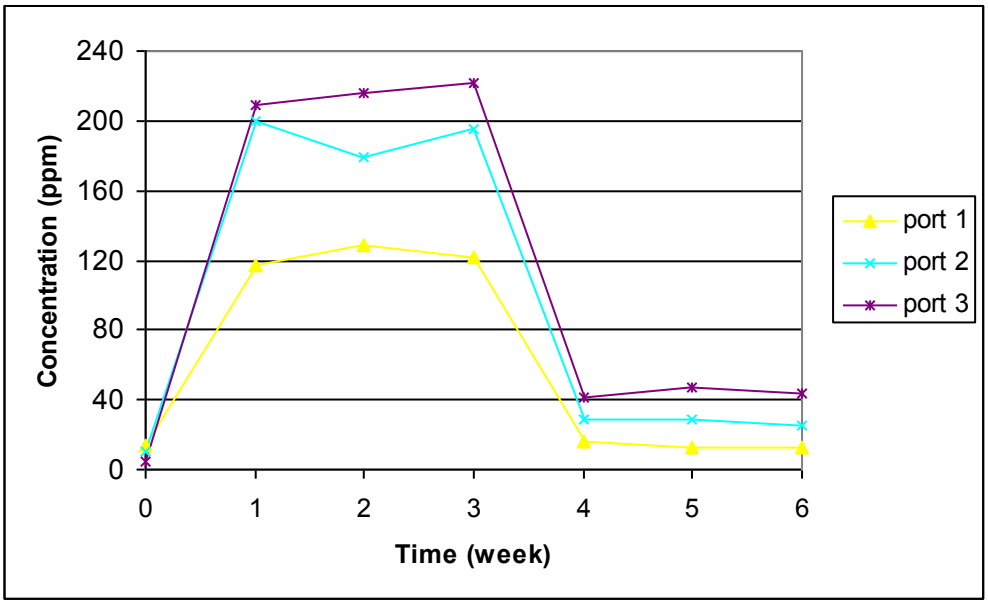

Figure G.41 EK Cell 7: Concentration curves describing the accumulation of chromium in the pore fluid sampling zones of the EK cell center compartment

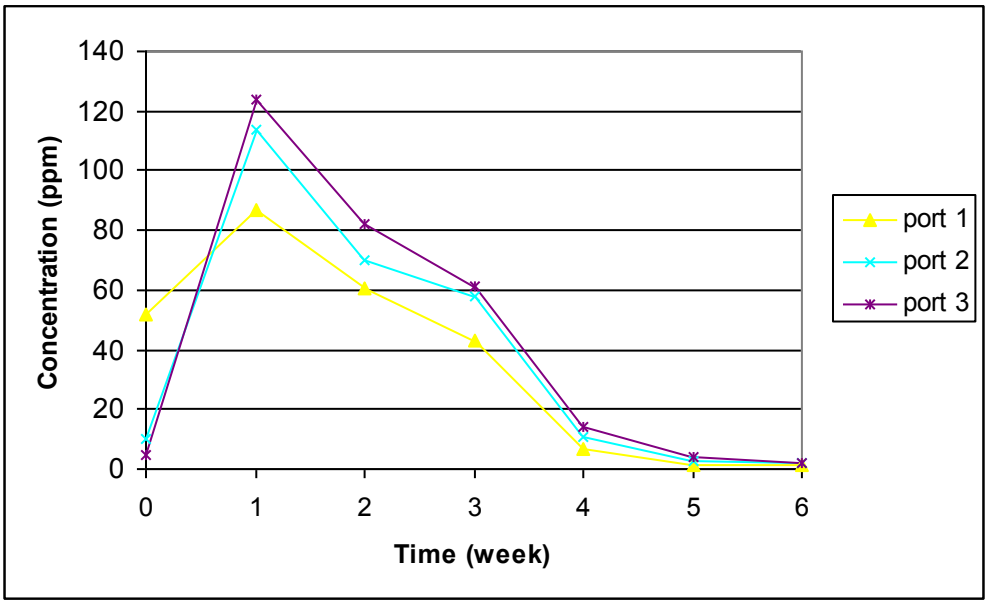

Figure G.42 EK Cell 7: Concentration curves describing the accumulation of copper in the pore fluid sampling zones of the EK cell center compartment

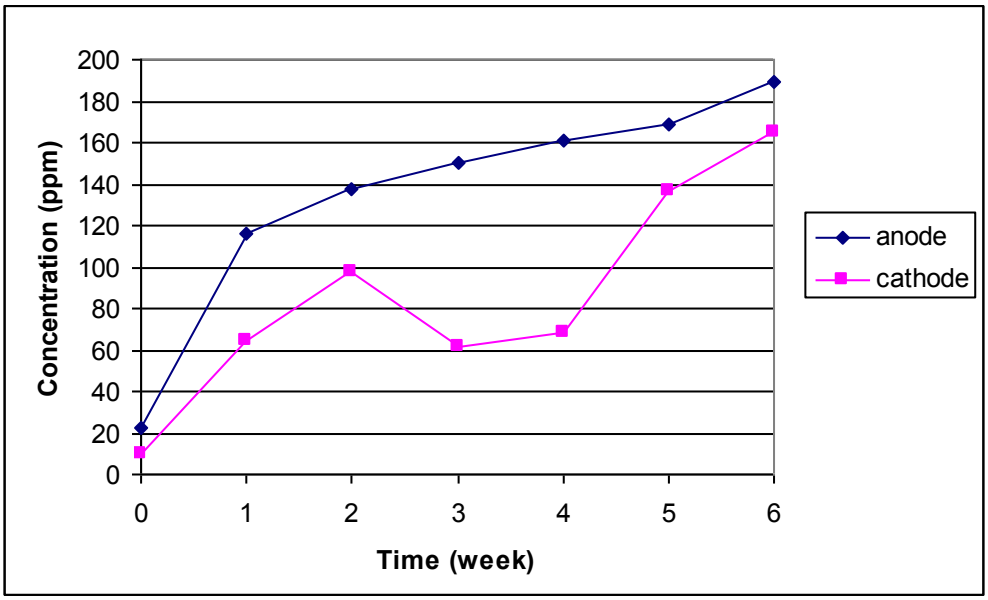

Figure G.43 EK Cell 8: Concentration curves describing the accumulation of arsenic in the anodic and cathodic half cells

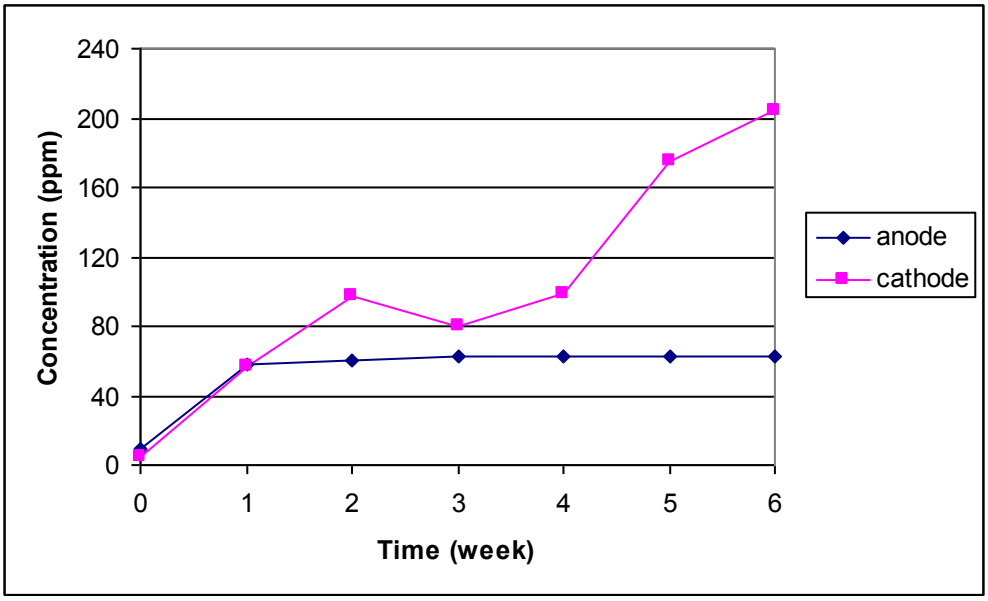

Figure G.44 EK Cell 8: Concentration curves describing the accumulation of chromium in the anodic and cathodic half cells

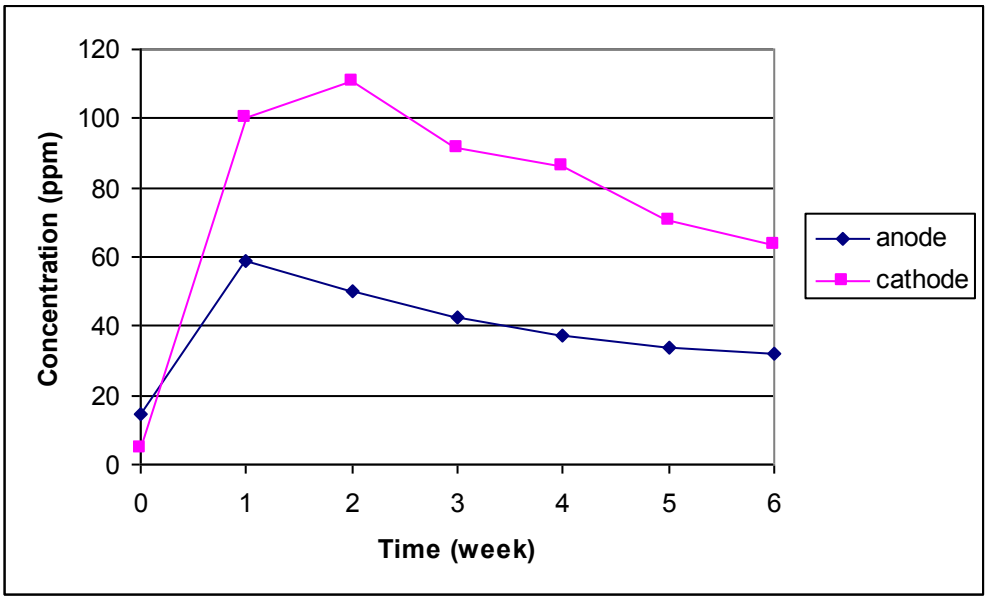

Figure G.45 EK Cell 8: Concentration curves describing the accumulation of copper in the anodic and cathodic half cells

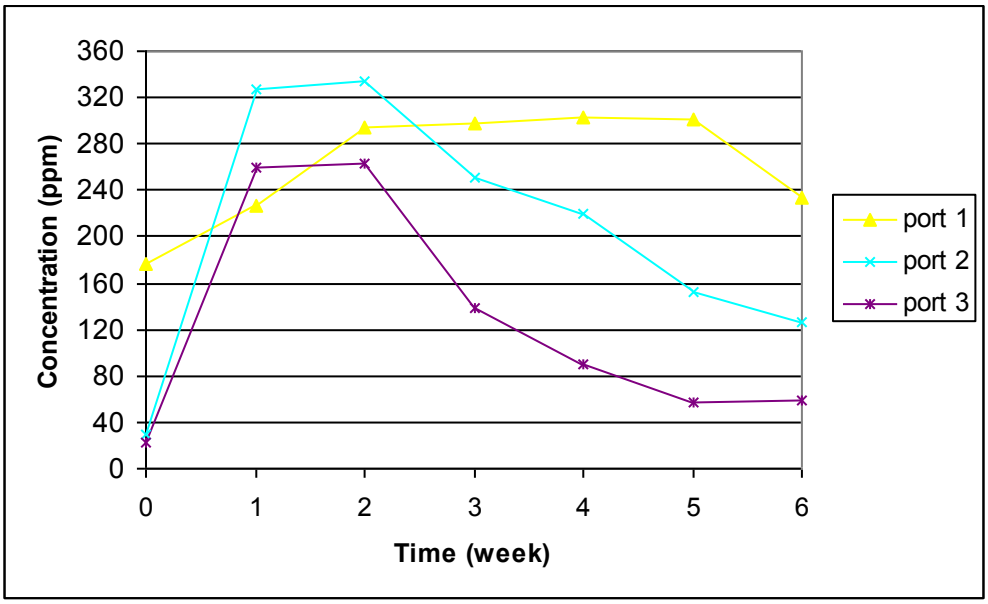

Figure G.46 EK Cell 8: Concentration curves describing the accumulation of arsenic in the pore fluid sampling zones of the EK cell center compartment

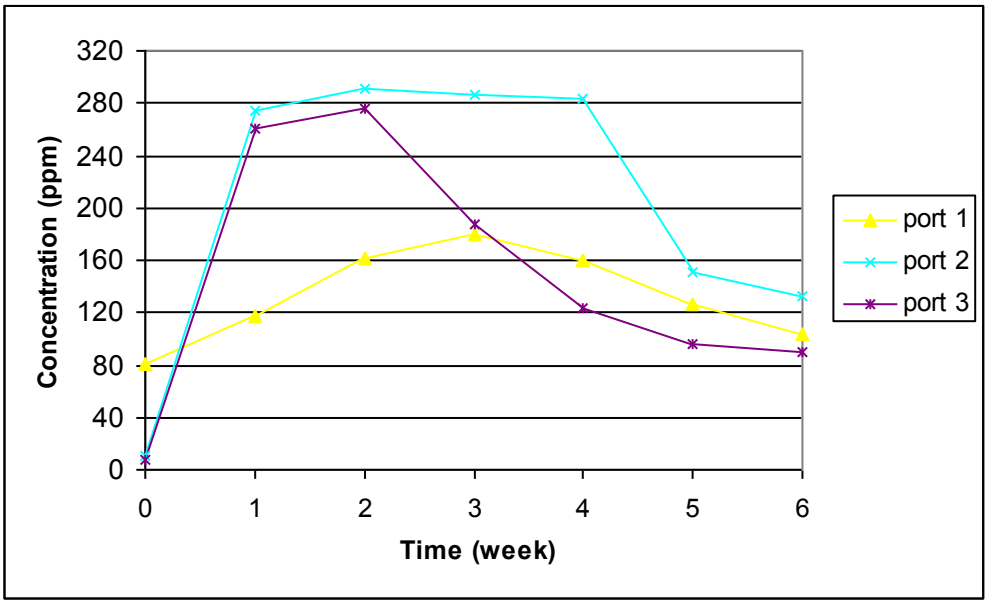

Figure G.47 EK Cell 8: Concentration curves describing the accumulation of chromium in the pore fluid sampling zones of the EK cell center compartment

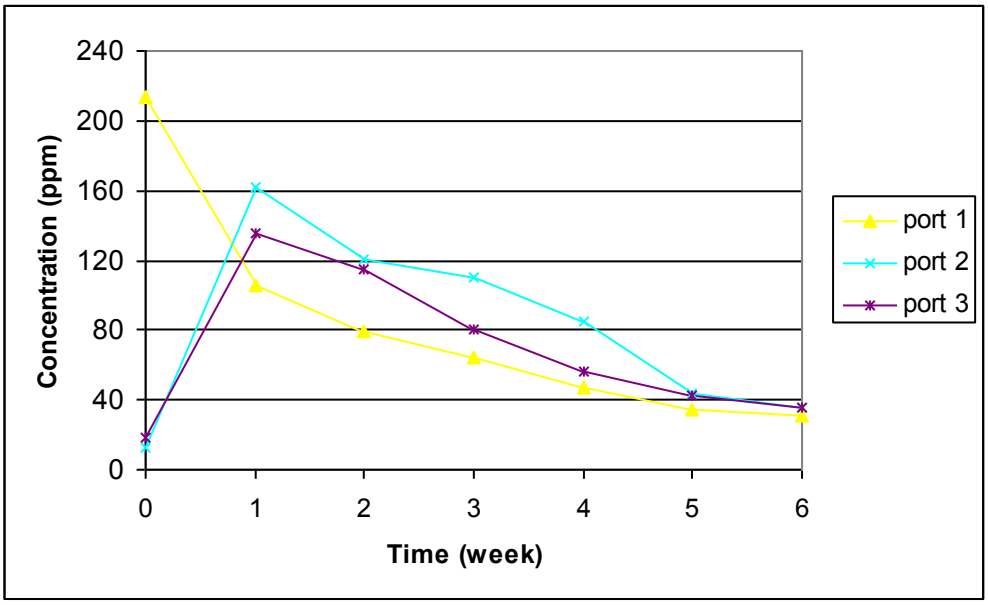

Figure G.48 EK Cell 8: Concentration curves describing the accumulation of copper in the pore fluid sampling zones of the EK cell center compartment

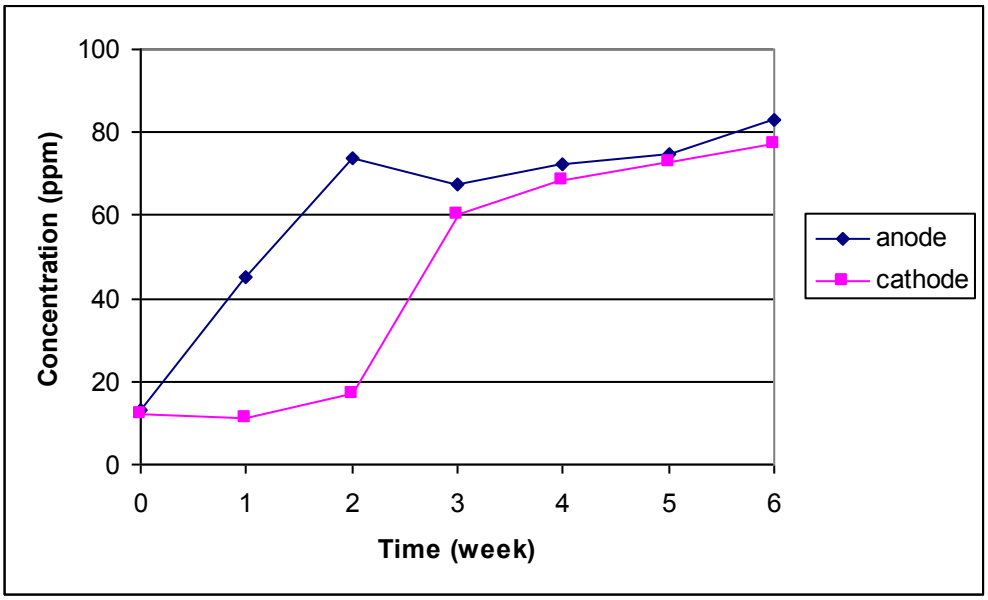

Figure G.49 EK Cell 9: Concentration curves describing the accumulation of arsenic in the anodic and cathodic half cells

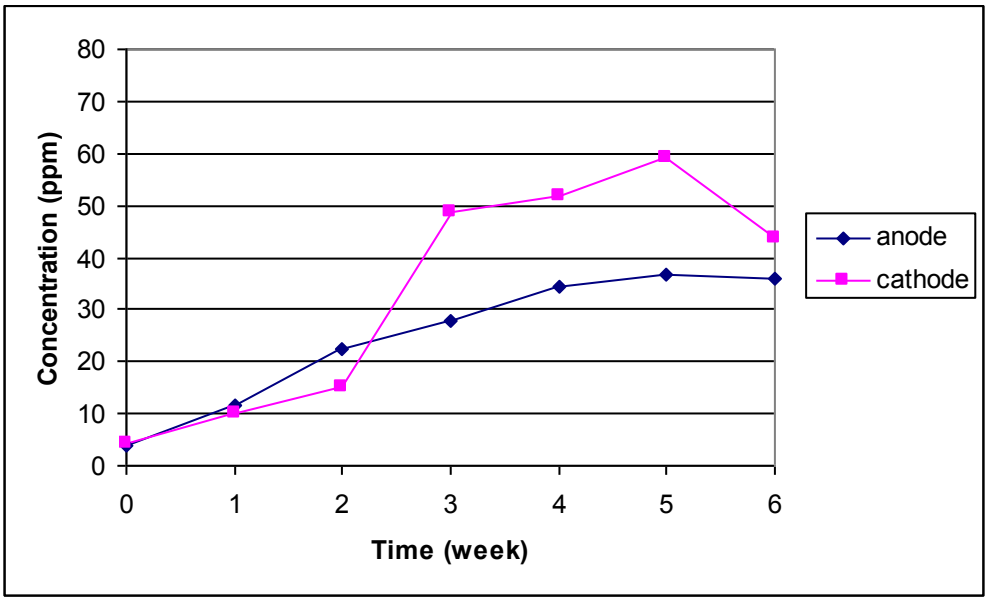

Figure G.50 EK Cell 9: Concentration curves describing the accumulation of chromium in the anodic and cathodic half cells

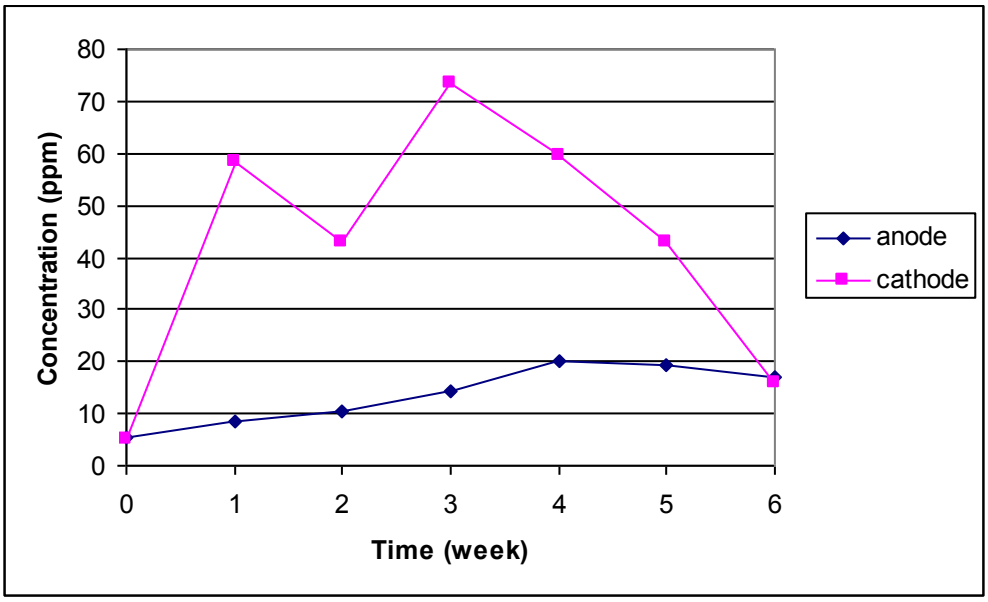

Figure G.51 EK Cell 9: Concentration curves describing the accumulation of copper in the anodic and cathodic half cells

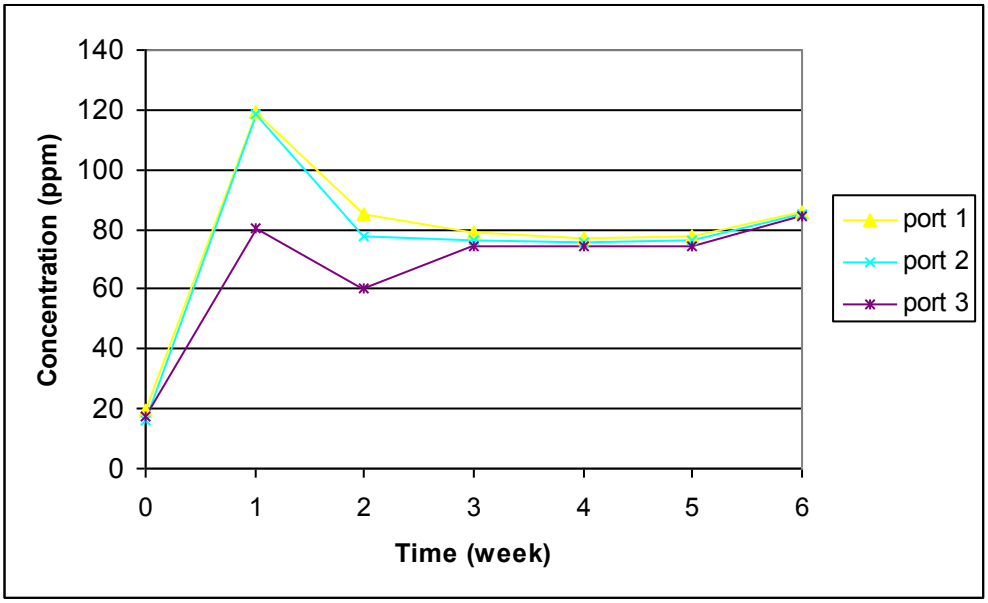

Figure G.52 EK Cell 9: Concentration curves describing the accumulation of arsenic in the pore fluid sampling zones of the EK cell center compartment

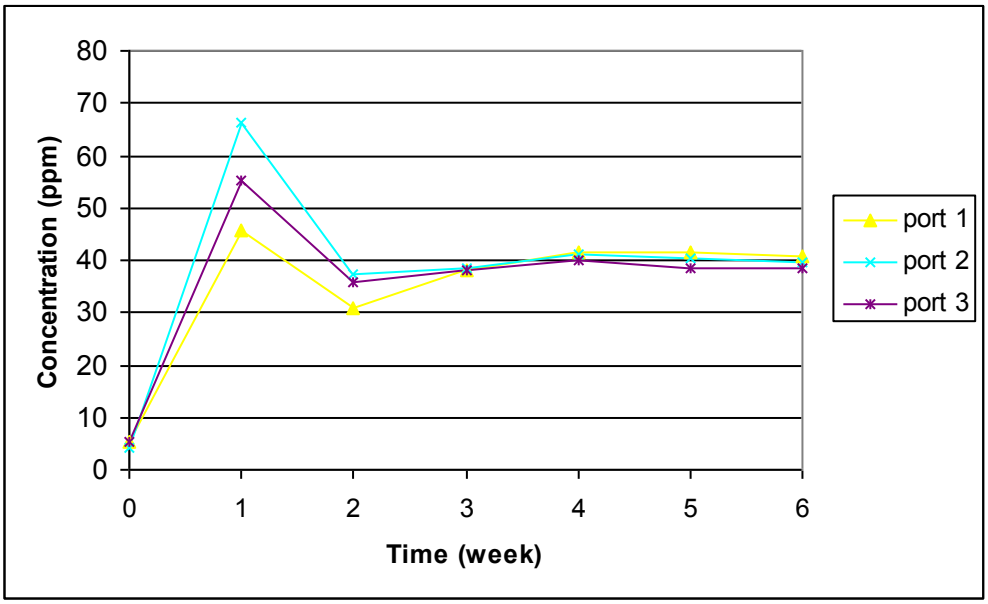

Figure G.53 EK Cell 9: Concentration curves describing the accumulation of chromium in the pore fluid sampling zones of the EK cell center compartment

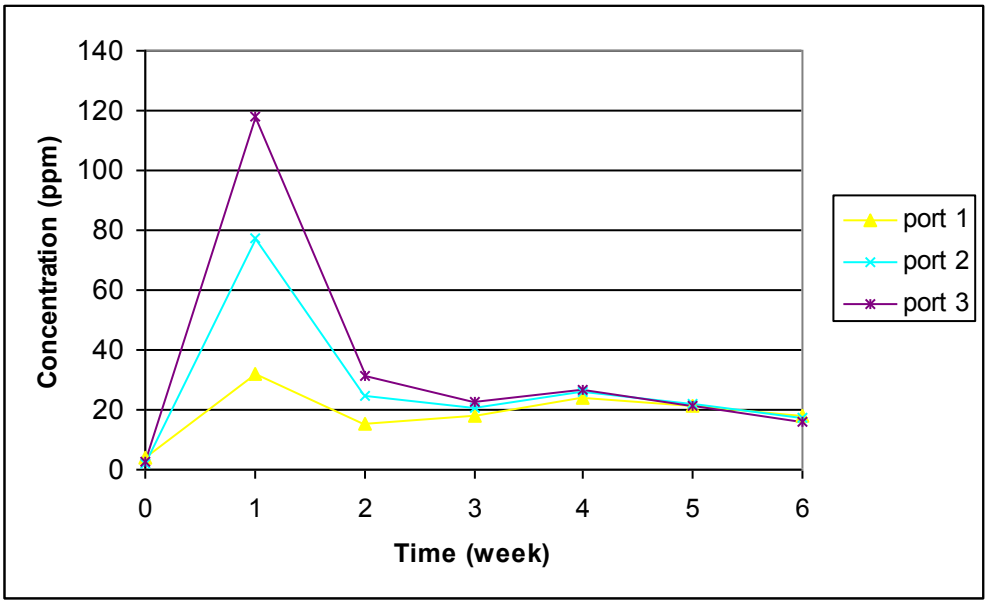

Figure G.54 EK Cell 9: Concentration curves describing the accumulation of copper in the pore fluid sampling zones of the EK cell center compartment

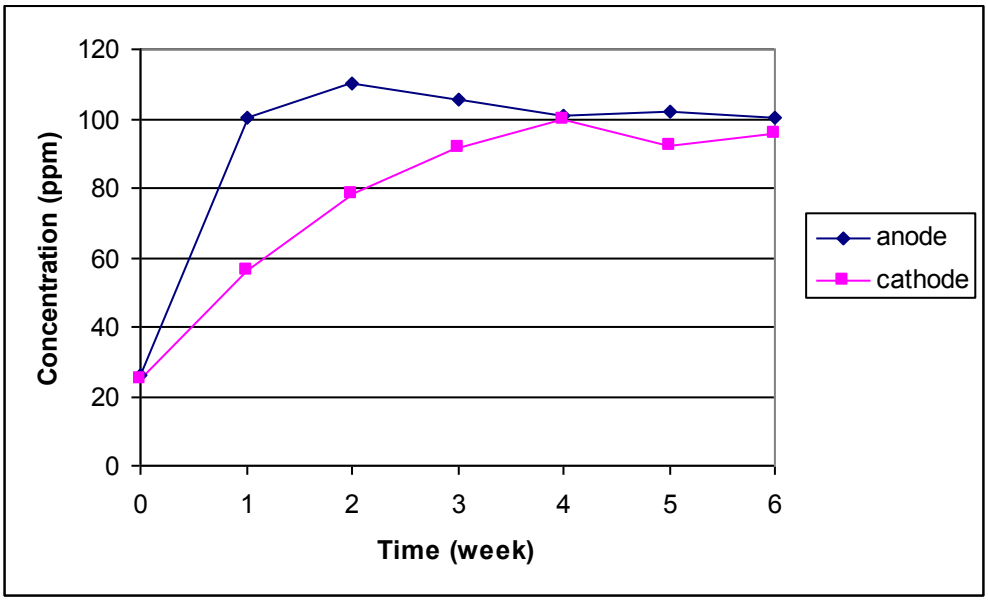

Figure G.55 EK Cell 10: Concentration curves describing the accumulation of arsenic in the anodic and cathodic half cells

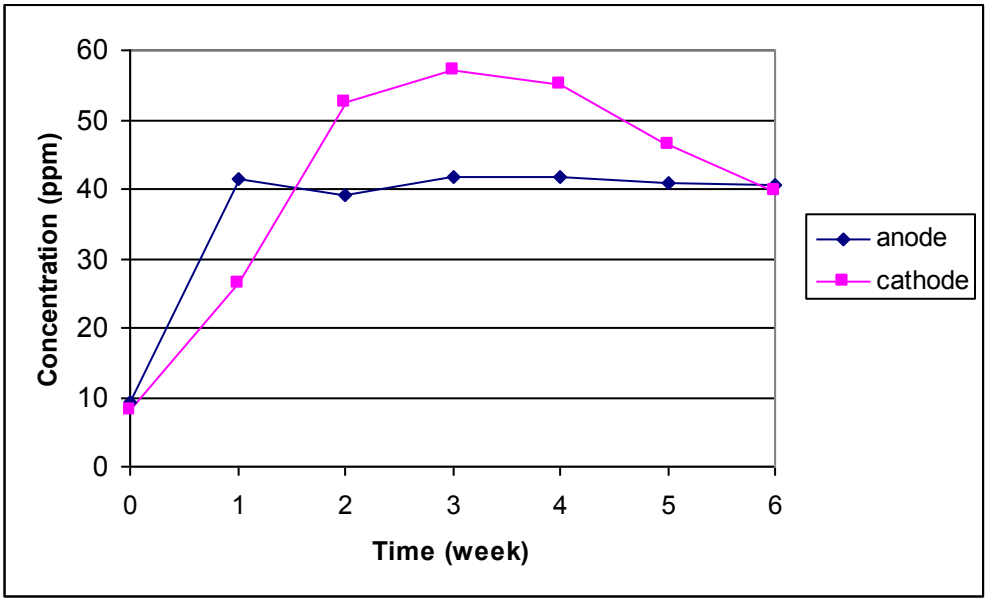

Figure G.56 EK Cell 10: Concentration curves describing the accumulation of chromium in the anodic and cathodic half cells

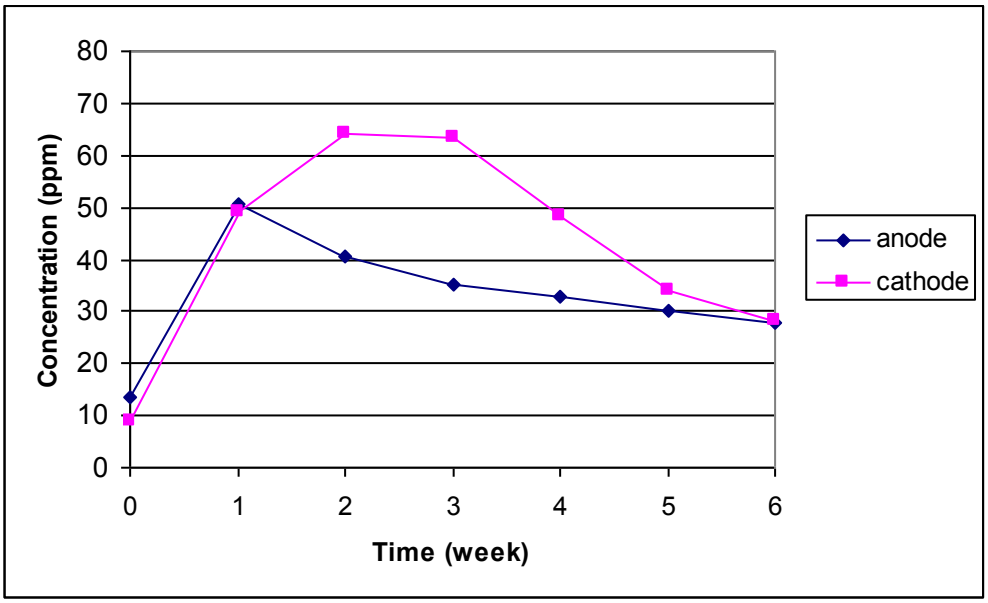

Figure G.57 EK Cell 10: Concentration curves describing the accumulation of copper in the anodic and cathodic half cells

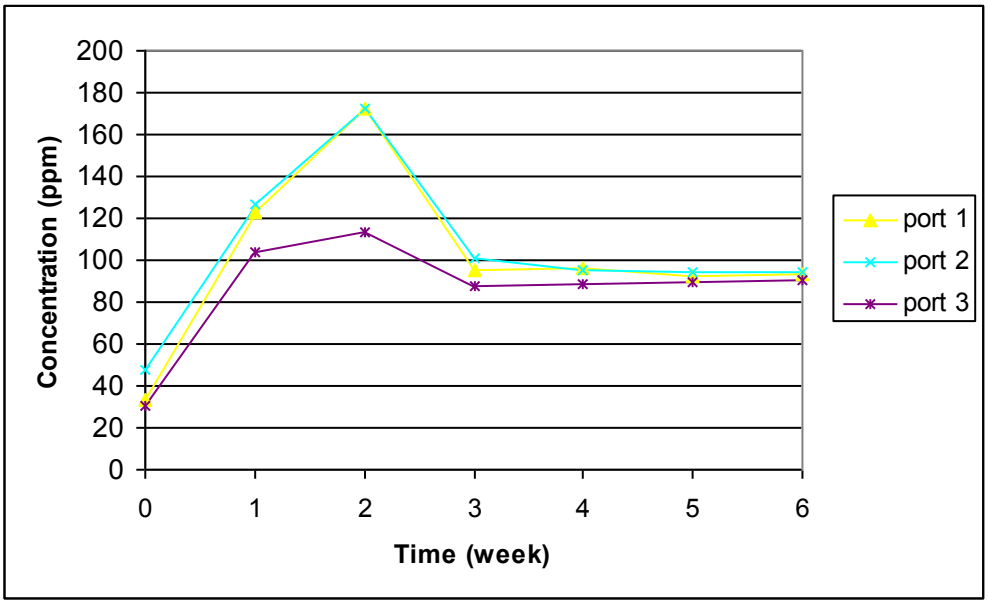

Figure G.58 EK Cell 10: Concentration curves describing the accumulation of arsenic in the pore fluid sampling zones of the EK cell center compartment.

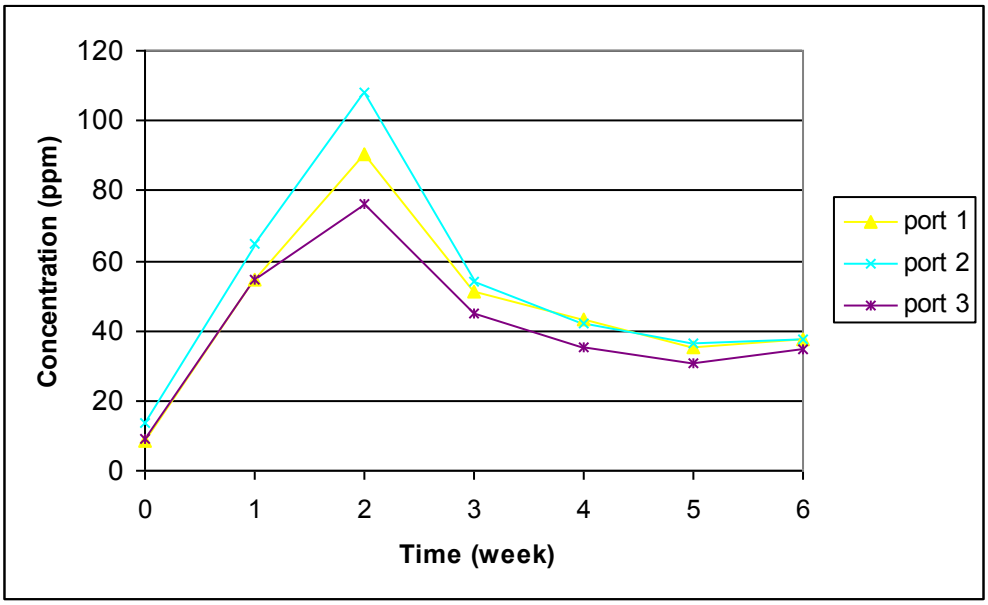

Figure G.59 EK Cell 10: Concentration curves describing the accumulation of chromium in the pore fluid sampling zones of the EK cell center compartment

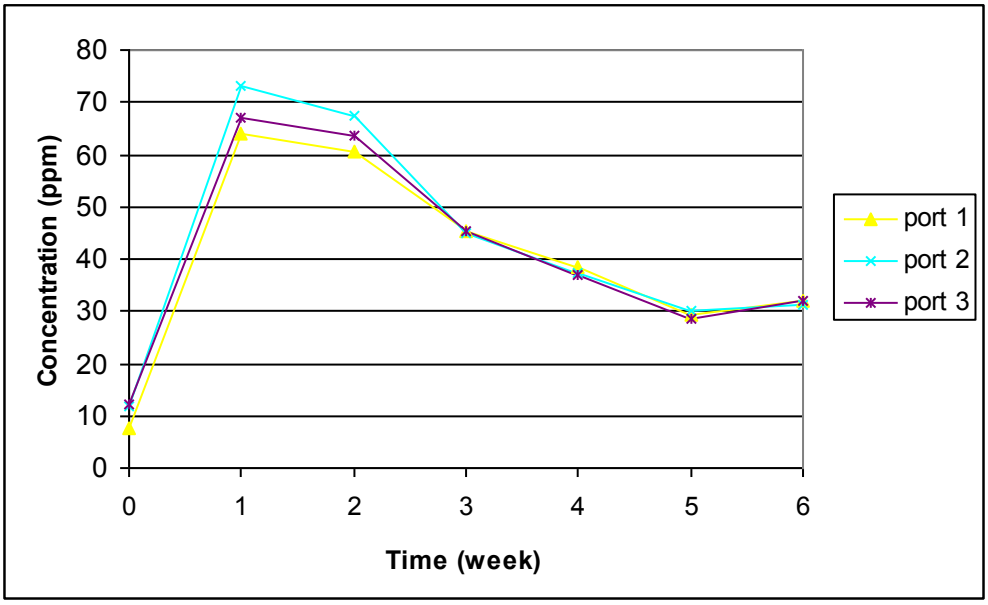

Figure G.60 EK Cell 10: Concentration curves describing the accumulation of copper in the pore fluid sampling zones of the EK cell center compartment

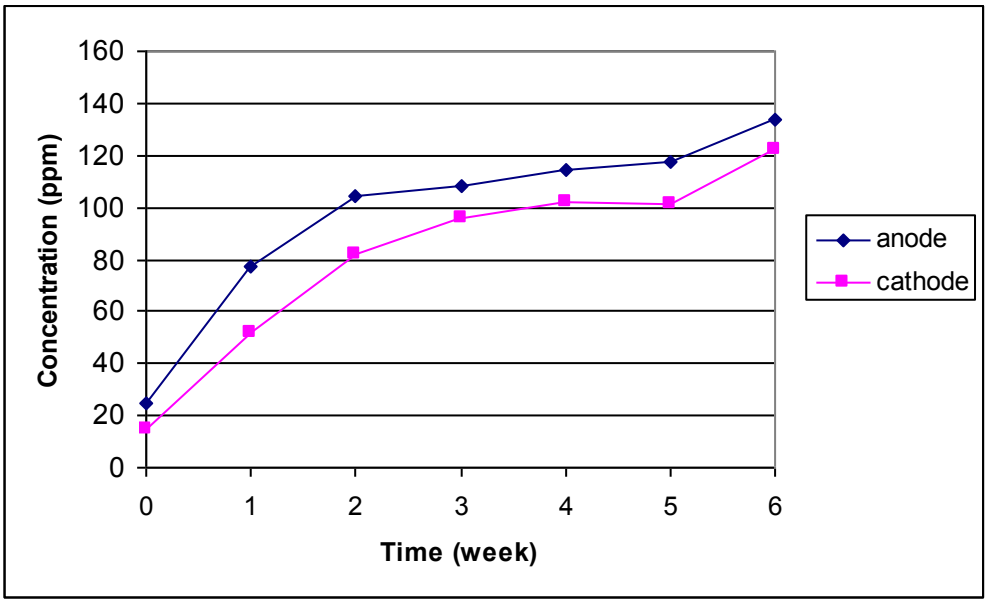

Figure G.61 EK Cell 11: Concentration curves describing the accumulation of arsenic in the anodic and cathodic half cells

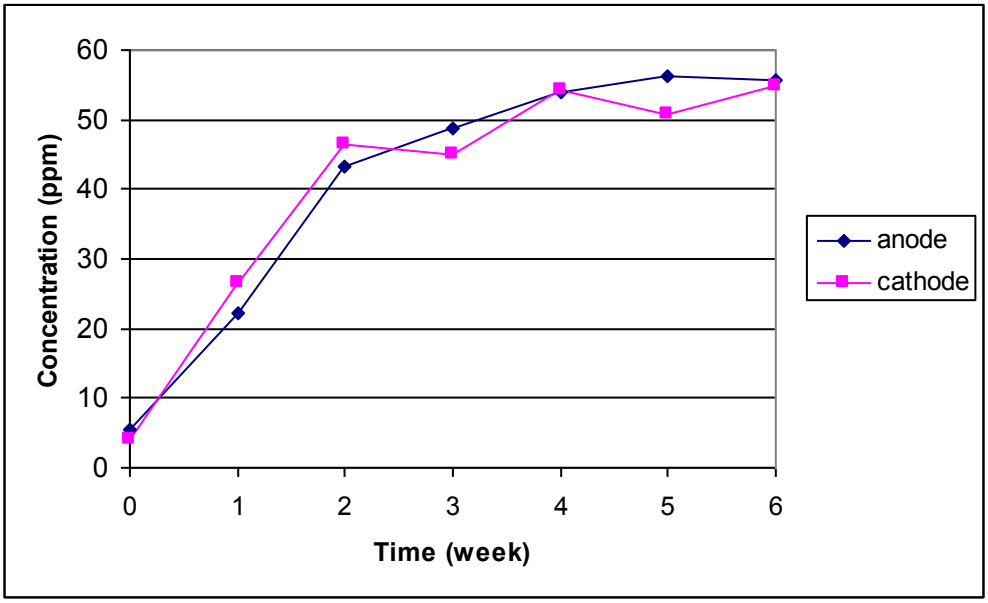

Figure G.62 EK Cell 11: Concentration curves describing the accumulation of chromium in the anodic and cathodic half cells

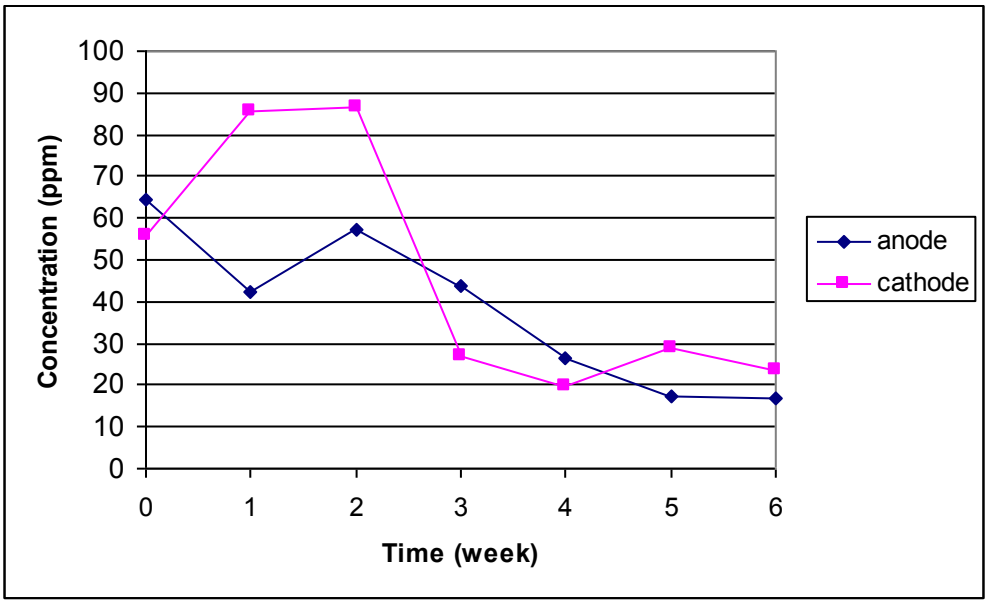

Figure G.63 EK Cell 11: Concentration curves describing the accumulation of copper in the anodic and cathodic half cells

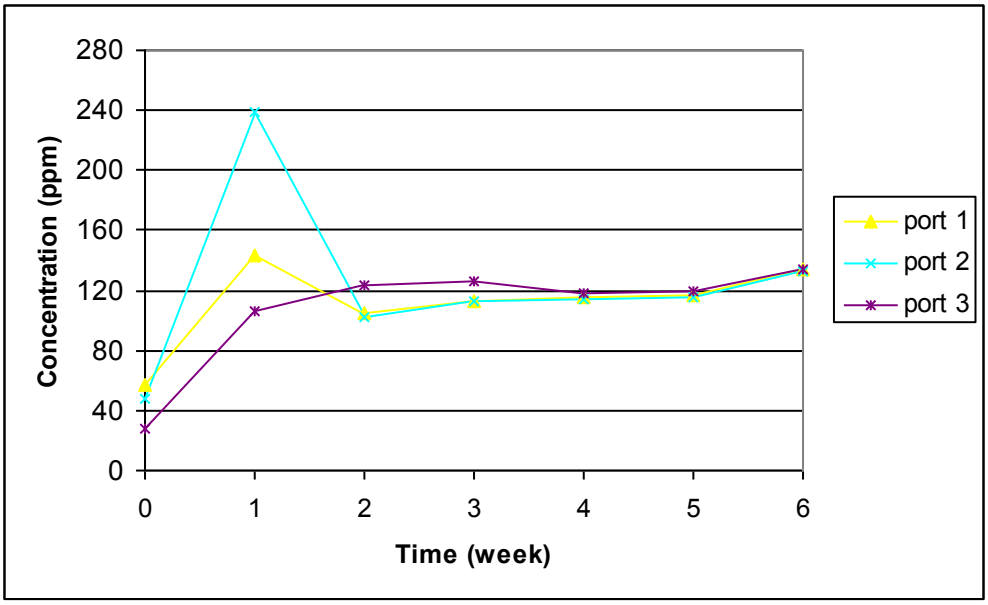

Figure G.64 EK Cell 11: Concentration curves describing the accumulation of arsenic in the pore fluid sampling zones of the EK cell center compartment

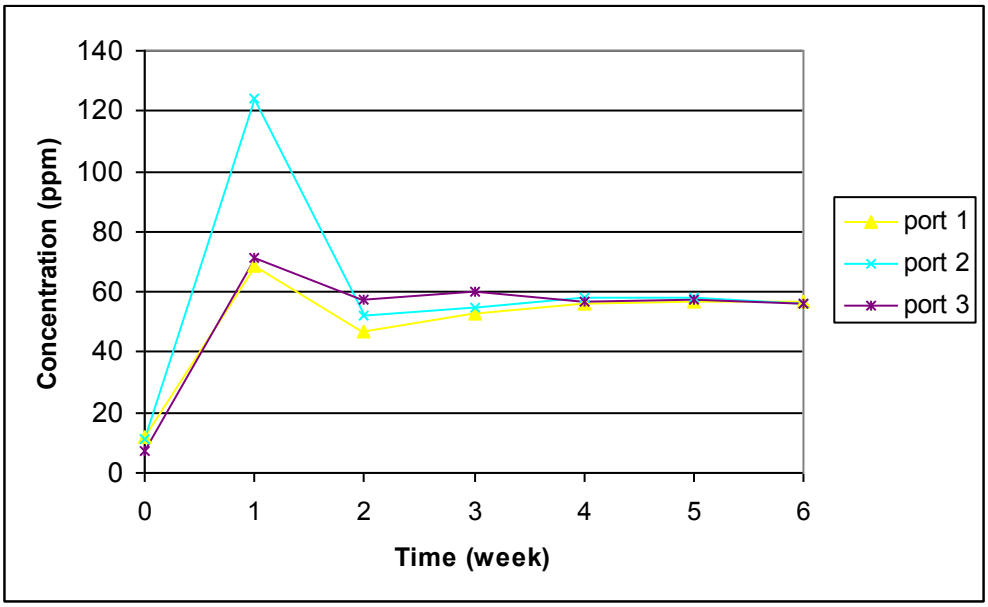

Figure G.65 EK Cell 11: Concentration curves describing the accumulation of chromium in the pore fluid sampling zones of the EK cell center compartment

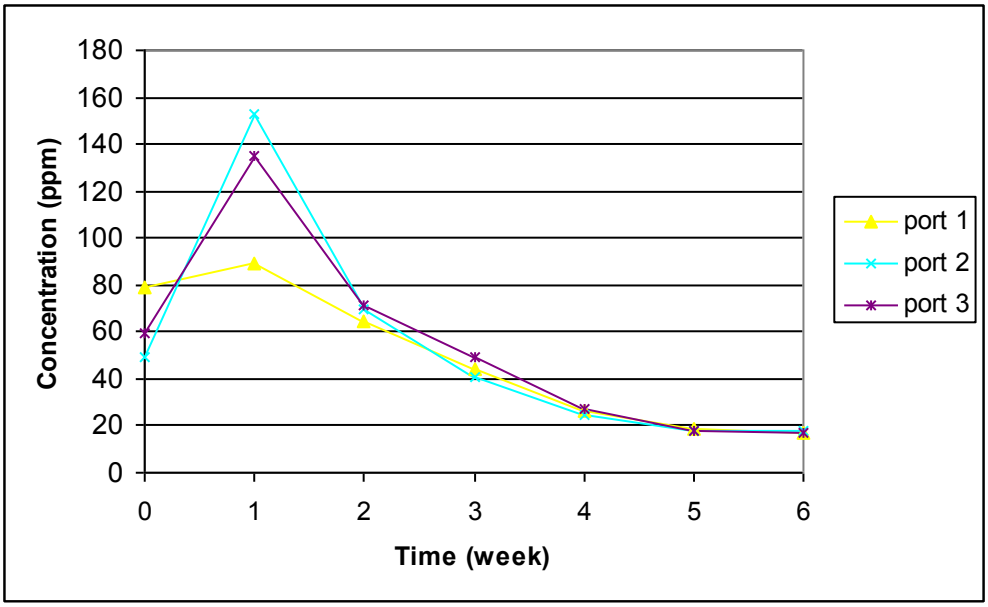

Figure G.66 EK Cell 11: Concentration curves describing the accumulation of copper in the pore fluid sampling zones of the EK cell center compartment

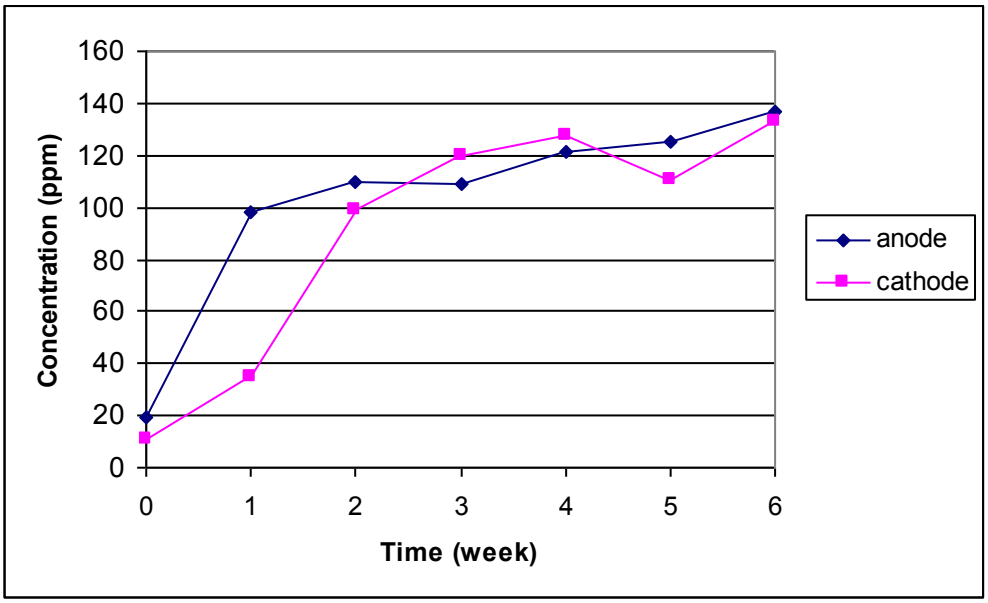

Figure G.67 EK Cell 12: Concentration curves describing the accumulation of arsenic in the anodic and cathodic half cells

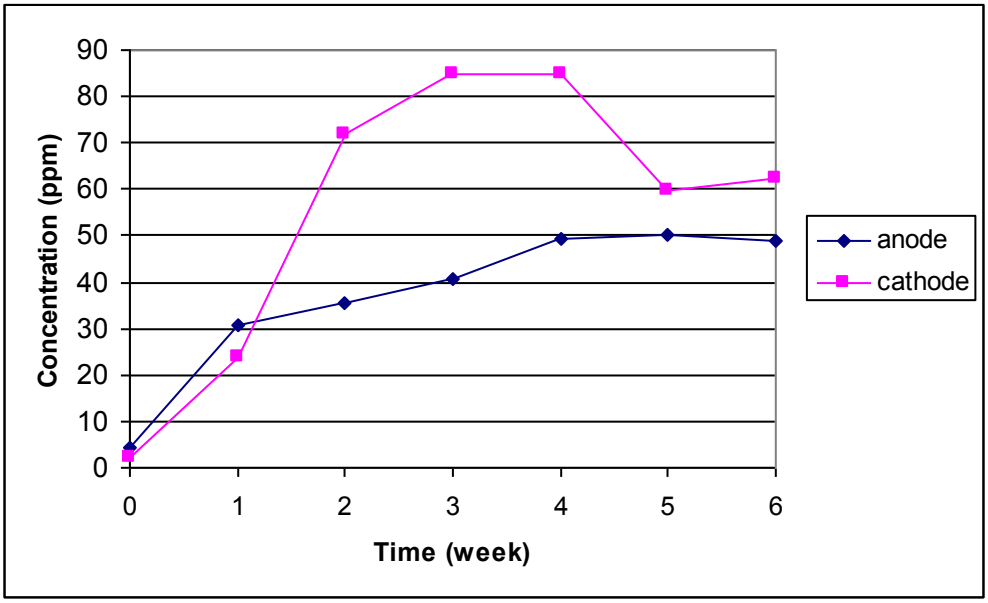

Figure G.68 EK Cell 12: Concentration curves describing the accumulation of chromium in the anodic and cathodic half cells

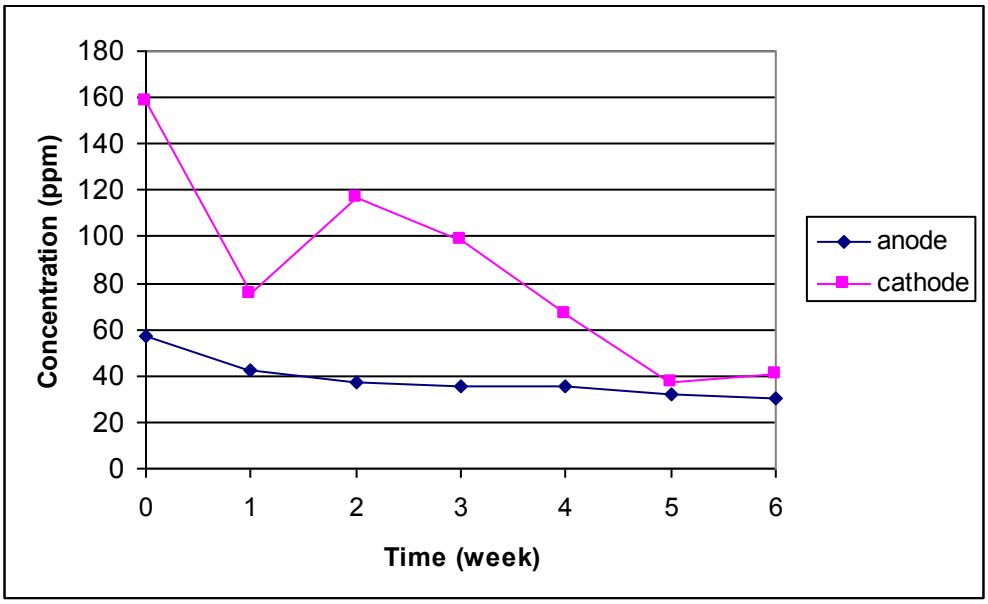

Figure G.69 EK Cell 12: Concentration curves describing the accumulation of copper in the anodic and cathodic half cells

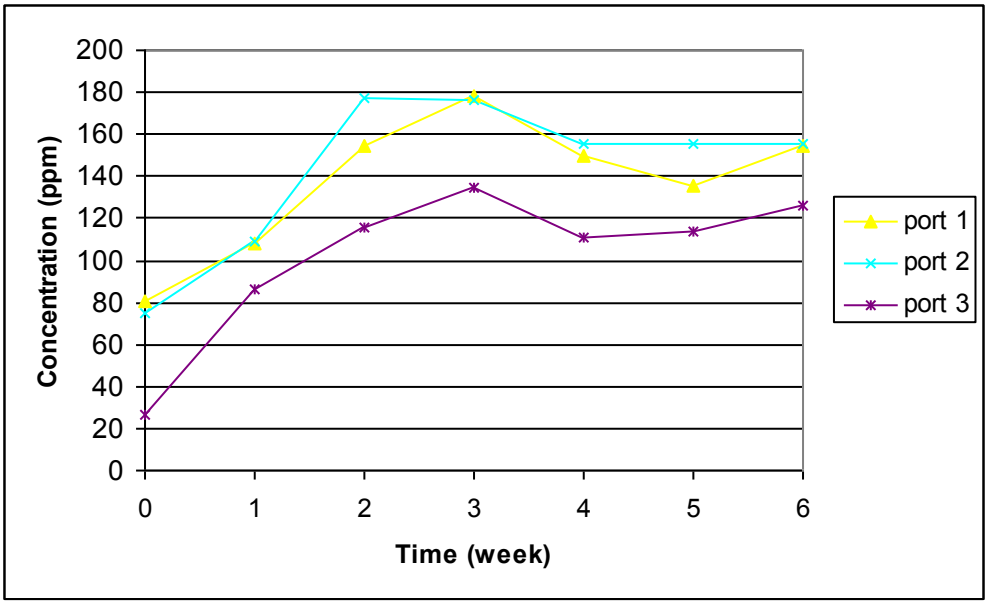

Figure G.70 EK Cell 12: Concentration curves describing the accumulation of arsenic in the pore fluid sampling zones of the EK cell center compartment

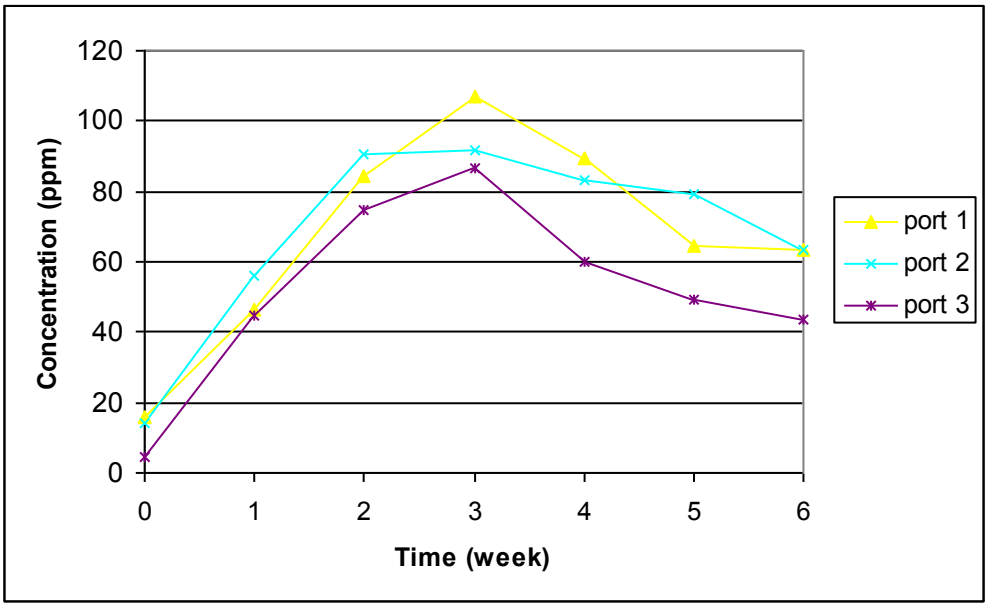

Figure G.71 EK Cell 12: Concentration curves describing the accumulation of chromium in the pore fluid sampling zones of the EK cell center compartment

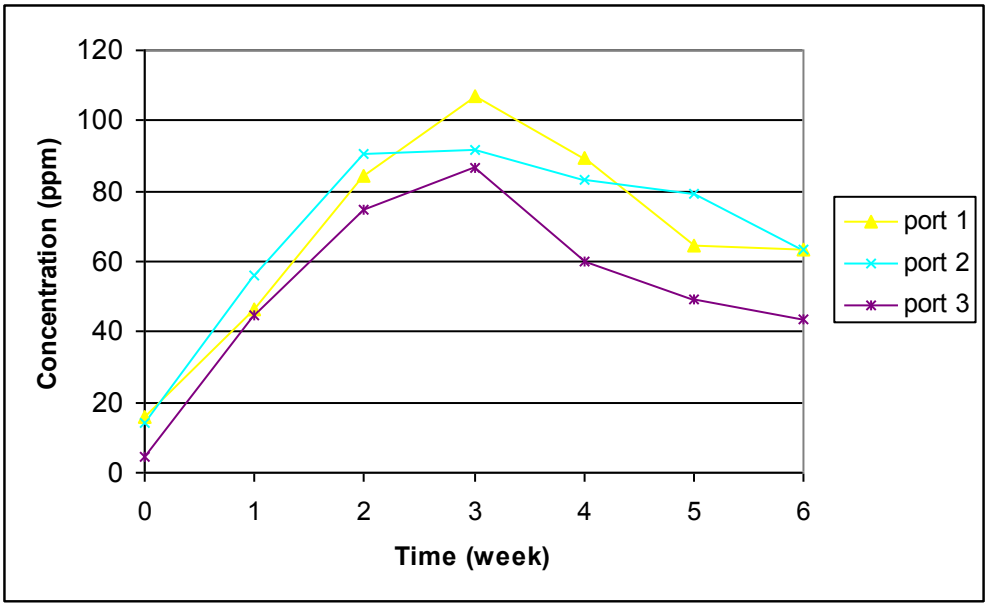

Figure G.72 EK Cell 12: Concentration curves describing the accumulation of copper in the pore fluid sampling zones of the EK cell center compartment

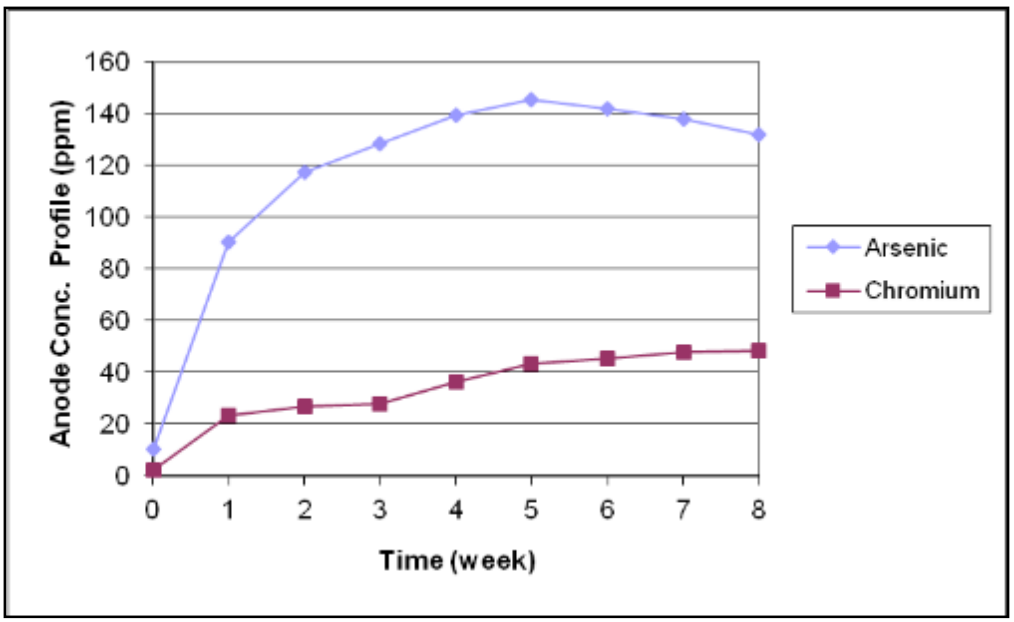

Figure G.73 EK Cell 1: Concentration curves describing the accumulation of arsenic and chromium in anodic half cell

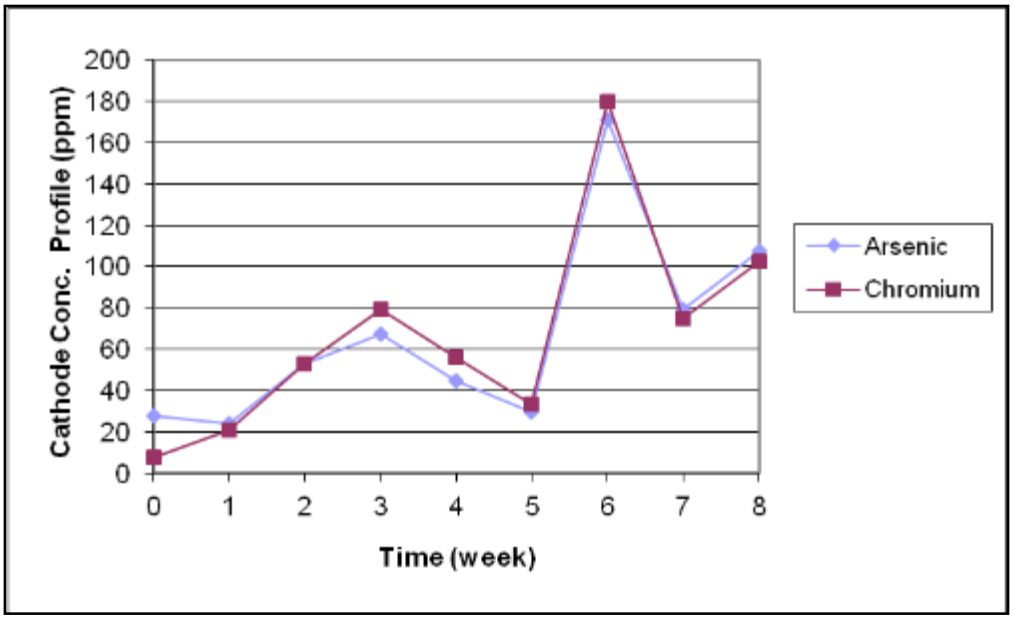

Figure G.74 EK Cell 2: Concentration curves describing the accumulation of arsenic and chromium in cathodic half cell

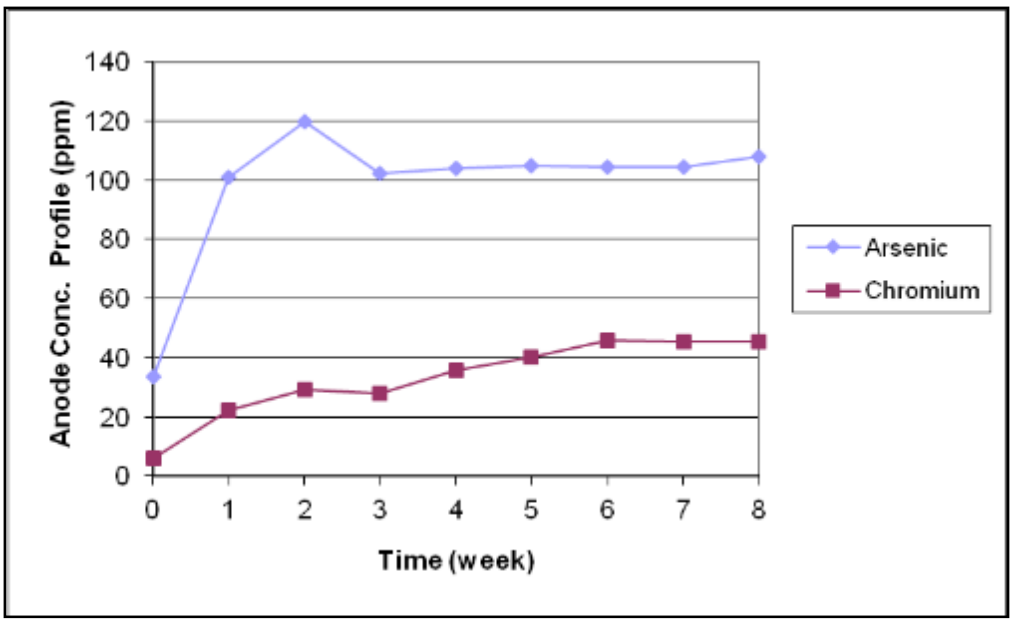

Figure G.75 EK Cell 3: Concentration curves describing the accumulation of arsenic and chromium in anodic half cell

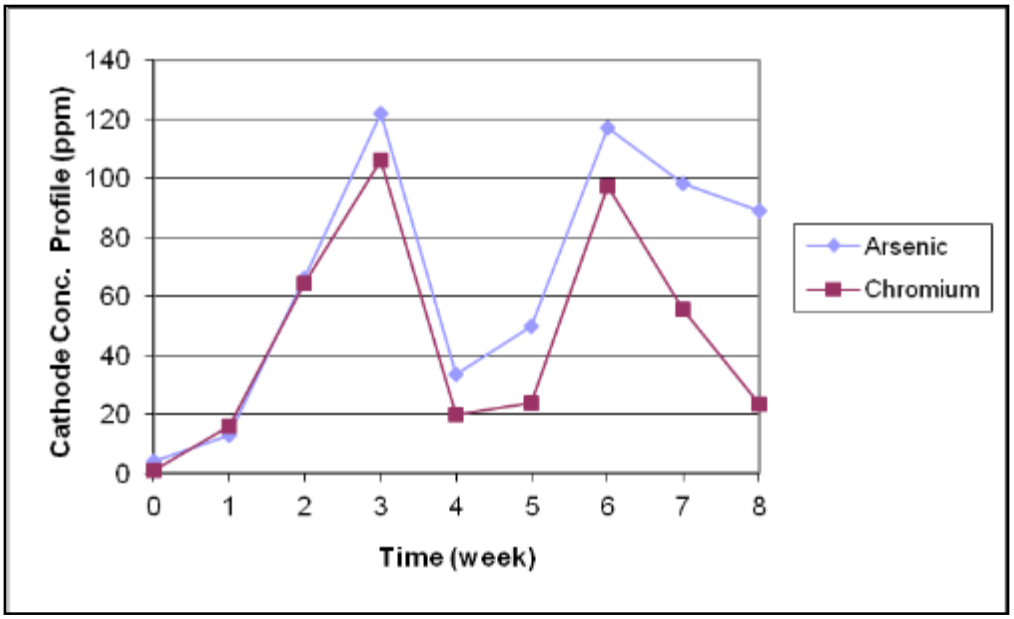

Figure G.76 EK Cell 3: Concentration curves describing the accumulation of arsenic and chromium in cathodic half cell

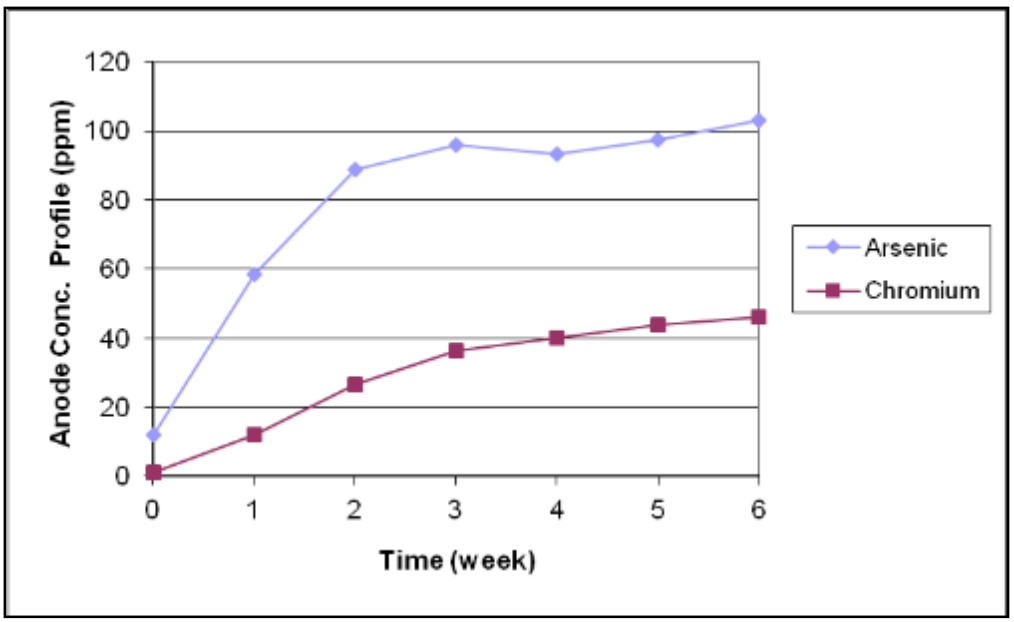

Figure G.77 EK Cell 5: Concentration curves describing the accumulation of arsenic and chromium in anodic half cell

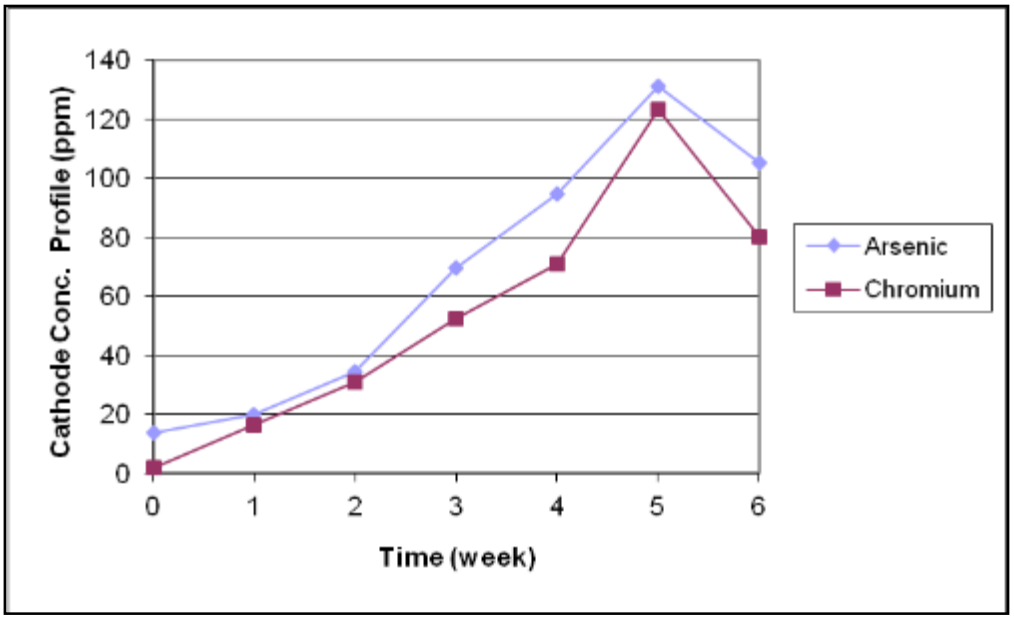

Figure G.78 EK Cell 5: Concentration curves describing the accumulation of arsenic and chromium in cathodic half cell

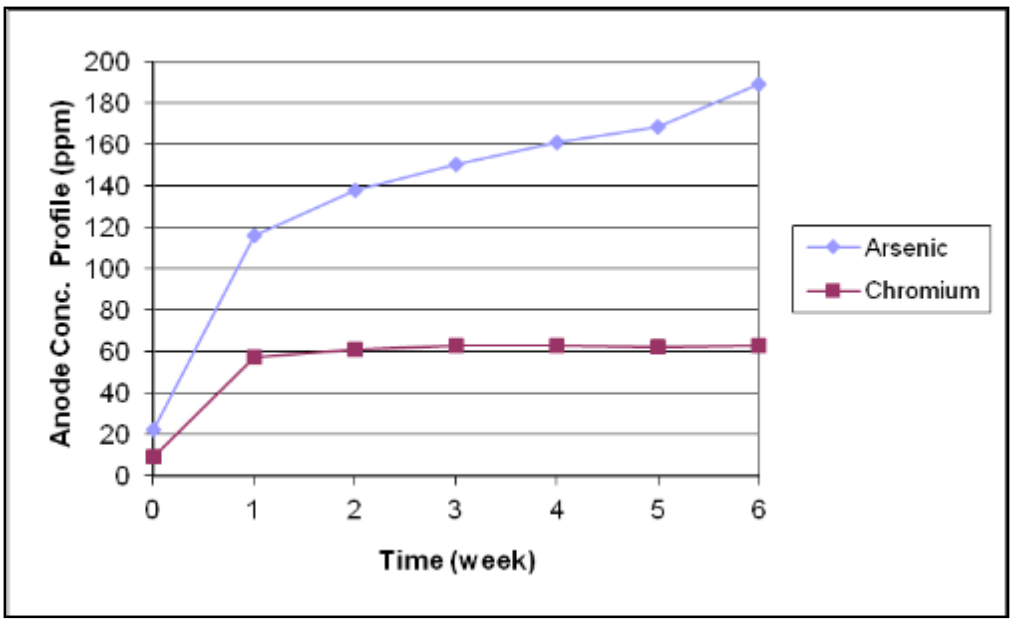

Figure G.79 EK Cell 8: Concentration curves describing the accumulation of arsenic and chromium in anodic half cell

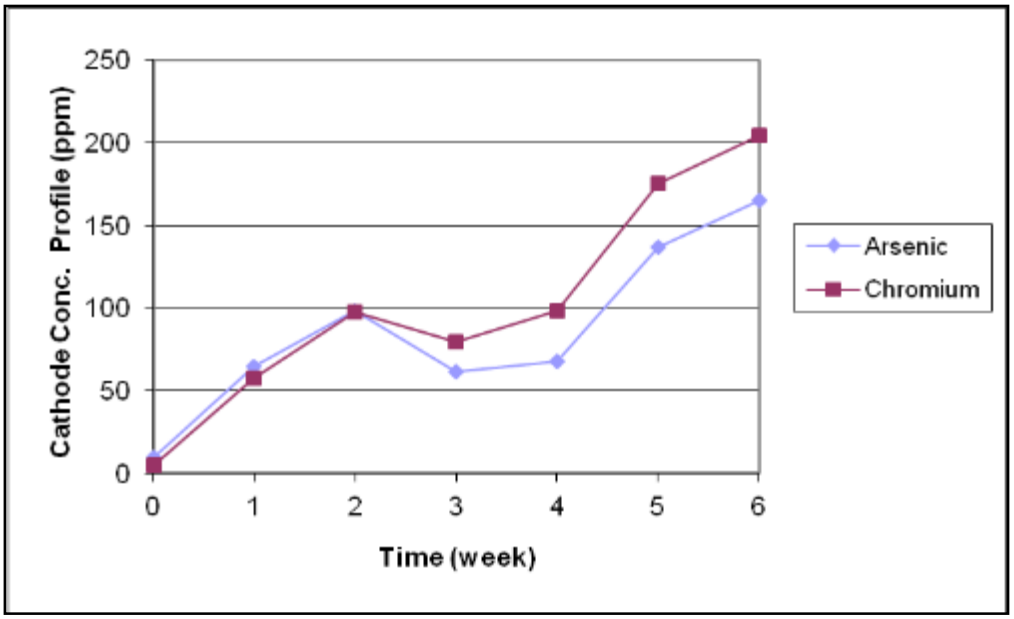

Figure G.80 EK Cell 8: Concentration curves describing the accumulation of arsenic and chromium in cathodic half cell

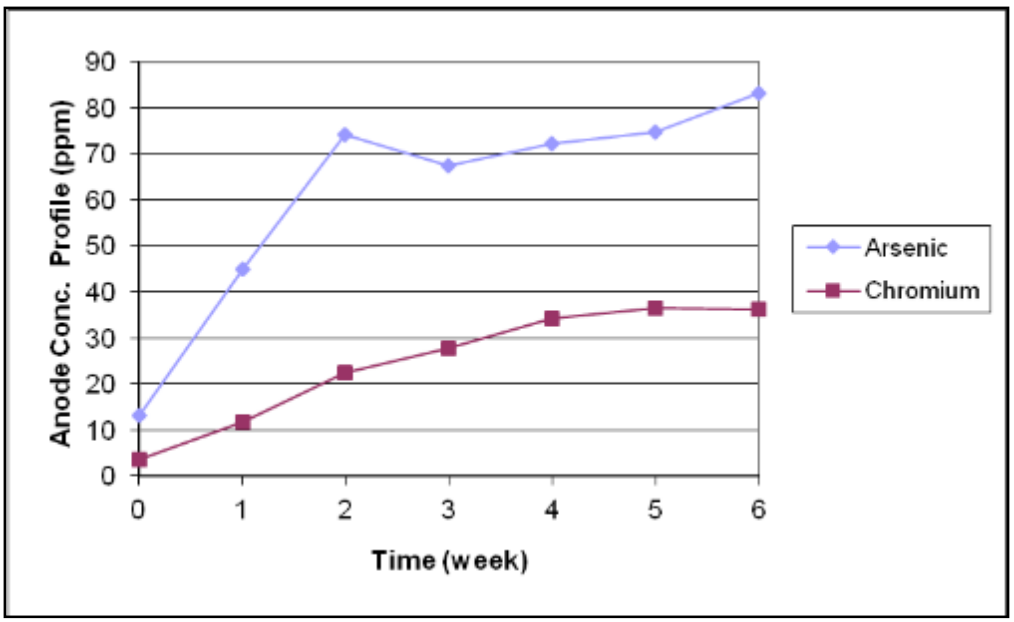

Figure G.81 EK Cell 9: Concentration curves describing the accumulation of arsenic and chromium in anodic half cell

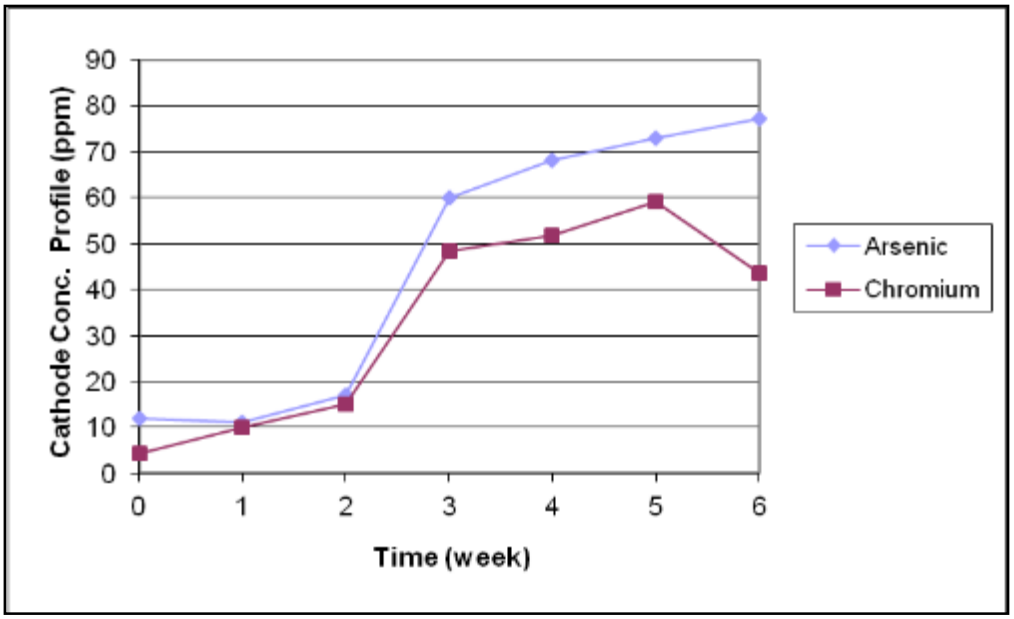

Figure G.82 EK Cell 9: Concentration curves describing the accumulation of arsenic and chromium in cathodic half cell

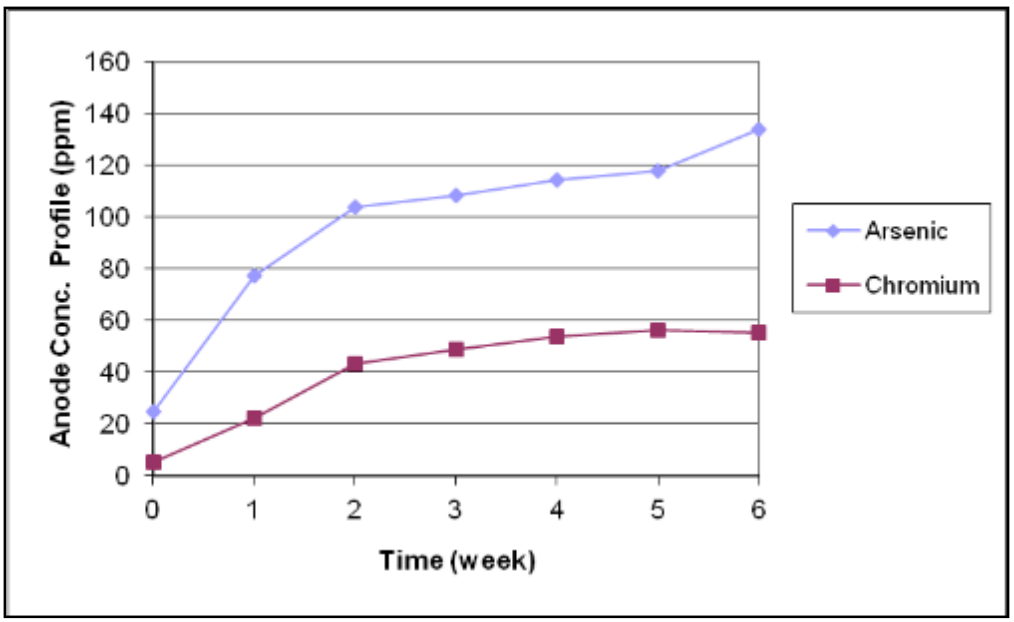

Figure G.83 EK Cell 11: Concentration curves describing the accumulation of arsenic and chromium in anodic half cell

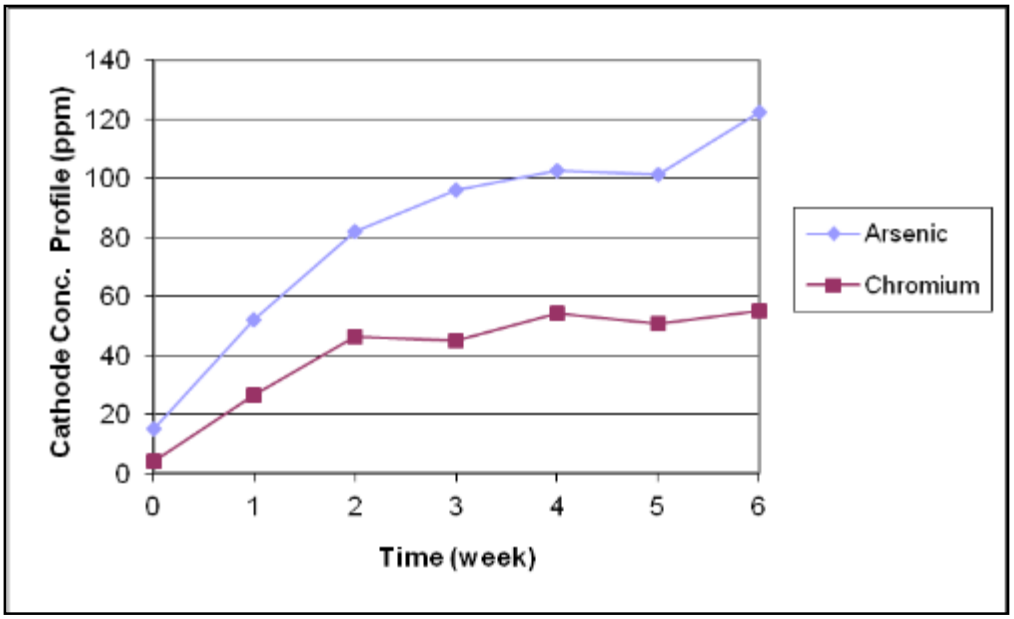

Figure G.84 EK Cell 11: Concentration curves describing the accumulation of arsenic and chromium in cathodic half cell